The Substitution Behaviour of Terpy polyglycoxyl and Ruthenium-Platinum Complexes with Biologically Significant Nucleophiles. A Kinetic and Mechanistic study.

Meshack Kituyi Sitati

Master of Science



School of Chemistry and Physics

Pietermaritzburg Campus

June 2014

The Substitution Behaviour of Terpy polyglycoxyl and Ruthenium-platinum Complexes with Biologically Significant Nucleophiles. A Kinetic and Mechanistic study.

Meshack Kituyi Sitati

Bsc. (Hons) (JKUAT, Kenya), Dip. Ed. (KSTC, Kenya)

Submitted in partial fulfilment of the academic requirements for the degree of

Master of Science

In the College of Agriculture, Engineering and Science

School of chemistry and Physics

University of KwaZulu-Natal

Pietermaritzburg

June 2014

Declaration

I M. K. Sitati do hereby declare that:

1. The search report in this thesis, except where otherwise indicated, is my original research.
2. This thesis has not been submitted for any degree or examination at any other university.
3. This thesis does not contain other persons' data, pictures, graphs or other information, unless specifically acknowledged as being sourced from other persons.
4. This thesis does not contain other persons' writing, unless specifically acknowledged as being sourced from other researchers. Where other written sources have been quoted, then:

   (a) Their words have been re-written but the general information attributed to them has been referenced

   (b) Where their exact words have been used then their writing has been placed in italics and inside quotation marks and referenced.
5. This thesis does not contain text, graphics or tables copied and pasted from the internet, unless specifically acknowledged and the source being detailed in the thesis and in the references sections.

Signed: ……..**M. K. Sitati** Date: …….

I hereby certify that these statements are correct, and as the candidates' supervisor I have approved this thesis for submission

Signed: …… **Professor D. Jaganyi (Supervisor)** Date: ……

Pietermaritzburg

June 2014

“Do not brood over your past mistakes and failures as this will only fill your mind with grief, regret and depression. Do not repeat them in the future.”

Swami Sivananda

*This work is **dedicated** to my family for being the firm support that was the springboard to accomplish this piece of work. I will forever be indebted to you. Above all God was the leading light to this accomplishment.*

Table of Contents

Abstract i

Acknowledgements ii

List of abbreviations and symbols iii

List of figures v

Chapter 1 Platinum complexes and cancer chemotherapy 1

1.1. Introduction 1

1.2 Cisplatin and analogues 1

1.3 DNA 2

1.4 Mechanism of action 3

1.5 Cisplatin resistance 4

1.6 Subsequent Platinum Anti-cancer complexes. 6

1.6.1. Platinum(IV) complexes 6

1.6.2. *Trans*-Platinum(II) complexes 7

1.6.3 Multinuclear complexes 7

1.7 Current research on platinum (II) terpyridine complexes. 9

1.8 Azoles 10

1.9 Other biologically relevant molecules 11

1.9.1 L-methionine 11

1.9.2 L-glutathione 12

1.9.3 Guanosine-5´-monophosphate 13

1.10 Aims of the study 13

1.11 References 15

Abstract

The kinetics of two sets of complexes was investigated under *pseudo* first order conditions using UV-Visible spectrophotometry as a function of concentration and temperature. The first set consisting 4'-substituted terpy polyglycoxyl complexes reacted with biological relevant N-donor nucleophiles showed that the oxygen on the polyglycoxyl group donates electrons to the Pt-metal resulting in a decrease in reactivity from **Pt** to **Pt(eg).** The first carbon-oxygen pendant bond plays a crucial role in regulating the electron density donated because there is insignificant change in the reactivity as the chain length is increased to **Pt(deg)** and then **Pt(teg).** The trend in the reactivity slightly increases in general from **Pt(eg)** to **Pt(teg)** due to reduction in steric hindrance imposed by the ethylene glycoxy unit on one side of the complex. The reactivity of the nucleophiles is p*K*a and steric dependent. It can be concluded that reactivity of the metal complexes is mostly electronically controlled while that of the nucleophiles is dependent on the basicity and steric bulk. The obtained kinetic data is supported by the DFT calculations that reveal a less electrophilic Pt(II) metal centre for complexes bearing the 4'-substituent. The temperature dependent studies support an associative mode of activation.

The second set of complexes studied included Ru(III)-Pt(II) complexes with a semi-rigid linker 4'-pyridyl-2,2':6',2''terpyridine (qpy) whose results indicated that increase in the overall charges of the respective complexes is the key reason for the observed increase in the reactivity. Additionally, replacing the *cis* pyridyl group in **Pt1** by Ru(III) polypyridyl to give **Pt2** and **Pt3** respectively lowers the energy of the LUMO (π^*) orbitals. The two qpy groups in the tri-nuclear complex **Pt3** only slightly increases the reactivity from that of **Pt2** because the qpy groups are in orthogonal positions preventing π-electron communication hence the two Pt(II) centres act independently of each other.

The observed activation parameters for both sets of complexes support an associative mode of substitution. The results of this project elucidate intrinsic, electronic and steric properties of the complexes that might be exploited for medicinal, photophysical or other applications.

Acknowledgements

First and foremost, I thank my advisor and mentor Professor Deogratius Jaganyi for offering me the opportunity to exploit my foresight. His guidance, leadership, timely feedback and support in every way throughout the project is greatly acknowledged.

I also very much appreciate the great input in this work from Dr. I. M. Wekesa (Post-doctoral fellow-UKZN)

The academic staff in the kinetics group; Dr. D. Reddy and Dr. A. Mambanda assisted greatly with the work.

I thank the University of KwaZulu-Natal for financial support.

The following people played important roles in this work;

- Mr. C. Grimmer for his expertise in running and analysing the NMR spectra and assisting in software applications.
- All academic staff in the school of chemistry who were readily available to assist at all times
- All friends and colleagues at the school of chemistry in Pietermaritzburg campus for their support and encouragement.
- My family, they had to endure my absence but more gave me strength to persist until it was done.
- Shawn for coordinating the deliveries. Hashim Desai for allocation of space in the masters' office and handling laboratory issues. All technicians and assistants for helping with issues in the laboratory.

List of abbreviations and symbols

5'-GMP	Guanosine-5'-monophosphate
aaa	$[Pt(diethylenediamine)OH_2]^{2+}$
aap	$[Pt(N\text{-}(pyridyl\text{-}2\text{-}methyl)\text{-}1,2\text{-}diamino\text{-}ethane)OH_2]^{2+}$
apa	$[Pt(2,6\text{-}bis\text{-}aminomethylpyridine)OH_2]^{2+}$
app	$[Pt(2,2'\text{-}bipyridine)(NH_3)OH_2]^{2+}$
BBR3464	$[\{trans\text{-}PtCl(NH_3)_2\}_2\{\mu\text{-}trans\text{-}Pt(NH_3)_2\text{-}(HN_2(CH_2)_6NH_2)_2\}]^{4+}$
DEDTC	Diethyldithiocarbamate
DNA	Deoxyribonucleic acid
GSH	Glutathione
HET	2-hydroxyethanethiol
HMG	High mobility group
HOMO	Highest occupied molecular orbital
L	Ligand
LUMO	Lowest unoccupied molecular orbital
mM	milliMolar
NER	Nuclear excision repair
pap	$[Pt(bis(2\text{-}pyridylmethyl)amine)OH_2]^{2+}$
ppp	$[Pt(2,2':6,2''\text{-}terpyridine)OH_2]^{2+}$
pt	$[Pt(2,2':6,2''\text{-}terpyridine)Cl]^{+}$
Pt(deg)	$[Pt\{4'\text{-}diethyleneglycoxyl)\text{-}\ 2,2':6,2''\text{-}terpyridine)Cl]^{+}$
Pt(eg)	$[Pt\{4'\text{-}ethyleneglycoxyl)\text{-}\ 2,2':6,2''\text{-}terpyridine)Cl]^{+}$
Pt(teg)	$[Pt\{4'\text{-}triethyleneglycoxyl)\text{-}\ 2,2':6,2''\text{-}terpyridine)Cl]^{+}$
Pt1	$[Pt(en)OH_2]^{2+}$
Pt2	$[H_2O(en)Pt(qpy)Ru(tpy)]^{4+}$
Pt3	$[H_2O(en)Pt(qpy)Ru(qpy)Pt(en)OH_2]^{6+}$
qpy	Quarterpyridine (4'-(pyridyl) 2,2':6,2''-terpyridine)
RNA	Ribonucleic acid
terpy/tpy	2,2':6,2''-terpyridine
TU	Thiourea

List of figures

Figure 1.1 Molecular structure of cisplatin. 1

Figure 1.2 Molecular structures of some cisplatin analogues in clinical trials. 2

Figure 1.3 Model DNA structure. 3

Figure 1.4 Models illustrating various DNA-cisplatin adducts. 4

Figure 1.5 The likely pathways of the Pt(II) complex drug may follow after uptake. ……..5

Figure 1.6 Selected Pt(IV) complexes 6

Figure 1.7 Molecular structures of dinuclear Pt(II) complexes cisplatinanalques…...7

Figure 1.8 Molecular structures of some doubly and singularly bridged multi-nuclear Pt(II) complexes bearing4'-dipyrazoylligand……..……8

Figure 1.9 Molecular structure of tri-nuclear Pt(II) complex, *BBR3464*……..….8

Figure 1.10 Structural formulae of the aqua Pt(II) complexes studied by Van Eldik *et al*……...10

Figure 1.11 pH dependent tautamers of Histidine……11

Figure 1.12 The zwitterionic form of L-methionine at pH 2……12

Figure 1.13 The zwitterionic form of L-glutathion at pH 2……..…….12

Figure 1.14 Resonance structures of GMP at pH 2……...……13

Figure 1.15 Structural formulae of the Pt(II) terpyridine complexes studied……..14

Figure 1.16 Structural formulae of the Ru(III)-Pt(II) polypyridyl complexes studied..14

Chapter 1

Platinum complexes and cancer chemotherapy

1.1. Introduction

A large number of platinum complexes have been synthesized and evaluated for potential to cure cancer since the discovery of cisplatin (figure 1.1).[1] Cisplatin, a complex of platinum metal is currently the most widely used for cancer chemotherapy after approval for clinical use in 1978,[2-6] though cancer chemotherapy remains a subject of keen interest due to the limitations of cisplatin. Cancer occurs when diseased cells grow uncontrollably forming a solid mass known as a tumour.[7] Benignant tumours do not invade the normal surrounding tissues while malignant tumours spread to neighbouring tissues or other parts of the body. A primary tumour becomes fatal if it obstructs vessels or a body organ however metastasis is the common cause of death. [8] Cancer accounts for about 13% of deaths worldwide. [9]

1.2 Cisplatin and analogues

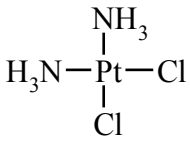


Figure 1.1 Molecular structure of cisplatin.

Due to resistance and toxicity in the administration of cisplatin,[10] a large number of cisplatin analogues were synthesised but only few merited clinical trials including carboplatin, oxaliplatin, nedaplatin, labaplatin (figure 1.2) *e.t.c.*[11,12]

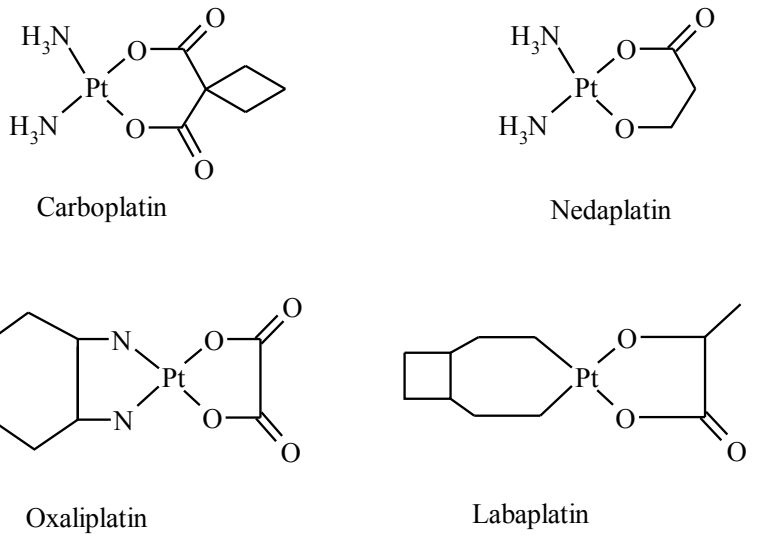


Figure 1.2 Molecular structures of some cisplatin analogues in clinical trials.

Although the cellular distribution of cisplatin and its exact mode of action are not well understood, its interaction with target **DNA** (deoxyribonucleic acid) is now accepted to be responsible for its anti-cancer activity.[12]

1.3 DNA

It's a nucleic acid macromolecule containing genetic instructions that allow living organisms to develop and function.[13] Molecules that can bind and interact with DNA provide access to genetic material which allows them applied as diagnostic probes, reactive agents or therapeutics.[14] DNA is a long polymer of simple units known as nucleosides each constituting a phosphate group, five carbon sugars (2-deoxyribose sugar) and a cyclic nitrogen containing compound called a base.[13,15] The phosphate group and sugar are joined by phosphodiester bonds forming the DNA backbone. The bases are attached to the sugar – phosphate backbone to form complete nucleotide. Bases commonly found in DNA are; adenine, quinine, thymine and cytosine. DNA macromolecule consists of double strands which intertwine to form a double helix (figure 1.3).[15] A nucleotide constitutes a backbone that holds the chain together and a base that interacts with the other strand in the helix.

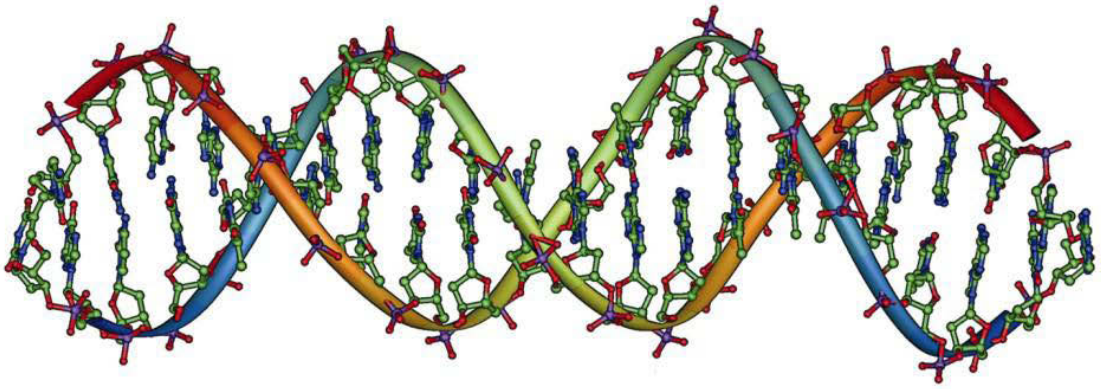


Figure 1.3 Model DNA structure.[16]

The strand backbones are closer together on one side of the helix than on the other. The major groove occurs where the backbones are far apart, the minor groove occurs where they are close together (figure 1.3). The grooves twist around the molecule on opposite sides. Certain proteins bind to DNA to alter its structure or to regulate transcription (copying DNA to RNA) or replication (copying DNA to DNA). It is easier for these DNA binding proteins to interact with the bases (the internal parts of the DNA molecule) on the major groove side because the backbones are not in the way.[16] The DNA is the ultimate target in the mechanism of cancer chemotherapy.

1.4 Mechanism of action

The antitumor activity of platinum drugs is ascribed to interaction between the metal complex and DNA, primarily with the genetic DNA located in the nucleus of the cell given that interactions with mitochondrial DNA are less responsible for antitumor activity.[15, 17] Experimental results affirm that there is high accumulation of the drug in the nuclei of cells[18] because the relatively high concentration of chloride ions in the extra cellular fluids (~ 100mM) keeps the drug neutral but after crossing the cell membrane one or both the chloride ions on the platinum drug are displaced by aqua ligands to form the cationic reactive species.[12] The first aquation is relatively rapid due to low chloride ion concentration in the cytosol (~4mM).[19] A two-step ligand exchange then occurs between the labile aqua ligands and the nucleobases of the DNA to form bifunctional adducts.[2] Binding to the DNA primarily occur through N7 atom of the guanine, while the binding to N7 and N1 of adenine and N3 of cytosine occur to a lesser degree.[3,20,21] The N7 position is preferred due to stabilising hydrogen bonding interactions and higher basicity.[3] Various bifunctional

adducts result after DNA binding *viz.* intrastrand cross-linking (GpG), interstrand cross-links of the type 1,2-(ApG), crosslinks between two deoxyquanosines separated by a third nucleosite (GnG), intrastrand crosslinks of the type GpG and mono adducts as illustrated in figure 1.4[11, 22]

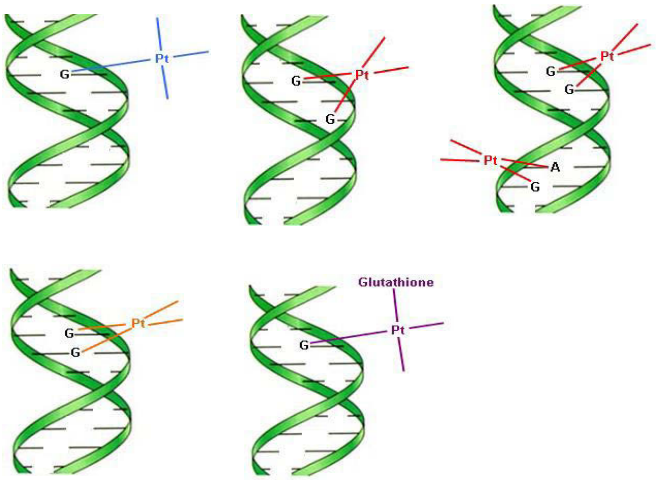


Figure 1.4 Models illustrating various DNA-cisplatin adducts.[11,12]

It is still unknown which are the most important adducts with respect to cytotoxicity, however research has shown that the adducts inhibit DNA replication or transcription but the exact mechanism of toxicity is a subject for further study.[23,24] Diamino-platinum(II) ($[(NH_3)_2Pt]^{2+}$) creates a unique junction between the strands , the distortion impedes DNA processing in the tumour cells. The distortion is characterised by a high mobility group (HMG); an 80 amino acid sequence present in many proteins that bend DNA dramatically.[25] The HMG protein binds to DNA-cisplatin adducts in a 1:1 ratio and protects them from DNA repair enzymes, thus it's not just the distortion that disrupts DNA functions but additionally the ability to attract HMGs[25,3,26] shields against effective repair of the DNA lesions by the nuclear excision repair (NER) machinery. Failure to repair lesions effectively triggers an abortive mitosis resulting in cell death by apoptosis pathway.[2,26,27]

1.5 Cisplatin resistance

A large number of the cancers have a natural resistance to treatment with the drug and some cancers that respond to the treatment would subsequently acquire resistance.[28] Acquired resistance results from, reduced cellular uptake, increased repair of the lesions, increased tolerance of the cisplatin-DNA lesions, and deactivation by preferential reactions or binding

to thiol containing proteins.[29] Reduced uptake of the drug prevents it from reaching its ultimate DNA target; deactivation could also occur when the drug reacts with other biomolecules like glutathione and metallothionein in the cytosol hence the drug that reaches the target is insufficient to inhibit tumour growth.[2] The sulphur coordinated forms of cisplatin are then excreted as conjugates coupled to the multi-drug resistance proteins through the golgi gateway.[29] However some of the sulphur containing bio-molecules especially the thioethers are under study as chemoprotecters in the platinum based chemotherapy. Pt-S(thiol) compounds are stable hence responsible for toxic side effects, but the bond can be broken in the presence of compounds known as 'rescue agents' which are exclusively sulphur-containing compounds such as diethyldithiocarbamate(DEDTC), thiourea(TU), thiosulphate, biotim, amifostine among others.[11,15, 30-32] Figure 1.5 summarises uptake of the cancer drug

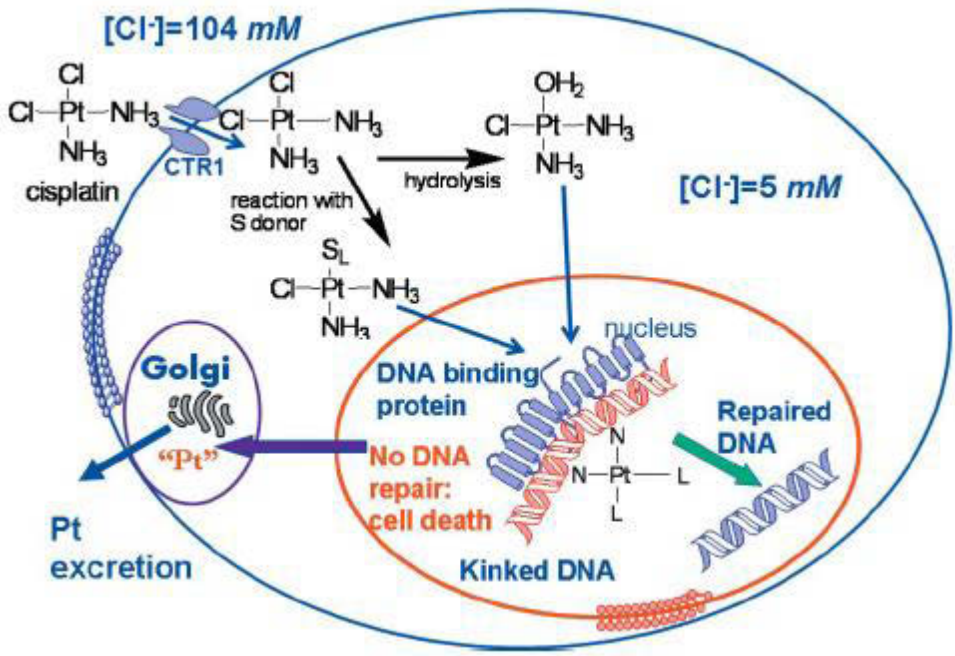


Figure 1.5 The likely pathways the Pt(II) complex drug may follow after uptake.[33]

Increased efflux reduces intracellular drug concentration. Cisplatin resistance is also enhanced by the repair of Pt-DNA lesions by nucleotide excision repair protein (NER), the nucleotide repair protein recognizes DNA damage, excises the damaged segments as base pair oligonucleotides which prompts gap filling by DNA polymerase.[5,34] Reduction in repair efficiency in insensitive tumour cells leads to resistance and drug tolerance. Further,

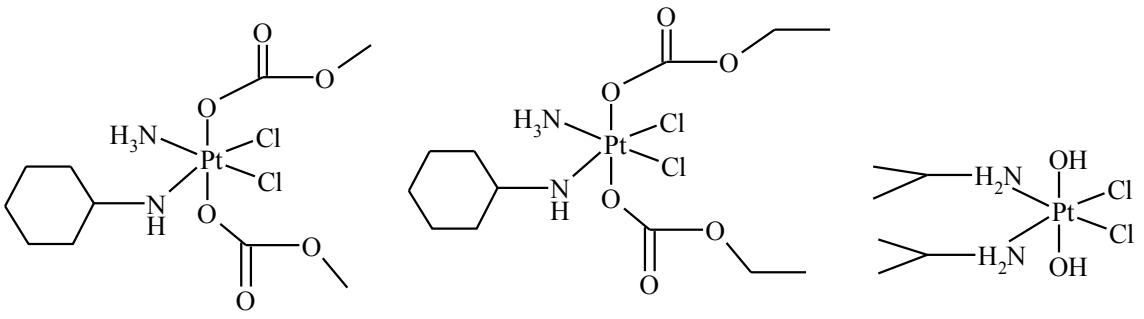
apoptotic malfunctions caused by mutant genes like the P^{53} proteins sequence can also lead to DNA lesions tolerance.[17] Continued research has produced more platinum(II) complexes some of which are on clinical trial as possible therapeutic agents.

1.6 Subsequent Platinum Anti-cancer complexes.

The development of analogues resulted in a few clinically useful complexes, most of which, cross-resistant to cisplatin.[35,36] A variety of platinum complexes have been synthesized, which are structurally distinct from cisplatin, and as a result bind to DNA in a fundamentally different manner.[37-39]

1.6.1. Platinum(IV) complexes

Though it has been shown that intravenous hydration has been able to reduce nephrotoxicity, side effects are still a problem in the use of cisplatin.[40] Intravenous injection and infusions being the only procedures of administration, novel Pt(IV) complexes were developed to overcome this limitation. One important member of this class of compounds is trans-bis(acetate) aminedichloro (cyclohexylamine) platinum(IV) (saraplatin) in figure 1.6 that is in phase (III) clinical trials in Europe and USA for the treatment of ovarian and lung cancers.[41] Saraplatin is regarded as a pro-drug of cisplatin since it undergoes reduction to yield cisplatin-like species once in the system. It has better activity than cisplatin in several cisplatin sensitive and resistant cell-lines with low nephrotoxicity and neurotoxicity.[42] Cis-aminodichloro(2-methylpyridine) platinum(II) (ZD0473) undergoing phase (II) trials displays good oral availability and anti-tumour activity.[43]



Satraplatin (JM221) Satraplatin derivative (JM216) Iproplatin

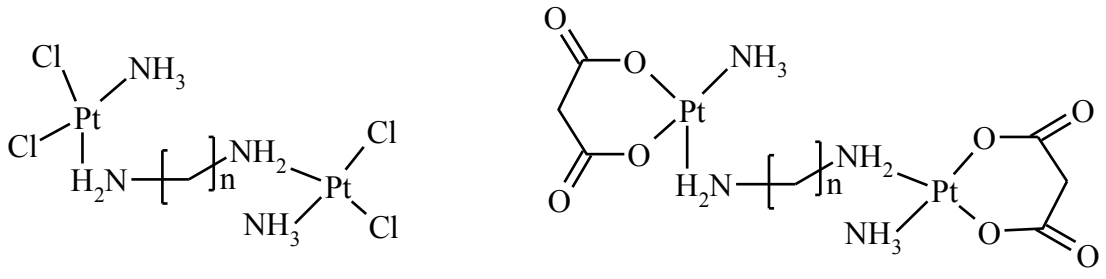
Figure 1.6 Selected Pt(IV) complexes

1.6.2. *Trans*-Platinum(II) complexes

Some *trans* complexes have anti-tumour activity with distinct DNA binding modes against the Cleare and Hosche rules.[44] These discoveries led to the development of more trans-platinum complexes with several of the compounds being characterised and showing favourable cytotoxocity against cancer cells especially the cisplatin-resistant cell lines.[45] The most notable *trans*-platinum(II) complexes with remarkable in-vitro anti-tumour activity include those bearing some planar aromatic ligand such as pyridine, N-methylimindazole, benzo-thiazole or quinoline and those carrying an alkylamine or imminoether.[46-48] Redesigning some *trans*-complexes slows their reactivity, increases solubility and cytotoxicity and makes them better cancer drugs.[49-53] Even with gains made in reduction of toxicity and overcoming resistance, there was little difference in cytotoxicity and spectrum of activity with cisplatin analogues because they form similar adducts as cisplatin.[29] Thus interest shifted to multinuclear platinum(II) complexes (figure 1.6-1.8) that can form a different range of DNA adducts that display unique anti-cancer activity vis-à-vis cisplatin (figure 1.1).

1.6.3 Multinuclear complexes

The first multinuclear platinum complexes were consistent with the traditional structure-activity relationships with examples being the compound with two cisplatin derivatives linked with flexible diamine linker and the other where the chloride groups replaced with malonate as shown in figure 1.7 which has improved water solubility and activity[54,55]



Where n = 2, 3, 4, 5, 6

Figure 1.7 Molecular structures of dinuclear Pt(II) complexes cisplatin analogues.

Subsequent multinuclear complexes were designed with either single or double bridge, mono-functional or multi-functional platinum centres and flexible or rigid linkers in an

attempt to improve cytotoxocity, increase charge and solubility as illustrated in the figure 1.8.[56-66]

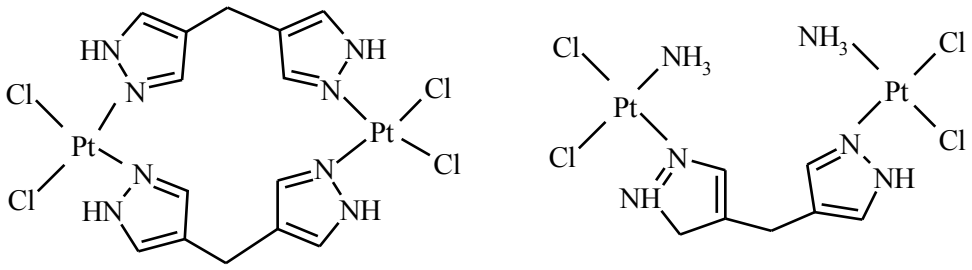
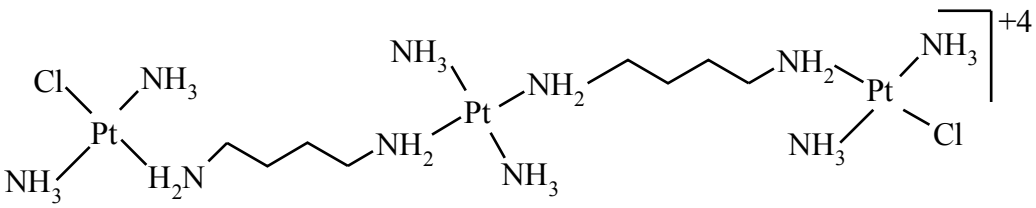


Figure 1.8 Molecular structures of some doubly and singularly bridged multinuclear Pt(II) complexes bearing the 4,4'-dipyrazolylmethane (dpzm) ligand

From the many multi-nuclear complexes synthesised and tested, tri-nuclear complex ***BBR3464***, figure 1.9 was the first to enter clinical trials because it's more active than cisplatin in all cell lines tested.[67] Based on the clinical trials, ***BBR3464*** will be much needed to treat non-small lung cancer, gastric cancer, ovarian cancer, small-cell lung cancer plus and not limited to pancreatic cancer.[68]



BBR3464

Figure 1.9 Molecular structure of tri-nuclear Pt(II)complex (***BBR3464***)

Studies of multi-nuclear complexes reveal that chain length and linker flexibility, hydrogen bonding potential of the linker, charge and geometry of leaving group to the linker are the key factors that dictate their design and potential for cancer therapy.[69-80]

1.7 Current research on platinum (II) terpyridine complexes.

Platinum(II) terpyridine complexes ($[Ptx(tpy)L]^{n+}$ where x is a substituent on the terpyridine ligand and L is the ligand in the fourth coordination site[81,82] were first synthesised in 1934.[81]

These complexes have versatile chemical benefits in biological and other fields and are important to account for ligand substitution reactions in square-planar d^8 metal complexes.[81] Platinum(II) complexes including terpyridine and1,10-phenanthroline have elicited a lot of interest currently due to their capacity to selectively bind to DNA[83] and inhibit telomerase activity. Pt(II) terpy complexes have been shown to have interactions with bio-molecules such as DNA and proteins hence the focus on them in the bioinorganic field.[82,84]

First evidence to their DNA binding was shown by Lippard and co-workers when they studied the interactions of the complex [Pt(terpy)(HET)]+ (HET=2-hydroxyethanethiol) with calf thymus DNA in 1974.[84] McFayden *et al.*[85]discovery that free terpy ligands do not intercalate to DNA at physiological pH illustrated the vital role of platinum in these reactions. Mechanistic studies on Pt(II) terpy complexes have been done with different variations on the basic terpy structure either by the addition of substituents onto the chelate or by adjusting the chelate itself to investigate the different effects that sterics and electronics play on the reaction kinetics. These investigations were envisaged to explain the substitution mechanism and behaviour of square planar d^8 transition metal complexes.[86-91]

The importance of the three joined pyridine rings in a planar configuration to the reaction kinetics of Pt(II) terpy as demonstrated by Van Eldik *et al.*[86] cannot be overemphasised Their studies on the aqua substitution reactions on complexes in figure 1.10 with thiourea nucleophiles show for instance that the rate of substitution with thiourea increases by a factor of 4 by just the addition of a single pyridine ring in going from **aaa** to **aap**, a further increase in the reaction rate by a factor of 4 on the addition of a second pyridine ring to **pap** and yet another increase by 4 orders on going from **aaa** to **ppp.** [86] This was explained to be mainly due to the increase of the electrophilicity of the metal centre as a result of increased electron back-donation to the ligand orbitals. Electronic communication between the π-acceptor ligands increases on going from **aaa** to **ppp**. The π-acceptor effects on their own (i.e in the *cis* or *trans* position) may have only a minor influence on the rate of the substitution reactions when there is no direct electronic communication.

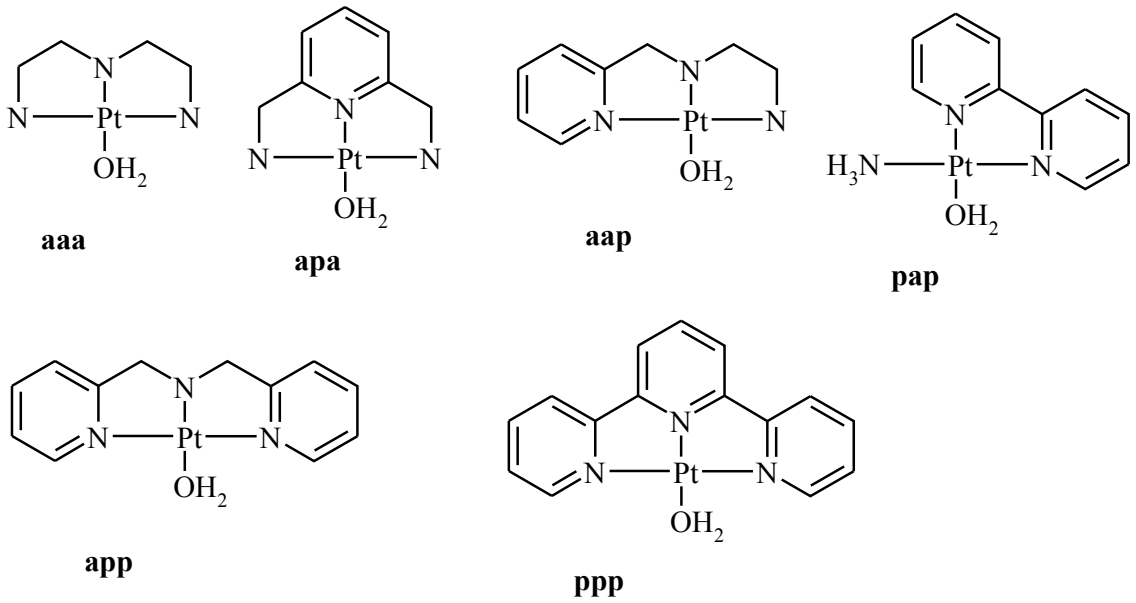


Figure 1.10 Structural formulae of the Pt(II) complexes studied by Van Eldik *et al.*

Studies by Jaganyi *et al.*[88] revealed that substituents on the terpy have different effects on the overall reactivity of the complex; Computational studies with complexes containing either electron-donating or electron-withdrawing groups in 4, 4′, 4″ positions showed electron-donating groups decrease the positive charge on the metal centre, as well as increasing the HOMO-LUMO gap of the ground state, making the complex less reactive while electron-withdrawing groups increase the positive charge on the metal centre and decreases the HOMO-LUMO gap of the ground state, enhancing the reactivity of the complex. From their observations they further concluded that substituents in both the *cis* and *trans*-positions affect reactivity with overall *trans*-influence greater than *trans*-effect and overall π *cis*-effect being greater than overall π *trans*-effect.[88,92-94] This study involves the reaction of Pt(II) complexes with nucleophiles of biological significance *viz.* azoles and bio-melecules, as such it is important to review their chemistry.

1.8 Azoles

The structure of azoles resembles that of DNA nucleic bases, thus, studies of reactions of Pt(II) complexes with azoles mimics the reaction of these complexes with the DNA base pairs[95]. Furthermore, imidazole derivatives have been shown to exhibit antineoplasic properties[96] (ability to prevent the development of neoplasm which can cause tumours). Substitution of azoles with platinum complexes is anticipated to throw more light on the designing of platinum-based cancer drugs. The coordination chemistry of five-membered

azole rings to transition metal is of interest because most reactions in biological systems involve the coordination of some form of azole to a metal centre.[97,98] Histidine, an amino acid which is essentially an imidazole derivative, forms an important fragment of many biological systems by binding to hemeproteins .[97,98] Its coordination to metal complexes varies with pH as illustrated in figure 1.11.

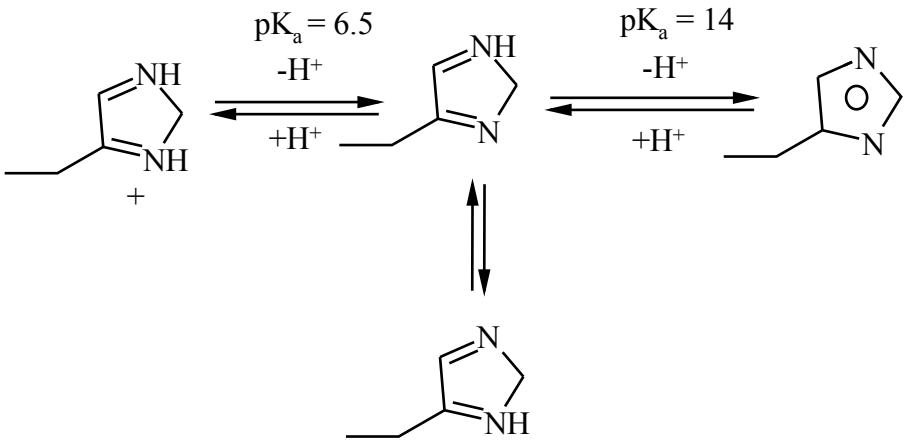


Figure 1.11 pH dependent tautamers of Histidine.

Hemeproteins consist of the iron(II) complex of protoporphyrin IX with an axially bound histidine responsible for the uptake, storage and transport of oxygen. Haemoglobin and myoglobin are hemeproteins responsible for oxygen transport and storage respectively. Since azoles form a part of hemeproteins they are part of the life-giving reactions in biological systems.[99] Azoles also form building blocks for the synthesis of higher complexes because they are good ligands and can serve to bridge complexes.[96] Apart from the azoles, substitution reaction using L-methione, guanosine-5'-monophosphate and reduced glutathione were investigated.

1.9 Other biologically relevant molecules

1.9.1 L-methionine

L-methione is thioether containing an essential amino acid having two acid dissociation constants, pK_{COOH} = 2.13[100] and pK_{NH3+} = 9.2.[101] Based on its p*K*a values, the carboxylate group is protonated to an extent of about 50 % at pH 2 where our reactions were studied resulting in an overall charge of +1. The residual 50 % exist in the form of zwitterions as shown in figure 1.12. The zwitterion is the one that coordinates to the metal complexes. Even if the positively charged species interacts with the Pt(II) complex, it will deprotonate

as a result of significant drop in the p*K*a value upon coordination to the metal centre giving the product complex with same charge as the starting complex. At pH 7.4 the zwitterionic form is predominantly present in solution and interacts with the platinum(II) compound.

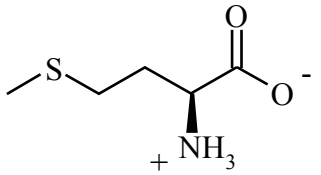


Figure 1.12 The zwitterionic form of L-methionine at pH 2

1.9.2 L-glutathione

The tripeptide glutathione is an ubiquitous thiol found in the cells of microorganisms, fungi, and plant and animal tissues, with intracellular concentrations varying between 0.1 and 10 mM consisting of the three amino acids glutamic acid, cysteine and glycine.[102] It has several cellular functions, including but not limited to working as an antioxidant to protect cells against reactive oxygen species, UV radiation, and heavy metals such as mercury, cadmium, and lead.[103,104] It is also applied in the biological detoxification processes as it's a known fact that formation of a complex between a heavy metal ion and GSH is the key step in detoxification.[105-108] Its presence in significant concentrations in cytoplasm predisposes it to react with platinum compounds before they can reach the DNA,[109] or after they bind to DNA.[109,110] The role of glutathione in the presence of cisplatin was studied in detail[111,112] revealing that glutathione can be used to reserve the drug since it readily binds on it lowering toxicity and other negative effects of the chemotherapy.[113] Glutathione exists as a zwitterions at pH 2 as shown in figure 1.13.

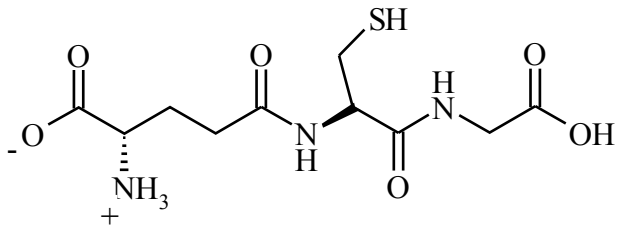


Figure 1.13 The zwitterionic form of L-glutathione at pH 2

1.9.3 Guanosine-5′-monophosphate

Guanosine-5'-monophosphate is a DNA model molecule which consists of a phosphate and sugar (2′-ribose) moiety connected to the nucleobase guanine. It includes N-donor atoms and is a model for binding to a nucleobase. Figure 1.14 shows structures of 5′-GMP with changing pH that includes atom numbering and p*K*a values. It is known that the N7-site of 5′-GMP is strongly favoured for binding to metal centres.[114-116]

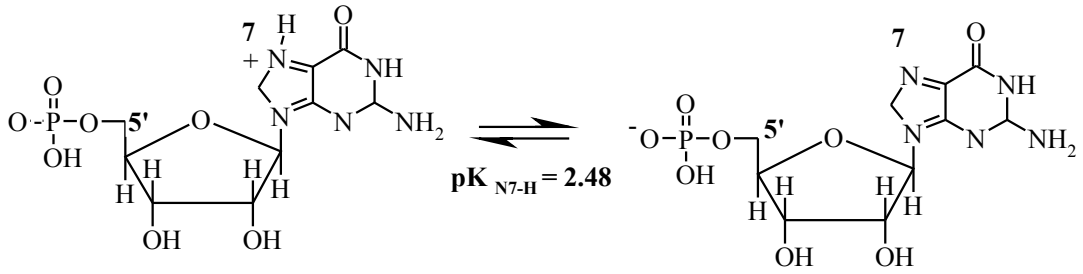


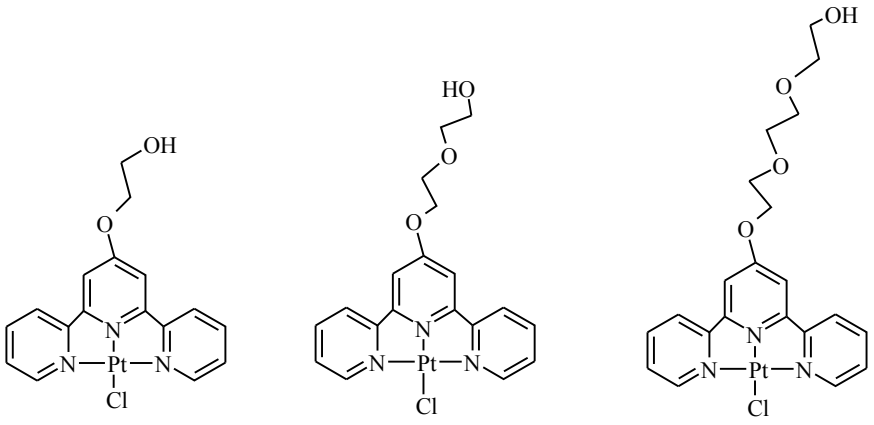
Figure 1.14 Resonance structures of 5'-GMP at pH 2.

From the p*K*a (N7) value of 2.48[116], 65 – 75 % of the 5′-GMP is protonated at N7 at pH 2 and therefore without charge while 25 – 35 % of 5′-GMP carry negative charge as they possess a singly deprotonated phosphate group. The non-protonated N7 of the negatively charged 5′-GMP is the one that reacts with the platinum centre with the acid–base equilibrium rapidly generating non-protonated N7.[117]

1.10 Aims of the study

Reedijk[118-120] underscores the importance of mechanistic studies as key to the design of new anticancer drugs with improved antitumor activities. Reactivity of the drug determines whether it reaches the target DNA molecule amid side reactions, lifetime in the body and of greatest importance the antitumor activity of the drug. The substitution reactions of platinum complexes with appropriate model nucleophiles have gained a lot of popularity today[121] with the hope of striking a platinum therapeutic drug of improved efficacy. To contribute to this pool of knowledge, we investigated the thermodynamic and kinetic properties of two sets of complexes. The first set of complexes that was studied, comprises of mononuclear Pt(II) terpy complexes (**Pt(eg)**, **Pt(deg)**, **Pt(teg)**) with a 4'-substituted polyglycoxyl pendant (figure 1.15). These were reacted with azole nucleophiles (imidazole, pyrazole, methylimidazole, 1, 2, 4-triazole and 1, 2-dimethylimidazole). Since the final target of the anticancer drugs is the N7 guanine of DNA, understanding substitution reactions of Pt(II)

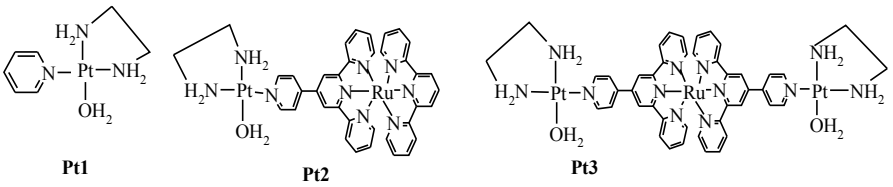
complexes with heterocyclic nitrogen donors with similar binding sites to that of guanine and other biologically relevant ligands like histidine is useful to understanding the mechanism of action of these drugs with DNA.



Pt(eg) **Pt(deg)** **Pt(teg)**

Figure 1.15 Structural formulae of the platinum (II) terpyridine complexes studied.

The second set of complexes were designed to determine the role of replacing the cis pyridyl group in **Pt1** with a (tpy)Ru(qpy) to give **Pt2** and then with $Ru(qpy)_2$ to form **Pt3** (figure 1.16) on the thermodynamic and kinetic properties of these complexes. They were reacted with biological nucleophiles L-methionine, glutathione and guanosine-5'-monophosphate never done before for this set of complexes. The sulphur containing nucleophiles (L-met and GSH) are good models for reactions involving sulfur-containing biomolecules which commonly take place in biological systems and are therefore available for competition reactions with Pt-based drugs while 5'-GMP is a model for DNA. The complexes were synthesised by standard procedures and reacted with the nucleophiles in aqueous lithium triflate medium at pH 2. Experimental data is supplemented by modelled DFT-calculations of the Pt(II) complexes to facilitate explanation of the observed trend in the reactivity.



Pt1 **Pt2** **Pt3**

Figure 1.16 Structural formulae the Ru(III)-Pt(II) polypyridyl complexes studied

1.11 References

1. F. R. Hartley, *Chemistry of the Platinum Group Metals Recent Developments*, Elsevier, Amsterdam, 1991, pgs 9, 23-30, 547-570.
2. E. R. Jameison, S. J. Lippard, *Chem. Rev.* 1999, **2467**; (b) K. R. Barnes and S. J. Lippard, *Metal ion in Biological systems*, A. Sigel, *Ed*., Marcel Dekker, New York, 2004, **42**, 143.
3. Y. Ho, S. F. Au-Yeung and K. W. T., *Med. Res. Rev.*, 2003, **23**, 633.
4. I. Kostava, *Recent Patents on Drug Discovery*, 2006, **1**, 1.
5. (a) M. J. Hannon, *Pure Appl. Chem*., 2007, **79**, 2243; (b) L. M. Pasetto, M. A. D'Andrea, A. A. Brandes, E. Rossi, S. Monfardini, *Critic. Rev. Onco. / Hemat.*, 2006, 59; (c) C. J. Jones and J. Thornback, *Medicinal Applications of Coordination Chemistry*, RSC Publishing, Cambridge, UK, 2007, pp. 218-257
6. S. M. Cohen and S. J. Lippard, *Prog. Nucleic acid Res. Mol. Bol*., 2001, **67**, 93. (b) J. Reedijk, *Eur. J. Inorg.,* 2009, 1312.
7. D. E. Thurston, *Chemistry and Pharmacology of Anti-cancer Drugs*, CRC Press Taylor & Francis Group, USA, 2007, pgs 1-27,61-63, 69-73.
8. M. Pan and C. Ho, *Chem. Soc. Rev.*, 2008, **37**, 2558; (b) http://www.diseasedatabase.com/dd28843.htm viewed on 2/11/2008; (c) S. B. Howell, *Cancer Cells*, 1990, **2**, 35; (d) H. Grunicke, W. Doppler and W. Helliger, *Arch Gerschwulstforsch*, 1999, **99**, 2711.
9. World Health Organisation, *Cancer*, http://www.who.int/cancer/en/,2009
10. B. Lippert, *Cisplatin. Chemistry and Biochemistry of a Leading Anti-cancer Drug*, Wiley-VCH, Weinheim, 1999, pgs 3-27,111-131,159-177.
11. M. A. Jakupec, M. Galanski and B. K. Keppler, *Rev. Physiol., Biochem., Pharmacol*., 2003, **146**, 1–54.
12. (a) J. Redijk, Eur. *J. Inorg. Chem*., 2009, 1303–1312. (b) *Chem. Rev*., 2007, 1387
13. D. P. Snustad and M. J. Simmons, *Principles of Genetics,* 4th ed., John Wiley & Sons, Inc., 2006, USA, pgs 210-219.
14. B. M. Zeglis, V. C. Pierre and J. K. Barton, *Chem.Commun.,* 2007, 4565-4579.
15. S. Kar, B. Sarkar, S. Ghumaan, M. Leboschka, J. Fielder, W. Kaim and G. Lahiri, *Dalton Trans.,* 2007, 1934.
16. DNA, htt://www.1musd.tehama.k12.ca.us/ date accessed-25/06/2014

17. (a) Y. Jung and S. J. Lippard, *Chem. Rev*., 2007, 1387. (b) S. Cruet-Hennequart, M. T. Glynn, L. S. Murillo, S. Coyne, M. P. Carty, *DNA Repair,* 2008, **7**, 582. (c) Y. Jung, S. J. Lippard, *J. Biol. Chem*., 2006, **281**, 1361.
18. (a) B. A. Jensen, P. Wielaard, G. V. Kalayda, M. Ferrari, C. Molenaar, J. H. Tanke, J. Bouwer and J. Reedijk, *J. Inorg. Chem*., 2003, **21**, 227. (b) *J. Biol. Chem.,* 2006, **281**, 1361
19. D. P. Bancroft, C. A. Lepre and S. J. Lippard, *J. Chem. Soc*., 1990, **112**, 6860.
20. B. Lippert, *Cisplatin, Chemistry and Biochemistry of Leading Antitumor Drugs*, ed., Wiley-VCH, Zürich, 1999.
21. J. Reedijk, *Chem. Rev*., 1999, **99**, 2499–2510.
22. J. Kozelka, F. Legendre, F. Reeder and J. C. Chottard, *Coord. Chem. Rev*., 1999, 190–192, 61–82.
23. E.R. Jamieson, S. J. Lippard, *Chem Rev.,* 1999, **99**, 2467-98.
24. K-B Lee, D. Wang, S. J. Lippard, P. A. Sharp., *Proc Natl. Acad. Sci.* USA 2002; **99**: 4239-44.
25. S. A. Kane, S. J. Lippard., *Biochemistry* 1996; **35**: 2180-8.
26. (a) M. J. Allday, G. J. Inman, D. H. Crawford and N. P. Farrell, *EMBO J*., 1995, **14**, 4994; (b). G. Wang, E. Reed and Q. Lid, *Onco*. *Rep*., 2004, **12**, 955; (c) U. M. Ohndorf, M. A. Rould, Q. He, C. O. Pabo and S. J. Lippard, *Nature*, 1999, **399**, 708.
27. (a) T. W. Sorenson, M. Eastman, *Cancer Res*., 1988, **48**, 4484; (b) M. Eastman, In *Cisplatin: Chemistry and biochemistry of a leading anticancer drug*, B. Lippert, *Ed*. Wiley VCH, Weinheim, 1999, 111.
28. B. Lippert, *Cisplatin: Chemistry and Biochemistry of a leading Anticancer Drug*, Wiley-VCH, Weinheim, 1999.
29. (a) C. H. Versantvoort, H. J. Broxterman, T. R. Badrij, J. Scheper and P. R. Twentyman, *J. Cancer*, 1995, **72**, 82, (b)E. Wong, C.M. Giandomenico, *Chem. Rev*., 1999, **9**, 2451
30. (a) J. Reedijk, *Chem. Rev*. 1999, **99**, 2499, (b) L. Ronconi and P. J. Sadler, *Coord. Chem. Rev*., 2007, **251**, 1633-1648.
31. A. E. C. Korst, C. M. Eeltink, J. B. Vermorken and W. J. F. van der Vijgh, *Eur. J. Cancer*, 1997, **33**, 1425–1429.
32. K. Lemma S. K. C. Elmroth and Elding, *J. Chem. Soc*., *Dalton Trans.,* 2002, 1288.

33. (a) J. Teuben, M. Rodriguez. I. Zubiri and J. Reeddijk, *J. Chem. Soc.*, *Dalton Trans.,* 2000, 369; (b) D. Petrović, B. Stojimirović, B. Petrović, Z. M. Bugarčića and Z. D. Bugarčić, *Bioorg. & Med. Chem*., 2007, **15**, 4203. (c) R. R. Crichton, *Biological Inorganic Chemistry: An Introduction*; Elsevier: New York, 2008, **1**, 341-344. (d) *Eur. J. Inorg. Chem.* 2009, 1303–1312

34. J. A. Mello, S. Acharya, R. Fishel, J. M. Essigmann, *Chem. Biol*., 1996, 579.

35. B. Lippert, V. Helvetica *Chimica Acta*, Zurich, Wiley-VCH, Weinheim, 1999.

36. M. A. Jakupec, M. Galanski, B. K. Keppler, *Rev. Physiol. Biochem. Pharmacol.* 2003, **146**, 1-53.

37. J. Reedijk, , *Proc. Natl. Acad. Sci. U. S. A*. 2003, **100**, 3611-3616.

38. N. J. Wheate, J. G. Collins, *Coord. Chem. Rev.* 2003, **241**, 133-145.

39. M. J. Clarke, *Coord. Chem. Rev.* 2003, **236**, 209-233.

40. R. B Weiss, M. C Giandamenico, *Chem. Rev.*, 1999, **99**, 2451

41. X. Anon, *Drug Res. Dev*., 2002, **3**, 67

42. E. Fokkema, H. J. Groen, M. N. Helder, E. G. Vries and C. Meijer, *Biochem. Pharmcol*., 2002, **63**, 1989.

43. Y. Chen, Z. Guo, S. Parsons and P. J. Sadler, *Chem. Eur. J.*, 1998, **4**, 672.

44. (a) N. Farrell, *Met. Ions Biol. Syst*., 1996, **32**, 603. (b) N. Farrell, *Eur. J. Inorg.,* 2009, 1293.

45. G. Natile M. Coluccia, *Coord. Chem. Rev*., 2001; 216-217: 383-410.

46. (a) N. Farrell, L. D. Kelland, J. D. Roberts and M. van Beusichem, *Cancer Res.*, 1992, **52**, 5065; (b) N. Farrell, T. T. Ha, J. P. Sourchard, F. L. Wimmer, S. Cross and N. P. Johnson, *J. Med. Chem*., 1992, **32**, 2240. (c) S. M. Aris and N. Farrell, *Eur. J. Inorg.,* 2009, 1293.

47. A. J. Kracker, J. D. Hoeschele, W. L. Elliot, H. D. Hollis, A. Showwalter, A. D. Sereel, N. Farrell, Y. Qu and M. P. Hacker, *J. Med. Chem*., 1992, **35**, 4526.

48. (a) M. Coluccia, A. Nassi, F. Loseto, A. Boccarelli. M. A. Mariggio, D. Giordano, F. P. Intini, P. Caputo and G. Natale, *J. Med. Chem.* 1992, **36**, 510; (b) M. Coluccia, A. Boccarelli, M. A. Mariggio, D. Giordano, F. P. Intini, P. Caputo and G. Natale, *Chem. Biol. Interac*., 1995, **98**, 251; (c) G. Natale, M. Coluccia, *Coord. Chem*., 2001, **216**, 384.

49. R. Prokop, J. Kasparkova, O. Novakova, *Biochem. Pharmacol.,* 2004; **67**: 1097-109.

50. N. Farrell, L. F. Povirk, Y. Dange, Cytotoxicity, *Biochem. Pharmacol.,* 2004; **68**: 857-66.
51. O. Novakova, J. Kasparkova, J. Malina, G. Natile, V. Brabec, *Nucleic Acids Res.,* 2003; **31**: 6450-60.
52. M. Coluccia, A. Nassi, A. Boccarelli, *J. Inorg. Biochem.,* 1999; **77**: 31-5.
53. Y. Najajreh, J. M. Perez, C. Alonso, C. Navarro-Ranninger and D. Gibson, *J. Med. Chem*., 2002, **45**, 5189.
54. N. Farell, L. R. Kelland, N. P. Farell, *Platinum-based Drugs in Cancer Therapy,* Humana Press, Ttowa, 2000, pp.321-338
55. L. Gatti, Supino, P. Perego, *Cell Death Differ.,* 2002; **9**: 1352-9.
56. S. Komeda, M. Lutz, A.L. Spek, M. Chikuma, J. Reedijk*, Inorg. Chem*., 2000, **39**, 4230.
57. S. Komeda, M. Lutz, A.L. Spek, Y. Yamanaka, T. Sato, M. Chikuma, J. Reedijk, *J. Am. Chem. Soc*., 2002, **124**, 4738.
58. V. Brabec, J. Kasparkova, O. Vrana, O. Novakova, J.W. Cox, Y. Qu, N. Farrell, *Biochemistry*, 1999, **38**, 6781.
59. P. Di Blasi, A. Bernareggi, G. Beggiolin, L. Piazzoni, E. Menta, M. Formento, *Anti-Cancer Res*., 1998, **18**, 3113.
60. P. Perego, C. Caserini, L. Gatti, N. Carenini, S. Romanelli, R. Supino, D. Colangelo, I. Viano, R. Leone, S. Spinelli, G. Pezzoni, C. Manzotti, N. Farrell, F. Zunino, *Mol. Pharm*., 1999, **55**, 528.
61. G. Pratesi, P. Perego, D. Polizzi, S.C. Righetti, R. Supino, C. Caserini, C. Manzotti, F.C. Giuliani, G. Pezzoni, S. Tognella, S. Spinelli, N. Farrell, F. Zunino, *Br. J. Cancer*, 1999, **80**, 1912.
62. S.Y. Sharp, L.R. Kelland, Curr. Opin. *Oncol. Endocr. Metab. Invest. Drugs*, 2000, **2**, 353.
63. A. Hegmans, Y. Qu, L.R. Kelland, J.D. Roberts, N. Farrell, *Inorg. Chem*., 2001, **40**, 6108.
64. L.R. Kelland, S.Y. Sharp, *Curr. Opin. Oncol. Endocr. Metab. Invest. Drugs*, 1999, **1**, 380.
65. L. Orlandi, G. Colella, A. Bearzatto, G. Abolafio, L. Manzotti, M.G. Daidone, N. Zaffaroni, *Eur. J. Cancer*, 2001, **37**, 649.

66. G. Collela, M. Pennati, A. Bearzatto, R. Leone, D. Colangelo, C. Manzotti, M.G. Daidone, N. Zaffaroni, *Br. J. Cancer*, 2001, **84**, 1387.
67. J. D. Roberts, J. Peroutka, G. Beggiolin, C. Manzotti, L. Piazzoni, N. Farrell, *J. Inorg. Biochem*., 1999, **77**, 47.
68. Novuspharma Product Profiles: *BBR3464, BBR3571, BBR3610, BBR3611*, November 2002.
69. N. Farrell, in: L. R. Kelland, N. P. Farrell (Eds.), *Platinum-Based Drugs in Cancer Therapy*, Humana Press, Totowa, 2000, **338**, pp. 321_ .
70. N. J. Wheate, C. Cullinane, L. K. Webster, J.G. Collins, *Anti- Cancer Drug Des*., 2001, **16**, 91.
71. C. Manzotti, G. Pratesi, E. Menta, R. Di Domenico, E. Cavalletti, H.H. Fiebig, L. R. Kelland, N. Farrell, D. Polizzi, R. Supino, G. Pezzoni, F. Zunino, *Clin. Cancer Res*., 2000, **6**, 2626.
72. Y. Wang, N. Farrell, J. D. Burgess, *J. Am. Chem. Soc*., 2001, **123**, 5576.
73. N. J. Wheate, J. G. Collins, *J. Inorg. Biochem*., 2000, **78**, 313.
74. N. J. Wheate, L. K. Webster, C. R. Brodie, J.G. Collins, *Anti- Cancer Drug Des*., 2000, **15**, 313.
75. N. J. Wheate, S .M. Cutts, D.R. Phillips, J. R. Aldrich-Wright, J. G. Collins, *J. Inorg. Biochem*., 2001, **84**, 119.
76. U. Sehlstedt, S.K. Kim, B. Norden, *J. Am. Chem. Soc*., 1993, **115**, 12258.
77. J. W. Cox, S.J. Berners-Price, M.S. Davies, Y. Qu, N. Farrell, *J. Am. Chem. Soc*., 2001, **123**, 1316.
78. Y. Qu, N. J. Scarsdale, M.-Y. Tran, N. P. Farrell, *J. Biol. Inorg. Chem*., 2003, **8**, 19.
79. T. D. McGregor, Z. Balcarova, Y. Qu, M.-C. Tran, R. Zaludova, V. Brabec, N. Farrell, *J. Inorg. Biochem*., 1999, **77**, 43.
80. T. D. McGregor, W. Bousfield, Y. Qu, N. Farrell, *J. Inorg. Biochem*., 2002, **91**, 212.
81. S. C. Cummings, *Coord. Chem.Rev*., 2009, **253**, 1495
82. S. D. Cummings, *Coord. Chem. Rev*., 2009, **253**, 449.
83. D.-L. Ma, C.-M. Che and S.-C. Yan, *J. Am. Chem. Soc*., 2009, **131**, 1835.
84. S. D. Cummings, *Coord. Chem. Rev*., 2009, **253**, 1495.
85. W. D. McFadyen, L. P. Wakelin, I. A. Roos and V. A. Leopold, *J. Med. Chem*., 1985, **28**, 1113.

86. A. Hofmann, D. Jaganyi, O. Q. Munro, G. Liehr, and R. van Eldik, *Inorg. Chem.*, 2003, **42**, 1688.
87. D. Jaganyi, K-L. De Boer, J. Gertenbach and J. Perils, *Int. J. Chem. Kinetics*, 2008, 808.
88. D. Reddy and D. Jaganyi, *Dalton Trans*., 2008, 6724.
89. R. Romeo, M. R. Plutino, L. M. Scolaro, S. Stoccoro and G. Minghetti, *Inorg. Chem.,* 2000, **39**, 4749.
90. D. Jaganyi, D. Reddy, J. A. Gertenbach, A. Hofmann and R. van Eldik, *Dalton Trans.*, 2004, 299.
91. A. Hofmann, L. Dahlenburg and R. van Eldik, *Inorg. Chem*., 2003, **42**, 6528.
92. R. Romeo, M. R. Plutino, L. M. Scolaro, S. Stoccoro and G. Minghetti*, Inorg. Chem.*, 2000, **39**, 4749.
93. M. L. Tobe and J. Burgess, *Inorganic Reaction Mechanisms*, Addison Wesley Longman Ltd., Essex, 1999, pgs 30-43, 70-112.
94. L. Canovese and M. L. Tobe, *Dalton Trans*., 1985, 27.
95. A. W. Roszak, O. Clement and E. Buncel, *Acta. Cryst.*, 1996, **C52**, 1654.
96. R. Conteras, A. Flores-Parra, E. Mijangos, F. Tellez, H. Lopez-Sandoval and N. Barba-Behrens, *Coord. Chem. Rev*., 2009, **253**, 1979.
97. J. Rosic, B. Petrovic, M. Djuran and Z. D Bugarcic, *Chemical Monthly*, 2007, **138**, 1.
98. Z. D. Bugarcic, S. T. Nandibewoor, M. S. A. Hamza, F. Heinemann and R. van Eldik, *Dalton Trans*., 2006, 2984.
99. P. R. Balding, C. S. Porro, K. J. McLean, M. J. Sutcliffe, J-D Mare´chal, A. W. Munro and S. P. de Visser, *J. Phys. Chem.,* 2008, **112***,* 12911.
100. D. R. Lide, *Handbook of Chemistry and Physics*; CRC press: New York, 1995.
101. E. J. Cohn, J. T. Edsall, *Proteins, Amino Acids and Peptides as Ions and Dipolar Ions*; Reinhold Publishing Corporation: New York, 1943.
102. Meister, *J. Biol. Chem.* 1988, **263**, 17205–17208.
103. A. Pompella, A. Visvikis, A. Paolicchi, V. De Tata, A. F. Casini, *Biochem. Pharmacol.* 2003, **66**, 1499–1503.
104. A. Meister, S. S. Tate, *Annu. Rev. Biochem.* 1976, **45**, 559–604.
105. K. Vido, D. Spector, G. Langniel, S. Lopez, M. B. Toledano, J. Labarre, *J. Biol. Chem.* 2001, **276**, 8469–8474.

106. D. Jamieson, *Nat. Genet.* 2002, **31**, 228–230.
107. M. Fauchon, G. Lagniel, J.-C. Aude, L. Lombardia, P. Soularue, C. Petat, G. Marguerie, A. Sentenac, M. Werner, J. Labarre, *Mol. Cell.* 2002, **9**, 713–723.
108. R. K. Singhal, M. E. Anderson, A. Meister, *FASEB J.* 1987, **1**, 220–223.
109. A. Eastman, *Chem. Biol. Interact.* 1987, **61***,* 241–248.
110. A. Eastman, M. A. Barry, *Biochemistry* 1987, **26***,* 3303–3307.
111. G. Pratesi, L. DalBo, A. Poalicchi, P. Tonarelli, R. Tongiani, F. Zunino, *Ann. Oncol.* 1995, **6**, 283–289.
112. J. Sastre, E. Diazrubio, J. Blanco, L. Cifuentes, *Oncol. Rep.* 1996, **3**, 1149–1152.
113. J. F. Smith, A. Bowman, T. Perren, P. Wilkinson, R. J. Presciott, K. J. Quinn, M. Tedeschi, *Ann. Oncol.* 1997, **8**, 569–574.
114. Ž. D. Bugarčić, F. W. Heinemann, R. van Eldik, *Dalton Trans.* 2004, **2**, 279–286.
115. B. Lippert, *Cisplatin: Chemistry and Biochemistry of a Leading Anticancer Drug*; Wiley-VCH: Zürich, Switzerland, 1999; pp. 183–221.
116. S. Zhu, A. Matilla, J. M. Tercero, V. Vijayaragavan, J. A. Walmsley, *Inorg. Chim. Acta* 2004, **357**, 411–420.
117. N. Summa, W. Schiessl, R. Puchta, N. van Eikema Hommes, R. van Eldik, *Inorg. Chem.* 2006, **45**, 2948–2959.
118. J. Reedijk, *Eur. J. Inorg.,* 2009, 1312.
119. J. Reedijk, *Chem. Rev*., 1999, **99**, 2499
120. J. Reedijk, *PNAS*., 2003, **100**, 3611.
121. D. Jaganyi, K. De Boer, J. Gertenbach, J. Perils, *Inte. J. Chem. Kinetics*, 2008, 809.

Table of contents

List of abbreviations and symbols……*i*

List of figures……..*ii*

List of schemes……...*iii*

List of tables.....*iv*

Chapter 2 Substitution Reactions…….. 1

2.1. Introduction to substitution reactions……... 1

2.2. Inorganic substitution reactions……1

2.2.1. Dissociative mechanism (**D**):……2

2.2.2. Associative mechanism (**A**):……2

2.2.3. Interchange Mechanism (**I**):……..2

2.2.3.1. Dissociative activated interchange mechanism ($\mathbf{I_D}$):……2

2.2.3.2. Associatively activated interchange mechanism ($\mathbf{I_A}$):……...3

2.3. Substitution reactions of the square planar complexes…… 4

2.3.1 Mechanism of reaction of square planar complexes……5

2.4 Factors affecting the rate of substitution reactions……7

2.4.1 Effect of the non-labile ligand…… 7

2.4.1.1 The polarization theory……... 10

2.4.1.2 The π-bonding theory…….. 11

2.4.2 The Molecular orbital theory…….. 12

2.4.3 Effect of incoming group…… 14

2.4.4 Nature of the *cis* Ligand……..15

2.4.5 Nature of the leaving group…… 16

2.4.6 Steric effect…… 17

2.4.7 Effect of the solvent……..17

2.5 Evidence of the dissociative pathway for the substitution reactions of square planar Pt(II) complexes…… 18

2.6 References…….. 19

List of abbreviations and symbols

η_{pt}/η_{pt}^{0}	Nucleophilicity constant/Standard nucleophilicity const
A	Associative
D	Dissociative
I	Interchange
$\mathbf{I_A}$	Associative activation
$\mathbf{I_D}$	Dissociative activation
k_S	Rate constant for attack by solvent
k_Y	Rate constant for entering nucleophile
L	Ligand
MeOH	Methanol
MO	Molecular orbital
py	pyridine
TS	Transition state
X	Leaving group unless stated otherwise
Y	Incoming group unless stated otherwise

List of figures

Figure 2.1 Diagrams to illustrate a (*a*) dissociatively activated and (*b*) associatively activated intimate mechanism……..3

Figure 2.2 Gibbs free energy diagrams showing D, A, and I mechanisms…….3

Figure 2.3 Plots of k_{obs} verses [NU] for the reaction of *Di*-Pt-But with thiourea nucleophiles. 6

Figure 2.4 Induced dipole moments along L-Pt-X 11

Figure 2.5 π-back donation of charge from the filled *d* orbitals of Pt(II) to the empty orbitals of the *trans* ligand. 12

Figure 2.6 A simple MO diagram of $[PtCl_4]$ 12

Figure 2.7 Representation of L-Pt-X bonding using σ_x MO; in (a) the strength of the σ-bonds are almost equal but stronger for the stronger σ-donor L in (b) 14

List of schemes

Scheme 2.1 Stereo-specific substitution reactions of square planar complexes. 5
Scheme 2.2 Reaction pathways of Pt(II) complexes 7
Scheme 2.3 Non-stereospecific substitution in dissociative mechanism 18

List of tables

Table 2.1 Effect of *cis* ligand, L, on the rate of reaction 16
Table 2.2 The effect of solvent on chloride substitution reactions.....17

Chapter 2

Substitution Reactions

2.1. Introduction

Substitution reactions involve bond breaking and subsequent bond formation and in the process a ligand from the environment replaces a ligand on a coordination shell. [1,2] Bond breaking according to Ingold and Hughes[3,4] can be categorised as homolytic or heterolytic based on electron distribution. Homolytic bond breaking involves dividing the bonding electron pair evenly between the products such that each species gets an electron as illustrated by equation 2.1. Heterolytic bond breaking on the other hand could either be nucleophilic heterolysis where the electrons of the bond leave with the leaving group (equation 2.2) or electrophilic heterolysis where the electrons of the bond remain with the reaction centre (equation 2.3).[5]

$A{:}B \longrightarrow A^{\cdot} + B^{\cdot}$ Homolysis (2.1)

$A{:}B \longrightarrow A^{+} + {:}B^{-}$ Nucleophilic heterolysis (2.2)

$A{:}B \longrightarrow A{:}^{-} + B^{+}$ Electrolytic heterolysis (2.3)

Where, *A = reaction centre, B = leaving group and : represent bonding electron pair.*

Ingold and Hughes classification is sufficient for describing substitutions on carbon centres, but limited in the area of inorganic reaction mechanisms.[1]

2.2 Inorganic substitution reactions

Inorganic reactions are divided into electrophilic substitution (SE) or nucleophilic substitutions (SN), and the latter could be represented by SN_1 or SN_2 depending on the molecularity of the rate determining step of the mechanism.[2] Most substitution reaction pathways are based on SN_1 or SN_2 mechanisms.[2] Investigations in the substitution reactions involving transition metal complexes in other solvents other than water revealed that the order of a reaction is not a reliable ground of molecularity and that often substitution occurs within a preformed aggregate.[1] Langford and Gray,[6] applied the operational approach to classify inorganic substitution reactions based on the concepts of stoichiometric mechanism and

intimate mechanisms.[7] The stoichiometric mechanism is determined from the kinetic behaviour and classified as;[7-10]

2.2.1. Dissociative mechanism (D):

The intermediate consists of a species with reduced coordination number because the bonds between the leaving group and the metal first breaks before the formation of the bond between the metal and the entering ligand. The mechanism is similar to SN_1 pathways. The bond breaking step is the rate-determining step hence rate of reaction depends on the nature of the leaving group.[11,12] The energy reaction profile is shown in figure 2.2 d.

2.2.2. Associative mechanism (A):

An intermediate of increased coordination number is formed because formation of the bond between the entering group and the metal, *M-Y*, occurs simultaneously with the breaking of the bond to the leaving group, *M-X*. The mechanism is similar to SN_2 reactions. Given that bond formation is the rate determining step, the rate of reaction is dependent on the entering group.[12-15] The energy reaction profile is shown in figure 2.2 a.

2.2.3. Interchange Mechanism (I):

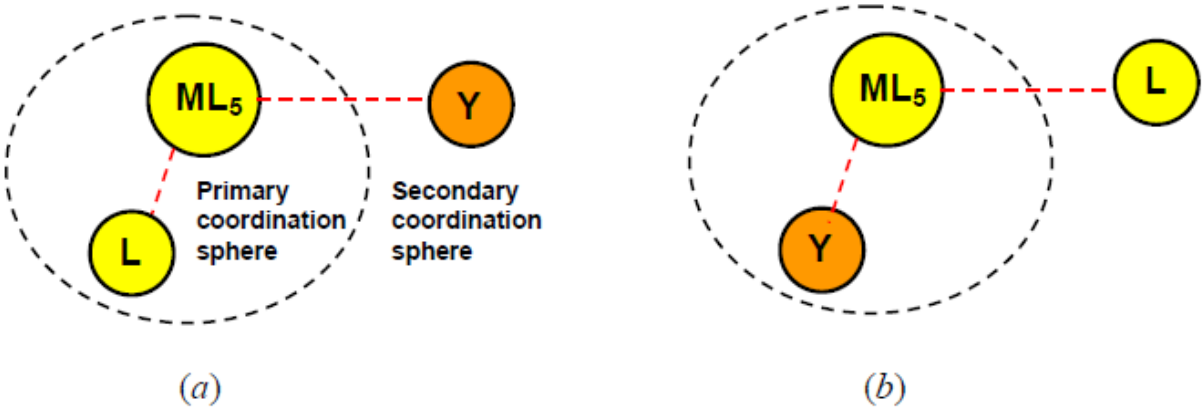
Concerns reactions where bond breaking between the metal and the leaving group and bond forming between the metal and entering group proceed simultaneously which is why no distinguishable intermediate is detected because of the rapidly exchanging activated complex. The interchange mechanisms can be further sub-divided into two groups based on which of the two mechanisms (**D** or **A**) is more favoured by the interchange transition state;[1,7,9]

2.2.3.1. Dissociative activated interchange mechanism (I_D):

Involves transition state that constitutes a very weak bond between the metal centre and the entering group because the leaving group is in the primary coordination sphere and the entering group is bound to the metal centre from the secondary coordination sphere (figure 2.1 a).[12,15] The entering group has a minor effect on the reaction rate but the reaction is more sensitive to the nature of the leaving group i.e. bond breaking is more important than bond formation.

2.2.3.2. Associatively activated interchange mechanism (I_A):

Its transition state consists of a weak bond between the metal centre and the leaving group. The rate is more sensitive to the changes in the entering group because it's in the primary coordination sphere and the leaving group is in the secondary coordination sphere (figure 2.1 b). Bond formation is superior to bond breaking. Most substitution reactions proceed by the associatively activated mechanism[7,9] as illustrated by figure 2.1



Where Y = *entering group*, L = *leaving group and* Y = *entering group*

Figure 2.1 Diagrams to illustrate a (*a*) dissociatively activated and (*b*) associatively activated intimate mechanism.[7,9]

A summarised energy profile diagram showing the different modes of substitution is presented in figure 2.2

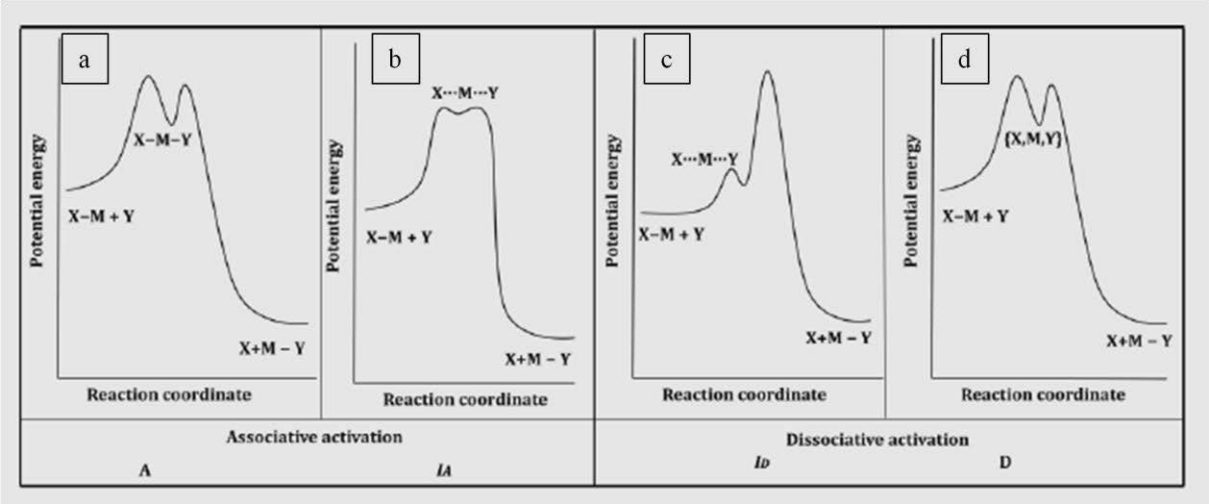


Figure 2.2 Gibbs free energy diagrams showing **D**, **A**, and **I** mechanisms.[9]

2.3. Substitution reactions of the square planar complexes

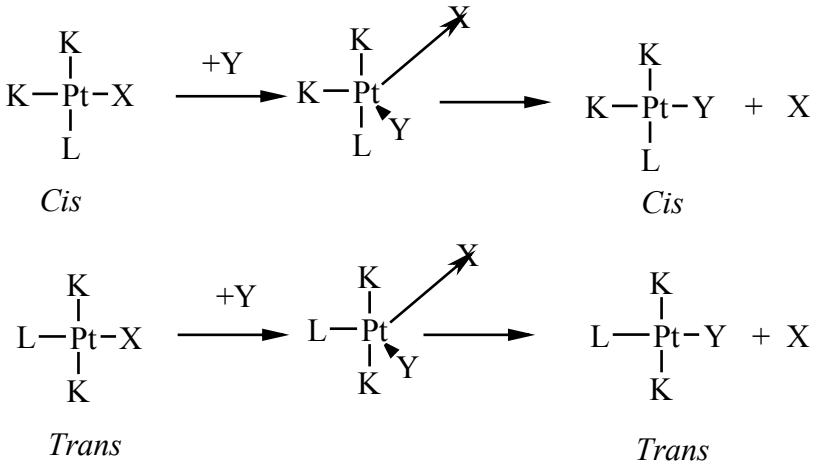
Square planar complexes are metal complexes where the metal ion contains eight electrons in the *d*-orbital that include Au(III), Ni(II), Ir(I), Pt(II), Rh(I) and Pd(II) which are invariably spin paired.[16,17] Square planar Pt(II) complexes are the most studied because platinum is easily available and has moderate reactivity allowing study by conventional sampling techniques.[18] The bias towards the Pt(II) complexes was renewed and sustained after the discovery of antitumor activity of cisplatin.[17] The rest of the square planar complexes *viz.* Ir(I) and Rh(I) have too rapid substitution reactions while Pd(II) is about five times more reactive than Pt(II) analogues,[19] Au(III)[20,21] complexes also show substitution by associative mechanism.

Since substitution reactions of all square planar complexes are similar, the reaction behaviour of Pt(II) complexes is similar to that of the other square planar complexes. Substitution reactions of square planar complexes proceed readily via the associative mechanism because *d*-block elements are stable with eighteen-electron valence shell and since four coordinate d^8 metal complexes have sixteen-electron valence shells, the five coordinate transition state is energetically more feasible as it leads to stable eighteen-electron system.[1] This is confirmed by voluminous data in literature on kinetic and thermodynamic studies of Pt(II) complexes.[7,10]

Based on steric and electronic reasons, the reactions in these systems would proceed most readily by an increase in the coordination number after inclusion of the entering ligand. The metal is open to attack above and below the plane, as there is no ligand perpendicular to the plane to obstruct it. Further, these low spin d^8 systems have a vacant p_z orbital of relatively low energy to accommodate the pair of electrons donated by the entering ligand.[21,22]

Reactions of *cis*- and *trans*-PtK_2LX with Y to yield PtK_2LY as shown in scheme 2.1 have been studied and reveal that the *cis* and *trans* conformations yield *cis* and *trans* products respectively.[22] The retention of configuration originates from a mechanism with precise stereo-specificity which excludes the dissociative mechanism where the three coordinated species assume a nearly regular planar structure with angles nearly 120° with equal chance to form the *cis* or *trans* isomer irrespective of whether Y enters PtK_2 LX adjacent to L or

opposite to L as illustrated by scheme 2.3. Stereo-specific displacement best assumes a nucleophilic attack via a trigonal bi-pyramidal intermediate illustrated in scheme 2.1



Where, Y = nucleophile, X = leaving group and K and L= non-labile ligands

Scheme 2.1 Stereo-specific substitution reactions of square planar complexes.

The observation illustrated by scheme 2.1 is evidence that substitution reactions of square planar complexes involve a bimolecular displacement mechanism although studies have revealed some dissociative character in square planar complexes.[23-26]

2.3.1 Mechanism of reaction of square planar complexes

Reactions of square planar complexes are best described in terms of bimolecular displacement mechanism.[22] It is important to note that kinetic studies are carried out in solvents, for the reactions represented by equation 2.4.[5,22,27]

$$[ML_3X] + Y \rightleftharpoons [ML_3Y] + X \qquad (2.4)$$

Where, M = metal ion, L = non-labile ligand, X = leaving group and Y = the nucleophile.

The rate law can be described as,

$$Rate = k_1 + k_2[ML_3X][Y] \qquad (2.5)$$

k_1 and k_2 are 1st and 2nd order rate constants respectively.

Applying pseudo-first-order conditions with at least ten-fold excess of nucleophile (Y), the experimental first-order rate constant ($k_{obs.}$) and the rate constant of the respective complex relate according to equation 2.6 known as the typical rate law for square planar complexes.

$$k_{obs} = k_1 + k_2[Y] \qquad (2.6)$$

A plot of k_{obs} against *[Y]* is linear with the slope equal to k_2 and the intercept equal to k_1 as illustrate by the sample plot in figure 2.3 where [Nu] represents [*Y*] which is concentration of L- methionine and glutathione nucleophiles.

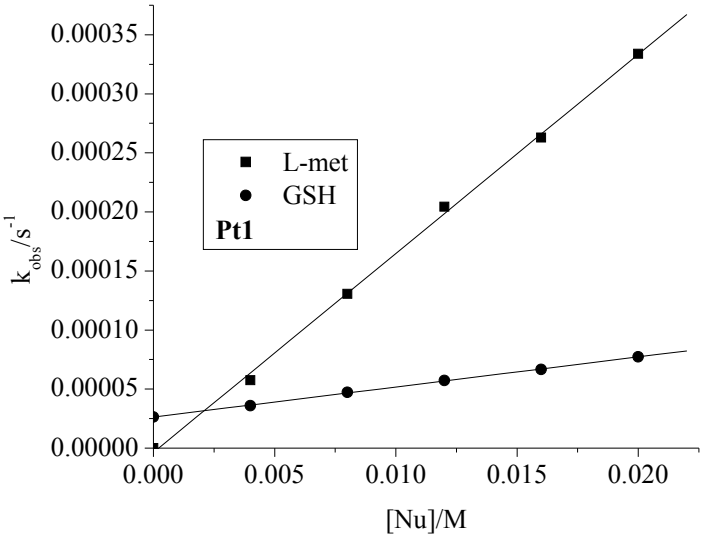
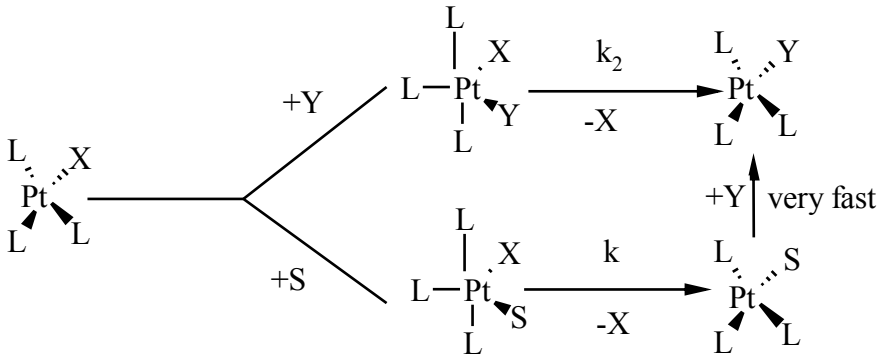


Figure 2.3 Plots of k_{obs} verses [Nu] for the reaction of **Pt1** with L-methionine and glutathione nucleophiles done in this thesis.[28]

Values of k_1 will normally be constant for different nucleophiles reacting with same metal complex, but k_2 values vary with nature of the entering nucleophile, Y. A positive intercept may not necessarily be attributed to k_1 but might represent the rate constant for the reverse reaction as shown in equation 2.4.[29,30] Coordinating solvents[19] commonly used like methanol or water usually present in large excess may be responsible for the k_1 term (solvosis pathway) if the reverse reaction is negligible.[8,10] Slow displacement of *X* by solvent is represented by k_1, but solvent is rapidly displaced by nucleophile, *Y* thus k_2 stands for direct displacement of *X* by *Y* as illustrated by scheme 2.2.



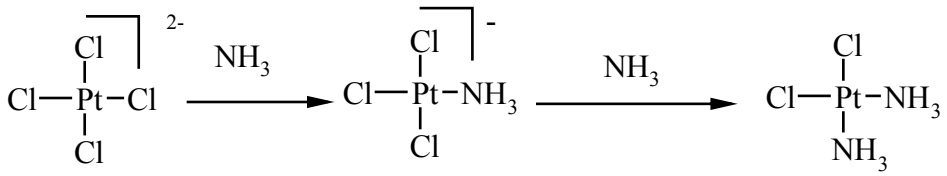
Scheme 2.2 Reaction pathways of Pt(II) complexes illustrating both direct nucleophilic attack and the solvolytic pathway.[29]

2.4 Factors affecting the rate of substitution reactions

The rate at which substitution reactions of square planar complexes proceeds is dependent on a number of factors.[21,31,32]

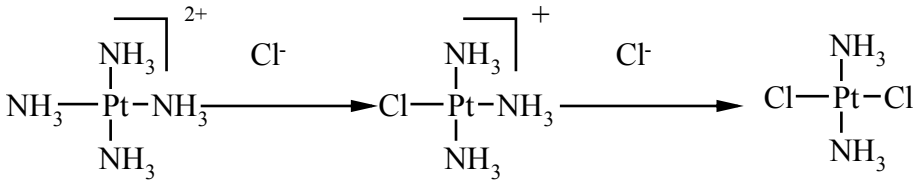
2.4.1 Effect of the non-labile ligand

Reactions of square planar complexes follow the associative pathway involving a trigonal bi-pyramidal transition state intermediate, in which the entering group, the leaving group and the trans-ligand are in the trigonal plane while the other two cis-ligands are out-of-plane.[22,32] The *trans*-ligand is able to exert a significant effect on the leaving group and consequently on the rate of substitution and this effect is called the *trans*-effect. The ligands *cis*- to the leaving group also exert an effect on the substitution reaction though less significant. This effect initially observed by Alfred Werner[33,34] was applied in 1926 when Chernayev and coworkers[35] initiated the idea of *trans*-effect to explain reactions of Pt(II) complexes. They reported that negatively charged ligands like chloride ions have higher labilizing effect on leaving groups *trans* to them than a leaving group *cis* to it, and overall the labilizing effect is greater than exhibited by a non π-bonding neutral ligand like ammonia. The *trans* effect is illustrated by substitution reactions of Pt(II) complexes in equations 2.7-2.14 . The phenomenon of *trans* effect has been applied in the synthesis of desired Pt(II) complex isomers.



(2.7)

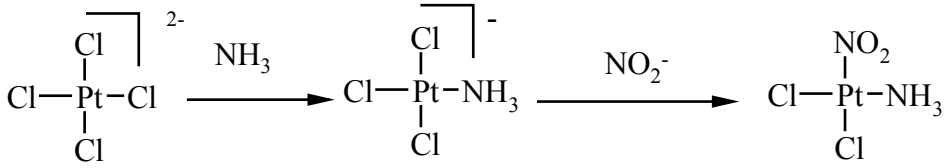
cis



(2.8)

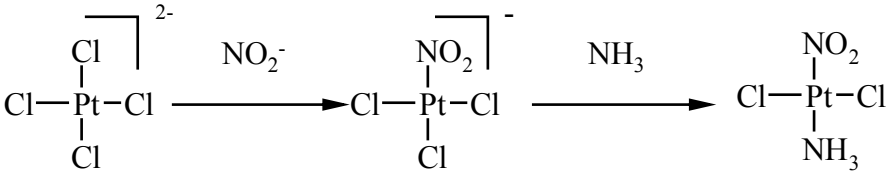
trans

In equation 2.7, the *cis* isomer of $Pt(NH_3)_2Cl_2$ is synthesised successfully due to the chloride ion having a larger *trans* directing influence than ammonia enabling the second ammonia to coordinate to the *cis* position confirming that the least reactive chloride group in $PtNH_3Cl_3$ is that opposite the ammonia group. In the second stage of the reaction represented by equation 2.8, the chloride ion replaces the most labile ammonia in $Pt(NH_3)_3Cl^+$ which is apparently the one opposite the chloride ion. From the observations in equations 2.7 and 2.8, the synthesis of *cis*- and *trans*- isomers of $[Pt(NH3)(NO_2)Cl_2]$[36] can be achieved by reversing the order of the incoming nucleophiles.



(2.9)

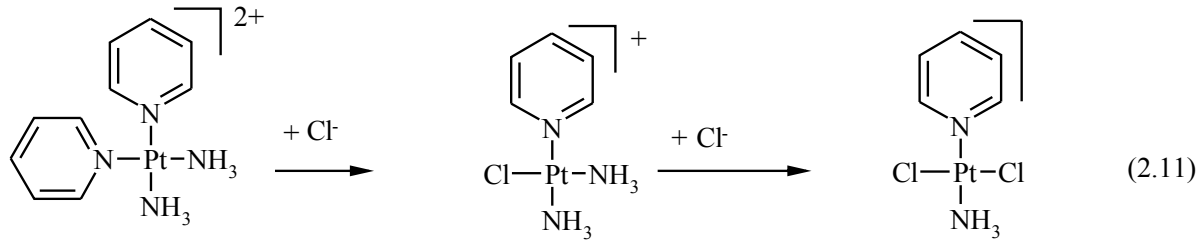
cis



(2.10)

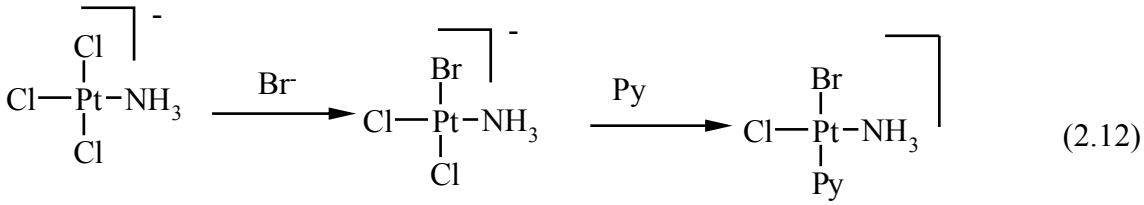
trans

Equation 2.10 shows that the *trans*-directing effect of the nitrite group is superior to that of chloride because the incoming ammonia molecule coordinates *trans* to the nitrite. Further examples to emphasize the idea of *trans*-effect appear in equations 2.11- 2.14.[22]

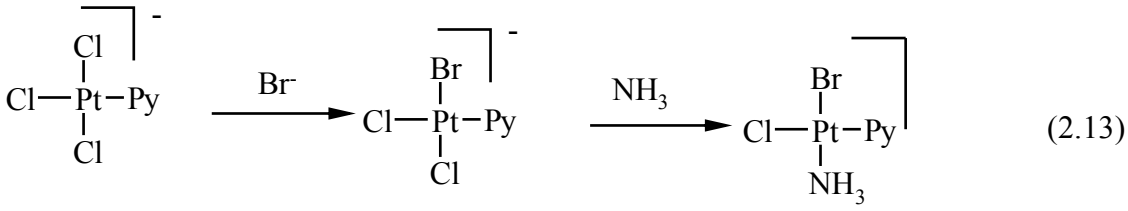


(2.11)

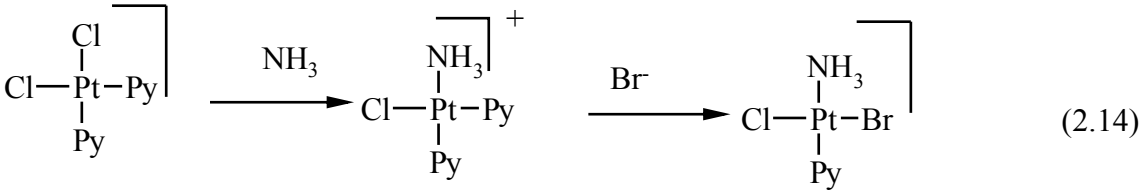
First chloride ion entered the complex and then labilised the ammonia ligand *trans* to it causing the second chloride ion to substitute the ammonia group showing that the chloride ion has a greater *trans*-labilizing effect than either pyridine or ammonia. Isomers of $[Pt(Py)(NH_3)(Cl)(Br)]$[22] were synthesised as shown by the subsequent equations.



(2.12)



(2.13)



(2.14)

The reactions already illustrated and many others indicated that strength of the metal-leaving group bond and the labilizing influence of the *trans*-group play important roles in substitution reactions. Ligands can be arranged in order of decreasing labizing strength as in the series;[7]

CO, CN", $C2H_4$ > PR_3, H > CH_3 > $SC(NH_2)_2$ > C_6H_5, $N0_2$, I , SCN > Br , CI > py, NH_3, OH , H_20

Effects at the ground state and transition state both play a role in understanding the *trans* effect and its role in increasing the rate of reactions. It is interesting to note that kinetically,

this effect can be large to a factor of 10^6 or higher in rates between complexes containing good *trans*-labilizing ligand to those containing weak *trans* labilizing ligand. Arguably, it is the most dramatic on the substitution reactions rates in metal complexes.[22] Basolo and Pearson[22] defined the *trans*-effect as the "effect of a coordinated group upon the rate of substitution reactions of ligands opposite to it in a metal complex". Possibly the best explanation takes to account both the σ-donating and π-accepting capabilities of the ligand; Strong σ-donation from a ligand, results in a weaker *trans*-bond (high ground state *trans*-influence), increasing the rate of substitution.

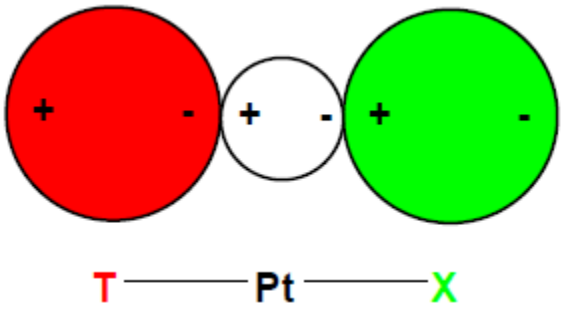
When charge is delocalized in the transition state, the species is stabilized which increases the rate. Strong π-acceptors typically facilitate this kind of stabilization leading to high *trans*-effects.[37,38] *Trans*-effect gives information about *trans*-ligand on the ground state and transition state. The effect of *trans*-ligand to ground state properties like bond lengths is called *trans*-influence while *trans*-effect is the influence of the *trans*-ligand to the transition state complex[9,39] A good π-accepter stabilises the five coordinate transition state because it accepts electrons donated from the filled π-orbitals of the metal (d_{xy}, d_{zy}, d_{yz}) to its empty *p*-orbitals or the *p*-orbitals of the leaving group.[22]

The metal-ligand bond is strengthened by the back donation if the ligand is a good π-acceptor and as a result the increase in the electron density due to increased coordination number on the metal centre in the transition state is reduced effectively lowering activation energy while increasing the reaction rate. σ-donation is a ground state stabilization of metal-leaving group bond since in the transition state, the leaving group and *trans* ligand don't directly share the same *p*-orbitals. A number of studies have been keen to account for *trans effect*[35,40,41] with the π-bonding and the polarisation theories being the most common.[42]

2.4.1.1 The polarization theory

Postulated by Grinberg[43], the polarization theory explains that the primary charge on the Pt(II) induces a dipole in the *trans*-ligand, which then induces a dipole in the metal as shown in figure 2.4. The dipole induced in the metal then repels the negative charge in the leaving group causing the metal-leaving group bond to stretch and weaken. There is indeed a link between the *trans*-influence of the *trans*-ligand and its polarisability e.g. $H^- \sim I^- > Cl^-$.[22] Objections to the electrostatic theory argue that the induced dipole on Pt(II) should depend

inversely to the distance from the *trans*-ligand which should depend on the net charge of the ligand more strongly than on its induced dipole moment.[22] On the basis of this contrary view, Cl^- would have greater *trans*-effect than I^- which is not true. This is however clarified by taking into account covalent bonding because highly polarizing ligands will also form more covalent bonds to Pt(II).



Where, T = *trans*-ligand and X = leaving group

Figure 2.4 Induced dipole moments along T-Pt-X[22]

2.4.1.2 The π-bonding theory

Pauling[44] first introduced the idea of π-bonding to account for the short Ni-C bond distance within the $Ni(C0)_4$ complex and the large stability of the cyanide complexes of transition metals as compared to non-transition metals. The existence and significance of such double bonding are now generally recognized and involves ligands capable of forming π-bonds like C_2H_4, CO and PR_3 due to their strong π-acceptor abilities making them strong *trans*-directors.[22] A σ-bond is formed between the ligand and metal by the donation of a pair of electrons from the ligand to the metal centre and the π-bond by the overlap of a filled *d*-orbital of the platinum centre and a vacant orbital of the ligand. In the ground state, it would appear that the removal of electrons from the metal by the π-bonding actually strengthens instead of weakening the metal leaving group bond but Chatt *et al.*[45]and Orgel[46,47] proposed π-bonding stabilization of the trigonal bi-pyramidal intermediate in the transition state to explain the *trans* effect. Chatt *et al.*[45] emphasised that decrease in electron density from Pt(II) centre in the transition state by π-bonding of the *trans*-ligand enhances addition of incoming group as activation energy is lowered. π-bonding according to Orgell[46,47] reduces the electron density on Pt(II) along the metal-leaving group and metal-incoming group directions which leads to a retention of configuration which is reffered to as the π-*trans* effect[22] as illustrated in figure 2.5.

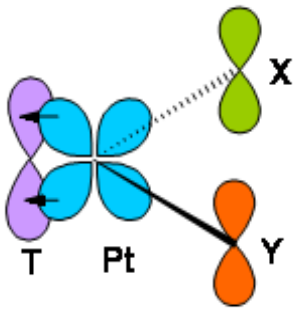


Figure 2.5 π-back donation of charge from the filled *d* orbitals of Pt(II) to the empty orbitals of the *trans* ligand.[22]

2.4.2 The Molecular orbital theory

The molecular orbital theory best explains *trans*-effect by considering both the σ-donation and π-accepting capacities of the *trans*-ligand.[22,48] Consider a simple molecular orbital (MO) diagram of $[PtCl_4]^{2-}$ as shown in figure 2.6.

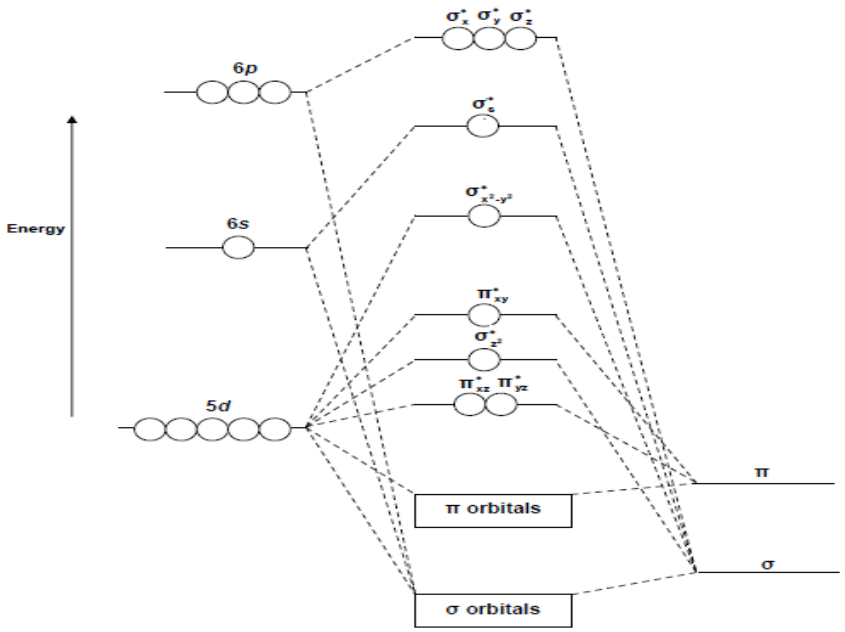
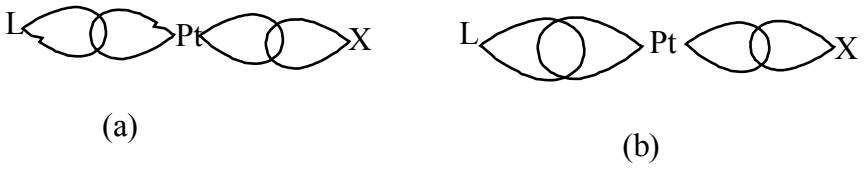


Figure 2.6 A simple MO diagram of $[PtCl_4]$ [2,22, 49]

The σ-bonding orbitals are the most stable followed by the π-bonding molecular orbitals, all mainly located on the four chlorines.[22,49] Next orbitals relatively stable are anti-bonding orbitals, $\pi^*_{xz}, \pi^*_{yz}, \pi^*_{z^2}, \sigma^*_{z^2}$ and π^*_{xy} while $\sigma^*_{x^2-y^2}$ are relatively unstable from the *5d* atomic orbitals of Pt(II).[22, 49] Anti-bonding σ orbitals $\sigma^*_s, \sigma^*_x, \sigma^*_y$ are at high energy.[49] Orbitals π^*_{xz}, π^*_{yz} and π^*_{xy} are the only ones with the correct orientation for π-bonding in square planar complexes.[23] On formation of the trigonal bipyrimidal intermediate after addition of *Y* (equation 2.4) , π^*_{xz} , π^*_{yz}, π^*_{xy} and $\pi^*_{x^2-y^2}$ are now in the strategic orientation for π interactions and are shared in π-bonding with the ligands, *L*, *X* and *Y* (equation 2.4) in the trigonal plane.[22]

The *trans*-ligand can thus greatly stabilize the transition state if it is capable of bonding to the π*-orbitals and delocalize the electronic charge to lower the energy. The transition state is stabilized as there are more filled π-orbitals than in the ground state the reason why a good *trans* π-acceptor ligand will lower the activation energy of the substitution reaction. According to Langford and Gray[11] in the ground state of a square planar complex, there is only one *p*-orbital p_x used to bond L–Pt–X, addition of the entering group, causes X to move out of the *x*-axis into the trigonal plane which has two *p*-orbitals, p_x and p_z increasing the number of orbitals available for bonding.

In the ground state there were only one *p*-orbital bonding two ligands but in the transition state there are two orbitals bonding three ligands, leading to increased stability of the transition state which means that good σ-bonding ligands which can donate into the extra *p*-orbitals can stabilize the σ-structure in the transition state.[22] The effect is known as the σ-*trans* effect.[11] Ground state stability of a complex can be affected by σ-bonding in that at ground state, the *trans*-ligand and the leaving group share the same p_x orbital as shown in figure 2.7, with a strong σ-donor *trans*-ligand, such as H^- and CH_3^- more electron density will be donated to the shared *p*-orbital strengthening the L–Pt bond and weakening the Pt–X bond which increases the rate of the reaction.[22]



(a) (b)

Figure 2.7 Representation of L-Pt-X bonding using σ_x MO; in (a) the strength of the σ-bonds are almost equal but stronger for the stronger σ-donor L in (b)

2.4.3 Effect of incoming group

The associative mechanism of reaction is sensitive to the nature of incoming nucleophile such that the rate of reaction is a manifestation of the reactivity (nucleophilicity) of the respective nucleophile.[14] Considering a standard reaction 2.15;

$$trans-\left[Pt(py_2)Cl_2\right] + L^n \rightarrow trans-\left[Pt(Py_2)(L)Cl\right]^{n+1} + Cl^{-1} \qquad (2.15)$$

The rate of the reaction will be given by equation 2.16

$$Rate = k_S\left[Pt(py_2)Cl_2\right] + k_L[L^-][Pt(py_2)(L)Cl] \qquad (2.16)$$

Where, py = pyridyl group, L = entering nucleophile, k_L = rate constant for the entering nucleophile and k_S = rate constant for attack by solvent on the complex

The nucleophilicity of a nucleophile is given by equation 2.17,

$$\eta_{pt} = \log\left(\frac{k_L}{k_S}\right) \qquad (2.17)$$

Most reactive nucleophiles are "soft" (species that are large, have low charge and are strongly polarisable) which accounts for sulphur being a better donor than oxygen.[14,33,34,50,51] For Pt(II) complexes, plots of $\log k_L$ verses η_{pt} were observed to be linear according to equation 2.18 which gives the linear free energy relationship.[22]

$$\log k_L = s.\eta_{pt} + \log k_S \qquad (2.18)$$

Where k_L is *second order rate constant for the nucleophile, L,* s is *nucleophilic discrimination factor (slope) and log* k_s *is the intrinsic reactivity of the complex (y-intercept)*

The nucleophilic discrimination factor is specific for a complex and measures the sensitivity of the metal centre to the nucleophilicity of the entering nucleophile.[22] A large value of the slope means the reaction is more sensitive to the changes in the nucleophilic nature. The y-intercept gives the rate constant for the weakest nucleophile measured in a solvent; a low value of k_S signifies that the complex is more sensitive to changes in the nucleophile. Ligands with capacity to form dative π-bonding with Pt(II) in the transition state exhibit high values of s (low values of k_S) which allows addition of electrons from the nucleophiles to the metal centre facilitating the entering group to participate in the transition state.[22] There are exceptions from the general trend illustrated by table 2.1 for certain nucleophiles like NO_2^-, $SeCN^-$ among others because of other factors including effective charge of the metal centre and shape and size of nucleophile.[14]

2.4.4 Nature of the *cis* Ligand

A ligand *cis* to the leaving group has generally less electronic effect on the reaction than when in the *trans*-position; however it will be more sensitive to steric hindrance in the *cis*-position.[51(b)] Steric hindrance magnifies when the tri-gonal bi-pyramidal complex is formed in the transition state because the *trans*-ligand is in the equatorial plane 120° from the incoming and leaving groups while the axial *cis*-ligand is separated from the groups by only 90° which lowers the rate of substitution the reaction. It has been shown that *trans*-activating ligand is a poor *cis*-activator.[22,52,53] There is contrary data however on this *cis* and *trans*-behaviour as illustrated by the reaction in equation 2.19,[54]

$$cis-\left[Pt\left(PEt_3\right)_2 LCl\right]+py \rightarrow cis-\left[Pt\left(PEt_3\right)_2 Lpy\right]+Cl^- \qquad (2.19)$$

The effect of the ligands, L; CH_3^-, $C_6H_5^-$ and Cl^- , on the reaction and order is same for *cis* and *trans*-complexes as shown in table 2.2,[54]

Table 2.1 Effect of *cis* ligand, L, on the rate of reaction in equation 2.19

L	$k_1(10^2)/s^{-1}$
Cl^-	1.7
$C_6H_5^-$	3.8
CH_3^-	6.0

Observations indicate that varying basicity of amines in the *cis* position affects reactivity significantly with the least reactive amine forming the most reactive complex to be substituted. When the *trans*-activator is weak, the *cis*-activator may have greater influence on the rate.[22,55] Generally, *cis*-effect is small and the order variable unless steric factors play a role.[9,22]

2.4.5 Nature of the leaving group

Effect of a leaving group is not very easy to account for because it's very closely connected with the nature of the incoming nucleophile and the *trans*-ligand. If a reaction is dissociative, the bond between the leaving ligand and the metal complex breaks in the transition state consequently there is a large dependence on the nature of the leaving group.[14] But for an associative reaction, effect of the leaving group depends on the extent to which bond breaking occurs in the transition state which is variable.[14] Effect of the leaving group has been investigated for the reaction shown in the equation 2.20, [13, 56]

$$[Pt(dien)X]^+ + py \rightarrow [Pt(dien)py] + X^- \qquad (2.20)$$

The rate of substitution of X follows the order;[14]

$NO_3^- > H_2O > Cl^- > Br^- > I^- > N^{3-} > SCN^- > NO_2^- > CN^-$

Leaving groups exert considerable influence to the rates of substitution which indicate that even associative modes of substitution encounter considerable bond breaking between metal and leaving group in the transition state which depends on the type of the reaction. The bond breaking doesn't automatically lead to dissociative process but only requires bond breaking to make a comparable contribution to bond formation between metal and incoming group.[22] Leaving groups high in the *trans*-effect series (strongly binding) are hard to replace consequently lead to a slower rate of substitution.

2.4.6 Steric effect

Steric hindrance could be caused by either bulky incoming ligand or bulky spectator ligand. Its worthy noting the fact that the transition state in an associative mode of substitution produces species with increased coordination number hence increased steric hindrance. Bulky non-labile ligands in the *cis* position significantly slow down the rate of reaction.

2.4.7 Effect of the solvent

Solvents may play a key role on the rate of a substitution reaction in square planar complexes with the effect of solvent increasing with increase in the coordination ability of the solvent.[22] In the case where the solvent coordinates, the rate law will include a reaction path attributed to solvent attack. The effect of solvent has been determined by investigating the chloride exchange reaction represented by equation 2.21 whose data is shown in table 2.2,[9,13]

$$trans-\left[Pt(py)_2Cl_2\right]+{}^{36}Cl \rightarrow trans-\left[Pt(py)_2Cl\left({}^{36}Cl\right)\right]+Cl^- \qquad (2.21)$$

Table 2.2 The effect of solvent on the chloride exchange reactions of equation 2.21.[13]

Coordinating solvents	k **x10^{-5} s^{-1}**	**Weakly coordinating solvents**	$K\ M^{-1}s^{-1}$
DMSO	380	CCl_4	10000
H_2O	3.5	C_6H_6	100
CH_3NO_2	3.2	*i*-BuOH	0.1
EtOH	1.4	EtOAc	0.01
PrOH	0.42	$(CH_3)CO$	0.01
		DMF	0.001

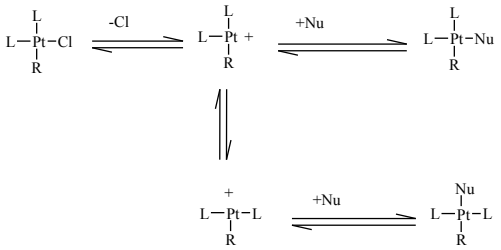
First column consists of solvents with good coordinating capacity where the rates depend on the nucleophilicity of the solvent ($k_S >> k_{Cl}[^{36}Cl^-]$). In the third column the solvents have low coordination capacity hence reactions proceed only by attack by incoming nucleophile ($k_{Cl}[^{36}Cl^-] >> k_S$). In the non-polar solvents, the rates are highest probably because the chloride is not solvated making it more reactive although in general the extent of solvation is uncertain.[22] For coordinating solvents, k_2 values go in the order,[22]

DMSO > CH_3NO_2 ~ H_2O > ROH

The significance of the order for coordinating solvents is that Pt-solvent bond formation is more important than bond breaking in the transition state because if solvating the leaving group was the sole role of the solvent then water will be superior to DMSO in solvent effects, however, DMSO is a more efficient nucleophile because sulphur is a better nucleophile than oxygen.[57,58]

2.5 Evidence of the dissociative pathway for the substitution reactions of square planar Pt(II) complexes.

Though rare, the dissociative mode of substitution in square planar complexes may occur if the metal complex is sterically hindered preventing axial approach by nucleophile, the nucleophile is weak so that the solvotic pathway is dominant or there is a sufficiently strong *trans* σ-donor which weakens the metal-leaving group bond enhancing bond breaking.[25] Complexes with strong σ-donor atoms like sulphur, carbon or phosphorus in the *cis*-position are observed to undergo the dissociative pathway during substitution reactions.[24-26,59] The strong σ-donor atoms stabilize the 14-electron three coordinate intermediate. Complexes whose nature is *cis*-$[Pt(Me)_2R_2]$ or *cis*-$[Pt(ph)_2R_2]$ (where R=DMSO or thioether) were found to exhibit dissociative mode of substitution. However, ligands with strong π-acceptor capacities like CO accept electrons from the metal centre making it more electrophilic facilitating the associative pathway.[59] One hallmark of the dissociative mechanism of substitution is its non-stereo selectivity possibly because the T-shaped 14 electron three coordinate intermediate species has long life enough to allow intermolecular rearrangements of '*cis*-like' form to a *trans-like'* form so that addition of nucleophile results in isomeration to give non-stereo specific products as shown in scheme 2.3. These mechanisms have small solvent effects.[24] With weak nucleophiles, the solvolytic pathway predorminates a shortcoming for the dissociative mechanism of substitution.



Scheme 2.3 Non-stereospecific substitution in dissociative mechanism of a Pt(II) square planar complex as a result of intermolecular rearrangement.

2.6 References

1. M. L. Tobe & J. Burgess, *Inorganic Reaction Mechanisms,* Addison Wesley Longman Ltd., Essex, 1999, p30-43, 70,112,73-90, 103-105
2. L. Arnaut, S. Formosinho and H. Burrows, *Chemical Kinetics From Molecular Structure to Chemical Reactivity*, Elsevier, New York, 2007, p. 273-294.
3. C.K. Ingold, *Structure and Mechanism in Organic Chemistry,* 2n Ed., Cornell University Press, Ithaca, NY, 1969, p 241.
4. C.K. Ingold, *Structure and Mechanism in Organic Chemistry,* G. Bell and Sons, Ltd., London, 1953, p205
5. S. Asperger, *Chemical Kinetics and Inorganic Reaction Mechanisms*, 2nd Ed., Kluwer Academic/Plenium Publishers, NY, 2003 p. 105-106, 108-110,140-153.
6. C.H. Langford, & H.B.Gray, *Ligand Substitution Processes,* Benjamin Inc., NY, 1965.
7. R.B. Jordan, *Reaction Mechanisms of Inorganic and Organometallic Systems,* Oxford University Press, 1991, p 23-30, 47-54, 58-60
8. (a) R. A. Henderson, *The mechanisms of reactions at Transition Metal Sites*, Oxford University Press, Oxford, 1993, p. 2-21 (b) G. L. Miessler, D. A. Tarr, *Inorganic Chemistry*; 3rd ed.; Pearson Education Internatioal: Singapore, 2004, 415- 426
9. J. D. Atwood, *Inorganic and Organometallic Reaction Mechanisms*, 2nd Ed., Wiley-VCH Inc., NY, 1997, p. 32-34, 43-61
10. R. G. Wilkins, *Kinetics and mechanisms of Reactions of Transition Metal Complexes*, 2nd Ed., VCH, Weinhelm, 1991, p. 199-201, 232-238
11. C. H. Langford, H.B. Gray, *Ligand Substitution Processes*, 1966, W.A. Benjamin, Inc., New York, p. 18-48.
12. P. Atkins, T. Overton, J. Rourke, M. Weller and F. Armstrong, *Shriver & Atkins Inorganic Chemistry 4th edition*, 2006, Oxford University Press, New York.
13. F. Basolo, H. B. Gray and R.G. Pearson, *Dalton Trans*., 1960, **82***,* 4200, 787
14. M. L. Tobe, *Inorganic Reaction Mechanisms Studies in modern Chemistry*, Nelson London, 1972, p. 199-201, 221, 232, 242.
15. G. Wulfsberg, *Inorganic chemistry*, 2000, university Science Books, USA.
16 . D. T. Richens, *Chem. Rev*., 2005, **105**, 1961
17. (a) B. Rosenberg, L. van camp, J. E. Trosko and H. V. mansour, *Nature***,** 1969, **222**, 385 (b) J. Reedijik, *PNAS*. **2003**, *100***,** 3611.

18. R. K. Murmann, R. T. M. Fraser and J. Bauman, *Mechanics of Inorganic reactions Reactions*, *Am. Chem. Soc*., Washington, D.C, 1965, p. 20-23, 81-97.
19. A. Peloso, *Coord. Chem. Rev*., 1973, **10**, 123
20. R. J. Cross, *Adv. Inorg. Chem*., 1989, **34**, 219.
21. L. Cattalini, *Progr. Inorg. Chem*., 1970, **13**, 263.
22. F. Basolo, & Pearson, R.J., *Mechanisms of Inorganic Reactions,* John Wiley & Sons., NY, 1967, p. 1,193-195, 351-356, 369-400
23. R. Romeo, *Comment Inorg. Chem*., 1990, **11**, 21
24. S. Lanza, D. Minniti, P. Moore, J. Sachinidis, R. Romeo and M. L. Tobe, *Inorg. Chem*., 1984, **23**, 4428
25. R. Romeo, L. Scolaro, M. R. Plutino, F. F. De Biani, G. Bottari and A. Romeo, *Inorg. Chim. Acta*, 2003, **350**, 143
26. M. R. Plutino, L. M. Scolaro, R. Romeo and A. Grassi, *Inorg. Chem*., 2000, **39**, 2712
27. U. Belluco, *coord. Chem. Rev***.,** 1966, **1**, 111.
28. D. Jaganyi, V. M. Munisamy, D. Reddy, *Wiley Interscience*, 2005
29. P. Haake, S. C. Chan and V. Jones, *Inorg. Chem*., 1970, **9**, 1925
30. J. K. Beattie, *Inorg. Chim Acta*., 1983,**76**, L69
31. D. Banerjie, F. Basolo and R. G. Pearson, *J. Am. Chem. Soc*., 1957, **79**, 4055.
32. (a) U. Belluco, L. Cattalini, F. Basolo, R. G. Pearson andA.Turko, *J. Am. Chem. Soc*., 1965, **87**, 241(b) J. Reedijik, *Eur.J.Inorg. Chem*., **2009**, 1303
33. R. J. Pearson, *J. Amer. Chem. Soc,* 1963, **85**, 3533.
34. R. J. Pearson, *J. Chem. Edit.,* 1987, **64**, 561.
35. I. I. Chernayev, *Ann. Inst. Platine* USSR, 1926, **4**, 243, 246,261
36. U. Belucco, *Organometallic and Coordination Chemistry of Platinum,* Academic press, London, 1974, pp 138-160.
37. N. Kuznik & O.F. Wendt, *J. Chem. Soc. Dalton Trans.,* 2002, 3074.
38. M. Plutino, S. Otto, A. Roodt, L.I. Elding, *Inorg. Chem.,* 1999, **38***,* 1233.
39. U. Belluco, *Organometallic Coordination Chemistry of Platinum*, Academic Press, London, 1974, p. 40-53, 138-160, 220-221
40. I. I. Chernayev, *Ann. Inst. Platine* USSR., 1928, **6**, 55.
41. Y. K. Syrkin, *Bull Acad Sci. U.S.S.R., Classe Sci. Chim*., 1948, 69.
42. D. Benson, *Mechanisms of inorganic reactions in solution*, McGraw-Hill, London, 1968, p. 19-31

43. A. A. Grinberg, *Acta Physicochim*, 1935, **3**, 573.
44. L. Pauling, *The nature of the Chemical Bond*, Ornel University Press, Ithaca, NY, 1960, p. 332
45. J. Chatt, L. A. Duncanson and L. M. Venanzi, *J. Chem. Soc*, 1955, 1955.
46. L. E. Orgel, *J. Inorg. Nucl. Chem*, 1956, **2**, 137.
47. J. Chatt, G. A. Gamlen and L. E Orgel, *J. Am. Chem. Soc*, 1959, 486.
48. S.S. Hupp, and G. Dahlgren, *Inorg. Chem*., 1976, **15**, 2349
49. C. W. Schwietert and J. P. McCue, *Coord. Chem. Rev*. 1999, **184**, 89.
50. F. A. Cotton, G. Wilkinson and P. L. Gaus, *Basic Inorganic Chemistry* 3rd edition, John Wiley & Sons, New York, 1995, pgs 228-229.
51. (a) R. G. Pearson, *J. Chem.Edu*., 1968, **45**, 643. (b) D. Jaganyi, D. Reddy *Dalton trans.,* 2008, 6724
52. A. A. Grinberg, *J. Inorg. Chem*. (USSR), 1959, 683
53. I. B. Bersuker, *J. Struct. Chem*., 1963, **4**, 419
54. F. Basolo, J. Chatt, H. B. Gray, R. G. Pearson and B. L. Shaw, *J. Chem. Soc*, 1961, 2207
55. M. A. Tucker, C. B. Colvin and Jr. D. S. Martin, *Inorg. Chem*., 1964, **3**, 1373
56. H. G. Gray and R. J. Olcott, *Inorg Chem*, 1962, **1,** 481.
57. F. A. Cotton, and R. Francis, *J. Am. Chem. Soc*., 1960, **82**, 2986
58. D. W. Meek, D. K. Straub and R. S. Drago, *ibid.,* 1960, **82**, 6013
59. R. Romeo, A. Grassi and L. M. Scolaro, *Inorg. Chem*., 1992, **31**, 4383.

Table of Contents

List of abbreviations and symbols ..... *i*

List of figures ..... *ii*

Chapter 3 Kinetic theory and associated techniques 1

3.1 Introduction to the kinetic theory 1

3.1.1 Concentration 1

3.1.2 Solvent Properties 2

3.1.3 Intensity of absorbed radiation 2

3.1.4 Physical conditions 2

3.2 Rate laws 2

3.3 Integrated rate laws 3

3.3.1 Irreversible first-order reactions 3

3.3.2 Reversible first-order reactions 5

3.3.3 Consecutive first-order reactions 7

3.3.4 Irreversible Second –Order reactions 10

3.3.5 Reversible Second-order Reactions 12

3.4 Activation parameters 14

3.4.1 The Arrhenius equation 15

3.4.2 The Transition-state Theory 15

3.5 Experimental kinetic techniques 18

3.5.1 UV/Visible Spectrophotometry 18

3.5.2 Flow methods 21

3.6 References 23

List of abbreviations and symbols

Å	Angstrom
A	Arrhenius pre-exponential factor ($M^{-1}s^{-1}$)
e	Exponential
E_a	Activation energy ($Jmol^{-1}$)
eq	Equilibrium
h	Plank's constant ($6.626 \times 10^{-34} Js^{-1}$)
IR	Infrared
K	Kelvin
k_1, k_{-1}	Rate constants
k_b	Boltzman's constant ($1.38 \times 10^{-23} JK^{-1}$)
k_{exp}	Experimental *pseudo* first-order rate constant
k_{obs}	Observed *pseudo* first-order rate constant
M	$moldm^{-3}$
$mgmL^{-1}$	Milligrams per millilitre
Nu	Nucleophile
R	Universal gas constant ($8.3145 JK^{-1}mol^{-1}$)
s	Nucleophilic discrimination factor
T	Absolute temperature (K) unless stated otherwise
t	Time
UV	Ultraviolet
VIS	Visible
$\Delta G^{\neq}$	Gibbs free energy of activation
$\Delta H^{\neq}$	Activation enthalpy
$\Delta S^{\neq}$	Activation entropy
ε	Molar absorptivity co-efficient

List of figures

Figure 3.1 A schematic diagram of a UV-Visible spectrophotometer. 19

Figure 3.2 UV-Visible spectrum for the reaction of Im (0.001 M) with Pt(eg) (5.0×10^{-5}) in methanol of ionic strength 0.01M (0.009M $LiCF_3SO_3$ and 0.001M LiCl) at 298K. 21

Figure 3.3 Schematic diagram of mechanistic action of stopped-flow apparatus.....22

Chapter 3

Kinetic theory and associated techniques

3.1 Introduction

The reaction rate can be defined as the amount of reactant converted into product per unit time or amount of product formed per unit time. The amount is expressed in terms of the concentrations of the *stoichiometric* reactants or products making it independent of the size of the sample but dependent on the molecular collisions. The study of reaction rates constitutes kinetics.[1] Kinetics is divided into physical kinetics and chemical kinetics where chemical kinetics deals with the rate of chemical reactions which covers a whole spectrum of reactions from those that proceed very fast to those which are exceedingly slow to the extent that they are unnoticed[2] and thermodynamics concerned with enthalpy and entropy among other quantities which depend only on initial and final states of a system. Chemical kinetics deals with how fast a chemical reaction occurs where measurements are made under dynamic conditions in which the concentrations of the reactants and products are changing as a function of time[3,4] which lead to the determination of the reaction rate.[5-8]

Kinetics not only explains a reaction and its parameters but also enlightens us on the factors that influence the rate of reactions. Data from chemical kinetics using a range of factors allows for the prediction of how fast a reaction would proceed under hypothetical conditions. Secondly the data provide some of the information needed to determine the mechanism of a reaction.[9] Kinetic methods allow many more chemical reactions to be applied for analytical purposes because it can make use of reactions that are too slow for thermodynamic studies. The factors that influence the rate of a reaction include those that can be controlled *viz.* temperature, concentration, pressure, available surface area, solvent properties and presence of catalysts plus other factors inherent to the process like identity of the chemical reagents or the set thermodynamic conditions which must all be taken into account to appreciate the kinetics of a given process.[10] The factors affecting the rate of reactions are briefly discussed in sub-sections 3.1.1-3.1.4.

3.1.1 Concentration

The higher the concentration of reagents the higher the number of reactant particles which increases the number of effective collisions increasing the rate of a reaction.

3.1.2 Solvent Properties

Solvents can directly affect a reaction by acting as a reactant or may form a solvent cage around the molecule consequently changing the kinetics of a reaction. Coordinating solvents slow down the rate with nucleophile as the solvent path predominates while weakly coordinating solvent have negligible effect on the reaction.

3.1.3 Intensity of absorbed radiation

For photosensitive reactions, exposure of a sample to white light will alter the rate at which the reaction proceeds. This could be due to the change in the nature of the reagents.

3.1.4 Physical conditions

Physical conditions including factors like temperature and pressure which are normally kept constant for a given kinetic measurement.

Change in the concentration of reactants or/and products with time is investigated in the study of kinetics. Since concentration cannot be measured directly, absorbance which is proportional to concentration is monitored during kinetic studies. This chapter presents a summary of the relevant rate laws and the experimental techniques applied in kinetic measurements.

3.2 Rate laws

Rate of a reaction is the change in the concentration of reactant or product as a function of time whose unit is mol $dm^{-3}s^{-1}$(Ms^{-1}).[11-13] Consider a chemical reaction represented by equation 3.1,

$$aA + bB \rightarrow cC + dD \qquad (3.1)$$

a, b, c and d represent the stoichiometry of the reaction and A, B, C *and* D *represent formulae of chemical compounds.*

The general rate law for a reaction is represented by equation 3.2,

$$Rate = \frac{-d[reac\tan t]}{dt} = \frac{d[product]}{dt} \qquad (3.2)$$

The negative sign in equation 3.2 shows that the concentration of the reactant reduces with time. With appropriate signs in the rate law, the rate itself is always a positive number. The rate law includes the concentration of all species that affect the rate.[14]

The rate law according to equation 3.2 if re-written to include reagents gives equation 3.3,

$$Rate = -\frac{1}{a}\frac{d[A]}{dt} = -\frac{1}{b}\frac{d[B]}{dt} = \frac{1}{c}\frac{d[C]}{dt} = \frac{1}{d}\frac{d[D]}{dt} \qquad (3.3)$$

In general the rate law may be written as;

$$Rate = -k\prod_i [A_i]^{\alpha_i}[X_j]^{\beta_j} \qquad (3.4)$$

A_i is *reactants, k* is *rate constant,* X_j is *other species such as catalysts that may affect the rate and* α *and* β are *rate orders with respect to reagents, A and, B respectively determined experimentally.*

The order of a reaction is defined as:[15]

$$Order \quad of \quad reaction = \sum_i \alpha_i \qquad (3.5)$$

While the unit for the rate of a reaction is mol $dm^{-3}s^{-1}$, the unit for the rate constant, *k*, depends on the reaction order.[11] The order of a reaction is not always related to the stiochiometry of the reaction hence it is determined experimentally.

3.3 Integrated rate laws

3.3.1 Irreversible first-order reactions

Most of the reactions fall under the category of first order or are studied under conditions that approximate first-order conditions. For a first-order reaction, the rate is directly proportional to a single reactant concentration thus the kinetics follow a rate law with the reaction order being unity.[16] The rate constant for the forward reaction is much greater than that for the reverse reaction. A first-order reaction can be simplified by the relation 3.6.

$$A \xrightarrow{k_1} B \qquad (3.6)$$

The rate law for the reaction represented by 3.6 will be given by equation 3.7.

$$Rate = \frac{-d[A]}{dt} = k_1[A]_t \tag{3.7}$$

Rearranging equation 3.7 forms equation 3.8.

$$\frac{-d[A]}{[A]_t} = k_1 dt \tag{3.8}$$

Integrating equation 3.8 from time $t = 0$ to $t = t$ during which concentration changes from $[A]_0$ to $[A]_t$ proceeds from equations 3.9 to 3.10.

$$\int_{[A]_0}^{[A]_t} \frac{d[A]}{[A]_t} = -k_1 \int_o^t dt \tag{3.9}$$

$$\ln \frac{[A]_t}{[A]_0} = -k_1 t \tag{3.10}$$

Equation 3.10 simplifies to equation 3.11.

$$\ln[A]_t = -kt + \ln[A]_0 \tag{3.11}$$

Equation 3.11 can be simplified further to equation 3.12.

$$[A]_t = [A]_0 e^{-kt} \tag{3.12}$$

$[A]_0$ *and* $[A]_t$ *are concentrations of A at time* t = 0 *and* t = t *respectively.*

From equation 3.10 which is consistent with the equation of a straight line $(y = mx + c)$, a plot of $\ln[A]_t$ verses *t* gives a straight line graph whose slope and intercept are equivalent to the rate constant, -*k*, and $\ln[A]_0$ respectively. Physical parameters proportional to concentration

viz. absorbance, pressure, conductivity or volume directly apply in the determination of the rate constant for first-order reactions.[10-12]

3.3.2 Reversible first-order reactions

A reaction that doesn't proceed to completion but establish equilibrium where some of the product formed is converted back into starting material is described as reversible (equation 3.13).[11,12]

$$A \underset{k_{-1}}{\overset{k_1}{\rightleftharpoons}} B \qquad (3.13)$$

Where, k_1 and k_{-1} are rate constants for the forward and reverse reactions respectively.

The rate law for this reaction is given by equation 3.14,

$$Rate = \frac{d[B]}{dt} = \frac{-d[A]}{dt} = k_1[A]_t - k_{-1}[B]_t \qquad (3.14)$$

At t = 0, $[B]_0 = 0$ and $[A]_t = [A]_0$ thus $[A]_0$, $[A]_t$ and $[B]_t$ are related by equation 3.15,

$$[B]_t = [A]_0 - [A]_t \qquad (3.15)$$

Substituting for $[B]_t$ in equation 3.14 gives equation 3.16,

$$\frac{-d[A]}{dt} = k_1[A]_t - k_{-1}([A]_0 - [A]_t) \qquad (3.16)$$

At equilibrium the net reaction is zero, hence equation 3.16 reduces to equation 3.17,

$$\frac{-d[A]}{dt} = 0 \qquad (3.17)$$

Applying equations 3.16 and 3.17 to equation 3.14 leads to equation 3.18,

$$k_1[A]_{eq} = k_{-1}[B]_{eq} = k_{-1}\left([A]_0 - [A]_{eq}\right) \tag{3.18}$$

Equation 3.18 can be rearranged to form equation 3.19,

$$[A]_0 = \frac{k_1 + k_{-1}}{k_{-1}}[A]_{eq} \tag{3.19}$$

Substituting equation 3.19 in 3.16 forms equation 3.20,

$$\frac{-d[A]}{dt} = (k_1 + k_{-1})[A]_t - (k_1 + k_{-1})[A]_{eq} \tag{3.20}$$

Rearranging equation 3.20 gives equation 3.21,

$$\frac{d[A]}{\left([A]_t - [A]_{eq}\right)} = -(k_1 + k_{-1})dt \tag{3.21}$$

Integrating equation 3.21as shown in equation 3.22 gives equation 3.23,

$$\int_{[A]_0}^{[A]_t} \frac{d[A]}{\left([A]_t - [A]_{eq}\right)} = -(k_1 + k_{-1})\int_0^t dt \tag{3.22}$$

Then,

$$\ln \frac{\left([A]_t - [A]_{eq}\right)}{\left([A]_0 - [A]_{eq}\right)} = -(k_1 + k_{-1})t \tag{3.23}$$

Rearranging equation 3.23 gives equation 3.24,

$$\ln\left([A]_t - [A]_{eq}\right) = -\left(k_1 + k_{-1}\right)\, t \, + \, \ln\left([A]_0 - [A]_{eq}\right) \tag{3.24}$$

Using equation 3.24 which is in the form, $y = mx + c$, a plot of $\ln\left([A]_t - [A]_{eq}\right)$ against, t, gives a straight line with the slope equal to $-\left(k_1 + k_{-1}\right)$. To determine k_1 and k_{-1}, the equilibrium constant, K_{eq}, must be evaluated.

Since,

$\frac{d[A]}{dt} = 0 = k_1[A]_{eq} - k_{-1}[B]_{eq}$, thus,

$$K_{eq} = \frac{[B]_{eq}}{[A]_{eq}} = \frac{k_1}{k_{-1}} \tag{3.25}$$

The experimentally observed rate constant becomes;

$$k_{obs} = \left(k_1 + k_{-1}\right) \tag{3.26}$$

To treat first-order reversible reactions, $[A]_{eq}$ must be measured accurately.[10-12,15]

3.3.3 Consecutive first-order reactions

Also known as series reactions, the product formed after the first reaction becomes the reactant for subsequent reactions. Ligand substitution reactions normally don't stop after one substitution but proceed to form a more highly substituted complex.[10,11] Consider a simple consecutive reaction represented in equation 3.27,

$$A \xrightarrow{k_1} B \xrightarrow{k_2} C \tag{3.27}$$

The rate law for the process is derived as follows,

$$\frac{-d[A]}{dt} = k_1[A] \tag{3.28}$$

$$\frac{d[B]}{dt} = k_1[A] - k_2[B] \tag{3.29}$$

$$\frac{d[C]}{dt} = k_2[B] \tag{3.30}$$

At time t = 0, $[A] = [A]_0$ while $[B]_0 = [C]_0 = 0$ and after a time, *t*,

$$[A]_0 = [A]_t + [B]_t + [C]_t \tag{3.31}$$

Integrating equation 3.27 gives equation 3.32,

$$[A]_t = [A]_0 e^{-k_1 t} \tag{3.32}$$

Equation 3.32 is substituted in equation 3.29 to give 3.33,

$$\frac{d[B]}{dt} = k_1[A]e^{-k_1 t} - k_2[B]_t \tag{3.33}$$

By integrating factor method, equation 3.33 is multiplied by the integrating factor, $e^{-k_2 t}$, followed by rearrangement to give;

$$\frac{d[B]e^{k_2 t}}{dt} = k_1[A]_0 e^{(k_2 - k_1)t} - k_2[B]_t e^{k_2 t} \tag{3.34}$$

With the initial conditions, t = 0, $[B]_0 = 0$ the product rule is applied to equation 3.34 and subsequent integration proceeds as follows to give equation 3.35,

$$\int_0^t \frac{d}{dt}\left([B]_t e^{k_2 t}\right) = k_1[A]_0 \int_0^t e^{\left(k_2 - k_1\right)t} dt \quad ,$$

$$[B]_t = k_1[A]_0 \frac{\int_0^t e^{\left(k_2 - k_1\right)t}}{e^{k_2 t}},$$

$$[B]_t = \frac{[A]_0 k_1}{k_2 - k_1}[e^{k_1 t} - e^{k_2 t}] \tag{3.35}$$

The mass law is applied to equation 3.35 to give equation 3.36;

$$[C]_t = [A]_0\left(1 - \frac{k_2}{k_2 - k_1}e^{-k_1 t} + \frac{k_1}{k_2 - k_1}e^{-k_2 t}\right) \tag{3.36}$$

For the *steady state approximation* (an assumption used for consecutive reactions), [B] is assumed to be very small and doesn't change during the reaction thus, $k_1 < k_2$[11] based on this assumption, equation 3.29 gives equation 3.37,

$$\frac{d[B]}{dt} = k_1[A]_t - k_2[B]_t \cong 0 \tag{3.37}$$

This rearranges to equation 3.38,

$$[B]_t = \frac{k_1}{k_2}[A]_t \tag{3.38}$$

Substituting equation 3.32 into 3.38 gives equation 3.39,

$$[B]_t = \frac{k_1}{k_2}[A]e^{-k_1 t} \tag{3.39}$$

Making $[C]_t$ the subject of the formula in equation 3.31 gives; $[C]_t = [A]_0 - [A]_t - [B]_t$, which when substituted with equations 3.32 and 3.39 gives equation 3.40,

$$[C]_t = [A]_0\left[\ 1 - e^{-k_1 t} - \frac{k_1}{k_2}e^{-k_1 t}\right] \cong [A]_0[1 - e^{-k_1 t}] \tag{3.40}$$

3.3.4 Irreversible Second –Order reactions

Second-order reactions include two types first, that in which the rate of the reaction is second order with respect to only one of the reactants and the second type is where the reaction is first-order with respect to two different reactants that forms our topic of discussion in this section. Consider a second order reaction represented by equation 3.41.

$$A + B \xrightarrow{k_2} C \tag{3.41}$$

The rate law for reaction 3.41 is given by equation 3.42,

$$Rate = k[A][B] \tag{3.42}$$

The rate law can be represented by equation 3.43,

$$Rate = \frac{d[C]}{dt} = -\frac{d[A]}{dt} = -\frac{d[B]}{dt} = k_2[A]_t[B]_t \tag{3.43}$$

If at t = 0, $[A] = [A]_0$ and $[B] = [B]_0$, and letting x be the amount of the reactants reacted after time, t, then concentration of [A] and [B] at time, t, will be, $[A]_t = \left([A]_0 - x\right)$ and $[B]_t = \left([B]_0 - x\right)$respectively.

The rate after time, t, is therefore given by equation 3.44,

$$-\frac{d[A]}{dt} = k_2\left([A]_0 - x\right)\left([B]_0 - x\right) \tag{3.44}$$

Given that $\frac{dx}{dt} = -\frac{d[A]}{dt} = -\frac{d[B]}{dt}$, equation 3.44 can be represented by equation 3.45,

$$\frac{dx}{dt} = k_2\left([A]_0 - x\right)\left([B]_0 - x\right) \tag{3.45}$$

When variables are separated, the new form of equation 3.45 is given by equation 3.46,

$$\frac{dx}{([A]_0 - x)([B]_0 - x)} = k_2 dt \tag{3.46}$$

Integrating equation 3.46 between the limits $x = 0$ to $x = x$ and $t = 0$ to $t = t$ respectively gives equation 3.47,

$$\int_0^x \frac{dx}{([A]_0 - x)([B]_0 - x)} = k_2 \int_0^t dt \tag{3.47}$$

Equation 3.47 solves to equation 3.48,

$$\frac{1}{[A]_0 - [B]_0} \ln \frac{[B]_0([A]_0 - x)}{[A]_0([B]_0 - x)} = k_2 t \tag{3.48}$$

Since $([A]_0 - x) = [A]_t$ and $([B]_0 - x) = [B]_t$, equation 3.48 changes to equation 3.49,

$$\frac{1}{[A]_0 - [B]_0} \ln \frac{[B]_0[A]_t}{[A]_0[B]_t} = k_2 t \tag{3.49}$$

For the second-order rate constant, k_2, to be calculated, $[A]_0$, $[B]_0$, $[A]_t$ and $[B]_t$ must be determined first as its implied in equation 3.49 which is cumbersome.[11,12] The rate law is thus commonly simplified by running reactions under *pseudo-first-order* conditions by having either concentration of *A* or *B* in excess (at least 10 fold) e.g. if $[B]_0 >> [A]_0$ then concentration of *B* remains relatively constant as the reaction proceeds. With the assumption that the reaction is *first-order* with respect to *A*, then *equation 3.43* converts to equation 3.50,

$$\frac{-d[A]}{dt} = (k_2[B]_0)[A]_t,$$

$$\frac{-d[A]}{dt} = k_{obs}[A]_t \tag{3.50}$$

Where k_{obs} *is the observed rate constant whose unit is per second* (s^{-1})

With the integrated form of equation 3.50, a graph of $\ln[A]$ verses time, *t,* is a straight line with the slope equal to k_{obs}. With several concentrations of *B* investigated each in large excess, respective values of k_{obs} are obtained which when plotted against $[B]_0$ according to equation 3.51give a straight line graph with slope equal to the second-order rate constant, k_2 ($M^{-1}s^{-1}$).[10-12,17]

$$k_{obs} = k_2[B]_0 \tag{3.51}$$

3.3.5 Reversible Second-order Reactions

Some second order reactions may not proceed to completion resulting to equilibrium state as illustrated by equation 3.52,

$$A + B \underset{k_{-2}}{\overset{k_2}{\rightleftharpoons}} C \tag{3.52}$$

The forward reaction is second order while the reverse reaction is first order meaning that the reaction is multi-order hence complex. The reaction is simplified by having pseudo first-order conditions for the forward reaction where $[B]_0 >> [A]_0$ which makes it resemble a reversible first-order reaction with rate given as, [11,12]

$$-\frac{d[A]}{dt} = -\frac{d[B]}{dt} = \frac{d[C]}{dt} \tag{3.53}$$

The rate of formation of C is given by equation 3.54,

$$Rate = k_2[A]_t[B]_t - k_{-2}[C]_t \tag{3.54}$$

Given the stoichiometry of the reaction is 1:1:1 and no product at time, $t = 0$, then after time, *t*, the masses remaining will be given by equations 3.55 and 3.56,

$$[A]_t = ([A]_0 - [C]_t) \tag{3.55}$$

$$[B]_t = ([B]_0 - [C]_t) \tag{3.56}$$

At equilibrium, the mass balances will be given by equations 3.57 and 3.58,

$$[A]_{eq} = ([A]_0 - [C]_{eq}) \tag{3.57}$$

$$[B]_{eq} = ([B]_0 - [C]_{eq}) \tag{3.58}$$

The forward and reverse reactions are equal and opposite represented by equation 3.59,

$-\frac{d[A]}{dt} = k_2[A]_{eq}[B]_{eq} - k_{-2}[C]_{eq} = 0$, thus,

$$k_2[A]_{eq}[B]_{eq} = k_{-2}[C]_{eq} \tag{3.59}$$

Substituting for $[C]_{eq}$ gives equation 3.60,

$$k_2[A]_{eq}[B]_{eq} = k_{-2}\left([A]_0 - [A]_{eq}\right) \tag{3.60}$$

With this, the rate works out to equation 3.61,

$k_{-2}[A]_0 = k_2[A]_{eq}[B]_{eq} + k_{-2}[A]_{eq}$ and

$[C]_t = ([A]_0 - [A]_t)$ Then,

$$-\frac{d[A]}{dt} = k_2[A]_t[B]_t - k_{-2}\left([A]_0 - [A]_t\right) = k_2[A]_t[B]_t - k_{-2}[A]_0 + k_{-2}[A]_t$$

$$= k_2[A]_t[B]_t - k_2[A]_{eq}[B]_{eq} - k_{-2}[A]_{eq} + k_{-2}[A]_t \tag{3.61}$$

Substituting for $[B]_t$ and $[B]_{eq}$ according to equations 3.56 and 3.58 and making the approximation that, $k_2[A]_0[A]_t \approx k_2[A]_{eq}[A]_0$ and $k_2[A]_t^2 \approx k_2[A]_{eq}^2$ gives equation 3.62,

$$-\frac{d[A]}{dt} = k_2[A]_t[B]_0 - k_2[A]_{eq}[B]_0 - k_{-2}[A]_{eq} + k_{-2}[A]_t \qquad (3.62)$$

Factorizing equation 3.62 gives equation 3.63,

$$-\frac{d[A]}{dt} = \left(k_2[B]_0 + k_{-2}\right)\left([A]_t - [A]_{eq}\right) \qquad (3.63)$$

Separating the variables and subsequent integration gives leads to equation 3.64,

$$\int_{[A]_0}^{[A]_t} \frac{d[A]}{\left([A]_t - [A]_{eq}\right)} = -\left(k_2[B]_0 + k_{-2}\right)\int_0^t dt\,,$$

$$\ln\left(\frac{[A]_t - [A]_{eq}}{[A]_0 - [A]_{eq}}\right) = -\left(k_2[B]_0 + k_{-2}\right)t = k_{obs}t \qquad (3.64)$$

Where $k_{obs} = k_2[B]_0 + k_{-2}$

A graph of k_{obs} verses $[B]_0$ is a straight line whose slope is k_2 and intercept equivalent to k_{-2}. The ratio of k_2 : k_{-2} gives equilibrium constant that can be measured thermodynamically.[17] Generally pseudo-first-order reactions are applied in the study of substitution reactions of square planar complexes.

3.4 Activation parameters

A rate law helps discern a reaction mechanism, however to obtain further information on the enthalpies of a reaction, the temperature dependence of the rate constant is often analysed which leads to the determination of the activation parameters.[11,12,18] This may also involve, for more complex rate laws, a study of concentration dependence of the rate at various temperatures, to determine the temperature dependence of different species in the rate law.

Experimental data for the rate constants can be analyzed according to the Arrhenius equation or transition state theory (absolute reaction rate theory) as follows.[11]

3.4.1 The Arrhenius equation

Equation 3.65 proposed by Svante Arrhenius in 1889,[19] states the relationship between temperature and rate constants.

$$k = Ae^{-\frac{E_a}{\mathrm{RT}}} \tag{3.65}$$

Taking natural logarithm of the Arrhenius equation gives equation 3.66,

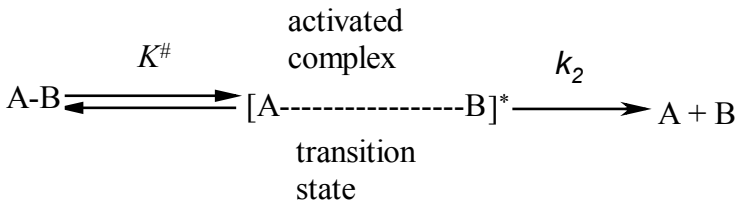
$$\ln k = \ln A - \frac{E_a}{\mathrm{R}}.\frac{1}{\mathrm{T}} \tag{3.66}$$

Where: A is *Arrhenius pre-exponential factor* ($M^{-1}s^{-1}$), E_a is *Arrhenius activation energy* ($Jmol^{-1}$), R is *Gas constant* ($8.315JK^{-1}mol^{-1}$) *and* T is *Absolute temperature (K)*

When appropriate experiments are done at different temperatures determining the respective rate constants, *k*, then a plot of $\ln k$ verses $\frac{1}{\mathrm{T}}$ gives a straight line graph whose slope is equal to $-\frac{E_a}{\mathrm{T}}$ from which E_a can be determined. The rate constant is expected to increase with temperature.[3,12,15,20] The Arrhenius equation comes in handy for complex systems where the determined rate constant, *k,* is thought to be a composite of specific rate constants.[12]

3.4.2 The Transition-state Theory

The transition-state theory originally known as the theory of absolute reaction states by H. Eyring, M. Evans and M. Polanyi in 1936[12,21,22] was developed for simple dissociation processes in gaseous phase. It's based on the assumption that most reactions proceed via a pre-equilibrium mechanism as illustrated by equation 3.67,



(3.67)

The reaction rate can be expressed by equation 3.68,

$$\frac{d[A]}{dt} = k_2\left[A---B\right]^* \tag{3.68}$$

Since $K^{\neq}$ is given by equation 3.69,

$$K^{\neq} = \frac{[A---B]^*}{[A-B]} \tag{3.69}$$

Equation 3.68 forms equation 3.70 after substituting for $[A\text{----}B]^*$.

$$\frac{d[A]}{dt} = k_2 K^{\neq}[A-B] = \frac{k_b \mathrm{T}}{h} K^{\neq}[A-B] \tag{3.70}$$

Where k_b is *Boltzmann's constant (1.38* x $10^{-23} JK^{-1}$*) and h* is *Plank's constant (6.626* x $10^{-34} Js^{-1}$*).*

The experimental rate constant can be incorporated in equation 3.70 to give equation 3.71,

$$\frac{d[A]}{dt} = k_{\exp}[A-B] \tag{3.71}$$

Where the experimental rate constant is given by equation 3.72,

$$k_{\exp} = \frac{k_b \mathrm{T}}{h} K^{\neq} \tag{3.72}$$

Given that Gibbs free energy of activation, $\Delta G^{\neq}$, is given by equation 3.73,

$$\Delta G^{\neq} = -\mathrm{RT}\ln K^{\neq},$$
$$= \Delta H^{\neq} - \mathrm{T}\Delta S^{\neq} \qquad (3.73)$$

Substituting for $K^{\neq}$ in equation 3.73 gives equation 3.74,

$$k_{\exp} = \frac{k_b \mathrm{T}}{h} e^{\left(-\frac{\Delta G^{\neq}}{\mathrm{RT}}\right)} \qquad (3.74)$$

Given that,

$-\mathrm{RT}\ln K^{\neq} = \Delta H^{\neq} - \mathrm{T}\Delta S^{\neq}$, where

$$K^{\neq} = e^{-\frac{\Delta H^{\neq}}{\mathrm{RT}}} e^{\frac{\Delta S^{\neq}}{\mathrm{R}}},$$

Equation 3.72 could also give equation 3.75,

$$k_{\exp} = \frac{k_b \mathrm{T}}{h} e^{\left(-\frac{\Delta H^{\neq}}{\mathrm{RT}}\right)} e^{\left(\frac{\Delta S^{\neq}}{\mathrm{R}}\right)} \qquad (3.75)$$

Rearranging, applying logarithms, linearization and simplifying equation 3.75 gives equation 3 76,

$$\ln\left(\frac{k_{\exp}}{\mathrm{T}}\right) = \frac{-\Delta H^{\neq}}{\mathrm{R}} . \frac{1}{\mathrm{T}} + \left[\ln\left(\frac{k_b}{h}\right) + \frac{\Delta S^{\neq}}{\mathrm{R}}\right] \qquad (3.76)$$

From the values of the constants k_b and h the value of $\ln\left(\frac{k_b}{h}\right)$ is given as 23.8 hence equation 3.76 will eventually form equation 3.77,

$$\ln\left(\frac{k_{\exp}}{\mathrm{T}}\right) = \frac{-\Delta H^{\neq}}{\mathrm{R}} . \frac{1}{\mathrm{T}} + \left[23.8 + \frac{\Delta S^{\neq}}{\mathrm{R}}\right] \qquad (3.77)$$

A plot of $\ln\left(\frac{k_{\exp}}{T}\right)$ verses $\frac{1}{T}$ gives a graph known as Erying plot, of slope $-\frac{\Delta H^{\neq}}{R}$ and an intercept equal to $23.8+\frac{\Delta S^{\neq}}{R}$ from which the enthalpy, $\Delta H^{\neq}$, of activation and entropy, $\Delta S^{\neq}$, of activation can be determined respectively.[12,15,23,24]

3.5 Experimental kinetic techniques

Kinetics of most chemical reactions in solutions has been studied in detail. There exists different methods for measuring reaction rates the choice of a method depends on whether the reaction of interest is fast or slow. The best technique to study chemical kinetics must involve mixing reactants in a time negligible to the time scale of the reaction, measure a variable that is proportional to concentration of reactants or products as a function of time and accurately measure and control temperature or pressure at which a reaction proceeds.[25] A slow reaction can be studied by conventional methods of analysis to determine the concentration of a reactant or product as a function of time but most reactions are too rapid so that the reaction has to be stopped while the measurement is done (quenching) or a technique that ensures continuous measurement of concentration as the reaction proceeds must be applied.[4]

Quenching is made possible by lowering temperature to slow the reaction to allow a measurement to be taken which is very slow and time-consuming hence more convenient to monitor the progress of a reaction continuously by spectrophotometry, conductometry, potentiometry or some other instrumental technique. With increasing availability of laboratory instrumentation, many kinetic studies have been studied by monitoring a physical property of a reaction mixture with time.[4] There are many techniques available for kinetic studies *viz.* pulse methods, infrared spectroscopy (IR) and nuclear magnetic resonance spectroscopy (NMR). UV/Visible absorption spectroscopy and stopped-flow analysis are the techniques applied in this study hence ones discussed in the proceeding sections.

3.5.1 UV/Visible Spectrophotometry

In a UV/Visible spectrophotometer, light from a continuous light source is passed through a monochromator (a prism, grating or even a filter) which allows a single wavelength. The selected wavelength with an intensity, I_o, strikes a sample in a cell called a cuvette of length, l, and emerges with reduced intensity, I, since the sample absorbs some light.[4] A double-beam

spectrophotometer facilitates light to pass alternately through the sample and reference cuvettes with pure solvent. Having a reference cuvette with pure solvent is important as it compensates for absorption due to the cuvette and solvent or light scattering.[4] A double-beam spectrophotometer, as shown in figure 1, alternates between cuvettes by using a chopper which is a motor that rotates a mirror into and out of the light path. When the chopper is not deflecting the beam, light passes through the sample and the detector measures the intensity; however, when the chopper deflects the beam through the reference cuvette, the detector reads the reference value *i.e.* the beam is chopped several times per second.

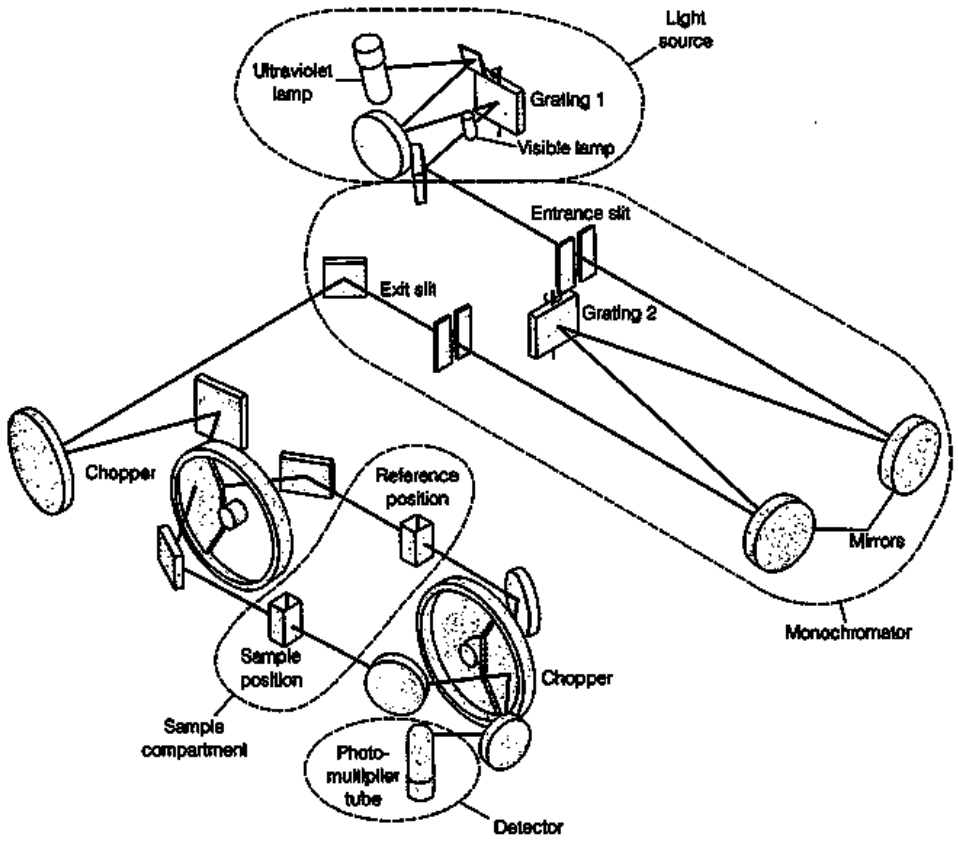


Figure 3.1 A schematic diagram of a UV-Visible spectrophotometer.[26]

Transmittance, T, measured by a spectrophotometer is defined as the fraction of light passing through the sample given by equation 3.78,

$$T = \frac{I}{I_o} \tag{3.78}$$

Where I_o is intensity of incident radiation and I is intensity of transmitted radiation

Absorbance, a more useful quantity because its directly related to concentration is given by equation 3.79,

$$A = \log \frac{I_0}{I} = -\log T \tag{3.79}$$

Absorbance is proportional to concentration hence more useful when expressed by by Beer's law in equation 3.80,

$$A = \varepsilon CL \tag{3.80}$$

Where A is optical absorbance (dimentionless), ε is molar absorptivity ($M^{-1}cm^{-1}$), C is concentration of the absorbing species (M) and L is path length(cm)

Consider a simple first-order reaction illustrated by equation 3.81,

$$X \xrightarrow{k_1} Y \tag{3.81}$$

Absorbance after a time, *t,* will be given by equation 3.82,

$$A_t = \varepsilon_X [X] + \varepsilon_Y [Y] \tag{3.82}$$

Where A_t is absorbance at time,t and $\varepsilon_X, \varepsilon_Y$ represent molar absorptivity of X and Y respectively

At the end of the reaction, the absorbance is given by equation 3.83,

$$A_\infty = \varepsilon_X [X]_0 + \varepsilon_Y [Y]_0 \tag{3.83}$$

Where A_∞ = absorbance at infinity

Kinetic analysis of a reaction represented by equation 3.81, can be done by the relation in equation 3.84,

$$\ln \frac{[X]_0}{[Y]_0} = \ln\left(\frac{A_0 - A_\infty}{A_t - A_\infty}\right) = k_1 t \qquad (3.84)$$

An example of the reaction profile obtained from the UV/Visible spectrophotometer for the substitution of chloride from [Pt{4'-ethyleneglycoxyl)- 2,2':6,2''-terpyridine)Cl]$^+$ by imidazole (studied in chapter 3) at 298K is shown in figure 3.2.The reaction was monitored from 200-800nm wavelength.

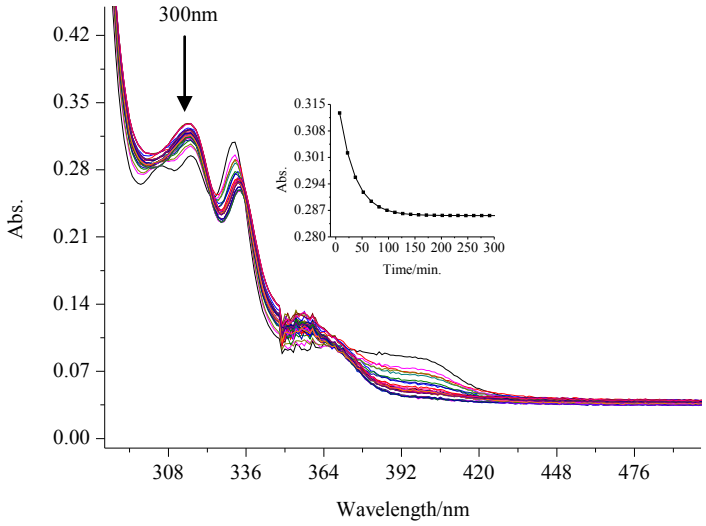


Figure 3.2 UV-Visible spectrum for the reaction of Imidazole (20 fold) with [Pt{4'-ethyleneglycoxyl)- 2,2':6,2''-terpyridine)Cl]$^+$ in methanol at 298K. (inset is the respective kinetic trace)

3.5.2 Flow methods

Many reactions happen too quickly hence impossible to monitor by standard absorption spectroscopy. The commonly applied method to monitor these rapid reactions is stopped-flow mixing which involves mixing reagents rapidly and stopping the flow of the mixed solution suddenly allowing the progress of the reaction to be analysed near the mixer.[9,11,19] The working of the stopped-flow apparatus is illustrated in figure 3.3

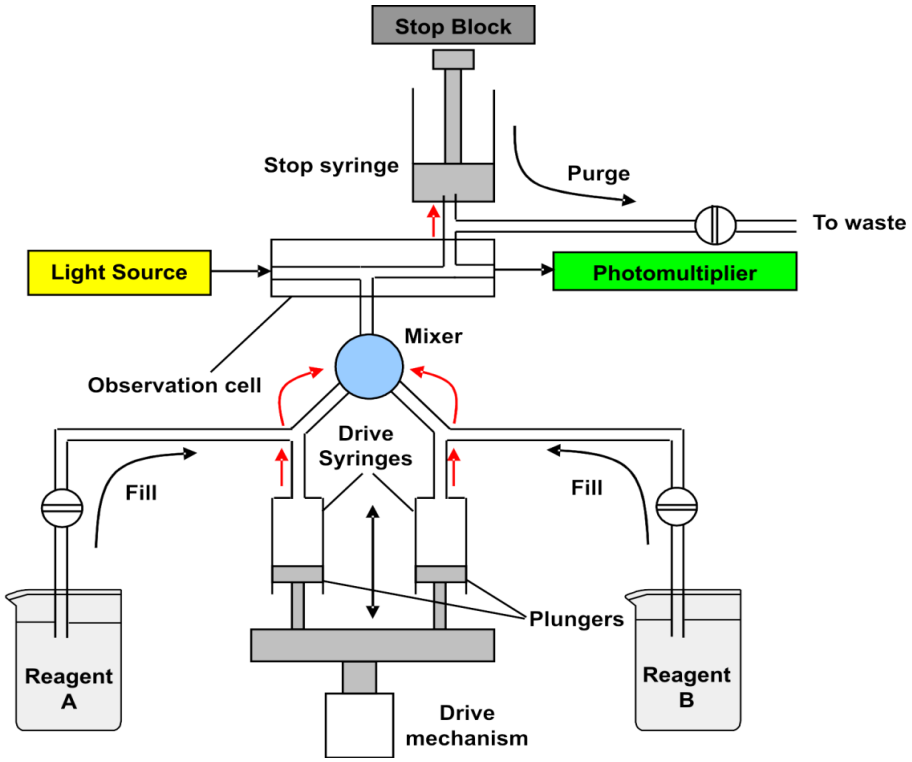


Figure 3.3 Schematic diagram of mechanistic action of stopped-flow apparatus[4]

Drive syringes are filled separately with the different reagents then the drive mechanism, which is usually piston driven, is activated causing the drive syringe plungers to go forward rapidly.[19, 27] The reagents then move into the mixer where there is rapid mixing within 0.001 s and the solution passes into the observation cell.[19, 27] The reaction solution then passes into the stop syringe until the stop syringe fills causing the plunger to strike the stop block instantly ceasing the flow, but leaving a recently mixed plug of solution in the observation cell.[19,27]

The mixed solution is stationary in the observation cell allowing a recording device like an oscilloscope to take readings. The method of detection is UV/visible spectrophotometry. Once the recording device starts, the intensity of light transmitted through the observation chamber at a specific wavelength changes as the reaction proceeds to completion.[19,27] A photomultiplier converts transmitted light into electric current interpreted by a computer as an absorption versus time spectrum which is analysed normaly.[19, 27] The stopped-flow analysis is a simple technique with some advantages as it allows very rapid first order reaction constants to be measured, $k \approx 40\ s^{-1}$, easy to analyse which allows small (≈ 0.2 ml) volumes of solutions to be used and permits the use of a number of different monitoring methods in conjunction with this technique.[19]

3.6 References

1 . A. Kenneth Connors, *Chemical Kinetics*; *The Study of reactions Rates in Solution*, Wiley- VCH, NY, 1990, pp 1-22, 59-67, 177-180, 207-209

2. E. L. King, *How Chemical Reactions Occur: An Introduction to Chemical Kinetics and Reaction Mechanics*, W. A. Benjamin, Inc, New York, 1964, p. 1.

3. S. R. Logan, *Fundamentals of Chemical Kinetics*, Longman, Essex, 1996, pgs 1-30, 8-44, 70-76

4. D. A. Skoog, D. M. West, F. J. Holler and S. R. Crouch, *Fundamentals of Analytical Chemistry*, 8th Ed., Brooks/Cole – Thomson Learning, Inc., United States, 2004, pgs 718-734, 771-775, 878-894.

5. D. W. Ball, *Physical Chemistry*, Brooks/Cole, Pacific Groove, 2003, p. 680-703.

6. M. Mortimer and P. Taylor, *Chemical Kinetics and Mechanism*, the Open University. Walton Hall, Miton Keys, MK76AA, London, 2002, p. 11

7. F. Wilkinson, *Chemical Kinetics and Reaction Mechanisms*, Van Nostrand Reinhold Company, New York, 1980, p. 1-11, 66-99

8. E. T. Denisov, O. M. Sarkisov and G. I. Likhtenshtein, *Chemical Kinetics: Fundamentals and New Development*,Elsevier Science and Technology Books, 2003, p.1-6

9. K. J. Laidler, J. H. Meiser and B. C. Sanctuary, *Physical Chemistry*, Houghton Mifflin Company, United States, 2003, pgs 363-376.

10. J. H. Espenson, *Chemical kinetics and Reaction mechanisms*, 2nd Ed., McGraw-Hill, N. Y., 1995, p. 1-72, 166, 254, 255.

11. J. D. Atwood, *Inorganic and Organometallic Reaction Mechanisms*, 2nd edition, Wiley-VCH, New York, 1997, pgs 1-32.

12. R. B. Jordan, *Reaction Mechanisms of Inorganic and Organometallic Systems*, Oxford University Press, New York, 1991, pgs 1-17.

13. D. Reddy, *PhD Thesis, Tuning the reactivity of Pt(II) Complexes,* University of Natal, Pietermarizburg, S.A, 2009, pp. 104,138-139

14. R. Büchner, C. T. Cunninggham, J. S. field, R. J. Haines, D. R. McMillin and G. C. Summerton, *J. Chem. Soc., Dalton trans.,* 1999, 711

15. B. G. Cox, *Modern Liquid Phase Kinetics,* Oxford University Press, NY, 1994, p 5, 59

16. K. T. Potts, A. Usifer, H. D. Guadalupe and H. D. Abruna, *J. Am. Chem. Soc.,* 1987, **109**, 3961

17. P. Atkins and J. de Paula, *Atkins' Physical Chemistry*, 8th edition., Oxford University Press, Oxford, 2006, pgs 479-815, 791-829.
18. D. Benson, *Mechanisms of Inorganic Reactions in Solution*, McGrow-Hill, London, 1968, p. 1-13
19. R.G. Wilkins, *Kinetics and Mechanism of Reactions of Transition Metal Complexes,* 2nd Ed., VCH, Weinheim, 1991, p 41-43
20. D. W. Ball, *Phsical Chemistry,* Brooks/Cole, Pacific Grove, 2003, p 680-703.
21. H. Erying, *J. Chem. Phys.,* 1935, **3**, 107
22. M. G. Evans, and M. Polanyi, *Trans. Faraday Soc.,* 1935, **31**, 875.
23. S. Asperger, *Chemical Kinetics and Inorganic Reaction Mechanisms*, 2nd Ed., Kluwer Academic/Plenum Publishers,NY, 2003, p 3, 17-23
24. R. J. Silbey, R. A. Alberty and G.B. Moungi, *Phys. Chem.,* 4th Ed., John Wiley & Sons, NY, 2005, p 642-652, 697, 698
25. M.J. Pilling and P.W. Seakins, *Reaction Kinetics,* Oxford Science Publications, Oxford, 1995, p 27, 38, 39.
26. D. C. Harris, *Quantitative Chemical Analysis*, 4th Ed., W. H. Freeman & Co., New York, 1995, pp. 480-417
27. M. S. Silberberg, *Chemistry. The Molecular Nature of Matter and Change*, 2nd edition., McGraw-Hill, United States, 2000, pgs 664-684.

Table of contents

List of abbreviations i

List of figures ii

List of tables iii

List of schemes iv

Chapter 4 1

The role of ethylene polyglycoxyl pendant units on the terpy based Platinum(II) complexes. A kinetic and mechanistic study. 1

4.1 Abstract 1

4.2 Introduction 2

4.3 Experimental 4

4.3.1 Materials 5

4.3.2 Synthesis of Ligands 5

4.3.3 Synthesis of Platinum(II) Complexes 6

4.3.4 Chemicals and solutions 7

4.3.5 Physical measurements and instrumentation 8

4.3.6 Computational details 11

4.3.7 Kinetic analysis 14

4.4 Results and discussion 15

4.5 Conclusions 20

4.6 References 21

4.7 Supplementary Information 26

List of abbreviations

Å	Angstrom
COD	Cyclooctadiene
DFT	Density functional theory
DIm	1,2-dimethylimidazole
eV	Electronvolt
HF	Hartree-Fock
HOMO	Highest occupied molecular orbital
Im	Imidazole
k_2, k_{-2}	Rate constants
k_{obs}	Observed *pseudo* first-order constant
LUMO	Lowest unoccupied molecular orbital
MIm	1-methylimidazole
NBO	Natural bond order
NMR	Nuclear magnetic resonance
Pt	$[Pt(2,2':6,2''\text{-terpyridine})Cl]^+$
Pt(deg)	$[Pt\{4'\text{-diethyleneglycoxyl})\text{- }2,2':6,2''\text{-terpyridine})Cl]^+$
Pt(eg)	$[Pt\{4'\text{-ethyleneglycoxyl})\text{- }2,2':6,2''\text{-terpyridine})Cl]^+$
Pt(teg)	$[Pt\{4'\text{-triethyleneglycoxyl})\text{- }2,2':6,2''\text{-terpyridine})Cl]^+$
Pz	Pyrazole
R	Universal gas constant ($8.3145 JK^{-1}mol^{-1}$)
T	Absolute temperature (K) unless stated otherwise
terpy/tpy	2,2':6,2''-terpyridine
tpy(deg)	4'-[2-(2-Hydroxyethoxy)ethoxy]-2,2':6',2"-terpyridine
tpy(eg)	4'-[2-(2-Hydroxyethoxy)]-2,2':6',2"-terpyridine
tpy(teg)	4'-{2-[2-(2-Hydroxyethoxy)ethoxy]ethoxy}-2,2':6',2"-terpyridine
Tz	Triazole
UV	Ultraviolet
VIS	Visible
$\Delta G^{\neq}$	Gibbs free energy of activation
$\Delta H^{\neq}$	Activation enthalpy
$\Delta S^{\neq}$	Activation entropy

List of figures

Figure 4.1 Absorbance spectra of Pt(eg) (5.0 x 10^{-5}M) and MIm (5.0 x 10^{-3}M) at 298 K.9

Figure 4.2 Concentration dependence plots to determine k_2 and k_{-2} from slopes intercepts respectively for the reaction of Pt(deg) with Im, Pz and Tz at 298K. ..... ……10

Figure 4.3 Eyring plots for the reaction of Pt(eg) with MIm, DIm and Tz 11

Figure 4.4 DFT calculated angles around the oxygen atoms on the polyglycoxyl group of Pt (teg).....14

Figure 4.5 Hydrogen bonding interactions in the polyglycoxyl pendant 17

List of tables

Table 4.1 DFT-calculated frontier molecular orbitals of the investigated Pt(II) complexes. ……...12

Table 4.2 Computational data of the complexes investigated……...13

Table 4.3 Rate constants and activation parameters for Pt(II) complexes with the azole nucleophiles……...15

List of schemes

Scheme 4.1 Structural formulae of the Platinum(II) complexes. 4
Scheme 4.2 Structural formulae of the azole nucleophiles. 4
Scheme 4.3 Proposed mechanism of substitution for the studied complexes. 15

Chapter 4

The role of ethylene polyglycoxyl pendant units on the terpy based Platinum(II) complexes. A kinetic and mechanistic study.

4.1 Abstract

The rate of Chloride substitution from [Pt{(4'-ethylglycoxyl)-2,2':6',2''-terpyridine}Cl]CF_3SO_3, **Pt(eg),** [Pt{(4'-diethylglycoxyl)-2,2':6',2''-terpyridine}Cl]CF_3SO_3, **Pt(deg)** and [Pt{(4'-triethylglycoxyl)-2,2':6',2''-terpyridine}Cl]CF_3SO_3, **Pt(teg)** by a series of biological nitrogen donor nucleophiles, *viz.* pyrazole (**Pz**), triazole (**Tz**), imidazole (**Im**), 1-methylimidazole (**MIm**) and 1,2-dimethylimidazole (**DIm**) under pseudo-first-order conditions in methanol using UV/Visible spectrophotometry were investigated. The analysis of kinetic trend on the candidate complexes show that the first carbon-oxygen pendant bond plays a crucial role in regulating the electron density donated by the polyethylenegycoxyl fragment. This is reflected in the significant reduction in reactivity from **Pt** to **Pt(eg)** followed by insignificant change in the reactivity as the chain length is increased. The trend in the reactivity slightly increases from **Pt(eg)** to **Pt(teg)** as the length of the polyethyleneglycoxyl is increased. This is attributed to reduction in steric hindrance imposed by the ethyleneglycoxy unit. The reactivity of the nucleophiles is in line with the basicity and the steric hinderance.

The obtained kinetic data is supported by the DFT calculations that reveal a less electrophilic Pt(II) metal centre for complexes bearing the 4'-substituent. The temperature dependent studies support an associative mode of activation where bond formation in the transition state is favoured.

4.2 Introduction

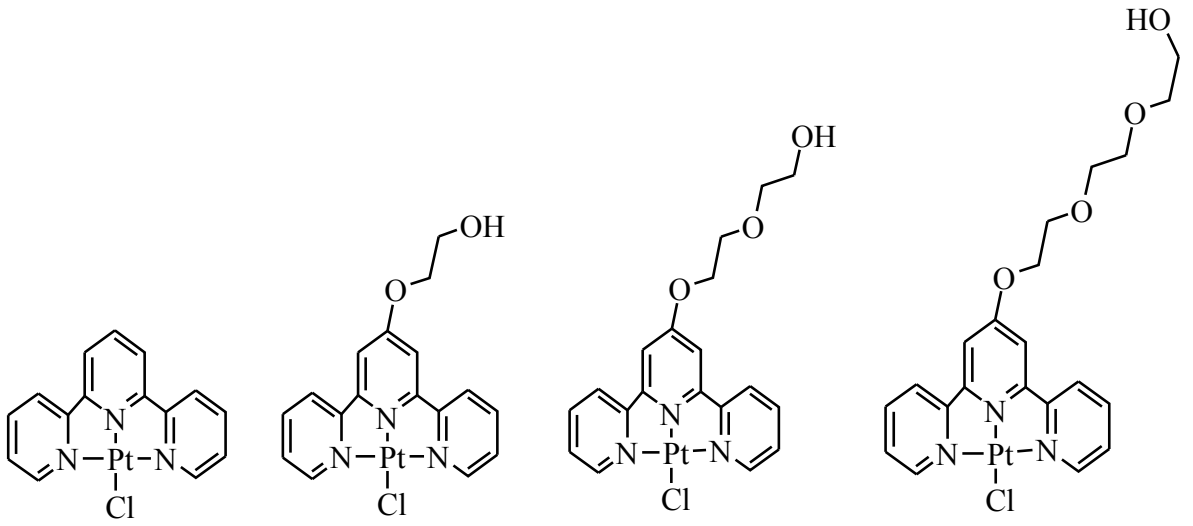
The voluminous number of Pt(II) complexes synthesized in the preceding decades informs of continuing research with the focus on tuning reactivity and other properties of Pt(II) complexes with a view to widen the biological spectrum of cisplatin.[1,2] Among the many synthesised compounds is 2,2':6",2"-terpyridine (tpy) whose derivatives are known to be good models for DNA intercalation.[3] 2,2':6",2"-terpyridine (tpy) first synthesised by Morgan in 1932[4,5] readily reacts with M^{n+} octahedral metal ions to give $[M(tpy)_2]^{n+}$ complexes.[6] For $[M(tpy)Cl]^+$ only the chloride ligand is labile due to the stable π-conjugated terpy ligand backbone,[7] thus π-conjugation explains the greater reactivity of platinum(II) terpyridine complexes relative to the less conjugated Platinum(II) ethylenediamine.[8,9] DNA-cisplatin adducts replication result to different strands of DNA with mutations leading to resistance which has elicited unmatched interest in substitution reactions of Pt(II) centre with nucleosides and other related compounds lately[10,11] unlike earlier research that focused on knowing the mechanism of ligand substitution and binding mode of complexes with sulphur and nitrogen donor nucleophiles.[12]

Research has shown that increasing the number of pyridine rings on the platinum (II) ethylenediamine increases its lability because the π-acceptor ability of subsequent complexes is enhanced.[9] The π-back-bonding of the terpy ligand enables the additional electron density from the incoming nucleophile to the π-acceptor orbitals of the pyridine groups to be stabilized in the transition state compared to the ground state,[8] a significant property of the terpy complexes. Recent attention has been paid to the mechanistic investigations into the substitution behaviour of platinum(II) terpy complexes with regard to the electronic tuning and the reactivity of the metal centre by changing the structure of the ligand.[13,14] Constable and Housecroft[15-22] have reported a variety of terpy ligands containing different functional groups at the 4'-position. Inclusion of these substituents alters the electronic as well as steric properties of the complexes. It is reported that different electron-withdrawing and donating groups change the electronic properties of the ruthenium complexes.[23,24] Lowe *et al.* reported alteration of the electronic property of the terpy ligand on addition of substituents at the 4' position.[25] A check in literature reveals that lability of the chloride ligand depends on the strength of π-back-bonding properties of the spectator terpy ligand backbone.[26] Substitution kinetics of $[Pd(bpma)(H_2O)]^{2+}$, $[Pd(dien)(H_2O)]^{2+}$ and $[Pd(dien)Cl]^+$ (bpma-bis(2-pyridylmethyl)amine and dien-diethylenetriamine) with azoles were reported by Bugarcic *et*

al.. Pitteri *et al*. also reported on the kinetics of reversible displacement of the chloride from [Pt(terpy)Cl] by some pyridines and heterocyclic compounds.[27-29]

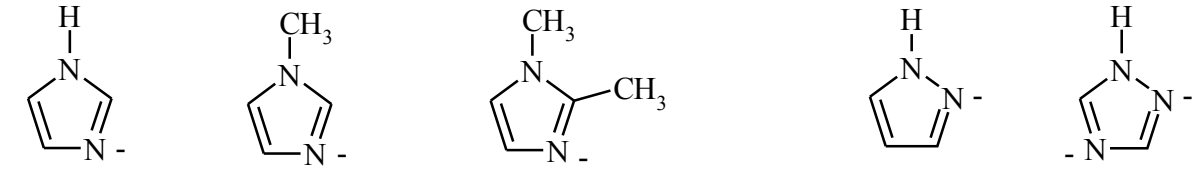
From a bioinorganic standpoint, azoles are essential given that the ligand histidine that binds to haemoproteins through its imidazole group is responsible for uptake of oxygen and electron transfer via cytochromes in plants and animals,[29] hence the need to probe the substitution behaviour of azole nucleophiles.[30,31] Furthermore, coordination chemists have a keen interest in imidazole and its derivatives because information on their ability to coordinate to metal complexes is linked to that of proton affinities in gaseous phase, aqueous solutions, aprotic solvents and hydrogen binding abilities.[32-36]

Data concerning the role of the π-acceptor ligands in the substitution reactions of square-planar platinum(II) complexes and the influence exerted by the substituents on the ancillary terpy ligand on the reactivity of these types of complexes[37,38] in the literature has no mention on the effect on the reaction of $[Pt(terpy)Cl]^+$ with polyglycoxyl at the 4'-position. It's on this basis that we extended the research to explore the effect the polyglycoxyl substituents at the 4'-position on the terpy ligand system will have on the rate of chloride substitution using azoles as the incoming nucleophiles. DFT calculations were used to aid in the interpretation of kinetic results. It is envisaged that this paper will throw more light on the mechanism and kinetics of these complexes with azoles given their relevance in biological systems. The structural formulae of the platinum complexes investigated and the respective azole nucleophiles are shown in schemes 4.1 and 4.2 respectively.



Pt **Pt(eg)** **Pt(deg)** **Pt(teg)**

Scheme 4.1 Structural formulae of the Platinum(II) complexes.



Imidazole **(Im)** 1-methylimidazole **(MIm)** 1,2-dimethylimidazole **(DIm)** Pyrazole **(Pz)** 1,2,4-triazole **(Tz)**

Scheme 4.2 Structural formulae of the azole nucleophiles.

4.3 Experimental

The Pt(II) complexes were synthesised in our group according to modified literature procedures.[39-44] The chemical analysis, UV-VIS spectra and ^{1}H NMR spectra data were in good agreement with those obtained in previous preparations. The purity of the ligands was confirmed by ^{1}H NMR and mass spectroscopy. The ^{1}H NMR spectra obtained are similar in the aromatic region for the ligands. The identity and the purity of the final complexes were confirmed by using ^{1}H NMR, ^{13}C NMR, ^{195}Pt NMR, elemental analyses, IR and mass spectroscopy. Similarly the ^{1}H NMR spectra of the complexes obtained show similarity in the aromatic region. Presence of a peak at about -2700 ppm on the ^{195}Pt NMR spectra confirms the Pt(NNN) coordination.[44(c-e),45(b)] Representative ^{1}H NMR, ^{13}C NMR, ^{195}Pt NMR, IR and mass spectra are given in figures SI 4.1-4.19 in the supporting information. The peak due to

the OH proton is not seen in any of the ^{1}H NMR spectra due to the proton exchange with the methanol solvent.[45(c)] IR spectra of the complexes show distinct broad bands at around 3200 to 3300 cm^{-1} due to the O-H stretches along with the C-H peaks at around 3000 cm^{-1}.[45(d-f)]

4.3.1 Materials

Methanol bought from Merck was distilled over magnesium[44(b)] prior to use for kinetic analysis. Dimethylsulfoxide (99.9%) from Aldrich was used without any further purification. Ethylene glycol (99.8%), diethylene glycol (99%) and triethylene glycol (99%) were bought from Sigma Aldrich. The ligand, 4'-chloro,2,2':6',2"-terpyridine (97%), tetraethylene glycol (99%), and the platinum salt, potassium tetrachloroplatinate(II) (99.9%) were bought from Aldrich. All other chemicals were purchased from Sigma Aldrich and were used without further purification.

4.3.2 Synthesis of Ligands

The syntheses of ligands were carried out by literature procedures.[39] To a suspension of KOH in dry DMSO at 50 °C was added the ethylene glycol and its respective polymer (n = 2, 3, 4) in excess to avoid the formation of the di-terpyridine ligand.[39(c)] After stirring for 30 minutes, 4'-chloro-2,2':6',2"-terpyridine was added and the reaction mixture stirred for 20 hours at this temperature. Upon cooling to room temperature, the reacting mixture was treated with deionised water and filtered. The crude product was extracted from the filtrate in dichloromethane (3 x 30 mL) dried over anhydrous magnesium sulfate and the solvent removed. 4'-[2-(2- Hydroxyethoxy)ethoxy]-2,2':6',2"-terpyridine (**tpy(eg)**) and 4'-[2-(2-Hydroxyethoxy)ethoxy]-2,2':6',2"-terpyridine (**tpy(deg)**) gave a white paste and a white powder respectively. The respective crude products were purified in THF to give white solids. 4'-{2-[2-(2-Hydroxyethoxy)ethoxy]ethoxy-2,2':6',2"-terpyridine (**tpy(teg)**) yielded pale yellow oil, pure enough for platination.

tpy(eg)

Yield: 250 mg, (70%), off white paste. ^{1}H NMR (400 MHz, $CDCl_3$)[1] δ/ ppm: 8.63 (d, 2H, 6 6''), 8.55 (2H, d, 3 3''), 7.99 (2H, s, 3' 5'), 7.79 (dt, 2H, 4 4''), 7.29 (dt, 2H, 5 5''), 4.23 (t, 2H, CH2), 3.97 (t, 2H, CH2). ^{13}C NMR (77 MHz, $CDCl_3$), δ / ppm: 61.1, 69.6, 107.6, 121.5, 123.8, 136.9, 148.9, 155.6, 157.2, 167.1. TOF MS-ES^{+}, m/z: 316.1062, $(M + Na)^{+}$.

tpy(deg)

Yield: 190 mg, (80%), white powder. ^{1}H NMR (400 MHz, $CDCl_3$) δ/ ppm: 8.69 (d, 2H, 6 6''), 8.62 (d, 2H, 3 3''), 8.13 (s, 2H, 3' 5'), 7.87 (t, 2H, 4 4''), 7.35 (t, 2H, 5 5''), 4.46 (t, 2H, CH2), 3.94 (t, 2H, CH2), 3.77 (t, 2H, CH2), 3.69 (t, 2H, CH2). ^{13}C NMR (77MHz, $CDCl_3$), δ / ppm: 61.7, 68.1, 69.9, 72.8, 108.3, 121.6, 124.0, 137.1, 148.9, 155.7, 156.7, 167.3. *Anal. Calc. for* $C_{19}H_{19}N_3O_3$: C, 67.64; H, 5.68; N, 12.46; *Found*: C, 68.00; H, 5.81; N, 11.97. TOF MS-ES$^+$, m/z: 360.1324, $(M + Na)^+$.

tpy(teg)

Yield: 175 mg, colourless oil (70%). ^{1}H NMR (400 MHz, $CDCl_3$) δ/ ppm: 8.66 (d, 2H, 6 6''), 8.59 (d, 2H, 3 3''), 8.03 (s, 2H, 3' 5'), 7.83 (t, 2H, 4 4''), 7.31 (t, 2H, 5 5''), 4.40 (t, 2H, CH2), 3.92 (t, 2H, CH2), 3.73 (m, 4H, CH2), 3.69 (t, 2H, CH2), 3.60 (t, 2H, CH2). ^{13}C NMR (77 MHz, $CDCl_3$), δ / ppm: 61.7, 67.9, 69.8, 70.4, 71.0, 72.9, 107.8, 121.4, 123.9, 136.9, 148.9, 155.9, 157.0, 167.1. TOF MS-ES$^+$, m/z: 404.1580, $(M + Na)^+$.

4.3.3 Synthesis of Platinum(II) Complexes

The syntheses of the complexes was carried out using the following procedure: To a stirred solution of $[Pt(COD)Cl_2]$[60(a)] in dry methanol at room temperature, a suspension of the appropriate ligand in dry methanol was added at 55 °C. The reaction mixture was stirred for 24 hours at the same temperature, after which the solution was cooled and filtered. When the bright yellow filtrate was concentrated under *vacuo*, the desired compound precipitated as pale yellow solid. The compound was filtered, washed with chloroform (20 mL), cold methanol (1 x 5 mL), diethylether (2 x 15 mL) and dried and stored in a desiccator.

Pt(eg)

Yield: 35 mg, (55%), pale yellow powder. ^{1}H NMR (400 MHz, CD_3OH) δ/ ppm: 10.23 (2H, d, 6 6''), 9.79 (2H, d, 3 3''), 9.78 (t, 2H, 4 4''), 9.39 (2H, s, 3' 5'), 9.20 (t, 2H, 5 5''), 5.88 (t, 2H, CH2), 5.44 (t, 2H, CH2). ^{195}Pt NMR (CD_3OH) δ/ ppm: -2715. IR (4000-650 cm-1) *υ*: 3237 (O-H), 3062 (C-H stretch), 1607 (C=H, pyridine), 1476 – 1423 (C-H stretch), 1222.43 (C-O), 788 (C-H stretch). *Anal. Calc. for* $C_{17}H_{15}Cl_2N_3O_2$: C, 36.51; H, 2.70; N, 7.51; *Found*: C, 36.38; H, 3.20; N, 7.92. TOF MS-ES$^+$, m/z: 524.0482, $(M + 1)^+$.

Pt(deg)

Yield: 46 mg, (64%), crystalline yellow powder. ^{1}H NMR (400 MHz, CD_3OH) δ/ ppm: 9.76 (d, 2H, 6 6''), 9.67 (d, 4H, 3 3''), 9.65 (t, 2H, 4 4''), 9.17 (s, 2H, 3' 5'), 9.07 (t, 2H, 5 5''), 5.87 (t, 2H, CH2), 5.38 (t, 2H, CH2), 5.21 (t, 2H, CH2), 5.11 (t, 2H, CH2). ^{13}C NMR (77 MHz, CD_3OH), δ / ppm: 62.26, 69.93, 72.01, 74.07, 112.07, 126.95, 130.28, 142.73, 152.27, 156.70, 159.58, 170.89. ^{195}Pt NMR (CD_3OH) δ/ ppm: -2705. IR (4000- 650 cm-1) *υ*: 3338 (O-H), 3071 (C-H stretch), 1607 (C=H, pyridine), 1476 - 1430(C-H stretch), 1219 (C-O), 773(C-H stretch). *Anal. Calc. for* $C_{19}H_{21}Cl_2N_3O_4$: C, 37.73; H, 3.41; N, 6.76; *Found*: C, 37.35; H, 3.75; N, 6.34. TOF MS-ES$^+$, m/z: 568.0847, $(M + 1)^+$.

Pt(teg)

Yield: 38 mg, dark orange powder (60%). ^{1}H NMR (400 MHz, CD_3OH) δ/ ppm: 9.98 (dd, 2H, 6 6''), 9.73 (s, 2H, 3' 5'), 9.71 (d, 2H, 3 3''), 9.29 (t, 2H, 4 4''), 9.13 (t, 2H, 5 5''), 5.90 (t, 2H, CH2), 5.40 (t, 2H, CH2), 5.22 (m, 2H, CH2), 5.14 (t, 2H, CH2), 5.11 (t, 2H, CH2), 5.04 (t, 2H, CH2). ^{195}Pt NMR (CD_3OH) δ/ ppm: -2708. IR (4000-650 cm-1) *υ*: 3332 (O-H), 3071 (C-H stretch), 1607 (C=H, pyridine), 1448 – 1429 (C-H stretch), 1220 (C-O), 774 (C-H stretch). *Anal. Calc. for* $C_{21}H_{23}Cl_2N_3O_4$: C, 38.96; H, 3.58; N, 6.49; *Found*: C, 38.48; H, 3.41; N, 6.32. TOF MS-ES$^+$, m/z: 612.1027, $(M + 1)^+$.

4.3.4 Chemicals and solutions

Solutions of chloro-complexes were prepared by dissolving known amount of the complex in methanol solution of constant ionic strength (*I*=0.01M, (0.009M $LiCF_3SO_3$ + 0.001M LiCl)). Solutions of **Pt(eg), Pt(deg)** and **Pt(teg)** were dissolved to give platinum concentrations of 5.00 x 10^{-5} M each. The 0.01 M ionic strength solution used to prepare complex and nucleophile solutions was made up of required amounts of $LiCF_3SO_3$ (0.009M) and LiCl (0.001M) dissolved in dry methanol since $CF_3SO_3^-$ does not coordinate to Pt(II).[45] Lithium chloride was added to suppress spontaneous solvolytic reactions. Nucleophile solutions were prepared by dissolving a known amount of the required nucleophile in 50 mL of methanol solution of constant ionic strength to afford a concentration of *ca.* 100 times that of the metal complex. Subsequent dilutions of the stock solution were done to afford a series of standards of 80, 60, 40 and 20 times that of the platinum complex.

4.3.5 Physical measurements and instrumentation

Kinetic measurements were done using a Varian Carry 100 Bio UV-VIS spectrophotometer with an attached Varian Peltier temperature control unit with online kinetics application. All the UV-VIS spectrophotometric measurements were thermostatically controlled to within ± 0.1^0 C. All kinetic measurements were performed under *pseudo*-first-order conditions *i.e.*, at least 10 fold excess of nucleophile concentration was used. The spectral changes resulting from mixing of complex and ligand solutions were recorded over the wavelength range of 200 - 800 nm and a suitable wavelength at which kinetic measurements could be performed was determined. Reactions were initiated by mixing equal volumes of metal complex and azole solutions in a tandem cuvette on the UV-visible spectrophotometer and the rate of complex formation was followed by monitoring the decrease in absorbance at 310 nm. All the kinetic measurements are reproducible within the limits of error of ± 0.5%. The quoted values are the average of three runs under identical experimental conditions. Figure 4.1 shows an absorbance spectrum for the reaction of **Pt(eg)** and **Im** at 298 K and *inset* is a kinetic trace obtained for the same reaction at 298 K . Other kinetic traces were presented in the supplementary information figures SI 4.17-4.22. Data for $\mathbf{Pt}^{60}$ was incorporated for comparison purposes.

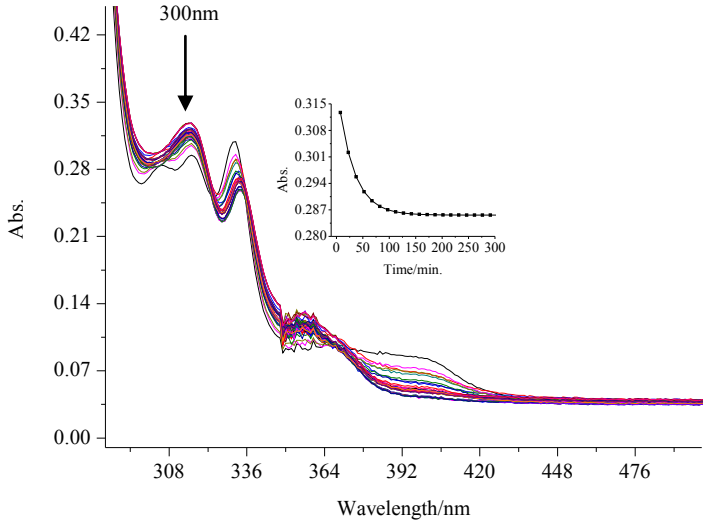


Figure 4.1 Absorbance spectra of Pt(eg) (5.0 x 10^{-5}M) and MIm (5.0 x 10^{-3}M) at 298 K.

The observed *pseudo* first-order rate constants, k_{obs}, were obtained from kinetic traces applying the online non-linear least-squares fit using equation 1

$$A_t = A_0 + (A_0 - A_\infty)e^{(-k_{obs}t)} \qquad (1)$$

Where; A_0 is initial absorbance of the mixture, A_t is absorbance of the reaction mixture at time, t and A_∞ is final absorbance. Second order rate constant, k_2, for the forward reaction and the solvolytic rate constant, k_{-2}, for each one of the Pt(II) complexes with a respective nucleophile were obtained from the slope and intercept respectively of the graph of k_{obs} verses nucleophile concentration drawn from graphical analysis software package, Origin 7.5®[46] from the relationship illustrated by equation 4.2

$$k_{obs} = k_2[Nu] + k_{-2} \approx k_2[Nu] \qquad (4.2)$$

A typical plot of k_{obs} verses $[Nu]$ is shown by figure 4.2 for the substitution reactions of **Pt(deg)** with **Im**, **Pz** and **Tz**. Other concentration dependence plots are presented in the

supplementary information figures SI 4.20, 4.22 and 4.24. Data for the concentration dependence is presented in supplementary information tables SI 4.1-4.3.

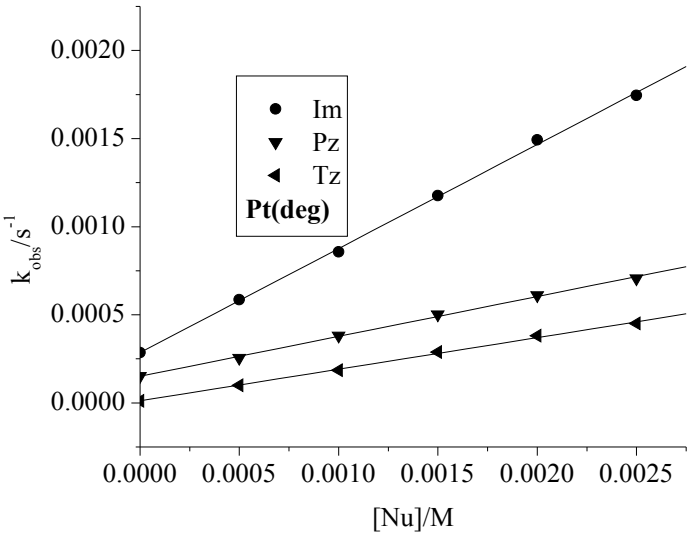


Figure 4.2 Concentration dependence plots to determine k_2 and k_{-2} from the reaction of **Pt(deg)** with **Im, Pz** and **Tz** at 298K.

The temperature dependence of the rate constants were studied over the temperature range of 20-40° C in increments of 5° C. Graphs of $\ln(k_2/T)$ verses $1/T$ were plotted using Origin 7.5®[46] from which activation parameters, enthalpy of activation, $\Delta H^{\neq}$ and entropy of activation, $\Delta S^{\neq}$ were obtained by applying the slope and the intercept respectively to the Eyring equation 3 where the letters represent their usual meaning.

$$\ln\frac{k_2}{T} = \left(\frac{\Delta H^{\neq}}{R}\right)\frac{1}{T} + \left(23.8 + \frac{\Delta S^{\neq}}{R}\right) \qquad (3)$$

A typical Eyring plot is shown in figure 4.3 for the reaction of **Pt(eg)** with **MIm**, **DIm** and **Tz**. Other Eyring plots are presented in the supplementary information figures SI 4.21, 4.23 and 4.25. Respective data for Eyring plots is presented in the supplementary information tables SI 4.4-4.6.

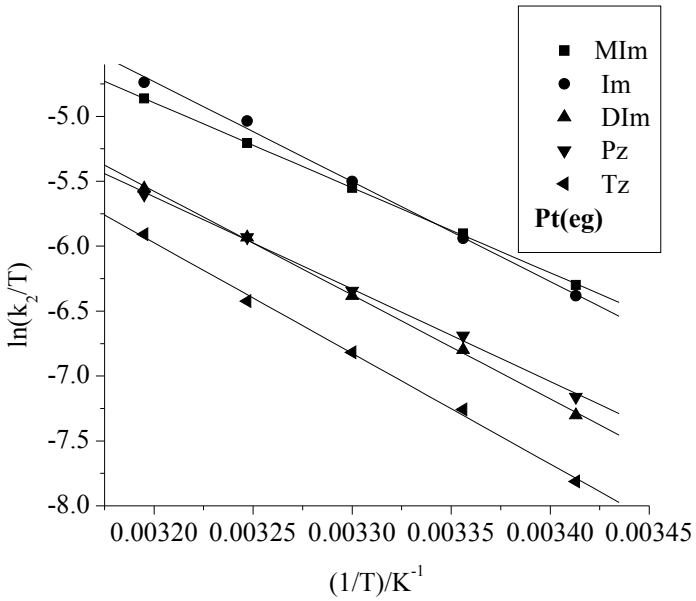


Figure 4.3 Eyring plots for the reaction of **Pt(eg)** with **MIm**, **DIm** and **Tz**

4.3.6 Computational details

To gain further insight on the structural and electronic differences among the complexes in this study, computational calculations were done at the DFT level of theory that has been applied by other researchers.[47-50] DFT calculation data in systems that contain transition metals have shown better agreement with experimental data than that obtained from Hartree–Fock (HF) calculations.[51] The LANL2DZ basis set was employed in the current case because it is known to provide reliable results in systems of this nature.[50,52-55] Singlet states were used due to the low electronic spin of Pt(II) complexes. The frontier molecular orbitals of the complexes were generated in Gauss view 5.0 applying the same level of theory. The Gaussian09 suite of programs was used for all DFT computations.[56] A summary of the DFT calculated frontier HOMO and LUMO molecular orbitals of the complexes in the study are shown in table 4.1 while the data processed for the complexes is included in table 4.2.

Table 4.1 DFT-calculated frontier molecular orbitals of the investigated Pt(II) complexes.

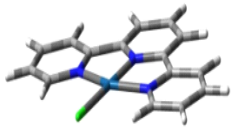
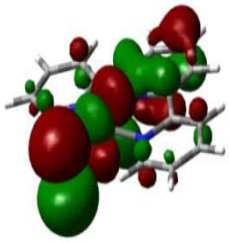
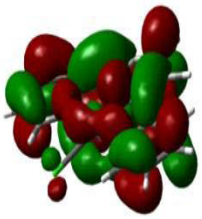
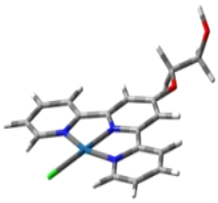
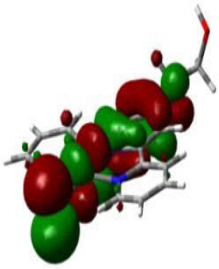
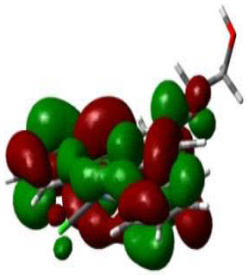
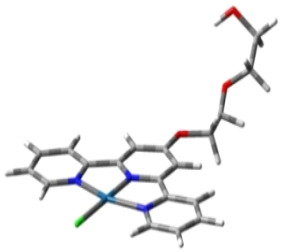
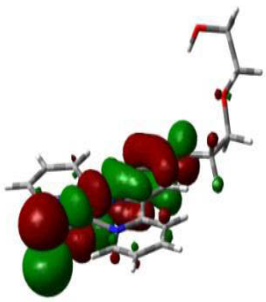
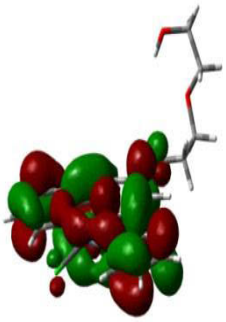
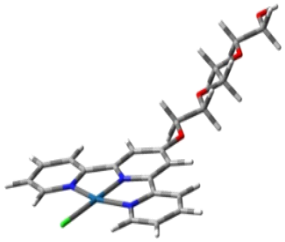
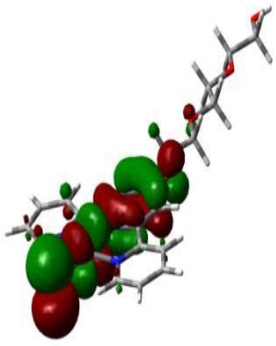
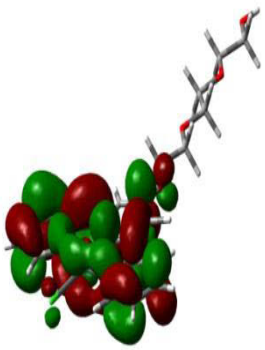
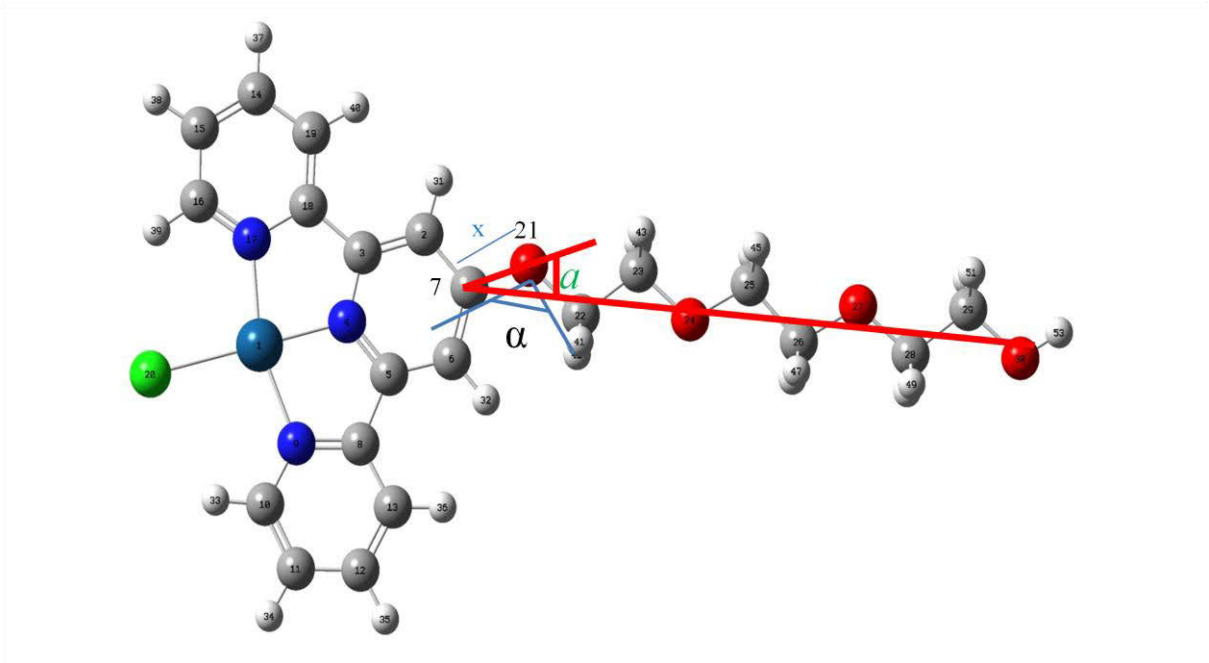
Complex	Lowest energy structure	Map	
		HOMO	LUMO
Pt			
Pt(eg)			
Pt(deg)			
Pt(teg)			

Table 4.2 Computational data of the complexes investigated

Property	**Pt**	**Pt(eg)**	**Pt(deg)**	**Pt(teg)**
Bond lengths (Å)				
Trans N-Pt	1.961	1.960	1.960	1.960
Cis N-Pt	2.049	2.048	2.051	2.048
Pt-Cl	2.443	2.444	2.444	2.442
C7 – O21, x, (Å)	-	1.369	1.369	1.369
Angles (^{0})				
Bite	161.90	161.69	161.70	161.71
Trans N-Pt-Cl	179.99	179.76	179.77	179.81
Angle of elevation ,***a***, of the ethylene glycoxy pendant. (°)	-	37.55	36.44	19.38
C7 O21 C22, α, (°)	-	120.2	120.5	120.7
Energy (eV)				
LUMO	-3.35	-3.23	-3.23	-3.23
HOMO	-7.04	-6.89	-6.89	-6.89
$\Delta E_{LUMO-HOMO}$	3.69	3.66	3.66	3.66
NBO Charges				
Pt^+	0.605	0.591	0.591	0.590
N(*trans*)	-0.453	-0.471	-0.470	-0.471
Dipole moment (D)	13.30	11.51	10.72	6.83
Electronic chemical potential (μ)	-5.20	-5.06	-5.06	-5.06
Electrophilicity index (ω)	7.31	6.94	6.97	7.00
Chemical hardness (η)	1.85	1.83	1.83	1.83
Point group	C_1	C_1	C_1	C_1

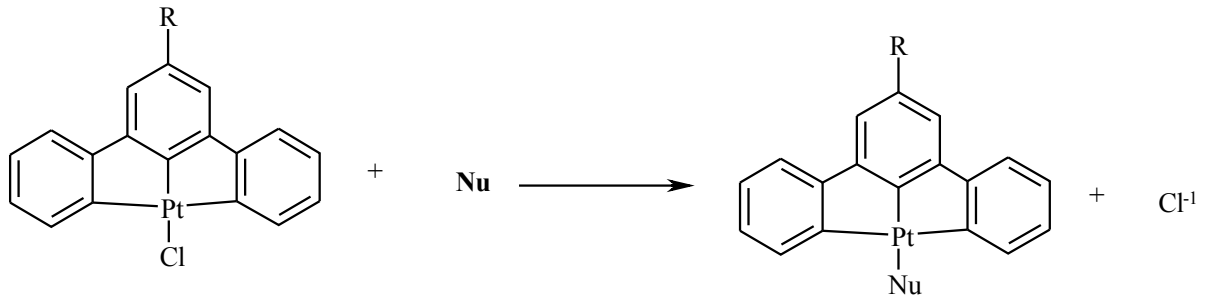


α = 120.7°, a = 19.38° x = 1.369Å

Figure 4.4 DFT calculated angles around the oxygen atoms on the polyglycoxyl group of **Pt (teg)**

4.3.7 Kinetic analysis

Substitution of the coordinated chloride from **Pt(eg), Pt(deg)** and **Pt(teg)** by the azole nucleophiles *viz* imidazole, 1,2-dimethylimidazole, pyrazole, 1,2,4-triazole and 1-methylimidazole was investigated. UV-visible spectrophotometry was used to track the progress of the reaction. All the kinetic traces were described by single exponentials with the *pseudo* first order rate constants calculated from the traces plotted against the concentration of incoming nucleophiles giving straight lines with negligible intercepts (figure 4.2). Values of second order rate constant, k_2, representing direct attack of by nucleophile according to equation 4.2 are shown in table 4.3. Solvolytic rate constants, k_{-2}, values are infinitesimal (averagely 10^5 times less than k_2) showing that the reaction proceeds predominantly by the direct attack by nucleophile. The proposed mechanism of substitution for the studied complexes can be represented by scheme 4.3.



R = eg, deg, teg Nu = MIm, Im, DIm, Pz, Tz

Scheme 4.3 Proposed mechanism of substitution for the studied complexes.

4.4 Results and discussion

Table 4.3 Rate constants and activation parameters for Pt(II) complexes with the azole nucleophiles.

Complex + Nu	k_2($M^{-1}s^{-1}$)	$\Delta H^{\neq}$ (Kj mol^{-1})	$\Delta S^{\neq}$ ($JK^{-1}mol^{-1}$)
Pt*			
Imidazole	3.98 ± 0.05	41 ± 3	-96 ± 10
Pyrazole	2.25 ± 0.11	42 ± 1	-96 ± 5
1-methylimidazole	3.84 ± 0.04	42 ± 2	-91 ± 5
1,2-dimethylimidazole	1.62 ± 0.04	46 ± 1	-88 ± 3
1,2,4-riazole	1.04 ± 0.07	40 ± 2	-107 ± 6
Pt(eg)			
Imidazole	0.610 ± 0.01	64 ± 3	-33 ± 10
Pyrazole	0.209 ± 0.004	59 ± 2	-55 ± 6
1-methylimidazole	0.734 ± 0.11	54 ± 1	-64 ± 3
1,2-dimethylimidazole	0.269 ± 0.004	67 ± 3	-31 ± 9
1,2,4-triazole	0.180 ± 0.01	71 ± 1	-21 ± 3
Pt(deg)			
Imidazole	0.611 ± 0.01	69 ± 3	-16 ±10
Pyrazole	0.226 ± 0.01	59 ± 1	-57 ± 3
1-methylimidazole	0.740 ± 0.02	57 ± 1	-56 ± 3
1,2-dimethylimidazole	0.284 ± 0.01	61 ± 3	-49 ± 9
1,2,4-triazole	0.185 ± 0.004	62 ± 1	-50 ± 5
Pt(teg)			
Imidazole	0.612 ± 0.02	62 ± 1	-40 ± 4
Pyrazole	0.242 ± 0.01	58 ± 2	-59 ± 5
1-methylimidazole	0.760 ± 0.02	65 ± 2	-28 ± 5
1,2-dimethylimidazole	0.293 ± 0.01	55 ± 1	-69 ± 3
1,2,4-triazole	0.158 ± 0.004	63 ± 2	-47 ± 5

(*) data extracted from Ref. 60 (b)

The data in table 4.3 indicate higher reactivity for **Pt*** complex than **Pt(eg), Pt(deg)** and **Pt(teg).** There is about six fold drop in the reactivity for most studied nucleophiles when the ethylene glycoxy unit is added in the 4'-position revealing that the substituent donate

electron-density towards the terpy system. The lone pair of electrons on the first oxygen atom (O21 figure 4.4) is in close proximity to the extended π-conjugation of the terpyridyl unit allowing greater delocalization into the pyridyl rings.[57,58] Donation of electron density towards the Pt(II) centre is also reflected in the raised LUMO energy of **Pt(eg)** (-3.23 eV) compared to that of **Pt** (-3.35 eV)(table 4.2) which makes it harder for π-back donation for **Pt(eg)**. The higher enthalpy of activation of **Pt(eg)** (table 4.3) also lends credence to its lower reactivity arising from the effects of electron donation hence higher energy is now needed to form the transition state complex. The π-donation along with σ-electron donation increases the negative charge on the *trans* nitrogen atom (table 4.2) of **Pt(eg)** compared to **Pt** and thus lowers the charge on the Pt(II) centre from 0.605 to 0.591 as well as the electrophilicity of the complex which changes from 7.31 to 6.94 revealing that there is electron flow towards the metal centre which can be accounted for in terms of *trans*-effect.

The C7- O21(figure 4.4) bond length (1.369Å) (table 4.2) is shorter than the other C-O bonds (range 1.456 - 1.467Å) also reported elsewhere,[59] further, α (figure 4.4) angles of about 120° indicate that the oxygen atom (figure 4.4) has sp^2 character and hence proves delocalization of the lone pair of electron into the π-system of the terpy. The donation of electron-density to the terpyridyl rings reduces the π-accepter capabilities of terpy bearing the polyglycoxyl substituents causing the platinum centre and the whole complex to be less electropositive hence less reactive.[57,58] The dipole moments of the Pt(II) complexes (table 4.2) corroborate the fact that the terpy unit of **Pt** has highest extended π-withdrawing character hence most electropositive platinum centre.[58] The substituent in the 4'-position on **Pt(eg)** being inclined at an angle of 120° introduces steric hindrance on one side of this complex unlike in **Pt** without any substituent. The inclined pendant hinders nucleophiles approaching the complex from the axial position an additional contribution to the reduction in the reactivity.

The reactivity remains fairly constant on addition of other substituents with more ethylene glycoxyl units in the 4'-position (table 4.3) for the studied complexes. A similar trend is observed for all the other incoming nucleophiles. One would have expected the reactivity to decrease due to increase in electron donation as the chain length increases but from DFT calculations, the charges on Pt(II) centre and on the *trans* nitrogen atom remain constant for **Pt(eg), Pt(deg)** and **Pt(teg)** indicating that there is no further electronic effects as the ethylene glycoxy unit grows beyond the first glycol unit. Even the global electrophilicity indices show insignificant increase with increase in the length of the pendant (table 4.2). It

can then be concluded that after the first glycol unit, both electronic and steric hindrance have minimal or no influence on the reactivity of the complexes. This is despite the angles of inclination, *a,* for **Pt(eg), Pt(deg)** and **Pt(teg)** decreasing from 37.55°, 36.44° and 19.38° respectively (table 4.2). Very weak intra-molecular hydrogen bonding interactions between the lone pairs of electrons on the oxygen atoms and neighbouring hydrogen atoms as shown in figure 4.5.[58(c)]

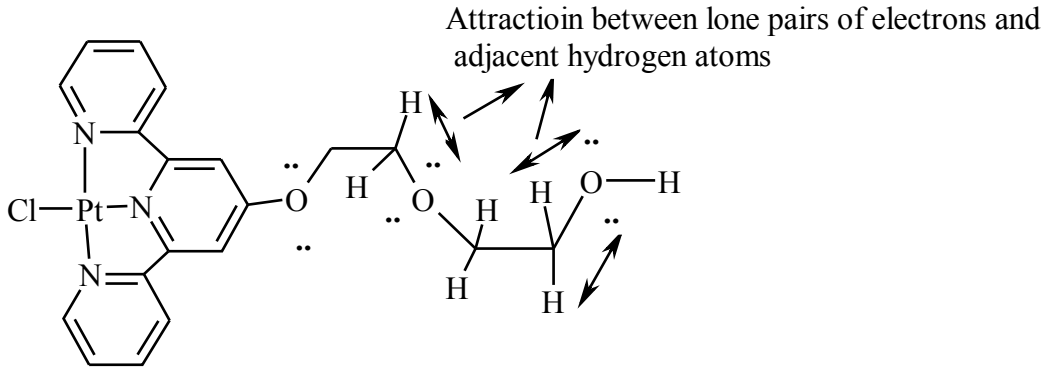


Figure 4.5 Hydrogen bonding interactions in the polyglycoxyl pendant

While the predominant factor remains electron donation to the terpyridyl ring, the stabilization by hydrogen bonding actually seems to play a significant role as increase in chain length of the glycol unit from **Pt(eg)** to **Pt(deg)** and **Pt(teg)** resulted in increase in k_2 values for all the nucleophiles.

It's worth noting that while the electron density in the chain increases with the increase in the chain length of the appended group; the donation of electron density towards the Pt atom becomes less effective as the chain length of the pendant increases.[59] The geometry of the platinum centres remains distorted square-planar with bite angles of 160 – 161° (table 4.2), a slight deviation from planarity typical of Pt(II) square planar complexes.[60] Table 4.2 has a summary of calculated bond lengths, energies of frontier molecular orbitals and electron density surrounding the Pt(II) centre for each of the Pt(II) complexes. It can be observed that the introduction of the ethylene glycoxyl units has negligible influence on the structural differences which was also observed by others working with similar compounds.[60] There is decrease in the positive charge (electrophilicity) on the Pt(II) centre on introduction of the polyglycoxyl units as already observed due to electron donation hence decrease in reactivity an effect previously noted in similar complexes.[61,62] The DFT-calculated ground-state

orbitals in table 4.1 show that the addition of the glycoxyl units causes the electron density of the HOMO to be centred above and below the Pt(II) metal centre and towards the glycoxyl substituent along the *trans* axis causing a less electrophilic metal centre, an effect reported by other researchers as well.[60] The electrophilicity index changes from **Pt**(7.31), to **Pt(eg)**(6.94), **Pt(deg)**(6.97) and **Pt(teg)**(7.00) (table 4.2) an indication **Pt** is the strongest electrophile compared to the rest of the nucleophiles.[63,64]

The trend in the reactivity of the nucleophiles investigated is **Im > Py** > **Tz** also observed in other reports.[52] The decrease in the reactivity correlates with their basicities; 7.00, 2.52 and 2.19 respectively though the trend is non-linear because **Tz** is unique as a result of its tautomerism even though the 1H form is predominant.[65] The reactivity of the other set of nucleophiles follows the order; **MIm** > **Im** > **DIm** having basicities of 7.30, 7.00 and 7.85 respectively.[65] The reactivity doesn't correlate with the basicities because steric hindrance brought about by the presence of methyl groups on **DIm** comes into play.[38] The overall trend in reactivity for the nucleophiles is **MIm** > **Im** > **DIm** > **Py** > **Tz**[38] consistent with their respective basicities except for **DIm** because of its steric bulk.

The observed trend agrees with previous studies on $[Pd(terpy)Cl]^+$ and $[Pt(terpy)Cl]^+$ complexes with pyridines[66,67] and $[Pt(terpy)Cl]^+$ complex with five membered N-donor heterocyclic ligands.[68] The magnitude of steric effects is attributed to the free rotation of the ligand around the Pt-N(azole) bond.[68] In the associative mode of reaction, the Pt-N(azole) bond is well formed and Pt-Cl bond weakened at the transition state, the trigonal bipyramidal intermediate contains pyridine rings on either side of the terpy in axial positions where the pyridyl protons sterically interact with α-methyl protons of the incoming nucleophiles which impede free rotation of the just formed Pt-N(azole) bond[68,69] effectively retarding the reaction. The effects of bulky azoles affect the energy of both ground state and transition state complexes hence the observed reaction rate (table 4.3).[70] Steric hindrance due to interaction between α-substituted methyl with solvent that causes charge dispersion through hydrogen bonding with solvent reducing basicity of the nucleophile in solution could have played a role in the slow reaction of **DIm**.[70,71] The higher reactivity of **MIm** is due to the inductive effects of the methyl group attached to N1 of the imidazole ring that results in the donation of electrons from the methyl group to N3 making it more basic. Since the methyl in **MIm** is further from the pyridyl rings on the terpy, steric congestion in the transition state is unlikely

or minimal. For **DIm**, steric effects prevail over inductive effects of the methyl groups,[69,72] accounting for the difference in reactivities.

The intercepts were insignificantly small indicating that the reverse reactions are very slow or absent the reason being that the Pt-N(azole) bond formed is stabilized by the π-back-bonding with the Pt(II) centre.[27] Values of enthalpy of activation, $\Delta H^{\neq}$, are relatively low while those of entropy of activation, $\Delta S^{\neq}$, are large and negative confirming an associative mode of substitution typical of Pt(II) square planar complexes.[73-76]

4.5 Conclusions

This study clearly reveals that electron donation towards the terpy chelate by the 4'-substituted polyglycoxyl units decreases the π-accepter ability of the chelate making the platinum centre of these complexes less electrophilic retarding their ligand substitutions reactions when compared to that of **Pt.** The electron donation is only effective up to the first oxygen atom (O21 figure 4.4) beyond which no significant electronic effect affect the Pt(II) centre. The overall decrease in reactivity from **Pt** to **Pt(eg)** mostly due to the electronic effect and to a minimal extent the steric factor. The reactivity of the nucleophiles is controlled by the basicity and steric hindrance, with the more basic nucleophiles being more reactive but steric factors come into play for the bulky nucleophiles.

4.6 References

1. T. Rau and R.van Eldik, *Met. Ions Biol. Syst*., 1996, **32**, 339
2. B. Lippert, *Cisplatin Chemistry and Biochemistry of Leading Anticancer Drugs*, ed., Wiley-VCH, Zùrich, 1999
3. C. S. Peyratout, T. K. Aldridge, D. K. Crites and D. R. McMillin, *Inorg. Chem*., 1995, **34**, 4484.
4. G. T. Morgan, and F. H Burstall, *J. Chem. Soc*., 1932, **20**.
5. G. T. Morgan, and F. H Burstall, *J. Chem. Soc*., 1937, 1649.
6. E. C. Constable, *Adv. Inorg. Chem. Radiochem.*, 1987, **30**, 69.
7. D. Jaganyi, F. Tiba, O. Q. Munro, B. Petrovic and Z. D. Bugarcic, *Dalton Trans*., 2006, 2943–2949.
8. D. Jaganyi, K. L. De Boer, J. Gertenbach and J. Perils, *Int. J. Chem. Kinet*., 2008, **40**, 808–818
9. R. Romeo, M. R. Plutino, L. M. Scolaro, S. Stoccoro and G. Minghetti, *Inorg. Chem*., 2000, **39**, 4749–4755.
10. B. Lippert , *Cisplatin Chemistry and Biochemistry of a Leading Anticancer Drug*. Wiley-VCH, Weinheim, 1999, pp1-27
11. P. Banerjee , *Coord Chem Rev.,*1999, 190-192: 19-28
12. A. Hofmann, D. Jaganyi, O. Q. Munro, G. Liehr and R. van Eldik, *Inorg. Chem*., 2003, **42**, 1688–1700.
13. D. Petrovic, B. Stojimirovic, B. Petrovic, Z. M. Bugarcic and Z. D. Bugarcic, *Bioorg. Med. Chem*., 2007, **15**, 4203–4211.
14. D. Jaganyi, A. Hofmann and R. van Eldik, *Angew. Chem., Int. Ed*., 2001, **40**, 1680–1683
15. E. C. Constable, A. J. Edwards, R. Martínez-Máñez, P. R. Raithby, and A. M. W. Cargill Thompson, *J. Chem. Soc., Dalton Trans.*, 1994, 645.
16. E. C. Constable, R. Handel, C. E. Housecroft, M. Neuburger, E. R. Schofield, and M. Zehnder, *Polyhedron*, 2004, **23**, 135.
17. E. C. Constable, B. Kariuki, and A. Mahmood, *Polyhedron*, 2003, **22**, 687.
18. E. C. Constable, C. E. Housecroft, L. A. Johnston, D. Armspach, M. Neuburger, and M. Zehnder, *Polyhedron*, 2001, **20**, 483.
19. D. Armspach, E. C. Constable, F. Diederich, C. E. Housecroft, and J.-F. Nierengarten, *Chem. Commun.*, 1996, 2009.

20. D. Armspach, E. C. Constable, F. Diederich, C. E. Housecroft, and J.-F. Nierengarten, *Chem. Eur. J.*, 1998, **4**, 723.
21. G. Albano, V. Balzani, E. C. Constable, M. Maestri, and D. R. Smith, *Inorg. Chim. Acta*, 1998, **277**, 225.
22. E. Figgemeier, V. Aranyos, E. C. Constable, R. W. Handel, C. E. Housecroft, C. Risinger, A. Hagfeldt, and E. Mukhtar, *Inorg. Chem. Commun.*, 2004, **7**, 117.
23. M. Maestri, N. Armaroli, V. Balzani, E. C. Constable, and A. M. W. Cargill Thompson, *Inorg. Chem.*, 1995, **34**, 2759.
24. E. C. Constable, and A. M. W. Cargill Thompson, *Polyhedron*, 1992, **11**, 2707.
25. C. A. Carr, J. M. Richards, S. A. Ross and G. Lowe, *J. Chem. Res*., 2000, **98**, 566.
26. P. O. Ongoma and D. Jaganyi, *Dalton Trans*., 2012, **41**, 10724–10730
27. B. Pitteri, M. Bortoluzzi, *Polyhedron*, 2006, **25**, 2698
28. J. D. Atwood, *Inorganic and organometallic reaction mechanisms, 2nd edn. Wiley-VCH inc., NY*, 1997**,** pp 43-61
29. R. J. Sundberg, R. B. Martin, *Chem Rev*., 1974, **74**, 471
30. Z. D. Bugarčič, A. T. Nandibewoor, M. S. A. Hamza, F. Heinemann, R. van Eldik., *Dalton trans*,2006, 2984
31. W. Kaim, B. Schwederski, *Bioinorganic chemistry: inorganic elements in the chemistry of life*, 1st edn. Wiley, NY, 1994, pp 16-35, 106-123
32. C. A. Hitchcock, *Bio-chem. Soc. Trans.,*1991, **19**, 782
33. M. H. Ibrahim, P.P.Duce, D.V. Prior, D. G. Barrat, J. J. Morris, P. J. Taylor, *J. Chem Soc.Perkin Trans.,*1989**,** **2**, 1355
34. M. Moet-Ner, *J Am Chem Soc*.,1988, **110**, 3071
35. J. Catalan, J. Elguero, *J. Chem. Soc. Perkin Trans.,*1983, **2**,1869
36. R. W. Taft, F. Anvia, M. Taageperia, J. Catalan, J. Elguerio, *J Am Chem Soc.,*1986**,** **108**, 3237
37. D. Jaganyi, D. Reddy, J. A. Gertenbach, A. Hofmann and R. van Eldik, *Dalton Trans*., 2004, 299–304.
38. D. Jaganyi, A. Shaira, D. Reddy, *Dalton trans*, 2013, **42**, 8426
39. (a) T. L. Gilchrist, *Heterocyclic Chemistry 2nd ed., Longman, Harlow*, 1992. (b) , U. Sampath, W. C. Putnam, T. A. Osiek, S. Touami, J. Xie, D. Cohen, A. Cagnolini, P. Droege, D. Klug, C. L. Barnes, A. Modak, J. K. Bashkin, S. S. Jurisson, *J. Chem. Soc., Dalton Trans.* 1999, 2049(c) P. R. Andres, Eindhoven University of Technology,

2004(d) H. S. Chow, PhD Thesis, University of Basel, Metal Complexes of 4'-Substituted-2,2':6',2"-Terpyridines in Supramolecular Chemistry, 2005, 33- 66.

40. G. R. Newkome, F. Cardullo, E. C. Constable, C. N. Moorefield, and A. M. W. Cargill Thompson, *J. Chem. Soc., Chem. Commun.*, 1993, 925.
41. D. Armspach, E. C. Constable, F. Diederich, C. E. Housecroft, and J.-F. Nierengarten, *Chem. Commun.*, 1996, 2009.
42. D. Armspach, E. C. Constable, F. Diederich, C. E. Housecroft, and J.-F. Nierengarten, *Chem. Eur. J.*, 1998, **4**, 723.
43. D. Armspach, E. C. Constable, C. E. Housecroft, M. Neuburger, and M. Zehnder, *J. Organomet. Chem.*, 1998, **550**, 193.
44. (a) E. C. Constable, and M. D. Ward, *J. Chem. Soc., Dalton Trans.*, 1990, 1405. (b) Perrin, D. D.; Armarego, W. L. F.; Perrin, D. R. *Purifiction of Laboratory Chemicals*; 2nd ed.; Pergamon: Oxford, 1980. (c) A. G. Becke, *J. Chem. Phys.* 1993, **98**, 5648(d) C. T. Lee, W. T. Yang, R. G. Parr, *Phys. Rev. B* 1988, **37**, 785(e) P. J. Hay, W. R. Wadt, *J. Chem. Phys.* 1985, **82**, 299.
45. (a) T. G. Appleton, J. R. Hall, S. F. Ralph, C. S. M.Thompson, *Inorg. Chem*., 1984, **23**, 3521. (b) R. C. Quardokus, Y. Lu, N. A. Wasio, C. S. Lent, F. Justaud, C. Lapinte, S. A. Kandel, *J. Am. Chem. Soc.* 2011, **134**, 1710. (c) *MOE (Molecular Operating Environment)*. (d) R. G. Parr, L. Szentpaly, S. Liu, *J. Am. Chem. Soc.* 1999, **121**, 1922(e) M. Elango, R. Parthasarathi, G. K. Narayanan, A. M. Sabeelullah, U. Sarkar, N. S. Venkatasubramaniyan, V. Subramanian, P. K. Chattaraj, *J. Chem. Sci.* 2005, **117**, 61(f) C. A. Mebi, *J. Chem. Sci.* 2011, **123**, 727.
46. Mocrocal^{TM}, Origin^{TM} Version 5.0, Microcal Software, Inc., One Roundhouse Plaza, Northampton, MA, 01060, USA, 1991-1997
47. C. Lee, W. Yang and R. G. Parr, Phys. Rev. B: Condens. *Matter*, 1988, **37**, 785.
48. A. D. Becke, *Phys. Rev. A*, 1988, **38**, 3098.
49. A. D. Becke, *J. Chem. Phys*., 1993, **98**, 5648
50. T. Shoeib and B. L. Sharp, *Metallomics*, 2012, **4**, 1308–1320.
51. T. Ziegler, *Chem. Rev*., 1991, **91**, 651–667.
52. H. -M. Wen, Y. -H. Wu, Y. Fan, L.-Y. Zhang, C.-N. Chen and Z.-N. Chen, *Inorg. Chem*., 2010, **49**, 2210–2221.
53. N. T. Abdel Ghani and A. M. Mansour, *Eur. J. Med. Chem*., **2012**, 47, 399–411.

54. A. B. Yongye, M. A. Giulianotti, A. Nefzi, R. A. Houghten and K. Martínez-Mayorga, J. Comput.-Aided Mol. Des., 2010, **24**, 225–235.

55. B. A. Blight, S.-B. Ko, J. Lu, L. F. Smith and S. Wang, *Dalton Trans*., 2013, **42**, 10089–10092.

56. G. W. Trucks, M. J. Frisch, H. B. Schlegel, G. E. Scuseria, J. R. Cheeseman, M. A. Robb, G. Scalmani, V. Barone, G. A. Petersson, B. Mennucci, H. Nakatsuji, M. Caricato, X. Li, A. F. Izmaylov, H. P. Hratchian, J. Bloino, G. Zheng, M. Hada, J. L. Sonnenberg, M. Ehara, K. Toyota, R. Fukuda, M. Ishida, J. Hasegawa, T. Nakajima, Y. Honda, O. Kitao, T. Vreven, H. Nakai, J. A. Montgomery Jr., J. E. Peralta, M. Bearpark, F. Ogliaro, J. J. Heyd, E. Brothers, K. N. Kudin, R. Kobayashi, V. N. Staroverov, J. Normand, K. Raghavachari, J. C. B. A. Rendell, S. S. Iyengar, J. Tomasi, M. Cossi, J. M. M. N. Rega, M. Klene, J. E. Knox, J. B. Cross, C. Adamo, V. Bakken, J. Jaramillo, R. Gomperts, R. E. Stratmann, O. Yazyev, A. J. Austin, R. Cammi, C. Pomelli, R. L. Martin, J. W. Ochterski, K. Morokuma, V. G. Zakrzewski, G. A. Voth, P. Salvador, J. J. Dannenberg, S. Dapprich, O. Farkas, A. D. Daniels, J. B. Foresman, J. V. Ortiz, J. Cioslowski and D. J. Fox, Gaussian 09 (RevisionA. 1), Inc., Wallingford, CT, 2009.

57. P. Y. Bruice, *Org. Chem.*, Prentice-Hall, Inc., New Jersey, 2nd edn, 1998.

58. (a)D. Stack, *Electron Withdrawing and Electron Donating Groups* (handout), University of Nebraska Omaha, http://myweb.unomaha.edu/~dstack/2250/overheads/EWG_EDG.pdf (b) D. P. Rillema, A. J. Cruz, C. Moore, K. Siam, A. Jehan, D. Base, T. Nguyen,W. Huang, *Inorg. Chem.,* 2013, **52**, 596 (c) P. O. Ongoma, D. Jaganyi, *Dalton Trans.,* 2013

59. (a) E. C. Constable, C. E. Housecroft, M. Neuburger, S. Schaffner, E. J. Shardlow, *Inorganica Chimica Acta,* 2007, **360**, 4069-4076 (b) D. Jaganyi, A. Mambanda, *Dalton Trans.,* 2011, **40**, 79 (c) D. Jaganyi, A. Mambanda, S. Hochreuther, R. van Eldik, *Dalton Trans.* 2010, **39**, 3595.

60. (a)D. Jaganyi, D. Reddy, *Dalton trans.*, 2008, 6724-6731. (b) D. Jaganyi, D. Reddy, J. Akerman, M. P. Akerman, *Trans. Met. Chem.,* 2011, **36,** 593-602

61. A. Hofmann, D. Jaganyi, O. Q. Munro G. Liehr and R. van Eldik, *inorg. Chem.*, 2003, **42**, 1688

62. C. J. Jones and J. R. Thornback, Medicinal Applications of Coordination Chemistry, Royal Society of Chemistry, Cambridge, 2007, p. 92–95.

63. R. Parthasarathi, M. Elango, V. Subramanian and P. K. Chattaraj., *Theor. Chem. Acc.,* 2005, **113,** 257
64. P. K. Chattaraj, U. Sarkar and D. R. Roy., *Chem. Rev.,* 2006, **106,** 2065
65. R. Katritzky, C. W. Rees, *Comprehensive Heterocyclic Chemistry*, vol 5. Pergamon Press, Oxford, 1984, 35-50, 169-225, 734-747
66. B. Pitteri and G. Marangoni, F. V. Viseutin, L. Cattalini and T. Bobbo, *polyhedron*, 1997, **17**, 475
67. Z. D. Bugargic, B. Petrovic and E. Zangrando, *Inorg. Chim. Acta.,* 2004, **357**, 2650
68. B. Pitteri and M. Bortoluzzi, *polyhedron,* 2006, **25**, 2698
69. B. Pitteri, G. Marangoni and L. Cattalini, *J. Chem. Soc. Dalton Trans.*, 1994, 3539
70. M. Bellicini, L. Cattalini, G. Marangoni and B. Pitteri, *J. Chem. Soc. Dalton Trans,*1994, 1805
71. J. Catalan and J. Elguero, *J. Chem. Soc. Parkin Trans.II.,* 1983, 1869
72. P. Bruno and M. Bortoluzzi, *polyhedron,* **25**, 2698
73. M. L. Tobe, & J. Burgess., *Inorganic Reaction Mechanisms,* Addison Wesley Longman Ltd., Essex, 1999, p30-43, 70-112
74. R. B. Jordan, *Reaction Mechanisms of Inorganic and Organometallic Systems,* Oxford University Press, 1991, p 29-74
75. J. D. Atwood, *Inorganic and Organometallic Reaction Mechanisms*, 2nd Ed., Wiley-VCH Inc., NY, 1997, p. 43-61
76. R. G. Wilkins., *Kinetics and mechanisms of Reactions of Transition Metal Complexes*, 2nd Ed., VCH, Weinhelm, 1991, p. 199-201, 221, 232-242

4.7 Supplementary Information

NMR, IR and mass spectra for ligands and complexes. Additionally, observed pseudo-first order rate constants, k_{obs}, at different concentrations and temperatures, concentration and temperature dependence plots for **Pt(eg)**, **Pt(deg)** and **Pt(teg)** and UV-visible kinetic traces.

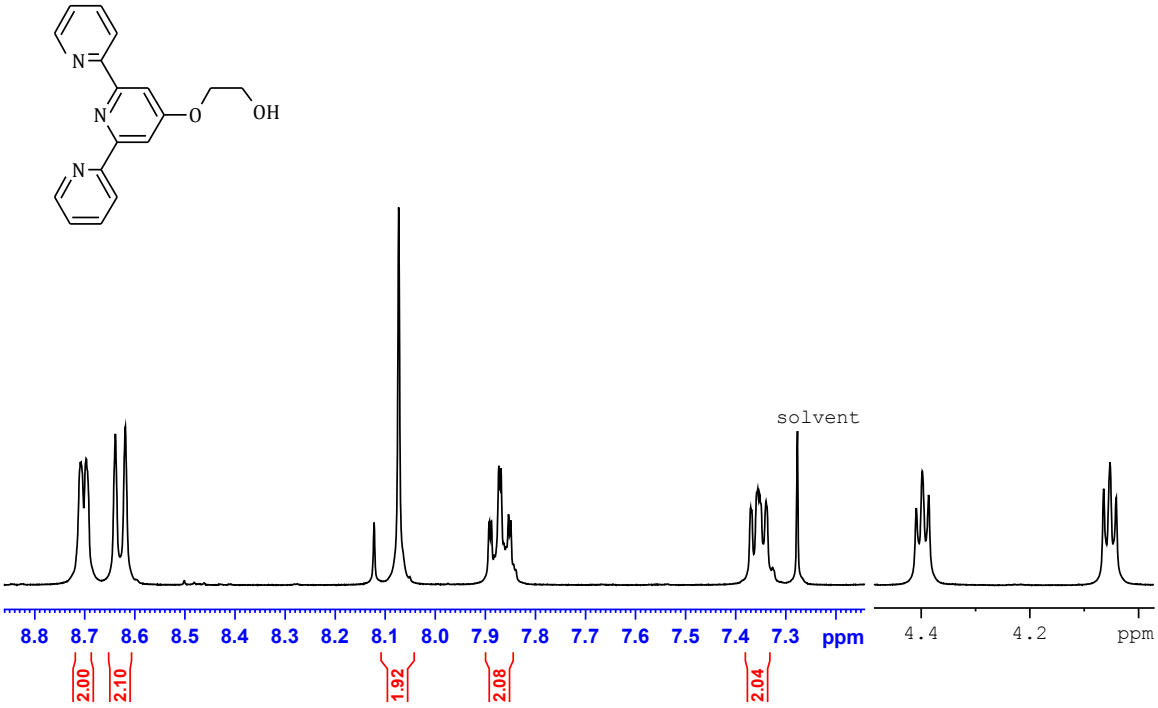


Figure SI 4.1 ^{1}H NMR spectrum of **tpy(eg)** in $CDCl_3$.

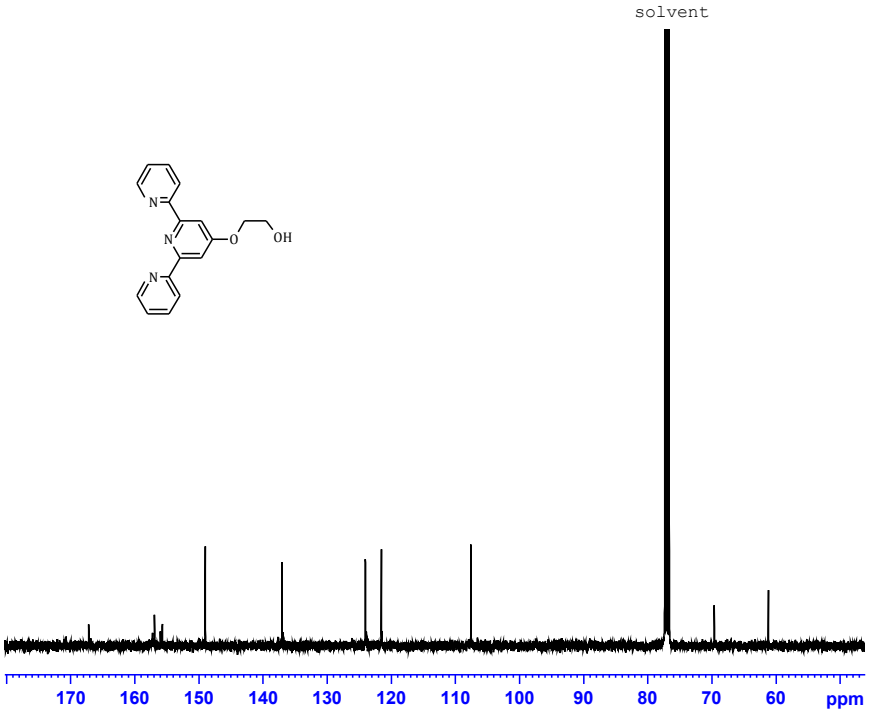


Figure SI 4.2 ^{3}C Spectrum of **tpy(eg)** in $CDCl_3$.

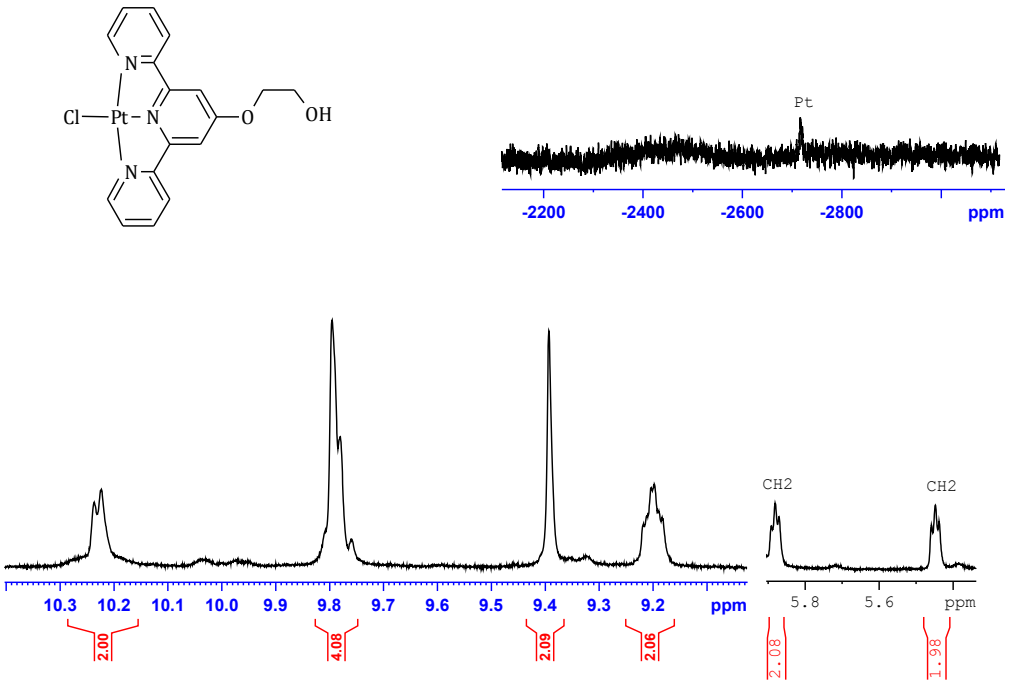


Figure SI 4.3 ^{1}H NMR and ^{195}Pt NMR spectra of **Pt(eg)**

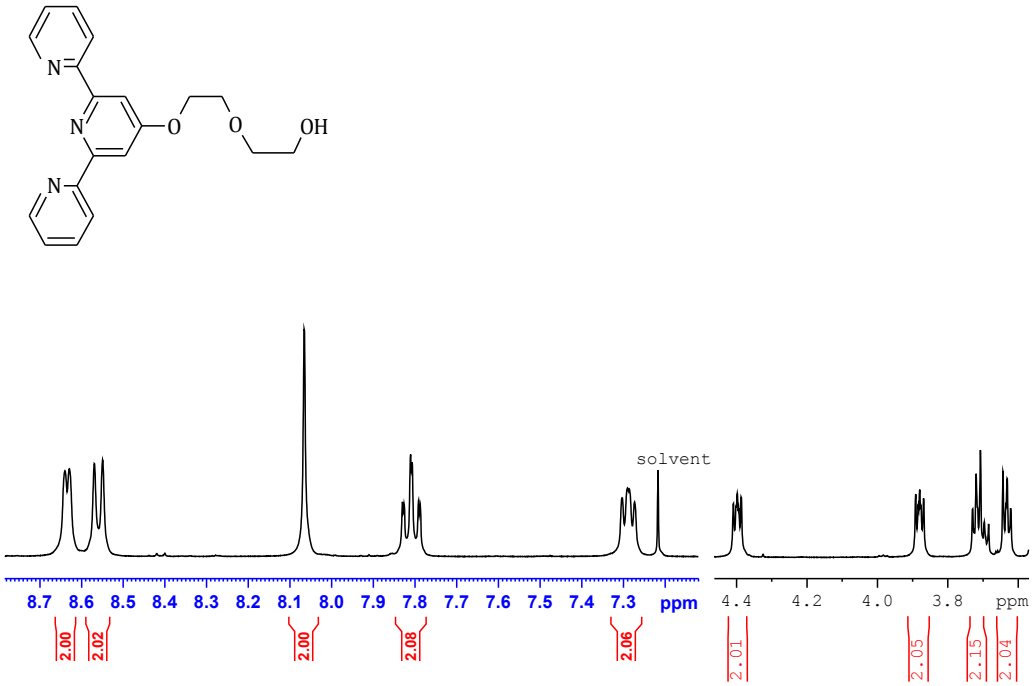


Figure SI 4.4 ^{1}H NMR spectrum of **tpy(deg)** in $CDCl_3$

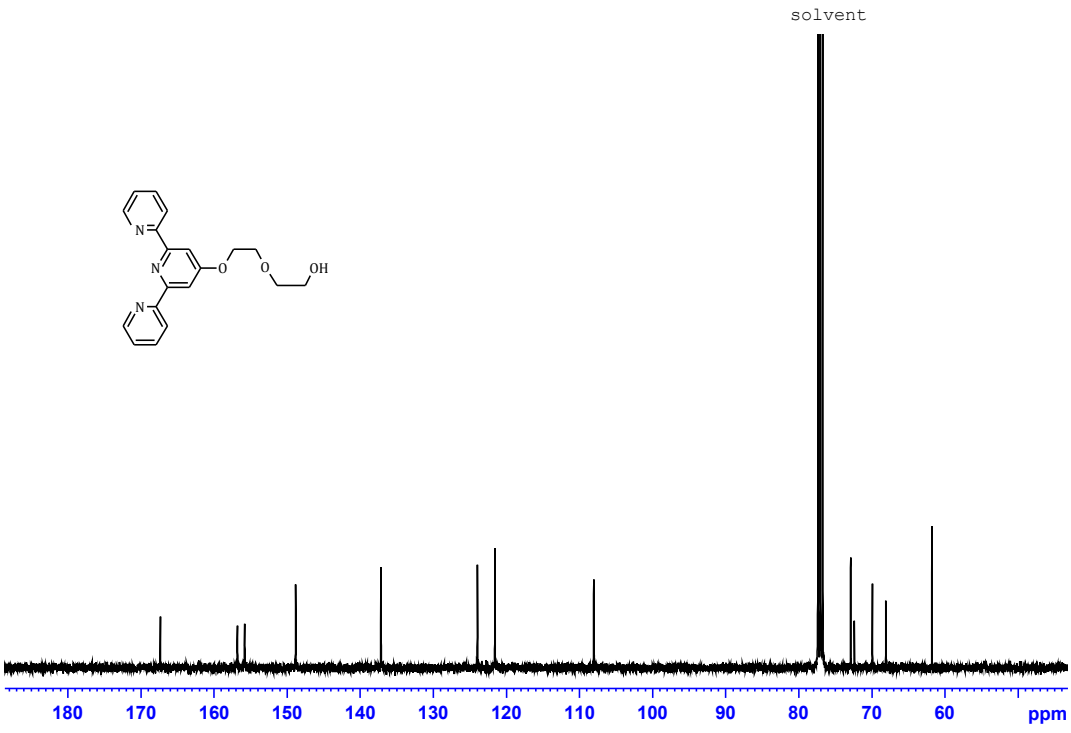


Figure SI 4.5 ^{13}C NMR spectrum of **tpy(deg)** in $CDCl_3$.

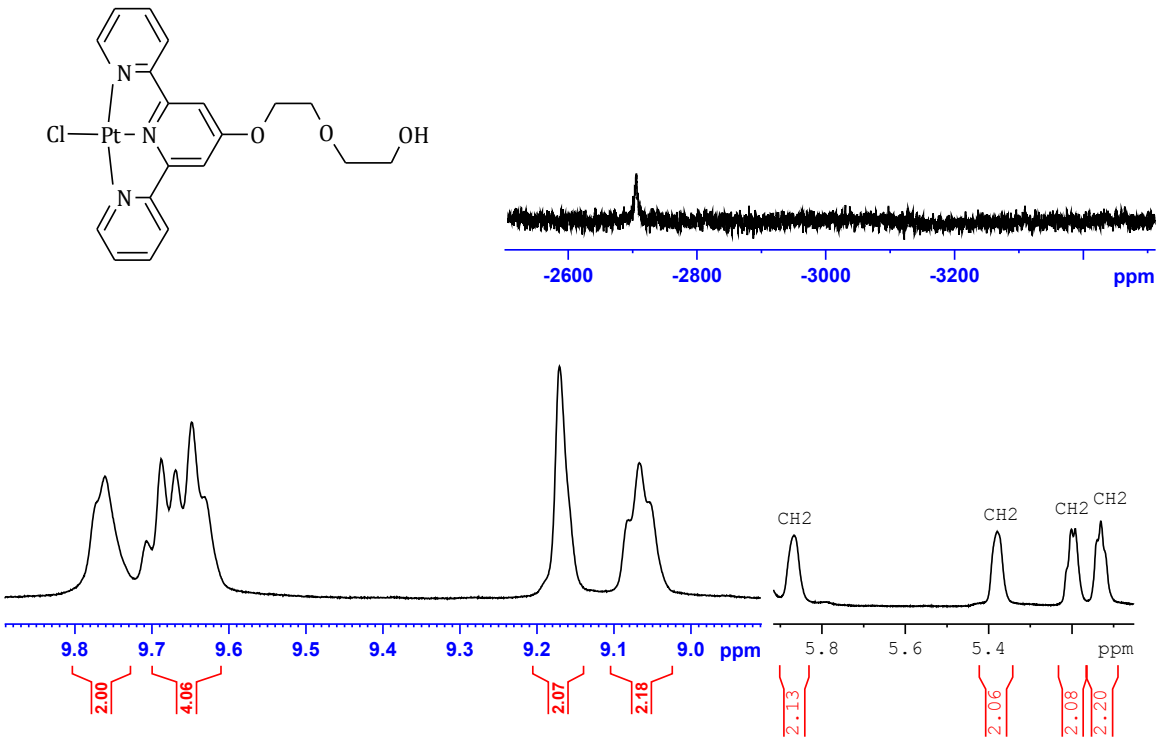


Figure SI 4.6 ^{1}H NMR and ^{195}Pt NMR spectra of **Pt(deg)**.

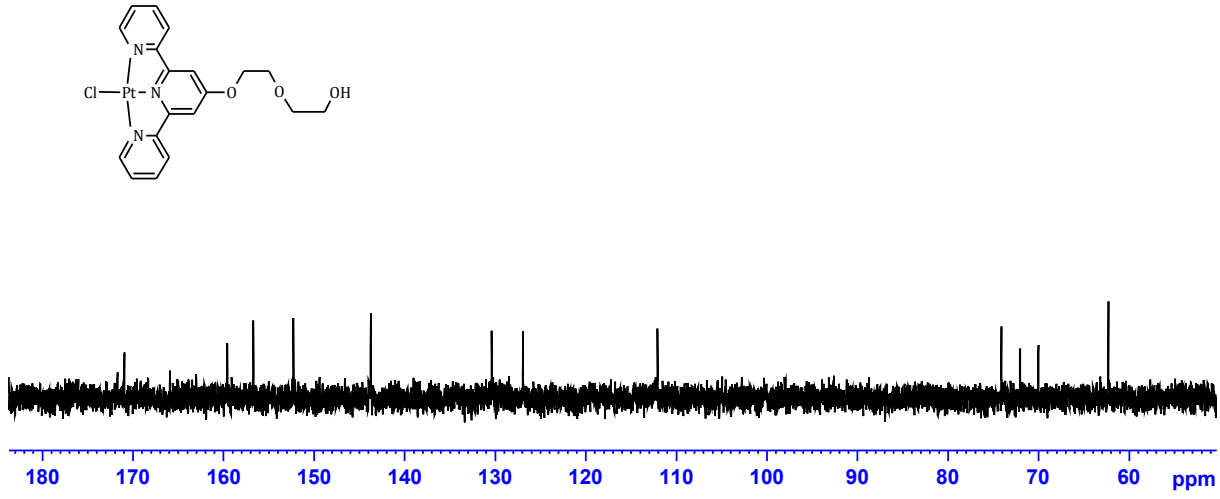


Figure SI 4.7 ^{13}C NMR spectrum of **Pt(deg)**

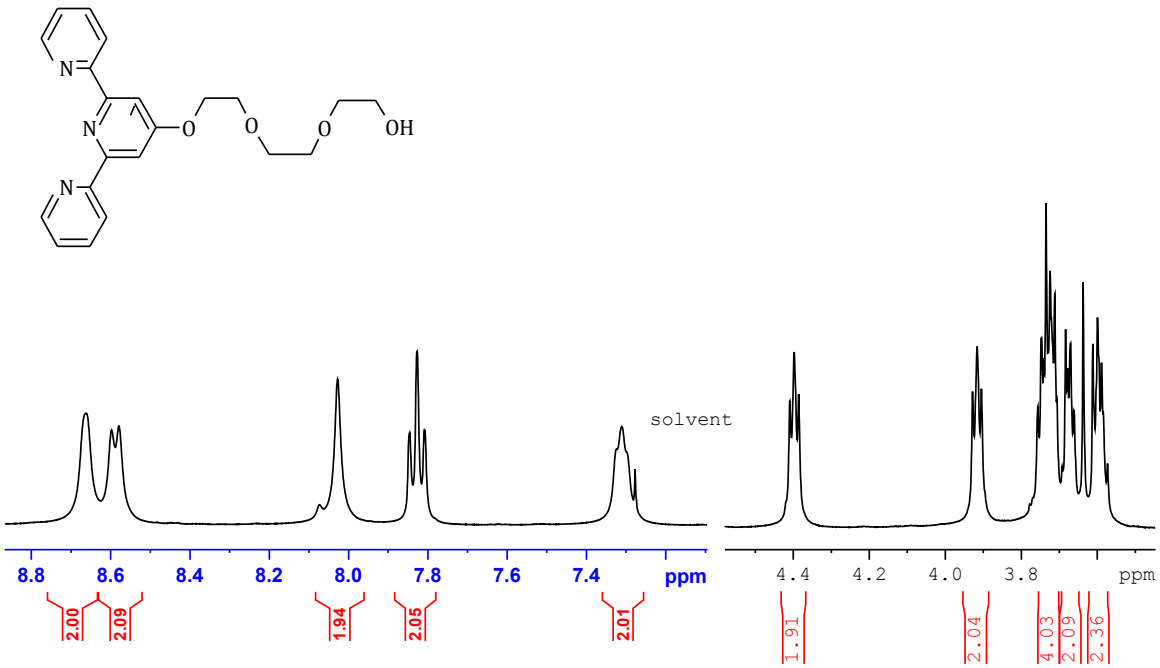


Figure SI 4.8 ^{1}H NMR spectrum of **tpy(teg)** in $CDCl_3$.

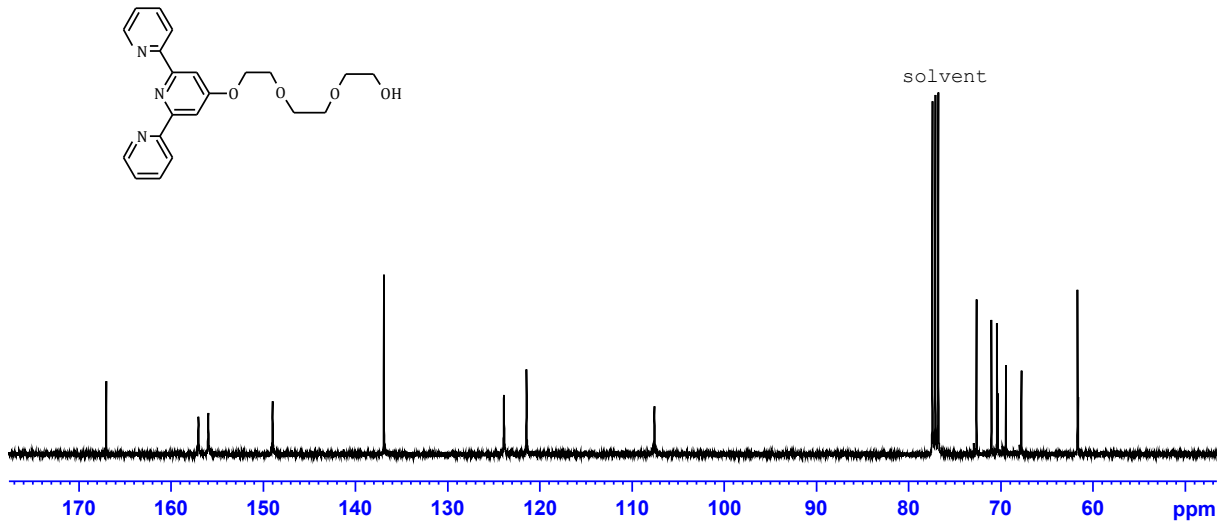


Figure SI 4.9 ^{13}C NMR spectrum of **tpy(teg)** in $CDCl_3$.

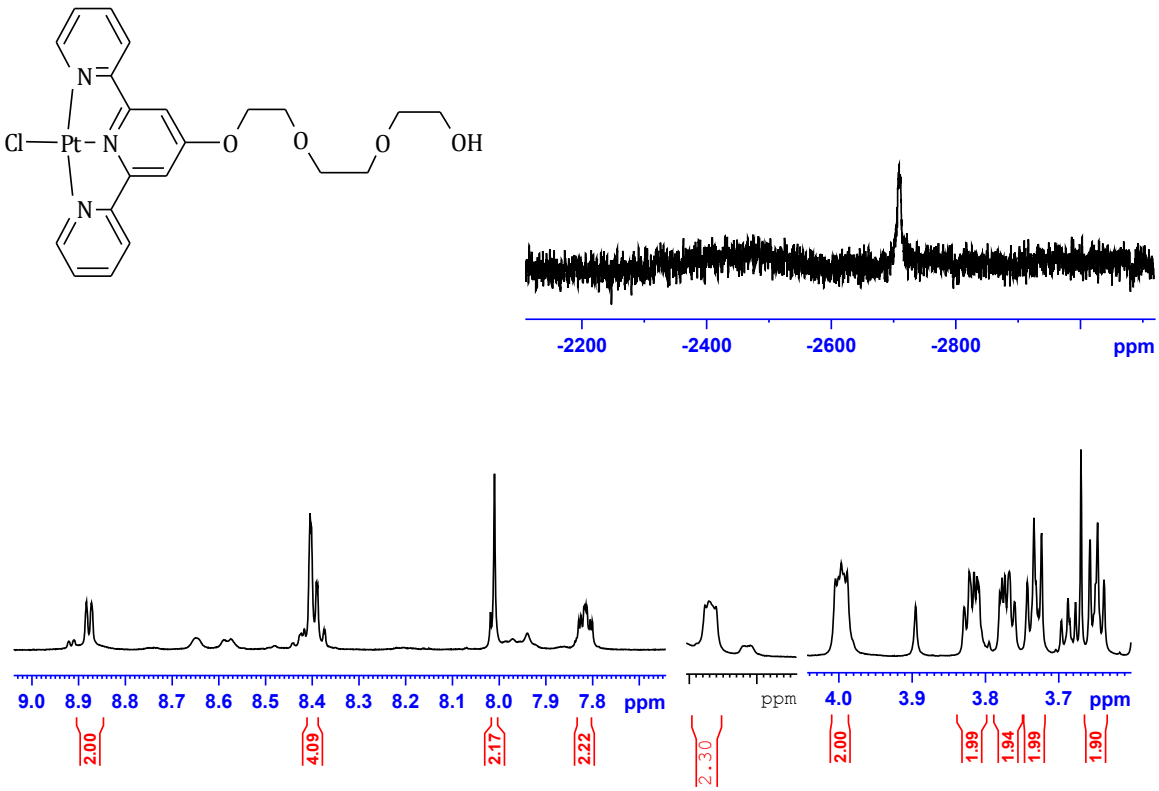


Figure SI 4.10 ^{1}HNMR and ^{195}Pt NMR spectra of of **Pt(teg).**

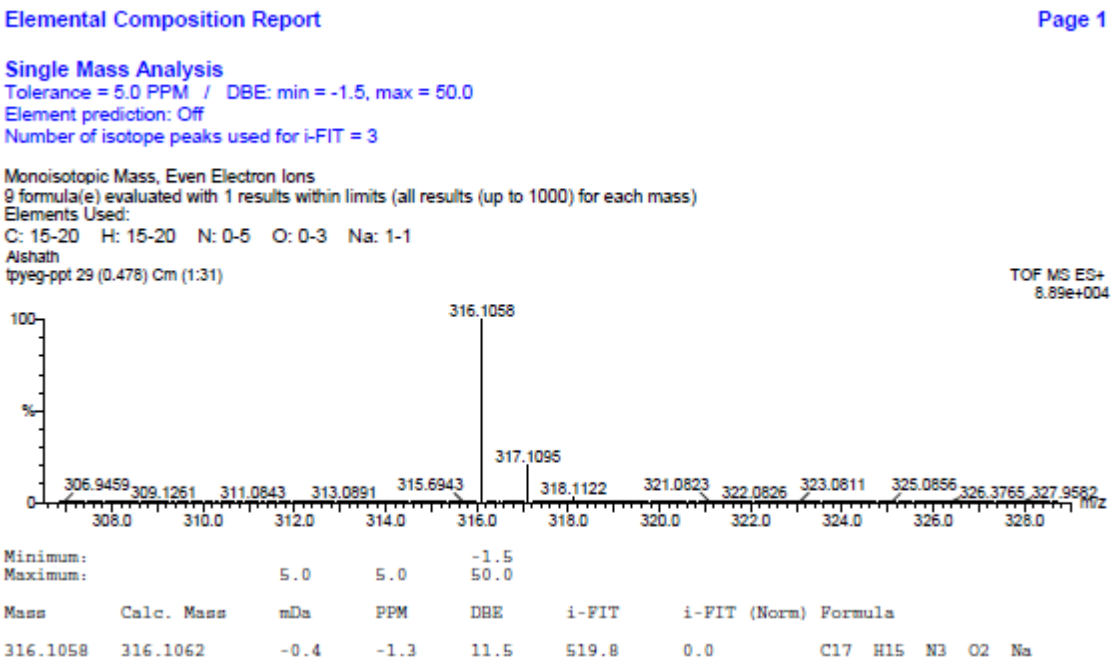


Figure SI 4.11 Low resolution ESI mass spectrum of **tpy(eg).**

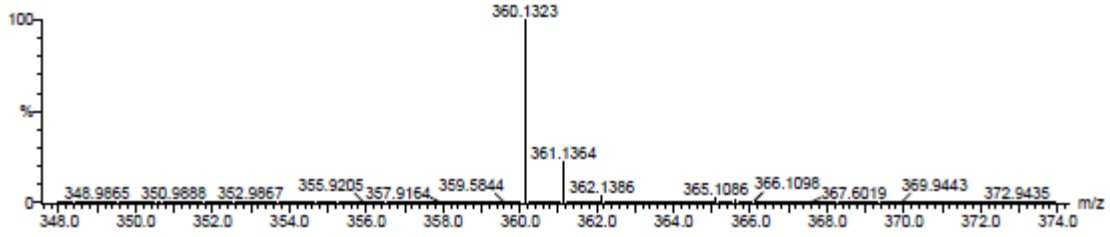
Elemental Composition Report Page 1

Single Mass Analysis
Tolerance = 5.0 PPM / DBE: min = -1.5, max = 50.0
Element prediction: Off
Number of isotope peaks used for i-FIT = 3

Monoisotopic Mass, Even Electron Ions
15 formula(e) evaluated with 1 results within limits (all results (up to 1000) for each mass)
Elements Used:
C: 15-20 H: 15-20 N: 0-5 O: 0-5 Na: 1-1

Alshath
tpydeg 16 (0.257) Cm (1:30)

TOF MS ES+
2.01e+005



Minimum:				-1.5			
Maximum:		5.0	5.0	50.0			
Mass	Calc. Mass	mDa	PPM	DBE	i-FIT	i-FIT (Norm)	Formula
360.1323	360.1324	-0.1	-0.3	11.5	565.0	0.0	C19 H19 N3 O3 Na

Figure SI 4.12 Low resolution ESI mass spectrum of **tpy(deg).**

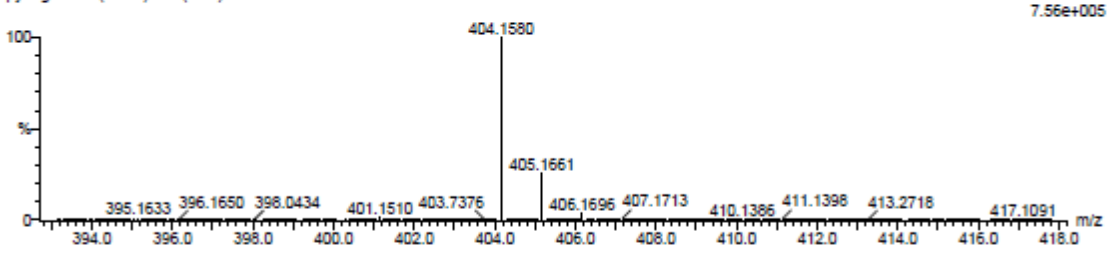
Elemental Composition Report Page 1

Single Mass Analysis
Tolerance = 5.0 PPM / DBE: min = -1.5, max = 50.0
Element prediction: Off
Number of isotope peaks used for i-FIT = 3

Monoisotopic Mass, Even Electron Ions
26 formula(e) evaluated with 1 results within limits (all results (up to 1000) for each mass)
Elements Used:
C: 20-25 H: 20-25 N: 0-5 O: 0-5 Na: 0-1

Alshath
tpy teg T1 30 (0.495) Cm (1:31)

TOF MS ES+
7.56e+005



Minimum:				-1.5			
Maximum:		5.0	5.0	50.0			
Mass	Calc. Mass	mDa	PPM	DBE	i-FIT	i-FIT (Norm)	Formula
404.1580	404.1586	-0.6	-1.5	11.5	606.7	0.0	C21 H23 N3 O4 Na

Figure SI 4.13 Low resolution ESI mass spectrum of **tpy(teg).**

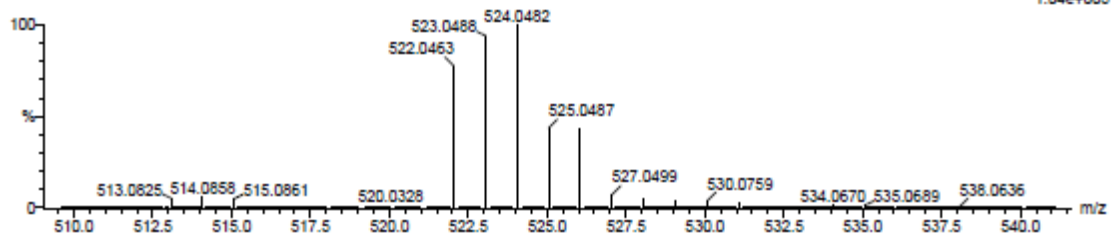
Elemental Composition Report Page 1

Single Mass Analysis
Tolerance = 5.0 PPM / DBE: min = -1.5, max = 50.0
Element prediction: Off
Number of isotope peaks used for i-FIT = 3

Monoisotopic Mass, Even Electron Ions
159 formula(e) evaluated with 1 results within limits (all results (up to 1000) for each mass)
Elements Used:
C: 15-20 H: 15-20 N: 0-5 O: 0-5 Cl: 0-2 Pt: 0-1

Alshath
tpy egPt dmso 16 (0.256) Cm (1:30)

TOF MS ES+
1.04e+005



Minimum:				-1.5								
Maximum:		5.0	5.0	50.0								
Mass	Calc. Mass	mDa	PPM	DBE	i-FIT	i-FIT (Norm)	Formula					
524.0482	524.0471	1.1	2.1	7.5	496.9	0.0	C15	H19	N2	O2	C12	Pt

Figure SI 4.14 Low resolution ESI mass spectrum of **Pt(eg).**

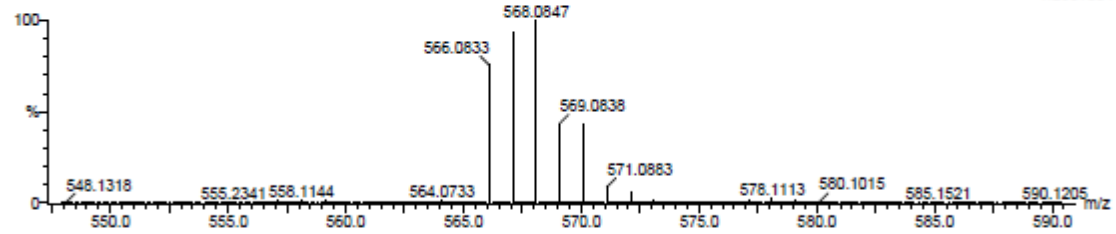
Elemental Composition Report Page 1

Single Mass Analysis
Tolerance = 4.0 PPM / DBE: min = -1.5, max = 50.0
Element prediction: Off
Number of isotope peaks used for i-FIT = 3

Monoisotopic Mass, Odd and Even Electron Ions
159 formula(e) evaluated with 1 results within limits (all results (up to 1000) for each mass)
Elements Used:
C: 15-20 H: 15-20 N: 0-5 O: 0-5 Cl: 0-2 Pt: 0-1

Alshath
tpydeg pt dmso ppt 25 (0.410) Cm (1:30)

TOF MS ES+
1.23e+004



Minimum:				-1.5								
Maximum:		5.0	4.0	50.0								
Mass	Calc. Mass	mDa	PPM	DBE	i-FIT	i-FIT (Norm)	Formula					
568.0847	568.0841	0.6	1.1	12.0	384.4	0.0	C19	H20	N3	O3	Cl	Pt

Figure SI 4.15 Low resolution ESI mass spectrum of **Pt(deg).**

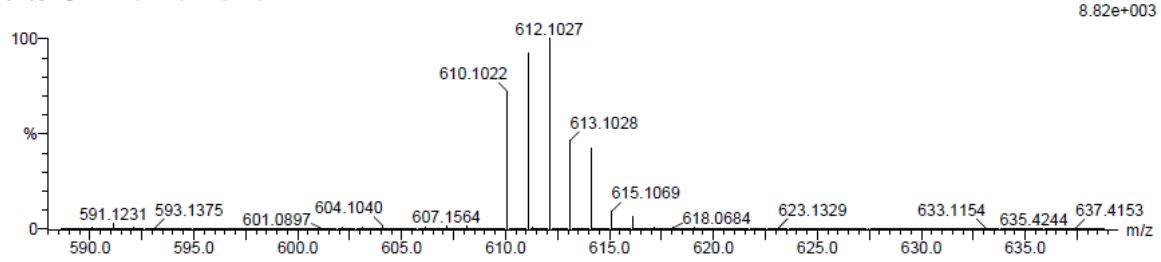
Elemental Composition Report **Page 1**

Single Mass Analysis
Tolerance = 5.0 PPM / DBE: min = -1.5, max = 50.0
Element prediction: Off
Number of isotope peaks used for i-FIT = 3

Monoisotopic Mass, Even Electron Ions
100 formula(e) evaluated with 1 results within limits (all results (up to 1000) for each mass)
Elements Used:
C: 20-25 H: 20-25 N: 0-5 O: 0-5 Cl: 0-1 Pt: 0-1

Aishath
pt tpy teg cod 30 (0.494) Cm (1:31)

TOF MS ES+
8.82e+003



Minimum:				-1.5			
Maximum:		5.0	5.0	50.0			
Mass	Calc. Mass	mDa	PPM	DBE	i-FIT	i-FIT (Norm)	Formula
611.1034	611.1025	0.9	1.5	12.5	338.6	0.0	C21 H23 N3 O4 Cl Pt

Figure SI 4.16 Low resolution ESI mass spectrum of **Pt(teg).**

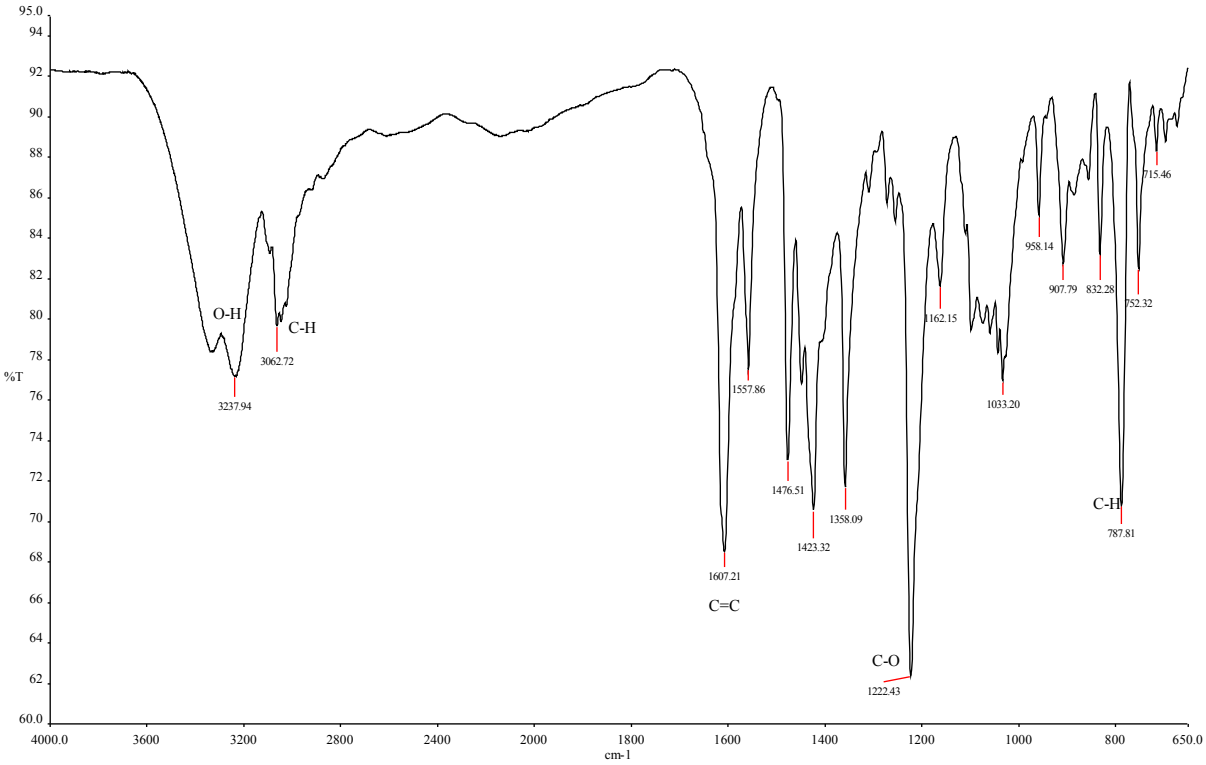


Figure SI 4.17 IR Spectrum of **Pt(eg).**

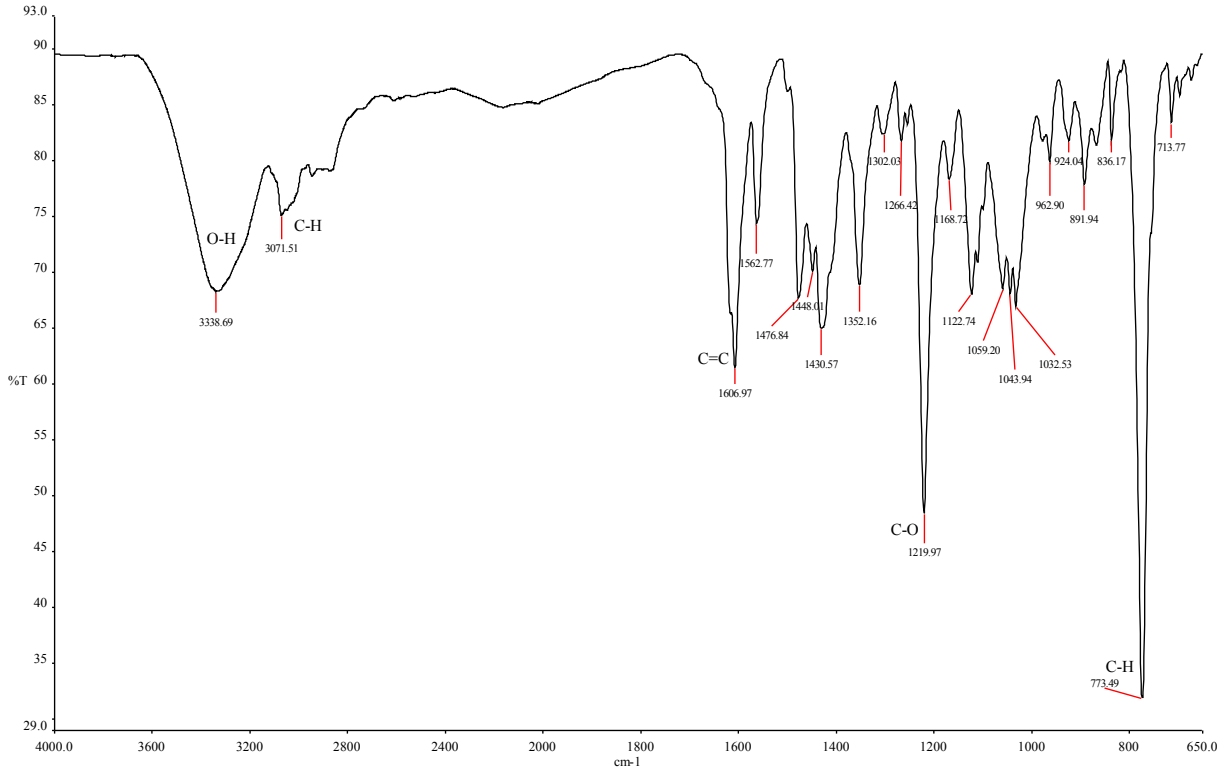


Figure SI 4.18 IR Spectrum of **Pt(deg).**



Figure SI 4.19 IR Spectrum of **Pt(teg).**

Table SI 4.1 Average observed rate constants, k_{obs}/s^{-1}, for the substitution of chloride from **Pt(eg)** by azole nucleophiles in methanolic solution at 298K

MIm(λ=310nm)		**Im** (λ=310nm)		**DIm**(λ=310nm)		**Pz** (λ=310nm)		**Tz** (λ=310nm)	
[Nu]/M	k_{obs},s^{-1} X10^{-4}	[Nu]/M	k_{obs},s^{-1} X10^{-4}	[Nu]/M	k_{obs},s^{-1} X10^{-4}	[Nu]/M	k_{obs},s^{-1} X10^{-4}	[Nu]/M	k_{obs},s^{-1} X10^{-4}
0.0005	4.497	0.0005	5.500	0.0005	2.310	0.0005	3.089	0.0005	1.138
0.0010	8.330	0.0010	8.571	0.0001	3.626	0.0010	4.140	0.0010	2.090
0.0015	12.217	0.0015	11.381	0.0015	4.988	0.0015	5.291	0.0015	3.147
0.0020	15.596	0.0020	14.517	0.0020	6.432	0.0020	6.201	0.0020	4.041
0.0025	19.226	0.0025	17.789	0.0025	7.636	0.0025	7.286	0.0025	4.653

Table SI 4.2 Average observed rate constants, k_{obs}/s^{-1}, for the substitution of chloride from **Pt(deg)** by azole nucleophiles in methanolic solution at 298K

MIm(λ=310nm)		**Im** (λ=310nm)		**DIm** (λ=310nm)		**Pz** (λ=310nm)		**Tz** (λ=310nm)	
[Nu]/M	k_{obs},s^{-1} X10^{-4}	[Nu]/M	k_{obs},s^{-1} X10^{-4}	[Nu]/M	k_{obs},s^{-1} X10^{-4}	[Nu]/M	k_{obs},s^{-1} X10^{-4}	[Nu]/M	k_{obs},s^{-1} X10^{-4}
0.0005	4.516	0.0005	5.859	0.0005	2.150	0.0005	2.550	0.0005	1.002
0.0010	8.355	0.0010	8.572	0.0010	3.602	0.0010	3.813	0.0010	1.854
0.0015	12.137	0.0015	11.763	0.0015	4.987	0.0015	5.009	0.0015	2.877
0.0020	16.094	0.0020	14.924	0.0020	6.631	0.0020	6.097	0.0020	3.805
0.0025	19.135	0.0025	17.967	0.0025	7.729	0.0025	7.065	0.0025	4.513

Table SI 4.3 Average observed rate constants, k_{obs}/s^{-1}, for the substitution of chloride from **Pt(teg)** by azole nucleophiles in methanolic solution at 298K.

MIm(λ=310nm)		**Im** (λ=310nm)		**DIm** (λ=310nm)		**Pz** (λ=310nm)		**Tz** (λ=310nm)	
[Nu]/M	k_{obs},s^{-1} X10^{-4}	[Nu]/M	k_{obs},s^{-1} X10^{-4}	[Nu]/M	k_{obs},s^{-1} X10^{-4}	[Nu]/M	k_{obs},s^{-1} X10^{-4}	[Nu]/M	k_{obs},s^{-1} X10^{-4}
0.0005	7.337	0.0005	4.167	0.0005	1.828	0.0005	2.374	0.0005	1.119
0.0010	11.321	0.0010	7.213	0.0010	3.225	0.0010	3.494	0.0010	1.891
0.0015	15.069	0.0015	10.097	0.0015	4.639	0.0015	4.457	0.0015	2.772
0.0020	18.434	0.0020	13.874	0.0020	6.285	0.0020	5.524	0.0020	3.591
0.0025	22.786	0.0025	16.140	0.0025	7.629	0.0025	6.530	0.0025	4.216

Table SI 4.4 Temperature dependence of $k_2/M^{-1}s^{-1}$ for the substitution of chloride from **Pt(eg)** by azole nucleophiles at 60 fold excess [metal complex] in methanolic soluion at 298K.

MIm(λ=310nm)		**Im** (λ=310nm)		**DIm**(λ=310nm)		**Pz** (λ=310nm)		**Tz** (λ=310nm)	
$(1/T)/K^{-1}$ X10^{-3}	$\ln(k_2/T)$	$(1/T)/K^{-1}$ X10^{-3}	$\ln(k_2/T)$	$(1/T)/K^{-1}$ X10^{-3}	$\ln(k_2/T)$	$(1/T)/K^{-1}$ X10^{-3}	$\ln(k_2/T)$	$(1/T)/K^{-1}$ X10^{-3}	$\ln(k_2/T)$
3.413	-6.29881	3.413	-6.38216	3.413	-7.30158	3.413	-7.16113	3.413	-7.81318
3.356	-5.90232	3.356	-5.94049	3.356	-6.79821	3.356	-6.68967	3.356	-7.25860
3.300	-5.55195	3.300	-5.50082	3.300	-6.38145	3.300	-6.34391	3.300	-6.81738
3.247	-5.20489	3.247	-5.03591	3.247	-5.93114	3.247	-5.93285	3.247	-6.42313
3.195	-4.86273	3.195	-4.73898	3.195	-5.55590	3.195	-5.60179	3.195	-5.90884

Table SI 4.5 Temperature dependence of $k_2/M^{-1}s^{-1}$ for the substitution of chloride from **Pt(deg)** by azole nucleophiles at 60 fold excess [metal complex] at 298K.

MIm(λ=310nm)		**Im** (λ=310nm)		**DIm**(λ=310nm)		**Pz** (λ=310nm)		**Tz** (λ=310nm)	
$(1/T)/K^{-1}$ X10^{-3}	$\ln(k_2/T)$	$(1/T)/K^{-1}$ X10^{-3}	$\ln(k_2/T)$	$(1/T)/K^{-1}$ X10^{-3}	$\ln(k_2/T)$	$(1/T)/K^{-1}$ X10^{-3}	$\ln(k_2/T)$	$(1/T)/K^{-1}$ X10^{-3}	$\ln(k_2/T)$
3.413	-6.28773	3.413	6.50900	3.413	-7.23413	3.413	-7.09174	3.413	-7.68681
3.356	-5.90885	3.356	-5.96401	3.356	-6.79839	3.356	-6.76444	3.356	-7.34850
3.300	-5.53059	3.300	-5.53507	3.300	-6.56344	3.300	-6.32973	3.300	-6.86486
3.247	-5.14005	3.247	-5.15285	3.247	-5.98639	3.247	-6.00296	3.247	-6.45490
3.195	-4.80934	3.195	-4.64948	3.195	-5.60580	3.195	-5.54819	3.195	-6.09383

Table SI 4.6 Temperature dependence of $k_2/M^{-1}s^{-1}$ for the substitution of chloride from **Pt(teg)** by azole nucleophiles at 60 fold excess [metal complex] in methanolic solution at 298K.

MIm(λ=310nm)		**Im** (λ=310nm)		**DIm**(λ=310nm)		**Pz** (λ=310nm)		**Tz** (λ=310nm)	
$(1/T)/K^{-1}$ X10^{-3}	$\ln(k_2/T)$	$(1/T)/K^{-1}$ X10^{-3}	$\ln(k_2/T)$	$(1/T)/K^{-1}$ X10^{-3}	$\ln(k_2/T)$	$(1/T)/K^{-1}$ X10^{-3}	$\ln(k_2/T)$	$(1/T)/K^{-1}$ X10^{-3}	$\ln(k_2/T)$
3.413	-6.18957	3.413	-6.66855	3.413	-7.27197	3.413	-7.30849	3.413	-7.87247
3.356	-5.70295	3.356	-6.17943	3.356	-6.88408	3.356	-6.91065	3.356	-7.38384
3.300	-5.25938	3.300	-5.78173	3.300	-6.48952	3.300	-6.56527	3.300	-6.97760
3.247	-4.89837	3.247	-5.44795	3.247	-6.15830	3.247	-6.12786	3.247	-6.60650
3.195	-4.46502	3.195	-4.99079	3.195	-5.82237	3.195	-5.78494	3.195	-6.18096

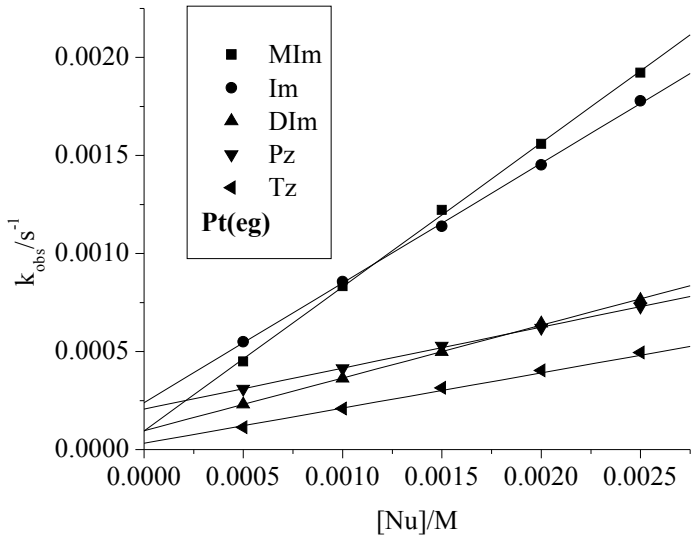


Figure SI 4.20 Concentration dependence plots for the chloride substitution on **Pt(eg)** in methanol solution at 298K

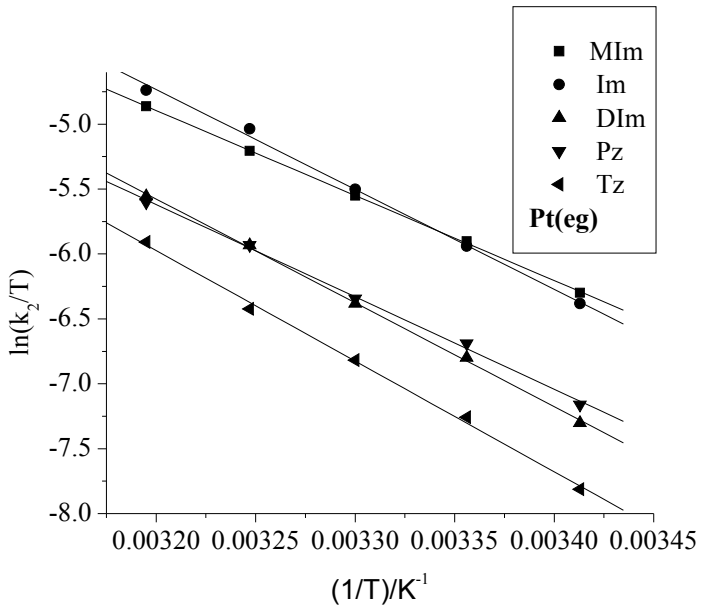


Figure SI 4.21 Eyring plots for the reactions of **Pt(eg)** with the azole nucleophiles at different temperatures in the range 20-40^0 C

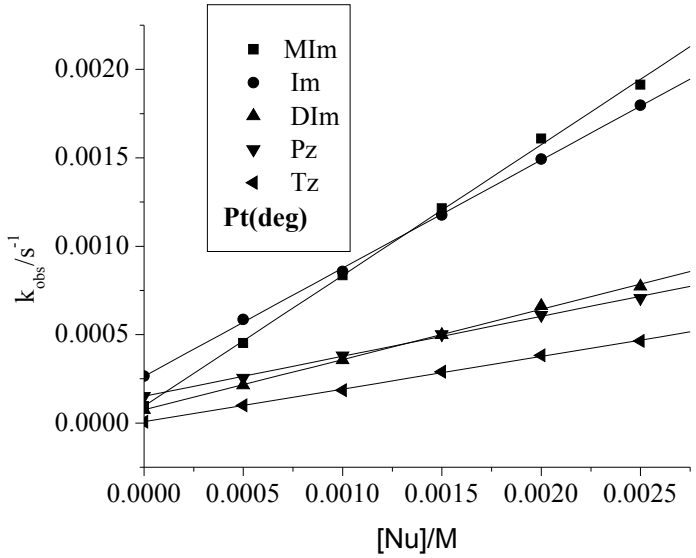


Figure SI 4.22 Concentration dependence plots of for the chloride substitution on **Pt(deg)** in methanol solution at 298K

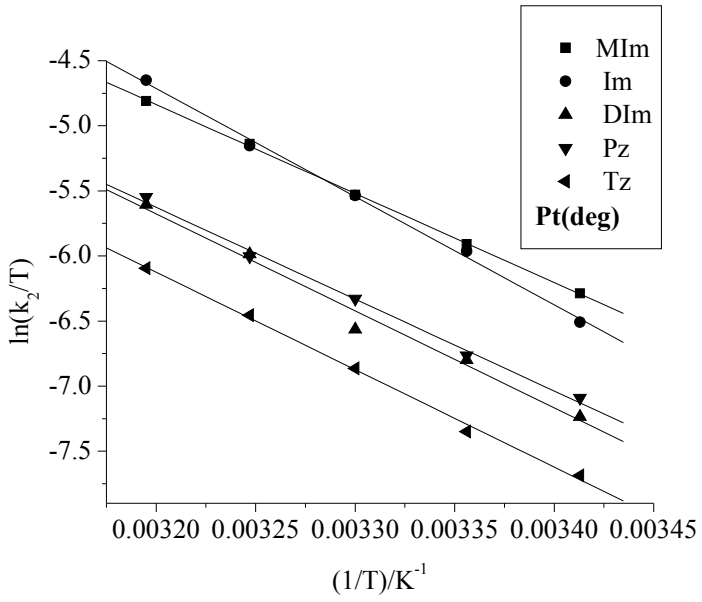


Figure SI 4.23 Eyring plots for the reactions of **Pt(deg)** with the azole nucleophiles at different temperatures in the range 20-40^0 C

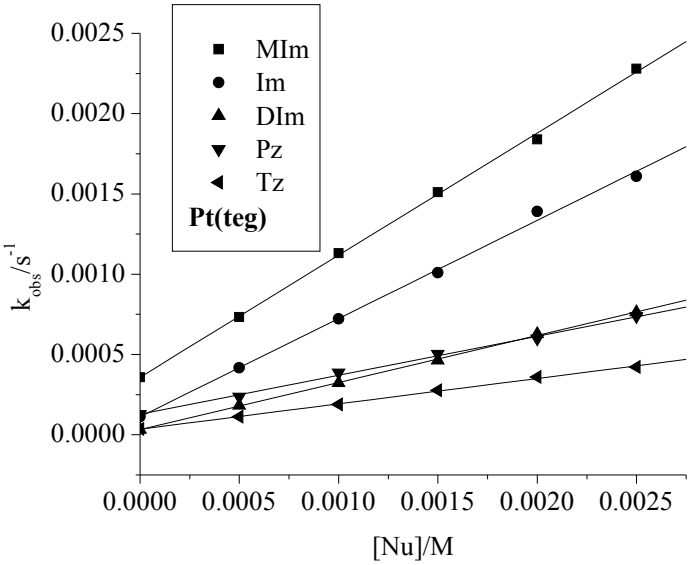


Figure SI 4.24 Concentration dependence plots for the chloride substitution on **Pt(teg)** in methanol solution at 298K

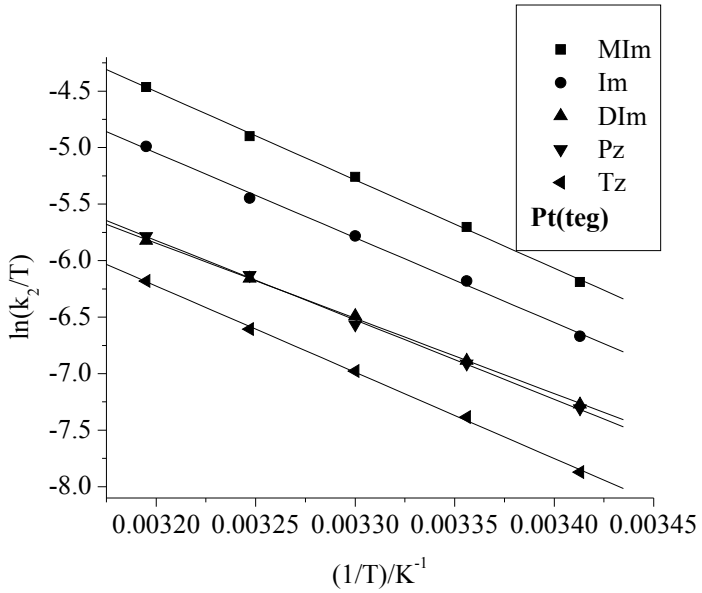


Figure SI 4.25 Eyring plots for the reactions of **Pt(teg)** with the azole nucleophiles at different temperatures in the range 20-40^0 C

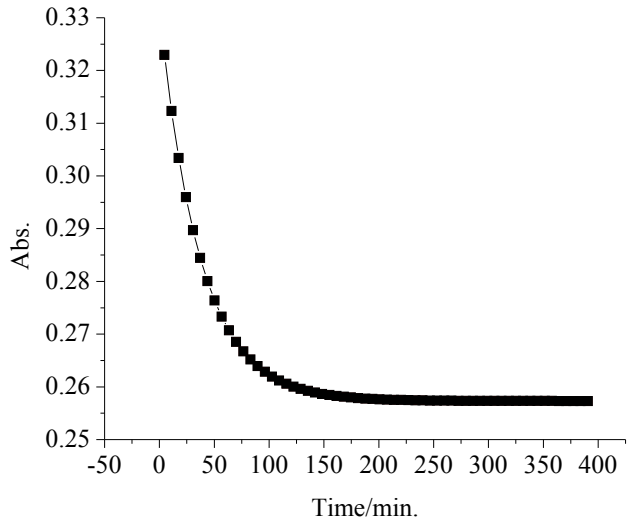


Figure SI 4.26 The kinetic trace for the reaction of **Pt(eg)** with 20 folds **MIm** in methanol at 298K

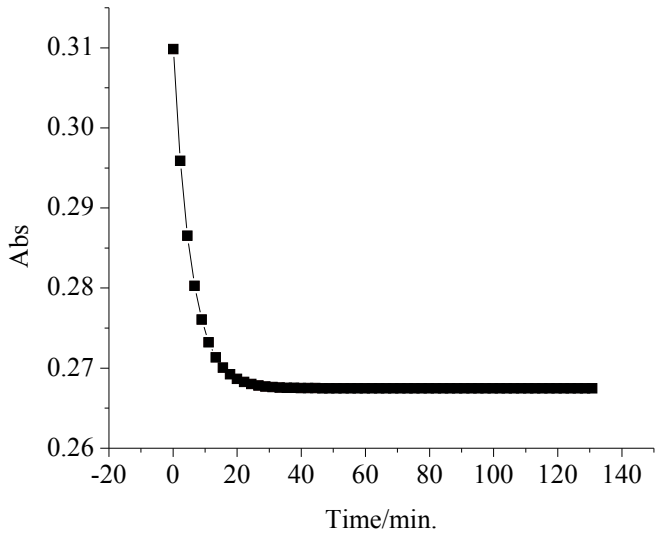


Figure SI 4.27 The kinetic trace for the reaction of **Pt(eg)** with 60 folds **Im** in methanol at 308K

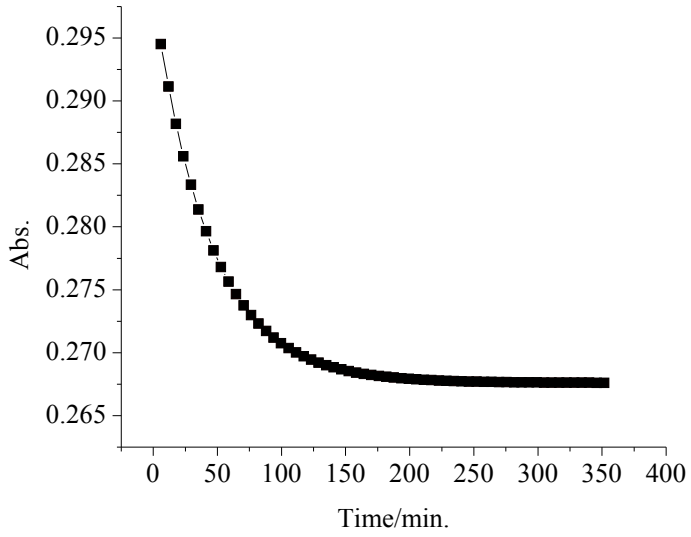


Figure SI 4.28 The kinetic trace for the reaction of **Pt(deg)** with 40 folds **Py** in methanol at 298K

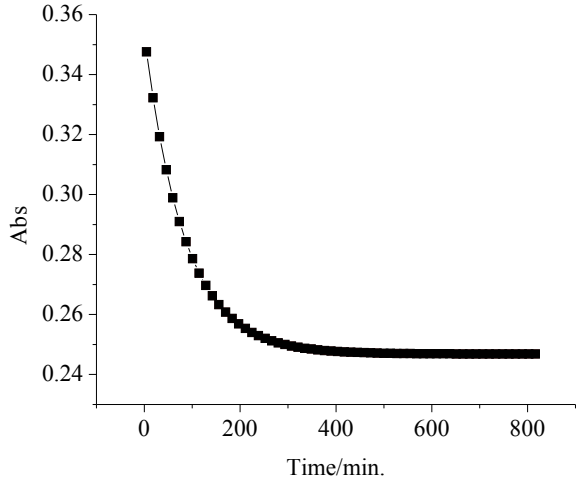


Figure SI 4.29 The kinetic trace for the reaction of **Pt(deg)** with 60 folds **Tz** in methanol at 293K

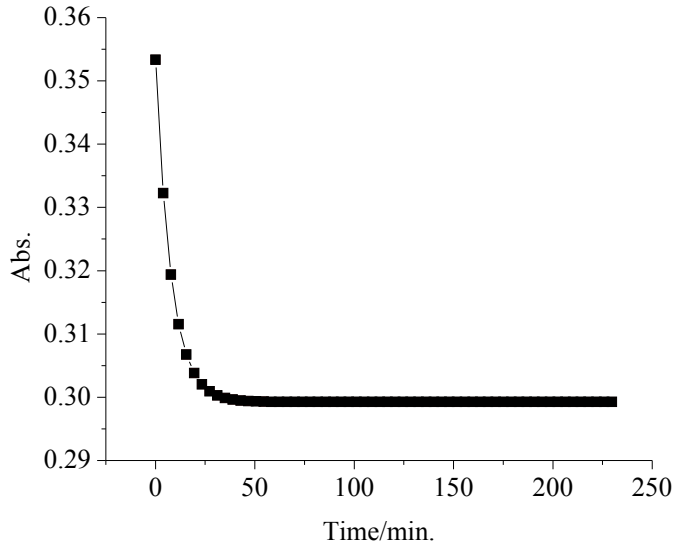


Figure SI 4.30 The kinetic trace for the reaction of **Pt(teg)** with 100 folds **MIm** in methanol at 298K

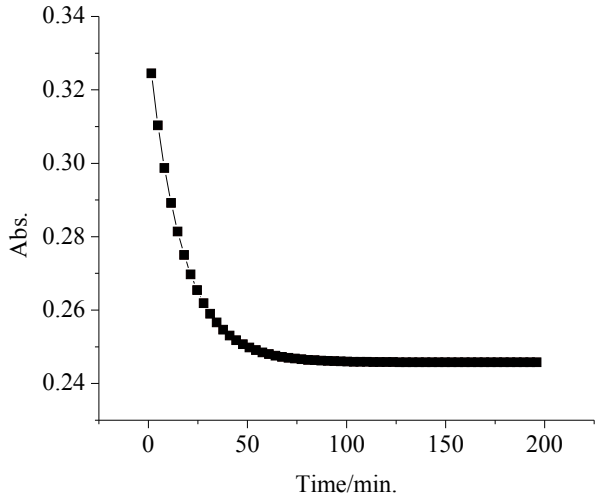


Figure SI 4.31 The kinetic trace for the reaction of **Pt(teg)** with 60 folds **Tz** in methanol at 313K

Table of contents

List of abbreviations i

List of figures ii

List of tables iii

List of schemes iv

Chapter 5 1

The role of Ruthenium Polypyridyl fragment on the reactivity of ethylene Pt(II) aqua units with biological nucleophiles. 1

5.1 Abstract 1

5.2 Introduction 2

5.3 Experimental 5

5.3.1 Synthesis 5

5.3.2 Materials 5

5.3.3 Synthesis of Ligand and Ruthenium Moieties 5

5.3.3.1 4'-pyridyl-2,2':6',2"-terpyridine (qpy) 5

5.3.3.2 $Ru(qpy)(tpy)Cl_2$ 6

5.3.3.3 $[Ru(qpy)_2]Cl_2$ 6

5.3.3.4 $Pt(en)Cl_2$ 7

5.3.4 Synthesis of Platinum(II) Complexes 7

5.3.4.1 Pt1-Cl 7

5.3.4.2 Pt2-Cl 8

5.3.4.3 Pt3-Cl 8

5.3.5 Preparation of Aqua Complexes 8

5.3.6 Chemical solutions 9

5.3.7 Instrumentation 9

5.3.8 Kinetic measurements 9

5.3.9 Computational modelling 12

5.4 Results and discussion 15

5.5 Conclusion 19

5.6 References 20

5.7 Supplementary information 26

List of abbreviations

LUMO	Lowest unoccupied molecular orbital
HOMO	Highest occupied molecular orbital
DNA	Deoxyribonucleic acid
5'-GMP	Guanosine-5'-monophosphate
DEDTC	Diethyldithiocarbamate
DFT	Density functional theory
GSH	Glutathione
k_2	Rate constants
k_{obs}	Observed *pseudo* first-order constant
mM	millimolar
NBO	Natural bond order
Nu	Nucleophile
[Nu]	Nucleophile concentration
Pt1	$[Pt(en)OH_2]^{2+}$
Pt2	$[H_2O(en)Pt(qpy)Ru(tpy)]^{4+}$
Pt3	$[H_2O(en)Pt(qpy)Ru(qpy)Pt(en)OH_2]^{6+}$
Pt1-Cl	$[Pt(en)Cl]^{+}$
Pt2-Cl	$[Cl(en)Pt(qpy)Ru(tpy)]^{3+}$
Pt3-Cl	$[Cl(en)Pt(qpy)Ru(qpy)Pt(en)Cl]^{4+}$
py	pyridine
qpy	Quarterpyridine (4'-(pyridyl) 2,2':6,2''-terpyridine)
T	Absolute temperature (K) unless stated otherwise
terpy/tpy	2,2':6,2''-terpyridine
TU	Thiourea
UV	Ultraviolet
$\Delta H^{\neq}$	Activation enthalpy
$\Delta S^{\neq}$	Activation entropy
L-met	L-methionine
en	ethylenediamine
NMR	Nuclear magnetic resonance
MLCT	metal to ligand charge transfer

List of figures

Figure 5.1 UV-visible spectrum of Pt3 (3.432×10^{-5}M) and L-met (200 fold) in 0.02M $LiCF_3SO_3$ at 298K.....10

Figure 5.2 Concentration dependence plots for the substitution of aqua ligand in Pt2 with GSH and L-met nucleophiles.....11

Figure 5.3 Eyring plots for the reaction of the complexes with L-met in the range of 20 - 40° C.....12

Figure 5.4 Structural formular of Pt2 showing the different N-atoms around the Pt(II) centre. 14

Figure 5.5 ^{195}Pt NMR arrays of Pt-Cl with excess GSH. 16

Figure 5.6 Schematic representation of GMP coordinated to the Pt(II) metal centre via N7. 18

List of tables

Table 5.1 DFT calculated minimum energy structures and frontier molecular orbitals (HOMO and LUMO) of the studied complexes 13

Table 5.2 Summary of DFT calculated data for the studied complexes.....14

Table 5.3 Rate constants and activation parameters for studied reactions at 298K 15

List of schemes

Scheme 5.1 Structural formulae of the biological nucleophiles and the Pt(II) complexes.' 4

Scheme 5.2 Aquation of the complexes 9

Chapter 5

The role of Ruthenium Polypyridyl fragment on the reactivity of ethylene Pt(II) aqua units with biological nucleophiles.

5.1 Abstract

Thermodynamic and kinetic study of Ru(II)-Pt(II) complexes with a semi-rigid linker 4'-pyridyl-2,2':6',2''terpyridine (qpy) with biological nucleophiles was carried out under *pseudo* first-order conditions as a function of concentration and temperature using UV-visible spectrophotometer. The reactions proceeded via a single step following first-order kinetics with the *pseudo* first-order rate constant obeying the rate law; $k_{obs} = k_2[Nu]$. The study revealed that increase in the overall charges of the respective complexes is the key reason for the observed increase in the reactivity. Additionally, replacing the *cis* pyridyl group in **Pt1** by Ru(III) polypyridyl to give **Pt2** and **Pt3** respectively lowers the energy of the LUMO (π^*) orbitals and HOMO-LUMO energy gap which influences the reactivity to some extent. The two qpy groups in the trinuclear complex **Pt3** only slightly increases the reactivity from that of **Pt2** because the qpy groups are in orthogonal positions preventing π-electron communication hence the two Pt(II) centres act independently of each other. The marginal increase in reactivity is due to increased charge and extension of the π-surface. The observed activation parameters support an associative mode of substitution.

5.2 Introduction

For the last two decades, platinum based chemotherapeutic regiments have been the mainstay in the treatment of cancer, diabetes and alzhelmer's [1,2] among others. The discovery of the anti-tumour activity of cisplatin elicited further research efforts towards more effective and wide-spectra drugs for the cure of cancer.[3] To this effect thousands of platinum complexes have been synthesised and evaluated for anti-tumour activity, though only few have entered clinical use.[4,5] Cisplatin is responsible for the cure of over 90% of testicular cancer cases and plays a vital role in the treatment of other forms of cancer.[6-9]

The binding of platinum complexes to S-containing bio-molecules in the cell before reaching target DNA molecule produces toxic effects[10-13] though a certain amount of the Pt drug eventually binds to N-donor biomolecules (amino acids or DNA) a mechanism which is now accepted to be responsible for the anti-cancer activity. The interactions with mitochondrial DNA are less responsible for the anti-tumour activity of the platinum complexes.[11,14] Different modes of binding exist but binding to DNA primarily occurs through the N7 atom of guanine.[15,16] The concentration of the thiols including glutathione (GSH) and L-cysteine in intracellular liquid is about 10 mM, it is assumed that most of the Platinum drug binds to sulphur before it reaches the DNA.[10,15,17-20] The resulting Pt–S(thioether) bond may be broken in the presence of DNA, *i.e.* the N7 atom of guanosine-5′-monophosphate (5′-GMP) can substitute the S-donor.[20,21] For these reasons the S-bound Pt(II) complexes are Pt-reservoirs in the body. On the other hand, Pt(II) complexes can bind to sulphur from thiol molecules with the resulting Pt–S(thiol) bond being very stable and compounds of this type are responsible for the occurrence of toxic side effects and resistance during the use of Pt(II) complexes as anti-tumour agents.[22-26] However the Pt–S(thiol) bond can be broken in the presence of "rescue agents", which are exclusively S-containing compounds, such as diethyldithiocarbamate (DEDTC), thiourea (TU), thiosulfate, glutathione(GSH), cysteine, biotin and amifostine.[1,11,15,27] Pt(IV) complexes being slower in reaction than Pt(II) complexes can act as precursors and undergo reduction within the body to form active Pt(II) species.[28-36]

On the other hand ruthenium complexes have been suitable candidates to fill the shortcomings of platinum based drugs as exhibited by cisplatin. Ruthenium complexes are very promising; given the fact that they overcome cisplatin resistant cell-lines with a low general toxicity and have found their way into the clinic, where their properties are exploited for many

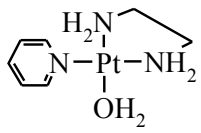
applications.[37-41] The wide range of accessible oxidation states of ruthenium under physiological conditions makes this metal unique amongst the platinum group.[42-45] For instance Ru(II) and Ru(III) show antitumor activity and chemical toxicity different from those of platinum. Their tendency to selectively bind bio-molecules partly accounts for their low toxicity.[40,41] Selectivity is enhanced due to the complexes binding to transferin and albumen that are usually supplied to cancerous and other diseased cell with great demand for iron which exposes the complexes to the target cells.[39,46-49] A lot of ruthenium complex groups have been synthesized namely; amino-chlorido,[47,50-68] ruthenium polyamino carboxylate,[39,58,69,70,71] organoruthenium[72-76] and photoreactive ruthenium complexes. [41,83]

It is therefore instructive that a combination of different metal centres provides a hybrid of properties which are advantageous for instance, platinum-ruthenium hetero-dinuclear complexes have the capacity to select and sequentially react with particular DNA sequences due to their unique interactions facilitating unique DNA modification.[84] In addition, the presence of non-binding metal centres in hetero-dinuclear metallic complexes considered has shown to increase the overall cationic charge thus enhancing their water solubility.[83] Furthermore, they also photo react with DNA through a light absorbing ruthenium metal centre which transfers the energy to the binding metal centre thus enhancing its reactivity.[83] These advantageous effects that results from hetero-dinuclear complexes inspired us to do a mechanistic investigation on the Pt(II)–Ru(III) complexes.

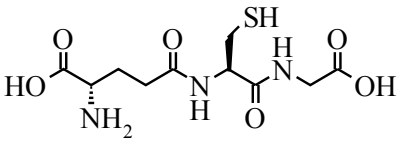
Two of the complexes used in this study consist of a bis(terpyridyl)-ruthenium(III) moiety, and one or two platinum-ethylenediamine centres, which coordinate to the fourth pyridine ligand of quarterpyridine and the third complex has a pyridyl coordinating to the platinum-ethylenediamine centre. The hetero-polynuclear ruthenium-platinum complexes has short and semi-rigid linking ligand 4'-pyridyl-2,2':6',2"-terpyridine (quaterpyridine or qpy) which presents a tridentate coordination site, and coordinate to a second metal via the fourth pyridine appended at the 4'-position of the terpyridine. The non-coordinated pyridyl groups of the bis(quaterpyridine) ruthenium complex have been shown to react with a range of electrophiles.[85] The bis(terpyridyl)-ruthenium(III) moiety, a constituent of two of the complexes can photo-react with DNA and subsequent energy transfer activates the platinum unit, which can coordinate to DNA.

We used biologically relevant nucleophiles *viz.* guanosine 5'-monophosphate (5'-GMP), L-methionine (L-Met) and reduced glutathione (GSH) for the kinetic investigation. The nucleophiles were selected based on the difference in nucleophilicity, steric hindrance, binding properties and biological relevance. The reactions were studied in aqueous solution using UV-visible spectrophotometric techniques. It is envisaged that this paper will throw more light on the mechanisms of interaction of the platinum(II) complexes with **N**- and **S**-donor ligands, give a better understanding on mechanistic competition between **S**- and **N** -donor ligands and reveal the role of the ruthenium polypyridyl fragment on the reactivity of the Pt(II) metal centre. The molecular structures of the studied complexes and nucleophiles are shown in scheme 5.1.

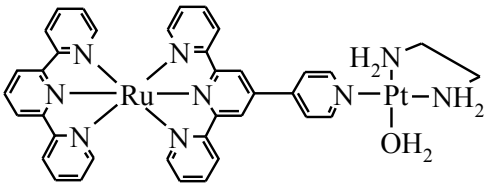
Complexes ***Nucleophiles***



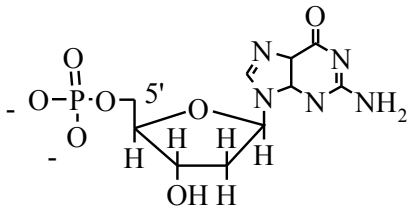
Pt1



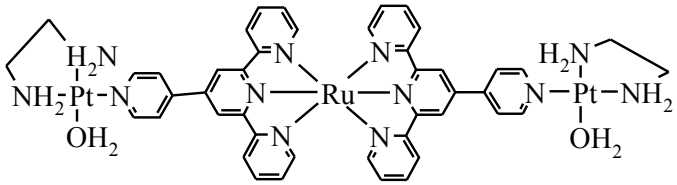
GSH



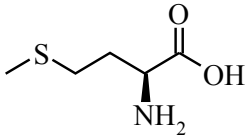
Pt2



5'-GMP



Pt3



L-met

Scheme 5.1 Structural formulae of the biological nucleophiles and the Pt(II) complexes.[86,87]

5.3 Experimental

5.3.1 Synthesis

The complexes; [Pt(en)OH_2], [H_2O(en)PtqtpyRutpy] and [H_2O(en)PtqtpyRuqtpyPt(en)OH_2] were prepared according to the literature methods.[88(a),89] Chemical analysis, UV-visible and ^{1}H NMR spectral data were in good agreement with those obtained in previous preparations.[88] Experimental procedures for 0.1 M Ru(III) solution,[88(a)] the Ru complexes, [Ru(tpy)CI_3],[88(b)] and [Ru(qpy)Cl_3],[88(a)] are summarized under Supporting Information (experimental SI). The details of the characterisation and spectroscopic data for ligands and complexes are included in the experimental section and also under Supporting Information figures 5.1- 5.14. Due to the poor solubility[89(d)] and the paramagnetic nature of [Ru(tpy)Cl_3][88(b)] and [Ru(qpy)Cl_3],[88(a)] the two precursors were used as synthesized.[85]

5.3.2 Materials

Buffer standards of pH 4.0, 7.0 and 10.0 were bought from Merck. ruthenium(III)chloride trihydrate (99%),1,5-cyclooctadiene and 4'-chloro-2,2':6',2" terpyridine (99%) were purchased from Aldrich. All other chemicals were purchased from Sigma Aldrich and used as received. For preparation of all aqueous solutions, ultra-pure water was used. The ruthenium precursors; [Ru(tpy)Cl_3],[88(b)] [Ru(qpy)Cl_3][88(a)] and 0.1 M Ru(III) solution[88(a)] were synthesized as described in literature.

5.3.3 Synthesis of Ligand and Ruthenium Moieties

5.3.3.1 4'-pyridyl-2,2':6',2"-terpyridine (qpy)

The ligand, 4'-pyridyl-2,2':6',2"-terpyridine (qpy) was synthesized as in literature.[88(c)]2-acetylpyridine (5 g, 4.13 mol), was added to a suspension of NaOH in polyethylene glycol (PEG 300) (35 mL) and the reaction mixture was stirred for 10 minutes at 0 °C. 4-pyridine carboxaldehyde (2.21 g, 2.06 mol) was added to the suspension and left at 0°C for 2 hours. The reaction mixture was stirred manually in every 15 minutes due to the high viscosity of the reaction mixture. After this time, excess NH_4OAc (10 g) was added and the suspension was heated at 100 °C for 2 hours. Brown precipitate was formed from the initially formed red solution. Water (75 mL) was added to the precipitate. The precipitate was filtered, washed with more water (50 mL) followed by cold ethanol (10 mL). The ligand was recrystallized from ethanol. Yield: 0.509 g, (70%), Colourless needles. ^{1}H NMR (400 MHz, $CDCl_3$) δ/ ppm: 8.79 (2H, m, 2''' 6'''), 8.77 (2H, s, 3' 5'), 8.74 (2H, br dm, 6 6''), 8.67 (2H, dd, 3 3''), 7.90

(2H, td, 4 4''), 7.80 (2H, dd, 3''' 5'''), 7.39 (2H, ddd, 5, 5''). TOF MS-ES$^+$, m/z: 333.1114, $(M+Na)^+$.

5.3.3.2 $Ru(qpy)(tpy)Cl_2$

This ruthenium moiety was synthesized by a slight modification of the literature method.[88(a)] To a filtered solution of $AgBF_4$ (240 mg; 1.232 mmol) in acetone (15 mL), $[Ru(tpy)Cl_3]$ (40 mg; 0.080 mmol) was added. The reaction mixture was refluxed for 18 hours in the dark after which the precipitated AgCl was removed by filtration. The filtrate was concentrated to 1 mL in *vacuo*. Into the resulting green oil the ligand qpy (43 mg, 0.148mmol) was added and the mixture was refluxed for 2 hours in DMF (20 mL) which reduced Ru(III) to Ru(II). The reaction mixture was filtered and concentrated in *vacuo* to (1.0 mL) which gave red oil. A saturated solution of LiCl (2 mL) in EtOH was added to the red oil. A precipitate was formed on adding the oil to acetone (200 mL). The precipitate obtained was purified by column chromatography on neutral alumina using CH_3CN: EtOH (50: 50) as the eluent. The first red band was collected and was lyophilised with diethylether. Recrystallization of the precipitate with a mixture of MeOH and diethylether yielded a relatively pure product. Yield: 35 mg, 0.0489 mmol (61%), Dark red powder. ^{1}H NMR (400 MHz, DMSO-d_6) δ/ ppm: 9.58 (2H, s, I3' 5'), 9.12 (2H, d, I33"), 9.10 (2H, s, II3' 5'), 8.99 (2H, d, I2''' 6'''), 8.85 (2H, d, II3 3'), 8.56 (2H, t, II4'), 8.45 (2H, d, I3''', 5'''), 8.09 (2H, t, I44''), 8.03 (2H, t, II4 4''), 7.52 (2H, d, II6 6''), 7.46 (2H, d, I6 6''), 7.30 (2H, t, I5 5''), 7.25 (2H, t, II5 5''). TOF MS-ES$^+$, m/z: 366.5616, (M^{2+}). *Anal. Calc. for* $C_{35}H_{25}C_{l2}N_7Ru$: C 58.75, N 13.70, H 3.52. *Found*: C 58.32, N 13.21, H 3.12.

5.3.3.3 $[Ru(qpy)_2]Cl_2$

The ruthenium moiety was synthesized by a slight modification of the literature method.[88(a)] To a filtered solution of $AgBF_4$ (350 mg; 1.798 mmol) in acetone (20 mL), $[Ru(qpy)Cl_3]$ (68.9 mg; 0.133 mmol) was added. The reaction mixture was refluxed for 18 hours in the dark after which the precipitated AgCl was removed by filtration. The filtrate was concentrated to 1 mL in *vacuo*. To the resulting green oil, the ligand qpy (46 mg, 0.147 mmol) was added and the mixture was refluxed for 2 hours in DMF (25 mL) which reduced Ru(III) to Ru(II). The reaction mixture was cooled to room temperature and filtered. The red filtrate was reduced to 1 mL to afford red oil. A saturated solution of LiCl (6 mL) in EtOH was then added to the red oil. A precipitate was formed on adding acetone (400 mL). The precipitate was purified by column chromatography on neutral alumina using acetone: MeOH: EtOH (3: 6: 1) as the

eluent. The first red band was collected and lyophilized with diethylether gave a relatively pure product. Yield: 50 mg, (46 %), Dark maroon powder. ^{1}H NMR (400 MHz, DMSOd_6) δ/ ppm: 9 .61 (2H, s, 3' 5'),9.12 (2H, d, 2''' 6'''), 9,00 (2H, d, 3 3''), 8.45 (2H, d, 3''' 5'''), 8.09 (2H, t, 4 4''), 7.57 (2H, d, 6 6''), 7.29 (2H, t, 5 5''). TOF MS-ES^{+}, m/z: 361.1088, (M^{2+}). *Anal. Calc. for* $C_{40}H_{28}C_{l2}N_8Ru$: C 60.61, N 14.14, H 3.56. *Found*: C 60.99, N 14.57, H 3.72.

5.3.3.4 Pt(en)Cl_2

The platinum complex precursor was synthesized following a literature procedure.[89(b)] Into an aqueous solution of K_2PtCl_4 (125 mg, 0.300 mmol), an aqueous solution of ethane-1,2-diamine (0.018, 0.300 mmol) was added drop wise. The pH of the solution was brought to 6. The reaction mixture was stirred at 313 K. During the reaction, the pH of the solution was maintained between 5- 6 using 0.1 M NaOH. The reaction was stopped when the pH of the solution no longer changed. The yellow precipitate which formed was filtered, washed with water and ethanol and dried. Yield: 0. 068 g, (70%), yellow powder. ^{1}HNMR (400 MHz, DMF) δ/ ppm: 5.54 (4H, br , NH), 2.79 (4H, br), ^{195}Pt (-3298).

5.3.4 Synthesis of Platinum(II) Complexes

The platinum complexes, **Pt1-Cl**, **Pt2-Cl** and **Pt3-Cl** were synthesized following a similar approach reported in literature.[88(a)]

5.3.4.1 Pt1-Cl

The compound was synthesized by a slight modification of the literaturemethod.[88(a)] To a stirred solution of [Pt(en)Cl_2] (42 mg; 0.126 mmol) in 10 mL of DMF at 310 K, silver nitrate ($AgNO_3$) (21 mg, 0.126 mmol) in dimethylformamide (DMF) (5 mL) was added drop wise. The reaction mixture was stirred for 24 hours at 313 K. After filtration of silver chloride (AgCl) precipitate using a 0.45 μm nylon membrane filter (Millipore), pyridine (0.010 mL, 0.126 mmol) was added to the filtrate and the mixture was stirred for another 18 hours. The reaction mixture was filtered and co-evaporated using EtOH/MeOH (v: v = 50:50) (20 mL) to remove DMF. The precipitate was dissolved in MeOH. The product was precipitated by slow diffusion of diethyl ether. Yield: 0. 032 g, (60%), off-white crystalline powder. ^{1}H NMR (400 MHz, DMF) δ/ ppm: 8.62 (2H, dd , *J*= 6.9, 1.4), 7.89 (1H, tt, *J*= 7.8, 1.5), 7.40 (2H, br), 6.04 (2H, br), 5.65 (2H, br), 3.01 (2H, t), 2.92 (2H, br), 195Pt NMR (500 MHz, DMF) δ/ ppm: -2501. TOF MS-ES^{+}, m/z: 369.0449, (M^{+}). *Anal. Calc. For* $C_7H_{13}ClN_4O_3Pt$: C 19.47, N 12.98, H 2.96. *Found*: C 19.21, N 12.51, H 2.98.

The purity and the identity of the complexes were confirmed by ^{1}H NMR, ^{195}Pt NMR, mass spectroscopy and elemental analyses. The ^{195}Pt NMR of all the complexes exhibited a characteristic signal at about -2500 ppm, typical to platinum coordinated to NNN chelate and a chloride. Due to the high charge and complexity of the complexes, the mass spectra obtained show characteristic fragmentations.

5.3.4.2 Pt2-Cl

Yield: 28 mg (15 %), Dark red powder. ^{1}H NMR (400 MHz, D_2O) δ/ ppm: 9.11 (2H, s, I3 5'), 9.00 (2H, d, I2''' 6'''), 8.78 (2H, d, II3' 5'), 8.61 (2H, d, I3 3''), 8.50 (2H, d, II3 3''), 8.42 (2H, t, II4'), 8.25 (2H, d, I3''' 5'''), 7.93 (2H, t, I4 4''), 7.89 (2H, t, II4 4''), 7.45 (2H, d, II6 6''), 7.35 (2H, d, I6 6'), 7.17 (2H, t, I5 5''), 7.11 (2H, t. II5 5''), 2.73 (2H, br, b), 2.66 (2H, br, c), ^{195}Pt NMR (500 MHz, D_2O) δ/ ppm: -2530. TOF MS-ES^{+}, m/z: 322.5963, (for water substituted M^{4+}). *Anal. Calc. For* $C_{37}H_{33}ClN_{12}O_9$ PtRu·$4H_2O$: C 37.24, N 14.08 , H 3.46. *Found*: C 36.81, N 13.76, H 3.01.

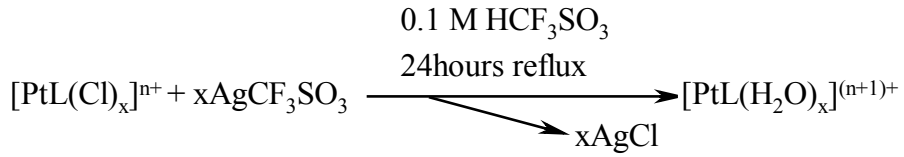
5.3.4.3 Pt3-Cl

Yield: 0. 035 g, (22 %), dark red powder. ^{1}H NMR (400 MHz, D_2O) δ/ ppm: 9.13 (2H, s, I3' 5'), 9.01 (2H, d, I2''' 6'''), 8.62 (2H, d, I3 3''), 8.25 (2H, d, I3''' 5'''), 7.93 (2H, t, I4 4''), 7.45 (2H, d, II6 6''), 7.17 (2H, t, I5 5''), 2.80 (2H, br, b), 2.73 (2H, br c) ^{195}Pt NMR (500 MHz, D_2O) δ/ ppm: -2532. TOF MS-ES^{+}, m/z: 2901.0024, (for water substituted M^{6+} -H_2O). *Anal. Calc. For* $C_{44}H_{44}C_{l2}N_{16}O_{12}$ Pt2Ru·$5H_2O$: C 32.90, N 13.95, H 3.64. *Found*: C 32.69, N 13.98, H 3.31.

5.3.5 Preparation of Aqua Complexes

The desired solutions for kinetic studies of aqua complexes (**Pt1**, **Pt2** and **Pt3**) were Prepared according to the literature procedure which is summarized in scheme 5.2. To a stirred solution of the Pt(II) compound (**Pt1-Cl**, **Pt2-Cl** and **Pt3-Cl**) (0.4 mmol) in 0.01 M triflic acid (CF_3SO_3H) (40 mL) was added silver triflate ($AgSO_3CF_3$) (equal amounts for mono chloro complexes, (**Pt1-Cl** and **Pt2-Cl**) and 2 equivalents for the di-chloro complex, (**Pt3-Cl**)). The mixture was stirred for 24 hours at 50° C in the dark. The precipitated silver chloride was removed by filtration using a 0.45 μm nylon membrane filter (Millipore). The filtrate was made up to 100 mL using 0.01 M CF_3SO_3H which had an ionic strength of 0.02 M adjusted with $LiSO_3CF_3$. For all kinetic studies, the pH of the solution was kept at pH 2, ionic strength

of 0.02 M adjusted with lithium triflate ($LiSO_3CF_3$). A pH of 2 was chosen to prevent the formation of the hydroxo species which are inert.[89(c)]



Where; L = py(en) for **Pt1-Cl,** tpyRuqpy(en) for **Pt2-Cl** and $Pt(en)_2(qpy)_2Ru$ for **Pt3-Cl,** x = 1 for **Pt1-Cl** and **Pt2-Cl** and 2 for **Pt3-Cl,** n = 1 for **Pt1-Cl,** 3 for **Pt2-Cl** and 5 for **Pt3-Cl**

Scheme 5.2 Aquation of the complexes

5.3.6 Chemical solutions

The nucleophiles quanosine-5-monophosphate sodium salt hydrate (5'-GMP), L-methionine (L-met), and reduced glutathione (GSH) were obtained from Sigma-Aldrich and used as received. Nucleophile stock solutions were prepared shortly before use by dissolving the chemicals in the aqua solvent. All other chemicals were of analytical reagent grade and ultra-pure water was used in preparation of all solutions. Since methanesulfonate ions do not coordinate to Pt(II) and Ru(III) in aqueous solution,[90] the kinetics of ligand substitution reaction were studied in 0.01M lithium methanesulfonate.

5.3.7 Instrumentation

^1H NMR were recorded on either a Bruker Avance DPX 400 or 500 MHz spectrometer, at 303 K using $Si(CH_3)_4$ as the reference for the chemical shifts. ^{195}Pt NMR were done on a 500 MHz spectrometer (^{195}Pt, 107.5 MHz) and chemical shifts externally referenced to $K_2[PtCl_6]$. Low resolution electron spray ionization (ESI^+) mass spectra were recorded on a TOF Micromass spectrometer. Elemental analyses were performed by a Thermal Scientific Flash 2000. UV-visible spectra and kinetic measurements were done on varian cary 100 Bio UV-visible spectrophotometer with an attached varian in thermostated 1.00 cm quartz suprasil cells the temperature was controlled throughout all kinetic exprriments to ± 0.1 ^0C.

5.3.8 Kinetic measurements

Spectral changes resulting from mixing complexes and nucleophile solutions respectively were recorded over the wavelength range of 200-800nm to establish a suitable wavelength at which kinetic measurements could be performed. Respective values of wavelength for the corresponding complexes are presented in supporting information table 5.1. The ligand substitution reactions were studied for the nucleophiles: GSH, L-met, and 5'-GMP. Reactions

were initiated by mixing equal volumes of the metal complex and ligand thermo-stated solutions in the UV-visible Spectrophotometric cell and the rate of complex formation was followed by monitoring the decrease in absorbance or otherwise. All kinetic measurements were performed under pseudo-first-order conditions with at least a 10-fold excess of the entering nucleophile being used. The values of reported pseudo-first-order rate constants are the average of three kinetic measurements. Kinetic runs were performed at pH 2 to ensure the aqua species is the one reacting based on the p*K*a values.[89(c)] The pH of the solution was adjusted by adding minute amounts of 0.01M triflic acid to the solution to lower the pH to the require value. A sample of the UV-visible spectrum for the reaction of **Pt3** with L-met is shown in figure 5.1 (inset is the respective kinetic trace at 310nm).

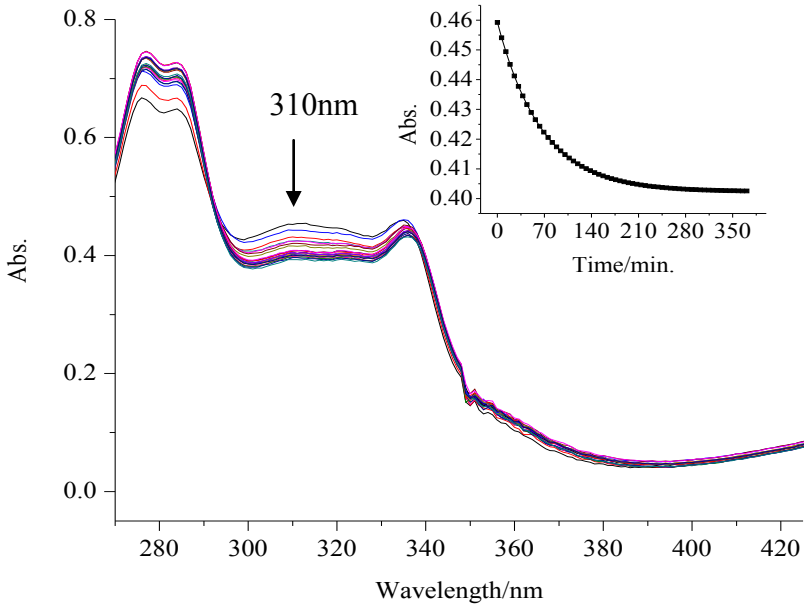


Figure 5.1 UV-visible spectrum of Pt3 (3.432 x 10^{-5}M) and L-met (200 fold) in 0.02M $LiCF_3SO_3$ at 298K

Other kinetic traces are presented in supporting information figures SI 5.24-5.41. In all cases, substitution reactions fitted to a single exponential equation. Observed *pseudo* first order constant, k_{obs}, values changed linearly with nucleophile concentrations with plots having small but noticeable intercepts; an indication that $k_{-2} \approx 0$. This means that the back reaction for the studied reactions is negligible; implying that substitution of the attached nucleophile is not effective.

$$k_{obs} = k_2[Nu] + k_{-2}[Nu] \approx k_2[Nu] \quad (5.1)$$

The proposed reaction mechanism therefore is as presented in equation 5.2.

$$PtL(OH_2)_x + xNu \xrightarrow{k_2} PtL(Nu)_x + xH_2O \quad (5.2)$$

Where; X = 1 for **Pt1** and **Pt2** and 2 for **Pt3,** Nu = GSH, L-met or GMP and L = py(en) for **Pt1** tpyRuqpy(en) for **Pt2** and $Pt(en)2(qpy)_2Ru$ for **Pt3**

A sample of concentration dependence plots is shown in figure 5.2. Other concentration dependent plots are presented in supporting information figures SI 5.15-5.20. Tables showing respective values of nucleophile concentration and k_{obs} are presented in tables SI 5.2-5.4.

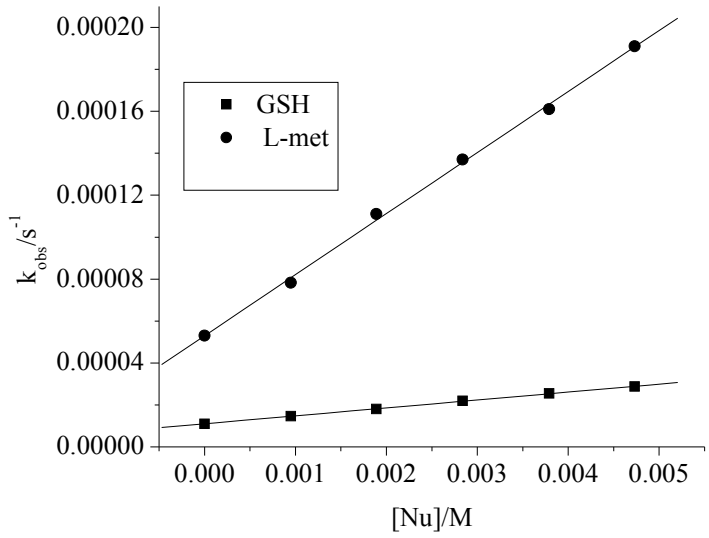


Figure 5.2 Concentration dependence plots for the substitution of aqua ligand in **Pt2** with GSH and L-met nucleophiles.

Slopes of the concentration dependence plots represented the second order rate constants, k_2, at 25 ^{0}C for the direct attack pathway summarised in table 5.3. The temperature dependence of the second order rate constants studied over the temperature range of 20-40^{0}C in intervals of 5^{0}C enabled the calculation of thermodynamic activation parameters; enthalpy of activation, $\Delta H^{\neq}$ and entropy of activation, $\Delta S^{\neq}$ by applying the Eyring equation whose values are summarised in table 5.3. Representative Eyring plots are shown in figure 5.3 while the rest

of the plots are presented in supporting information figures SI 5.21-5.23. Respective values of $\ln(k_2/T)$ and T^{-1}/K^{-1} are presented in tables SI 5.5-5.7

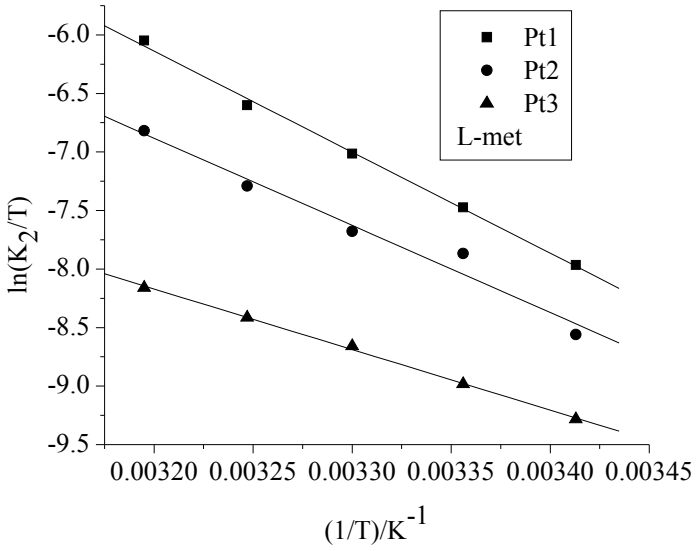
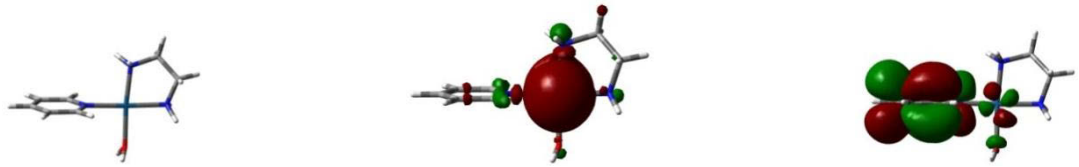
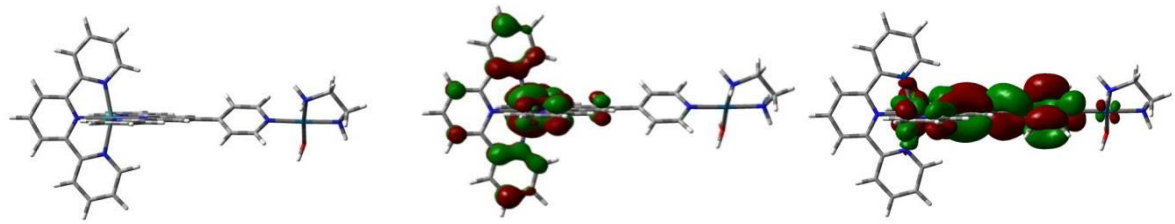
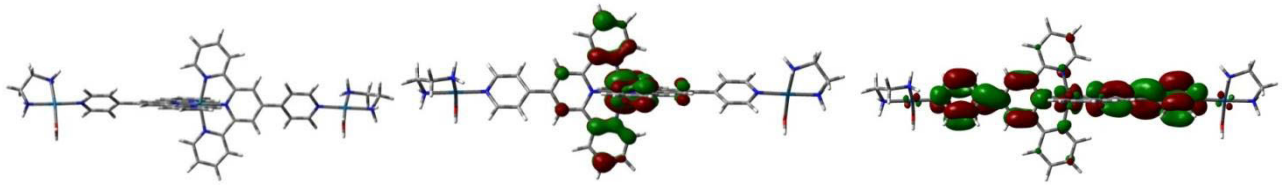


Figure 5.3 Eyring plots for the reaction of the complexes with L-met in the range of 20 - 40° C

5.3.9 Computational modelling

Density functional theory (DFT) was performed using Gaussian 09 suite of programs at the DFT B3LYP/LanL2DZ level of theory.[91] Pt(II) have low electronic spin hence the DFT calculations of the complexes were done at singlet state. Table 5.1 shows minimum energy structures and frontier molecular orbitals of the studied complexes. A Summary of bond lengths, bond angles, DFT-calculated NBO charges, HOMO and LUMO energies plus other parameters obtained from the modelled structures of the platinum-ruthenium complexes are presented in table 5.2.

Table 5.1 DFT calculated minimum energy structures and frontier molecular orbitals (HOMO and LUMO) of the studied complexes

Structures	HOMO Map	LUMO Map
 **Pt1**		
 **Pt2**		
 **Pt3**		

Complexes **Pt1** and **Pt2** have both C_1 symmetry while **Pt3** has C_2 symmetry. DFT calculations (table 5.2) reveal slightly distorted square planar structures around the Pt (II) centres typical of Pt (NNN) centres.[92] As expected, the ruthenium centre takes up distorted octahedral coordination geometry with *trans* angles ranging from 158° to 180° (table 5.2) common in octahedral complexes.[93,94] Bond lengths (table 5.2) are comparable to corresponding bond lengths of other Ru(II) complexes containing tridentate 2,2:2',2''-terpyridine ligands.[93,94] The DFT calculated structures in table 5.1 show that the 4'-pyridyl group on the qpy is out of the plane with the terpy ligand backbone bonded to Ru(II) expected to reduce anticipated steric strain when the hydrogens on the 4'-pyridyl group and those on the central pyridine interact an observation reported in previous studies.[95,96]

Table 5.2 Summary of DFT calculated data for the studied complexes.

Parameter	Pt1	Pt2	Pt3
Bond lengths (Å)			
Pt-OH_2	2.110	2.111	2.107
Pt-N_{trans}	2.052	2.052	2.050
Pt-$N_{cis(NH2)}$	2.082	2.085	2.085
Pt-$N_{cis(py)}$	2.051	2.057	2.058
Bond angles (°)			
N_{cis}-Pt-N_{cis}	177.51	177.95	178.16
OH_2-Pt-N_{trans}	174.51	175.36	174.99
NBO charges			
Pt	0.736	0.740	0.742
Ru	-	0.315	0.320
N_{trans}	-0.831	-0.837	-0.812
$N_{cis(py)}$	-0.516	-0.510	-0.510
$N_{cis(NH2)}$	-0.837	-0.812	-0.812
Orbital energy (eV)			
HOMO	-7.00	-6.30	-6.40
LUMO	-2.11	-3.16	-3.25
$\Delta E_{HOMO-LUMO}$	4.89	3.14	3.15
η/eV	2.44	1.57	1.58
μ/eV	-4.56	-4.73	-4.83
ω/eV	4.25	7.13	7.38
Point group	C_1	C_1	C_2

μ - Chemical potential, η – Chemical hardness and ω – global electrophilicity index

Figure 5.4 shows the different nitrogen atoms referred to in table 5.2

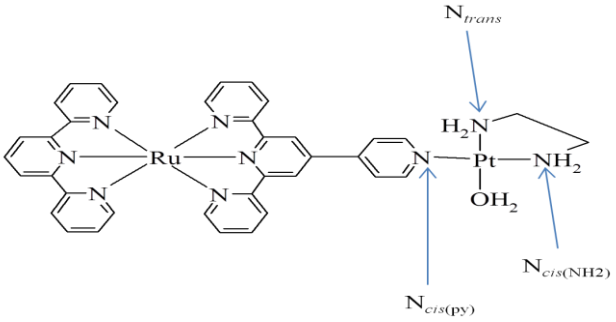


Figure 5.4 Structural formular of Pt2 showing the different N-atoms around the Pt(II) centre.

Due to steric interactions between the pyridyl and *trans*-amino protons in **Pt1**, the pyridyl group lies in a plane almost perpendicular (87.93°) to the plane containing Pt and N atoms reducing π-back bonding between Pt(II) centre and the *cis* pyridyl entity hence lower electrophilicity of the platinum centre.[97] DFT calculated HOMO electron density of **Pt1** lies

predominantly on the Pt(II) centre while that for **Pt2** and **Pt3** complexes lies on the Ru(II) centre and sparsely distributed on the pyridyl ligands but none on the Pt(II) centre resulting **Pt2** and **Pt3** being slightly electrophilic than **Pt1**. The LUMO electron density in table 5.1 comprises MLCT (Metal-to-ligand charge transfer) which is concentrated on the pyridyl group in **Pt1** and on the qpy ligand in the case of **Pt2** and **Pt3** complexes. The incorporation of Ru(II) moiety narrows the HOMO-LUMO energy gap as is evident from the DFT calculations in table 5.2. The k_2 values for **Pt2** and **Pt3** are close indicating that the doubling of the ligand qpy doesn't cause a significant effect to the rate of reaction because the qpy-tpy and qpy-qpy ligands in **Pt2** and **Pt3** respectively are oriented in planes perpendicular (89.58°) to each other hence no π communication that should have led to extended π-conjugation.[94]

5.4 Results and discussion

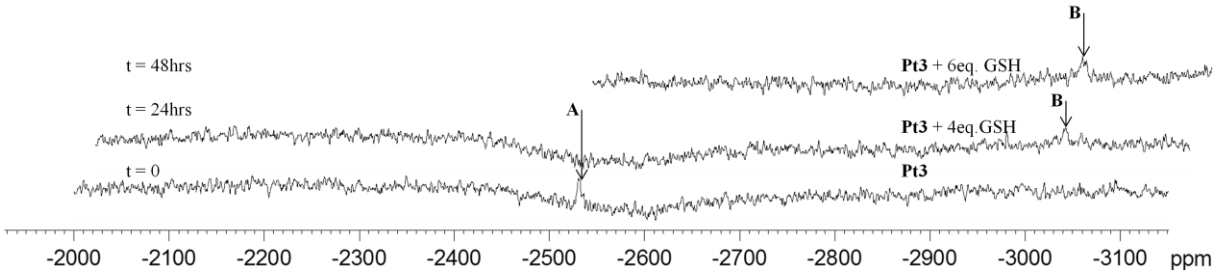
To investigate the impact of the ruthenium polypyridyl ligands on the reactivity of the platinum centre and the competition between the S- and N-ligands, ligand substitution reactions of the metal complexes with the chosen nucleophiles; GMP, L-met and GSH were studied. The experiment on the dependence of reactions on nucleophile concentrations and temperature resulted in rate constants and activation parameters enthalpy of activation, $\Delta H^{\neq}$, and entropy of activation, $\Delta S^{\neq}$, for the displacement of coordinated water as shown in table 5.3.

Table 5.3 Rate constants and activation parameters for studied reactions at 298K

Complex +[Nu]	k_2 (M^{-1} s^{-1})	k_{-2} (s^{-1})	$\Delta H_2^{\neq}$ (kJ mol^{-1})	$\Delta S_2^{\neq}$ ($JK^{-1}mol^{1}$)	$K/(M^{-1})(k_2/k_{-2})$
Pt1					
GMP	0.050 ± 0.001	(6.39 ± 0.2) x 10^{-6}	50 ± 1	-91 ± 3	7825
L-met	0.034 ± 0.001	(-7.76 ± 5.1) x 10^{-6}	72 ± 1	-32 ± 3	4381
GSH	0.005 ± 0.0001	(2.63 ± 0.1) x 10^{-5}	77 ± 1	-26 ± 3	190
Pt2					
GMP	0.059 ± 0.002	(3.36 ± 0.2) x 10^{-5}	68 ± 1	-36 ± 4	1756
L-met	0.058 ± 0.002	(5.32 ± 0.3) x 10^{-5}	62 ± 1	-58 ± 3	1090
GSH	0.008 ± 0.0001	(1.10 ± 0.1) x 10^{-5}	75 ± 1	-23 ± 3	727
Pt3					
GMP	0.057 ± 0.002	(4.16 ± 0.1) x 10^{-5}	64 ± 1	-47 ± 3	1370
L-met	0.065 ± 0.002	(2.64 ± 0.4) x 10^{-5}	43 ± 1	-122 ± 4	2462
GSH	0.010 ± 0.0001	(1.77 ± 0.1) x 10^{-5}	62 ± 1	-66 ± 3	565

The substitution reactions of the Pt(II) complexes with the biological nucleophiles studied as a function of nucleophile concentration at 25° C on the UV-visible spectrophotometer showed

only one reaction step in all cases. The hetero-dinuclear complex **Pt3,** is symmetrical as observed from the DFT calculated structures with the platinum nuclei far apart (22.31Å) which makes them act independent of each other an observation reported in other studies for dinuclear complexes.[98] To confirm the simultaneous substitution on **Pt3**, the complex was subjected to ^{195}Pt NMR spectroscopy at 303 K with excess GSH in deuterated water, and the results are displayed by the NMR arrays in figure 5.5.



*Where **A** is the platinum signal due to the starting complex while **B** platinum signals corresponding to the formation of PtN_3S core.*

Figure 5.5 ^{195}Pt NMR arrays of **Pt-Cl** with excess GSH.

Prior to addition of the nucleophile a signal is observed at $\delta \approx -2530\,\text{ppm}$[88] due to the starting complex **Pt3**. A new signal is observed up-field at $\delta \approx -3020\,\text{ppm}$ confirming the formation of PtN_3S core.[99] The ^{195}Pt NMR results confirm that the aqua ligands in **Pt3** are substituted simultaneously. Since there was no shift in the **Pt** peak after a further 48 hrs, it can be concluded that no dechelation is induced by the substituted S-donor nucleophile, an observation similar to that done with thiourea nucleophiles.[100]

From the k_2 values in table 5.3, the replacement of the pyridyl of Pt(en)py in **Pt1** with tpy(Ru)qpy to form **Pt2** through the 4'- pyridine of the qpy increases slightly the reactivity of the Pt(II) centre with the studied nucleophiles. The rate constants, k_2, for the reaction of **Pt1**, **Pt2** and **Pt3** with L-met are $0.034\text{M}^{-1}\text{s}^{-1}$, $0.058\text{M}^{-1}\text{s}^{-1}$ and $0.065\text{M}^{-1}\text{s}^{-1}$ respectively. Using **Pt1** as reference the ratio is 1: 1.7: 1.9 respectively. The trend for the reaction of the Pt(II) complexes with the rest of the nucleophiles also indicate that the reactivity increases in the order **Pt1** < **Pt2** < **Pt3** for most studied nucleophiles. The increase in overall charge of the complexes **Pt1**(+2) and **Pt2**(+4) due to addition of the tpy(Ru)qpy(+2) increases the overall electrophilicity of the complex as shown by the global electrophilicity index, ω, in table 5.2 resulting in enhancing reactivity from **Pt1** to **Pt3**. Additionally, the tridentate coordination of

the qpy to ruthenium enhances the electronic transitions from the Pt(II) metal centre towards the pyridyl group due to lowering of the energy of the LUMO π^* orbitals.[101,101,102]

The slight increase in Pt-$N_{cis(py)}$ bond length from **Pt1**(2.051Å) to **Pt2**(2.057) (table 5.2) is attributed to pulling of σ-bonding electrons towards the qpy linker, contributing to the slight increase in the positive charge on the Pt(II) metal centre in both **Pt2** and **Pt3.** This shows that the introduction of the qpy ligand enhances to a slight extent electronic transition (MLCT) of the Pt(II) centre.

The introduction of Ru(III) terpyridyl complex results in the narrowing of the HOMO-LUMO energy gap from **Pt1**(4.89eV) to **Pt2**(3.14eV) ≈ **Pt3**(3.15eV) (table 5.2*)* making it easier to transfer electrons from the ground state HOMO to the empty LUMO (π^*).[94,96,101,102] This also accounts for the slight increase in reactivity. **Pt3** is only slightly more reactive than **Pt2** despite the increase in the overall charge. This is because the linker, qpy(Ru)qpy does not allow π-communication between the back-to-back coordinated qpy ligands that would have increased the reactivity. This means that the observed reactivity is independent of each side of the qpy since they are aligned orthogonal to each other at the Ru(III) metal centre. Thus the higher overall charge of **Pt3**(+6) account for the slight increase in the observed reactivity of **Pt3**. The chemical hardness of the complexes decreases from **Pt1** to **Pt3** (table 5.2) showing that stability of the complexes reduces respectively hence the observed increase in reactivity(table 5.2)[103-105] The trend in reactivity is in agreement with the pKa_1 values *viz.* 3.01, 3.61, and 5.53 for **Pt1, Pt3** and **Pt3** respectively. [100]

Reactivity of the nucleophiles follows the order GMP > L-met >GSH for most of the studied complexes. Based on the structures of the nucleophiles, one would expect GMP to be the least reactive because of its bulkiness, however its unexpected reactivity points to the existence of an anchimeric effect. This feature arises from hydrogen bonding interactions between the keto group of the base and the amine protons of the ethylene diamine ligand (figure 5.6)[106] during the transition state with a net reduction in activation energy of substitution. This neighbouring group participation has been observed by other researchers[107] and is well known in organic reactions.[108]

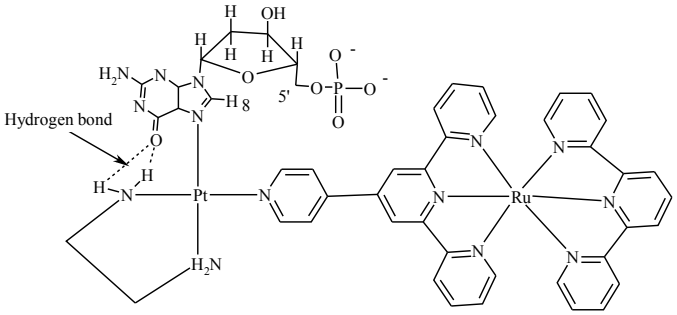


Figure 5.6 Schematic representation of GMP coordinated to the Pt(II) metal centre via N7.

L-met is more reactive than GSH in agreement with previously published results.[109,110] This is attributed to the presence of a methyl group on the sulphur donor atom which through a positive inductive effect increases the nucleophilicity of the atom.[109,110] It can therefore be concluded that the reactivity of the nucleophiles at pH 2 is largely affected by their charge, electronic, steric factors and anchimeric effects. The stability constants ($K = k_2/k_{-2}$) for the platinum complexes listed in table 3 indicate that the products are very stable based on the large values.[107] Relatively low values of the enthalpy of activation ($\Delta H^{\neq}$) and the large and negative entropy of activation ($\Delta S^{\neq}$) support the associative mechanism typical of square planar complexes.[111]

5.5 Conclusion

This study has shown that the replacement of the pyridyl group by tpy(Ru)qpy results in the lowering of the energy of the anti-bonding LUMO orbital and the net HOMO-LUMO energy gap. DFT calculation has shown that qpy ligands lie orthorgonal at the Ru(III) centre eliminating any possibility of π-communication between the ligands hence between the metal centres. The net result of this is that the two Pt(II) centres in **Pt3** act independently of each other. In general the reactivity of these complexes is influenced by both the electronic as well as steric effects. The dominant factor is the increase in the overall cationic charge from **Pt1** to **Pt3.** The trend in pKa values are in line with the observed trend in reactivity. The higher reactivity of **Pt3** is mainly due to the increase in the charge which increases the overall electrophilicity of the complex. ^{195}Pt NMR confirmed simultaneous substitution of the two aqua ligands in **Pt3**. The anchimeric effects of GMP make the nucleophile slightly more reactive than others in the studied complexes. The observed activation parameters support an associative mode of substitution.

5.6 References

1. L. Ronconi and P. J. Sadler, Coord. *Chem. Rev*., 2007, **251**, 1633–1648.
2. P. C. A. Bruijnincx and P. J. Sadler, *Adv. Inorg. Chem*., 2009, **61**, 1–62.
3. B. Rosenberg, L. V. Camp, J. E. Trosko and V. H. Mansour, *Nature*, 1969, **222**, 385–386.
4. B. Rosenberg, *Plat. Met. Rev.* 1971, **15***,* 42–51.
5. Z. Guo, P. J. Sadler, *Adv. Inorg. Chem.* 2000, **49,** 183–306.
6. T. W. Hambley, *Coord. Chem. Rev.* 1997, **166***,* 181–223.
7. E. Wong, C. M. Giandomenico, *Chem. Rev.* 1999, **99***,* 2451–2466.
8. R. B. Weiss, M. C. Christian, *Drugs* 1993, **46,** 360–377.
9. P. J. O'Dwyer, J. P. Stevenson, S. W. Johnson, *Cisplatin: Chemistry and Biochemistry of a Leading Anticancer Drug;* Lippert, B., Ed.; Verlag Helvetica *Chimica Acta*: Zurich; Wiley-VCH: Weinheim, Germany, 1999; pp 31–69.
10. B. Lippert, *Cisplatin, Chemistry and Biochemistry of Leading Antitumor Drugs*, Wiley-VCH, Zürich, 1999.
11. M. A. Fuertes, C. Alonso and J. M. Perez, *Chem. Rev*., 2003, **103**, 645–662.
12. J. Reedijk, *Chem. Rev*., 1999, **99**, 2499–2510.
13. L. R. Kelland, *Drugs Suppl.*, 2000, **59**, 1–8.
14. A. Eastman, *Cisplatin: Chemistry and Biochemistry of a Leading Anticancer Drug;* Lippert, B., Ed.; Verlag Helvetica Chimica Acta: Zurich; Wiley-VCH: Weinheim, Germany, 1999; pp 111–134.
15. M. A. Jakupec, M. Galanski and B. K. Keppler, *Rev. Physiol., Biochem., Pharmacol*., 2003, **146**, 1–54.
16. J. Kozelka, F. Legendre, F. Reeder and J. C. Chottard, *Coord. Chem. Rev*., 1999, 190–192, 61–82.
17. R. G. Pearson, *J. Am. Chem. Soc.* 1963, **85***,* 3533–3539.
18. R. G. Pearson, *J. Chem. Educ.* 1968, **45**, 581–587.
19. R. G. Pearson, *J. Chem. Educ.* 1968, **45**, 643–648
20. J. Redijk*, Eur. J. Inorg. Chem*., 2009, 1303–1312
21. T. Soldatović and Ž. D. Bugarčić, *J. Inorg. Biochem*., 2005, **99**, 1472–1479
22. F. Kratz, *Metal Complexes in Cancer Chemotherapy;* B. K. Keppler, Ed.; VCH: Weinheim, Germany, 1993; pp 391–429

23. K. J. Barnham, M. I. Djuran, P. d. S. Murdoch, J. D. Ranford, P. J. Sadler, *Inorg. Chem.* 1996, **35***,* 1065–1072.
24. E. L. M. Lempers, J. Reedijk, *Adv. Inorg. Chem.* 1991, **37***,* 175–217.
25. P. A. Andrews, W. E. Wung, S. B. Howell, *Anal. Biochem.* 1984, **143**, 46–56.
26. R. C. Dolman, G. B. Deacon, T. W. Hambley, *J. Inorg. Biochem.* 2002**, 88**, 260–267.
27. A. E. C. Korst, C. M. Eeltink, J. B. Vermorken and W. J. F. van der Vijgh, *Eur. J. Cancer*, 1997, **33**, 1425–1429
28. M. S. Ali, S. R. A. Khan, H. Ojima, I. Y. Guzman, K. H. Whitmire, Z. H. Siddik and A. R. Khokhar, *J. Inorg. Biochem*., 2005, **99**, 795–804.
29. W. Arg, I. Khalaila, C. S. Allardyce, L. Juillerat-Jeanneret and P. J. Dyson, *J. Am. Chem. Soc.,* 2005, **127**, 1382–1383.
30. E. G. Talman, W. Bruning, J. Reedijk, A. L. Spek and N. Veldman, *Inorg. Chem.,* 1997, **36**, 854**–**851.
31. K. Lemma, T. Shi and L. I. Elding, *Inorg. Chem*., 2000, **39**, 1728
32. K. Lemma, A. M. Sargeson and L. I. Elding, *J. Chem. Soc., Dalton Trans.,* 2000, 1167**–**1172.
33. J. N. Jolley, A. I. Yanovsky, L. R. Kelland and K. B. Nolan, *J. Inorg. Biochem*., 2001, **83**, 91**–**100.
34. G. Natile and M. Coluccia, *Coord. Chem. Rev*., 2001, 216**–**217, 383**–**410.
35. P. A. Nguewa, M. A. Fuertes, S. Ibbora, Y. Najajreh, D. Gibson, E. Martinez, C. Alonso and J. M. Perez, *J. Inorg. Biochem*., 2005, **99**,727.
36. B. A. J. Jansen, J. Brouwer and J. Reedijk, *J. Inorg. Biochem*., 2002, **89**, 197**–**202.
37. I. Zanzi, S. C. Srivastava, G. E. Meinken, W. Robeson, L. F. Mausner, R. G. Fairchild, D. Margouleff, *Nucl. Med. Biol.* 1989, **16**, 397-403.
38. S. C. Srivastava, *Semin. Nucl. Med.* 1996, **26**, 119-131
39. M. J. Clarke, *Coord. Chem. Rev.* 2003, **236**, 209-233
40. C. S. Allardyce, P. J. Dyson, *Platinum Metals Rev.* 2001, **45**, 62-69.
41. O. Lentzen, C. Moucheron, Kirsch-De Mesmaeker, A., *Metallotherapeutic drugs & metal-based diagnostic agents*. John Wiley & Sons, Ltd: West Sussex, 2005; p 359-378
42. M. J. Clarke, S. Bitler, D. Rennert, M. Buchbinder, A. D. Kelman, *J. Inorg.Biochem.* **1980,** *12*, 79-87.

43. D. M. Stanbury, O. Haas, H. Taube, *Inorg. Chem.* 1980, **19**, 518-524
44. D. M. Stanbury, W. A. Mulac, J. C. Sullivan, H. Taube, *Inorg. Chem.* 1980, **19**, 3735-3740.
45. D. M. Stanbury, D. Gaswick, G. M. Brown, H. Taube, *Inorg. Chem.* 1983, **22**,1975-1982.
46. C. A. Smith, A. J. Sutherland-Smith, B. K. Keppler, F. Kratz, E. N. Baker, *J. Biol. Inorg. Chem.* 1996, **1**, 424-431.
47. M. J. Clarke, F. C. Zhu, D. R. Frasca, *Chem. Rev.,* 1999, **99**, 2511-2533.
48. C. G. Hartinger, S. Zorbas-Seifried, M. A. Jakupec, B. Kynast, H. Zorbas, B. K. Keppler, *J. Inorg. Biochem.* 2006**, 100**, 891-904.
49. K. Polec-Pawlak, J. K. Abramski, O. Semenova, C. G. Hartinger, A. R. Timerbaev, B. K. Keppler, M. Jarosz, *Electrophoresis* 2006, **27**, 1128-1135.
50. M. J. Clarke, M. Buchbinder, A. D. Kelman, *Inorg. Chim. Acta* 1978, **27**, L87-L88.
51. M. J. Clarke, B. Jansen, K. A. Marx, R. Kruger, *Inorg. Chim. Acta* 1986, **124**, 13-28.
52. V. M. Rodriguez-Bailey, K. J. La Chance-Galang, P. E. Doan, M. J. Clarke, *Inorg. Chem.* 1997, **36**, 1873-1883.
53. J. R. Durig, W. D. DannemanBehnke, E. E. Mercer, *Chem.-Biol. Interact.* 1976**, 13**, 287-294.
54. E. Alessio, G. Mestroni, G. Nardin, W. M. Attia, M. Calligaris, G. Sava, S. Zorzet, *Inorg. Chem.* 1988, **27**, 4099-4106.
55. M. Coluccia, G. Sava, F. Loseto, A. Nassi, A. Boccarelli, D. Giordano, E. Alessio, G. Mestroni, *Eur. J. Cancer* 1993, **29A**, 1873-1879.
56. A. Bergamo B. Gava, E. Alessio, G. Mestroni, B. Serli, M. Cocchietto, S. Zorzet, G. Sava, *Int. J. Oncol.* 2002, **21**, 1331-1338.
57. I. Kostova, *Curr. Med. Chem.* 2006, **13**, 1085-1107.
58. E. Gallori, C. Vettori, E. Alessio, F. González-Vílchez, R. Vilaplana, P. Orioli, A. Casini, L. Messori, *Arch. Biochem. Biophys.* 2000, **376**, 156-162.
59. Messori, L.; Orioli, P.; Vullo, D.; Alessio, E.; Iengo, E., *Eur. J. Biochem.* 2000, **267**, 1206-1213.
60. A. Barca, B. Pani, M. Tamaro, E. Russo, *Mutat. Res.-Fundam. Mol. Mech. Mutagen.* 1999, **423**, 171-181.
61. B. Sanna, M. Debidda, G. Pintus, B. Tadolini, A. M. Posadino, F. Bennardini, G. Sava, C. Ventura, *Arch. Biochem. Biophys.* 2002, **403**, 209-218.

62. S. Kapitza, M. Pongratz, M. A. Jakupec, P. Heffeter, W. Berger, L. Lackinger, Keppler, B. K.; Marian, B., *J. Cancer Res. Clin. Oncol.* 2005, **131**, 101-110.
63. O. Nováková, J. Kaspárková, O. Vrána, P. M. van Vliet, J. Reedijk, V. Brabec, *Biochemistry* 1995, **34**, 12369-12378.
64. P. M. Van Vliet, J. G. Haasnoot, J. Reedijk, *Inorg. Chem.* 1994, **33**, 1934-1939
65. P. M. Van Vliet, S. M. S. Toekimin, J. G. Haasnoot, J. Reedijk, O. Nováková, O. Vrána, V. Brabec, *Inorg. Chim. Acta* 1995, **231**, 57-64.
66. F. Zobi, M. Hohl, W. Zimmermann, R. Alberto, *Inorg. Chem.* 2004, **43**, 2771-2772.
67. A. H. Velders, H. Kooijman, A. L. Spek, J. G. Haasnoot, D. de Vos, J. Reedijk, *Inorg. Chem.* 2000, **39**, 2966-2967.
68. A. C. G. Hotze, A. H. Velders, F. Ugozzoli, M. Biagini-Cingi, A. M. Manotti-Lanfredi, J. G. Haasnoot, J. Reedijk, *Inorg. Chem.* 2000, **39**, 3838-3844.
69. F. González-Vílchez, R. Vilaplana, G. Blasco, L. Messori, *J. Inorg. Biochem.* 1998, **71**, 45-51.
70. D. Chatterjee, M. S. Ward, R. E. Shepherd, *Inorg. Chim. Acta* 1999, **285**, 170-177.
71. R. E. Shepherd,Y. Chen, R. A. Kortes, M. S. Ward, *Inorg. Chim. Acta* 2000, **303**, 30-39.
72. R. E. Morris, R. E. Aird, P. D. Murdoch, H. M. Chen, J. Cummings, N. D. Hughes, S. Parsons, A. Parkin, G. Boyd, D. I. Jodrell, P. J. Sadler, *J. Med. Chem.* 2001, **44**, 3616-3621.
73. R. E. Aird, J. Cummings, A. A. Ritchie, M. Muir, R. E. Morris, H. Chen, P. J. Sadler, D. I. Jodrell, *Br. J. Cancer* 2002, **86**, 1652-1657.
74. O. Nováková, H. M. Chen, O. Vrána, A. Rodger, P. J. Sadler, V. Brabec, *Biochemistry* 2003, **42**, 11544-11554.
75. O. Nováková, J. Kaspárková, V. Bursova, C. Hofr, M. Vojtiskova, H. M. Chen, P. J. Sadler, V. Brabec, *Chem. Biol.* 2005, **12**, 121-129.
76. F. Wang, H. M. Chen, S. Parsons, L. D. H. Oswald, J. E. Davidson, P. J. Sadler, *Chem.-Eur. J.* 2003, **9**, 5810-5820.
77. B. Armitage, *Chem. Rev.* 1998, **98**, 1171-1200
78. C. Creutz, H. Taube, *J. Am. Chem. Soc.* 1973, **95**, 1086-1094
79. E. Iengo, G. Mestroni, S. Geremia, M. Calligaris, E. Alessio, *J. Chem. Soc.-Dalton Trans.* 1999, 3361-3371.
80. R. S. Srivastava, F. R. Fronczek, *Inorg. Chim. Acta* 2001, **322**, 32-36
81. A. Wu, D. C. Kennedy, B. O. Patrick, B. R. James, *Inorg. Chem.* 2003, **42**, 7579-

7586.

82. R. S. Srivastava, F. R. Fronczek, L. M. Romero, *Inorg. Chim. Acta* 2004, **357**, 2410-2414.
83. M. A. S. Aquino, *Coord. Chem. Rev.* 2004, **248**, 1025-1045
84. V. Brabec, O. Nováková, *Drug Resist. Update* 2006, **9**, 111-122
85. E. C. Constable, A. M. W. Cargill Thompson, *J. Chem. Soc.-Dalton Trans.* 1994, 1409-1418.
86. *Inorganic Chemistry*, 2006, **45**, No. 7, 2953
87. *J. Chem. Soc*., *Dalton Trans*., 2002, 951–956
88. (a) K. van der schilden., *design and development of polypyridyl complexes in search of a new anti-cancer agents (*PhD thesis*)*. 2006, 133-149. (b) K. J. Takeuchi, M. S. Thompson, D. W. Pipes, T. J. Meyer., *Inorg. Chem.,* 1984, **23**, 1845 (c) C. B. Smith, C. L. Raston, A. N. Sobolev., *Green Chem.,* 2005, **7**, 650
89. (a) L. S. Hollis, A. R. Amundsen, E. W. Stern, *J. Med. Chem.* 1989, **32**, 128-136. (b) H. Brunner, K. -M. Schellerer, *Inorg. Chim. Acta.* **2003**, *350*, 39. (c) G. Mahal, R. van Eldik, *Inorg. Chem.* **1987**, *127*, 203. (d) E. C. Constable, *Inorg. Chem. Radiochem.* **1986**, *30*, 69.
90. T. G. Appleton, J. R.Hall, S. F. Ralph and C. S. M. Thompson, inorg. Chem., 1984, **23**, 3521
91. M. J. Frisch, *Gaussian 09, Revision A.02*, 2009, Gaussian, Inc., Wallingford CT.
92. (a) D. Jaganyi, K. L. De Boer, J. Gertenbach and J. Perils, Int. J. Chem. Kinet., 2008, **40**, 808–818; (b) D. Jaganyi, D. Reddy, J. A. Gertenbach, A. Hofmann and R. van Eldik, Dalton Trans., 2004, 299–304
93. E. C. Constable, C. E. Housecroft, L. A. Johnston, D. Armspach, M. Neuburger, and M. Zehnder, *Polyhedron*, 2001, **20**, 483.
94. H. S. Chow, Ph. D. Thesis Universty of Basel Switzerland, 2005
95. J. A. Thomas, C. Metcalfe, S. Spey, H. Adams, *J. Chem. Soc. Dalton Trans.,* 2002, 4732-4739
96. (a) J. S. Field, J. Gertenbach, R. J. Haines, L. P. Ledwaba, N. T. Mashapa, D. R. McMillin, O. Q. Munro, G. C. Summerton, *Dalton Trans.,* 2003, 1176-1180. (b) E. C. Constable, J. Lewis, M. C. Liptrot and P. R. Raithby, *Inorg. Chim. Acta*, 1990, **178**, 47.
97. B. Petrović, Z. D. Bugarčić, A. Dees, I. Ivavanović-Burmazović, F. W. Heinemann, R. Puchta, S. N. Steinmann, C. Corminboeuf, R. V. Eldik, *Inorg. Chem.,* 2011

98 . (a) R. A. Ruhayel, J. S. Langner, M. J. Oke, S. J. Berners-Price, I. Zgani, N. P. Farrel, *J. Am. Chem. Soc,* 2012, **134**, 7135. (b) J. Maigut, H. Ertürk, R. Puchta, R. Van Eldik, *Dalton Trans.*, 2008, 2759

99 . E. L. Crossley, D. Caia and L. M. Rending, *Dalton Trans.,* 2005, 2825

100. D. Jaganyi, A. Shaira, Manuscript in preparation

101. S. Swavey, Z. Fang, K. J. Brewer, *Inorg. Chem.,* 2002, **41**, 2598

102. A. Jain, J. Wang, E. R. Mashack, B. S. J. Winkel, K. J. Brewer, *Inorg. Chem.,* 2009, 48, 9077

103. *J. Chem. Sci.* Vol. 123, No. 5, September 2011, pp. 727–731.

104. P. K. Chattaraj and B. Maiti, *J. Am. Chem. Soc.,* 2003, **125,** 2705

105. (a) A. Vektariene, G. Vektaris and J. Svoboda, 2009, *ARKIVOC* **7**, 311(b) R. G. Parr, L. Szentpaly and S. Liu *J. Am. Chem. Soc.,* 1999, **121,** 1922

106. K. Van der Schilden, Ph. D. Thesis, Leiden University, 2005

107. (a) D. Jaganyi, F. Tiba, *Trans. Met. Chem*., 2003, **28**, 803 (b) G. Annibale, M. Brandolisio, _Z. D. Bugarcic and L. Cattalini, *Trans. Met. Chem*., 1998, **23**, 715 (c) ZZ.D. Bugar_ci_c, D. Ilic and M.I. Djuran, *Austr. J. Chem*., 2001, **54**, 237 (d) T. Shi and L.I. Elding, Inorg. Chem., 35, 735 (1996); T. Shi and L.I. Elding, *Inorg. Chem*., 1997, **36**, 528 (e) Z. D. Bugarcic and B.V. Djordjevic´ , *Monatsh. Chem*., 1998, **129**, 1267

108. R.G. Wilkins, *Kinetics and Mechanism of Reactions of Transition Metal Complexes*, 2nd edit., Verlag, Berlin, 1991, p. 300.

109. T. Soldatovic, Z. D. Bugarcic, *Dalton Trans*., 2009,4526

110. B. V. Petrovic, *J. coord Chem*. 2001, **53**, 35

111. J. D. Atwood, *Inorganic and organic reaction mechanisms;* 2nd Edition, Wiley-VCH Inc., NY, 1997, 32-34, 43-61

5.7 Supplementary Information

Support information (ESI) available. Selected mass and NMR spectra, kinetic traces and data corresponding to concentration dependence plots and Eyring plots and wavelengths for kinetic measurements for **Pt1**, **Pt2** and **Pt3** are presented.

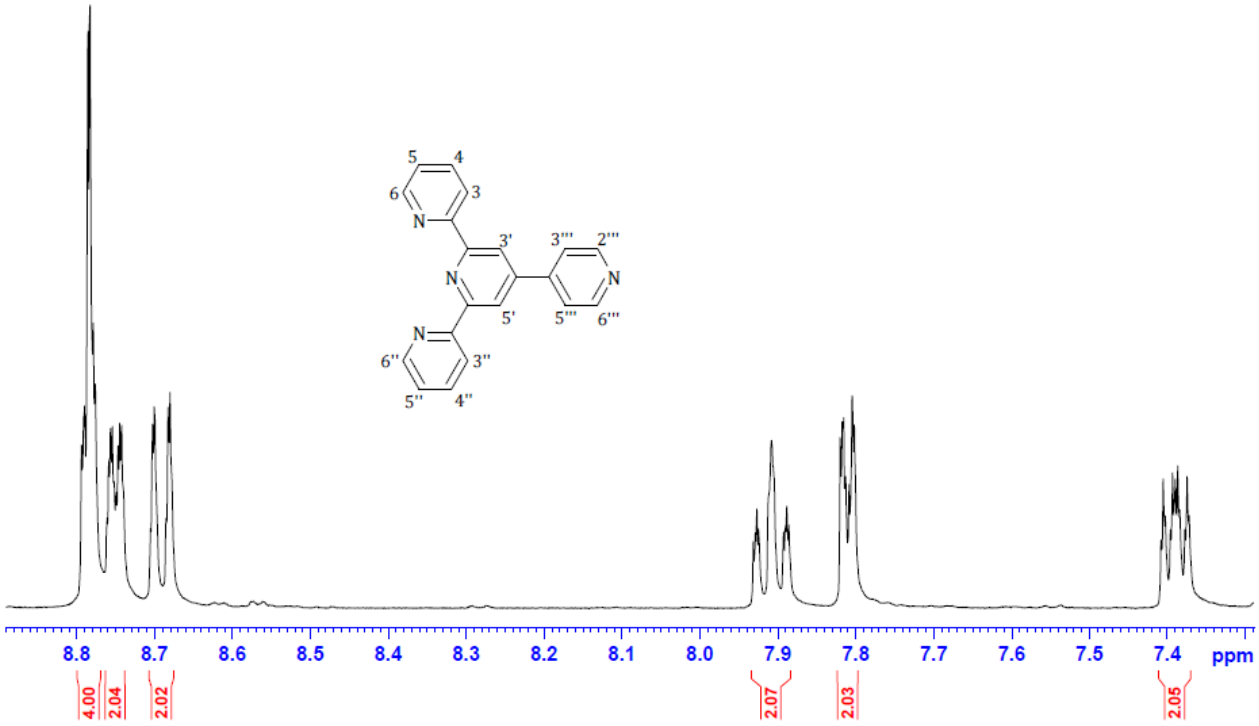


Figure SI 5.1 ^{1}H NMR spectrum of 4'-(4'''-pyridyl)2,2':6',2''-terpyridine in $CDCl_3$.

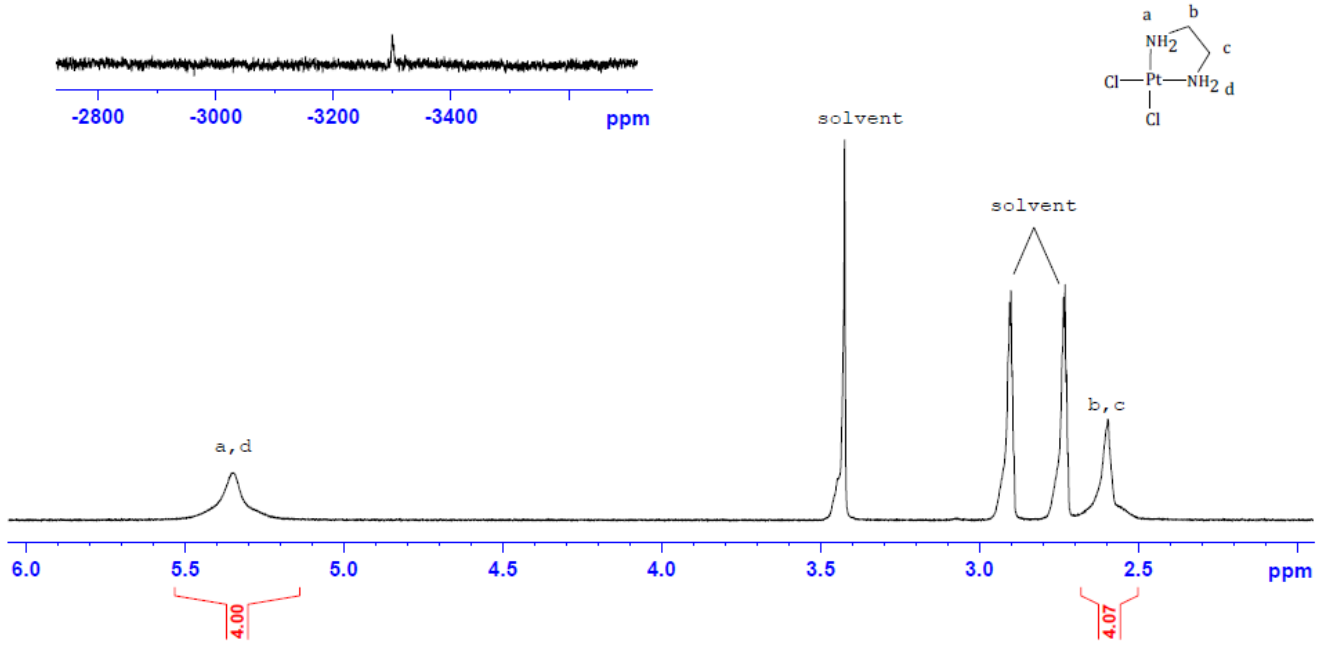


Figure SI 5.2 ^{1}H NMR and ^{195}Pt NMR spectra of $Pt(en)Cl_2$ in DMF-d^7.

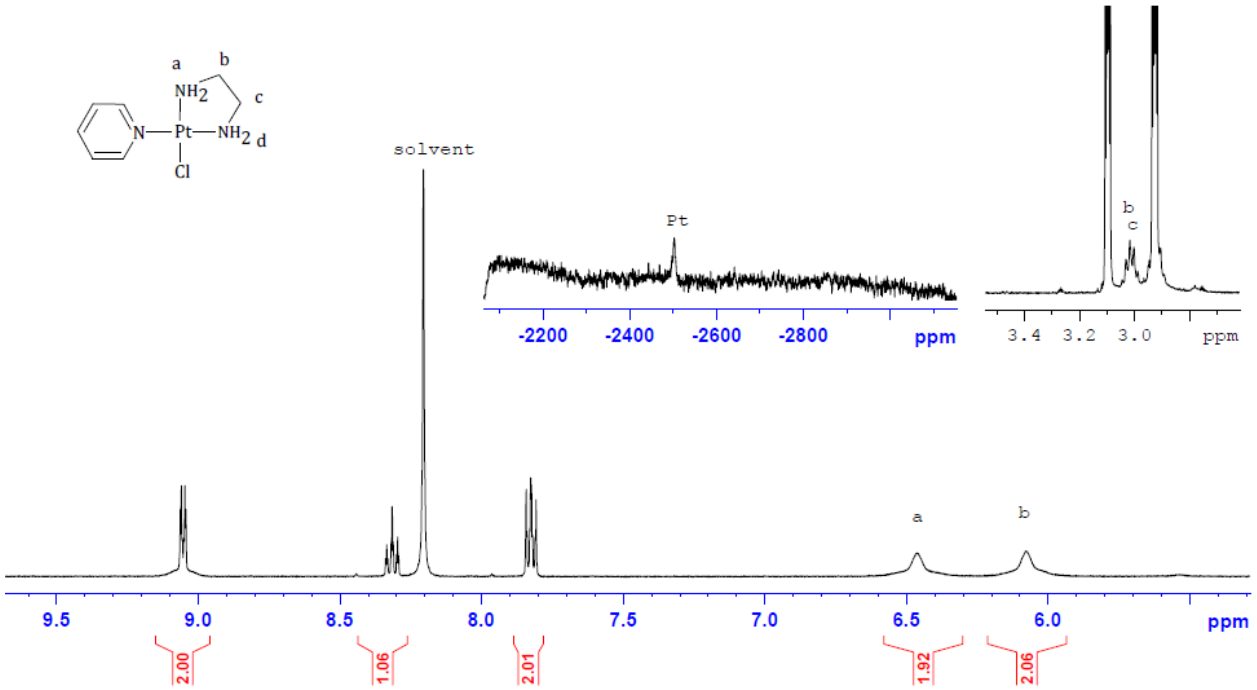


Figure SI 5.3 ^{1}H NMR and ^{195}Pt NMR spectrum of **Pt1-Cl** in DMF-d^7.

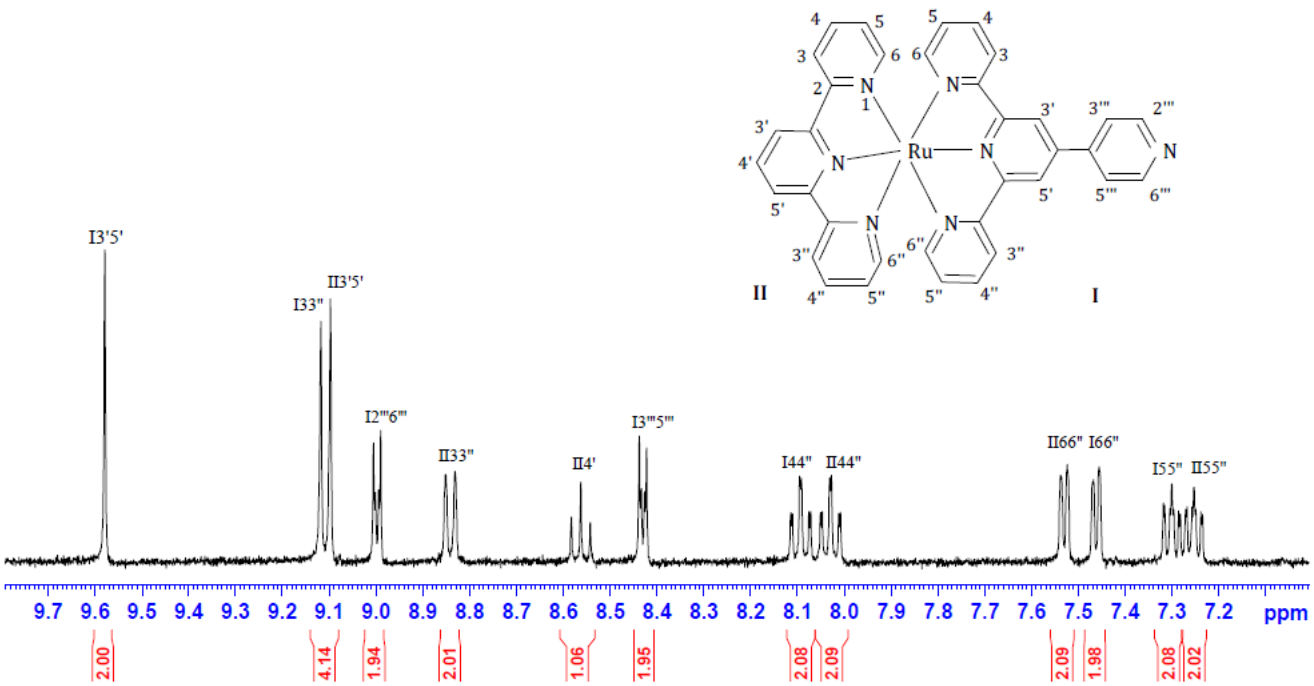


Figure SI 5.4 ^{1}H NMR spectrum of Ru(qpy)(tpy)Cl_2 .

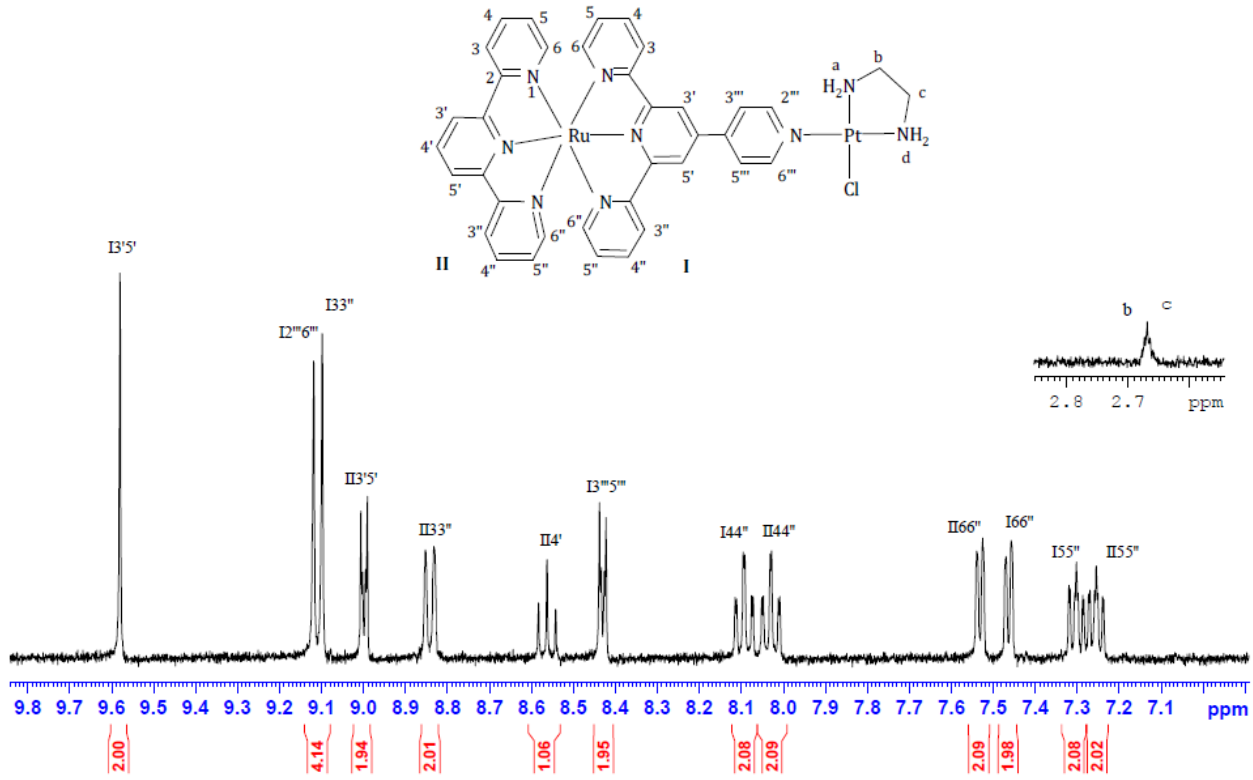


Figure SI 5.5 ^{1}H NMR spectrum of **Pt2-Cl**. Inset is the signal due to the alkyl protons.

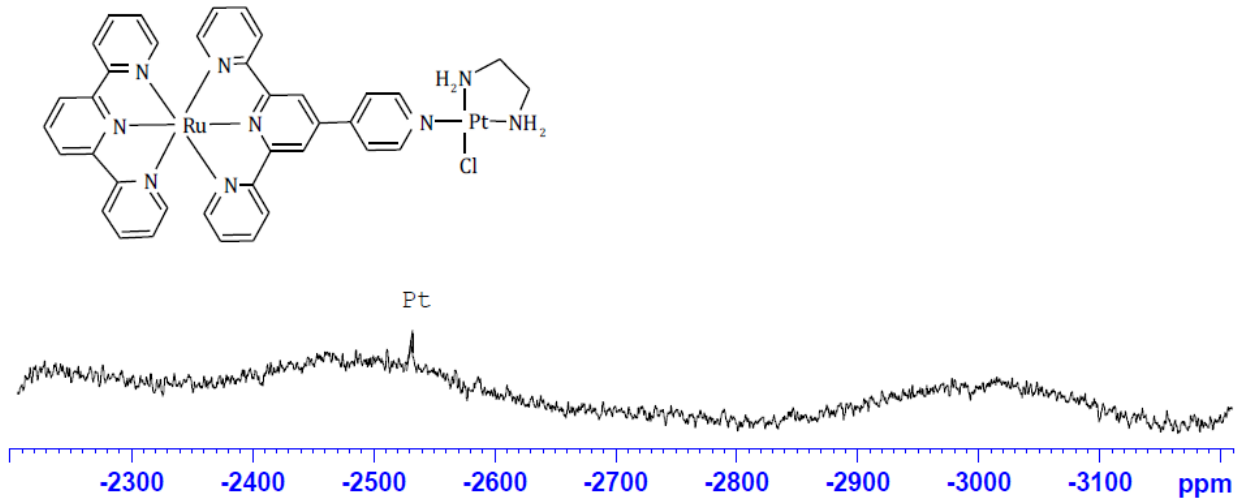


Figure SI 5.6 ^{195}Pt NMR spectrum of **Pt2-Cl**.

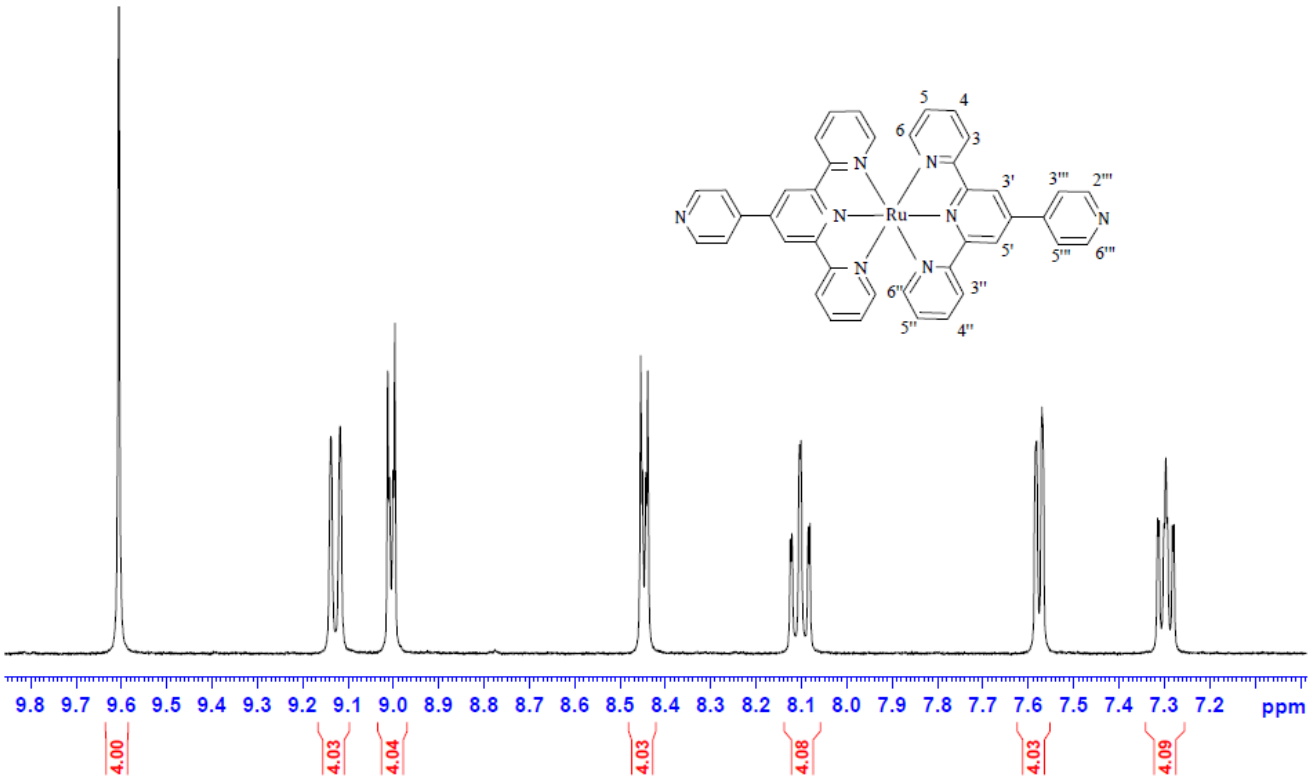


Figure SI 5.7 ^{1}HNMR spectrum of $[Ru(qpy)_2]Cl_2$.

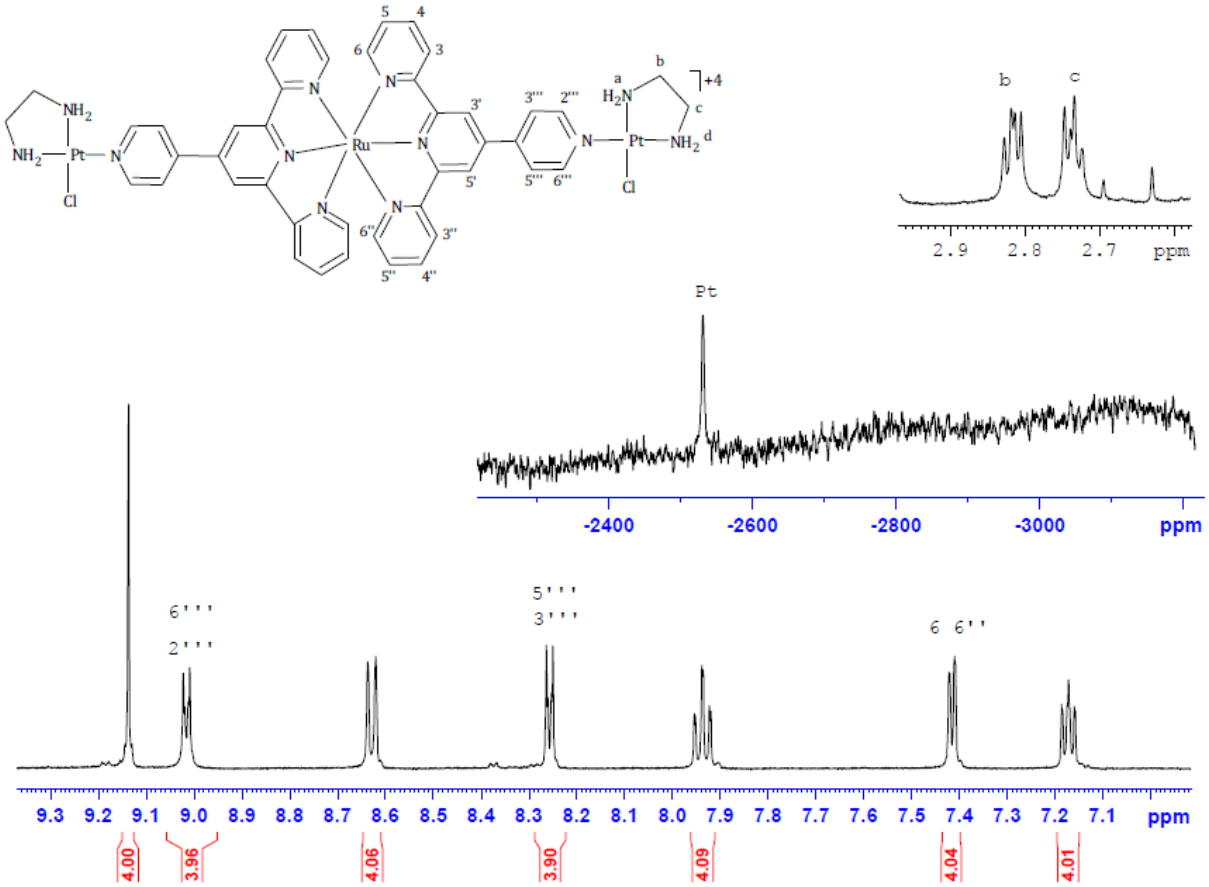


Figure SI 5.8 ^{1}H NMR and ^{195}Pt NMR spectra of **Pt3-Cl**. Insets are the signals due to the alkyl protons and due to Pt.

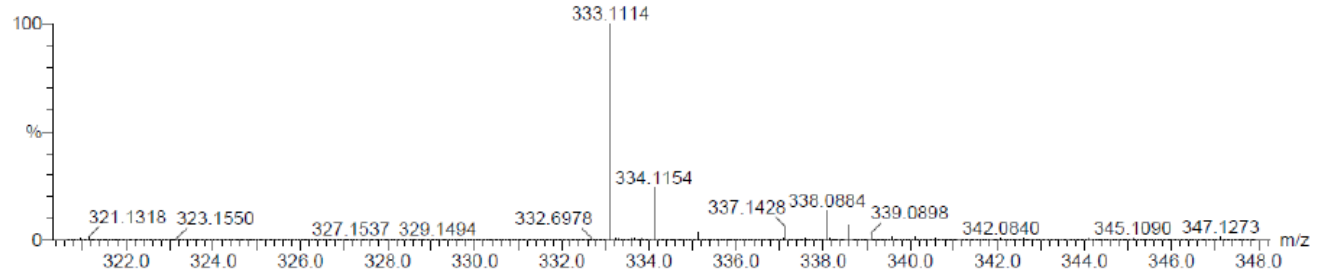
Elemental Composition Report **Page 1**

Single Mass Analysis
Tolerance = 5.0 PPM / DBE: min = -1.5, max = 50.0
Element prediction: Off
Number of isotope peaks used for i-FIT = 3

Monoisotopic Mass, Even Electron Ions
6 formula(e) evaluated with 1 results within limits (all results (up to 1000) for each mass)
Elements Used:
C: 15-20 H: 10-15 N: 0-5 Na: 0-1

Aishath
qtpy 11 (0.170) Cm (1:30)

TOF MS ES+
1.18e+005



Minimum:				-1.5			
Maximum:		5.0	5.0	50.0			
Mass	Calc. Mass	mDa	PPM	DBE	i-FIT	i-FIT (Norm)	Formula
333.1114	333.1116	-0.2	-0.6	15.5	540.3	0.0	C20 H14 N4 Na

Figure SI 5.9 High resolution ESI mass spectrum of qpy.

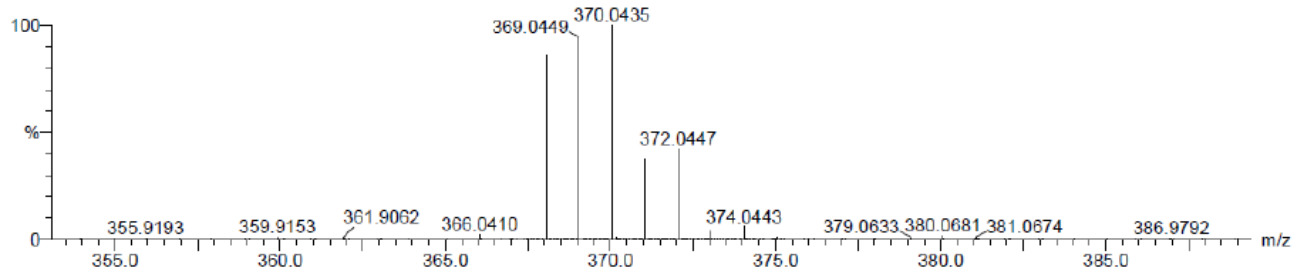
Elemental Composition Report **Page 1**

Single Mass Analysis
Tolerance = 5.0 PPM / DBE: min = -1.5, max = 50.0
Element prediction: Off
Number of isotope peaks used for i-FIT = 3

Monoisotopic Mass, Even Electron Ions
19 formula(e) evaluated with 1 results within limits (all results (up to 1000) for each mass)
Elements Used:
C: 5-10 H: 10-15 N: 0-5 Cl: 0-1 Pt: 0-1

Aishath
Ptenpy 2 (0.017) Cm (1:29)

TOF MS ES+
2.07e+004



Minimum:				-1.5			
Maximum:		5.0	5.0	50.0			
Mass	Calc. Mass	mDa	PPM	DBE	i-FIT	i-FIT (Norm)	Formula
369.0449	369.0446	0.3	0.8	3.5	450.2	0.0	C7 H13 N3 Cl Pt

Figure SI 5.10 High resolution ESI mass spectrum of **Pt1-Cl**.

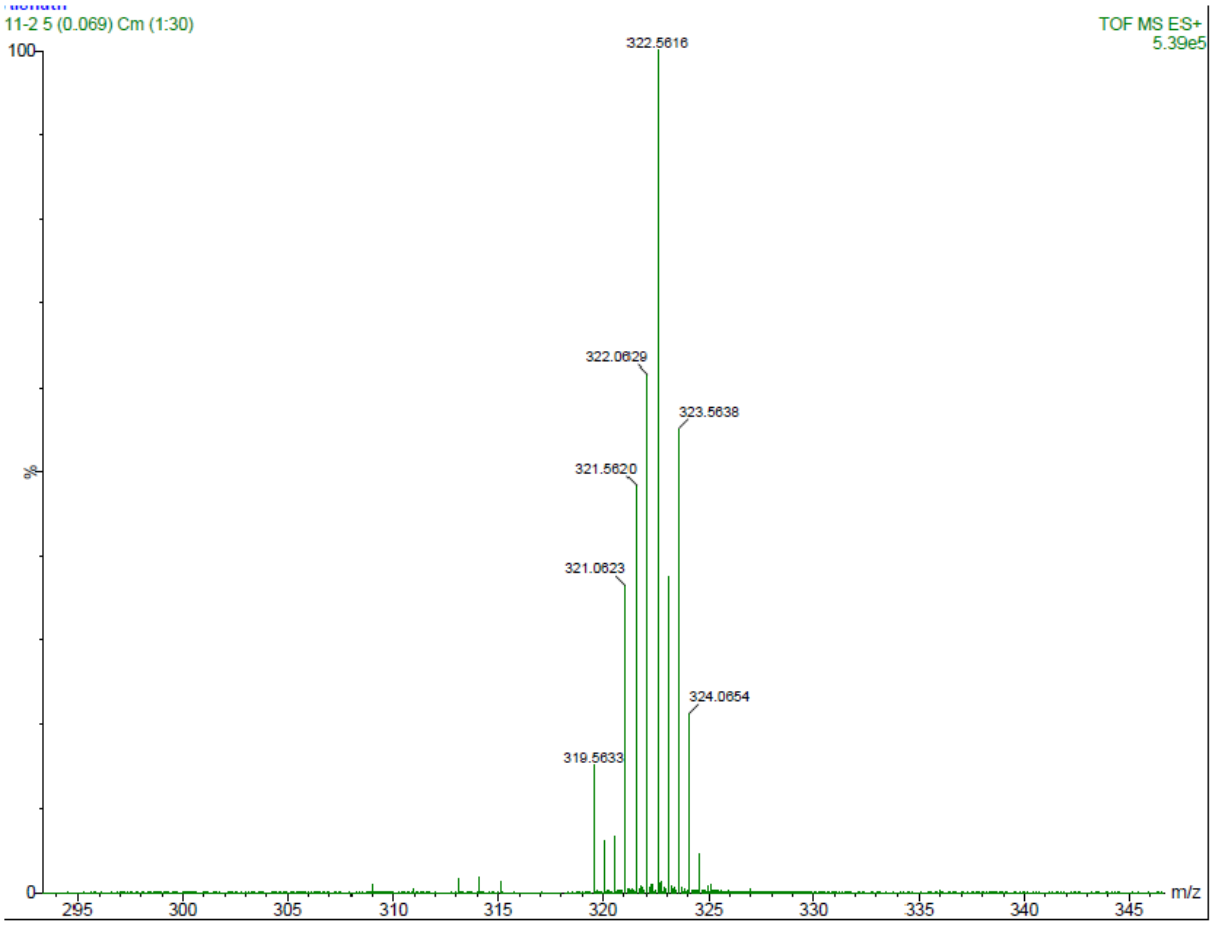


Figure SI 5.11 Low resolution ESI mass spectrum of [Ru(qpy)(tpy)Cl_2].

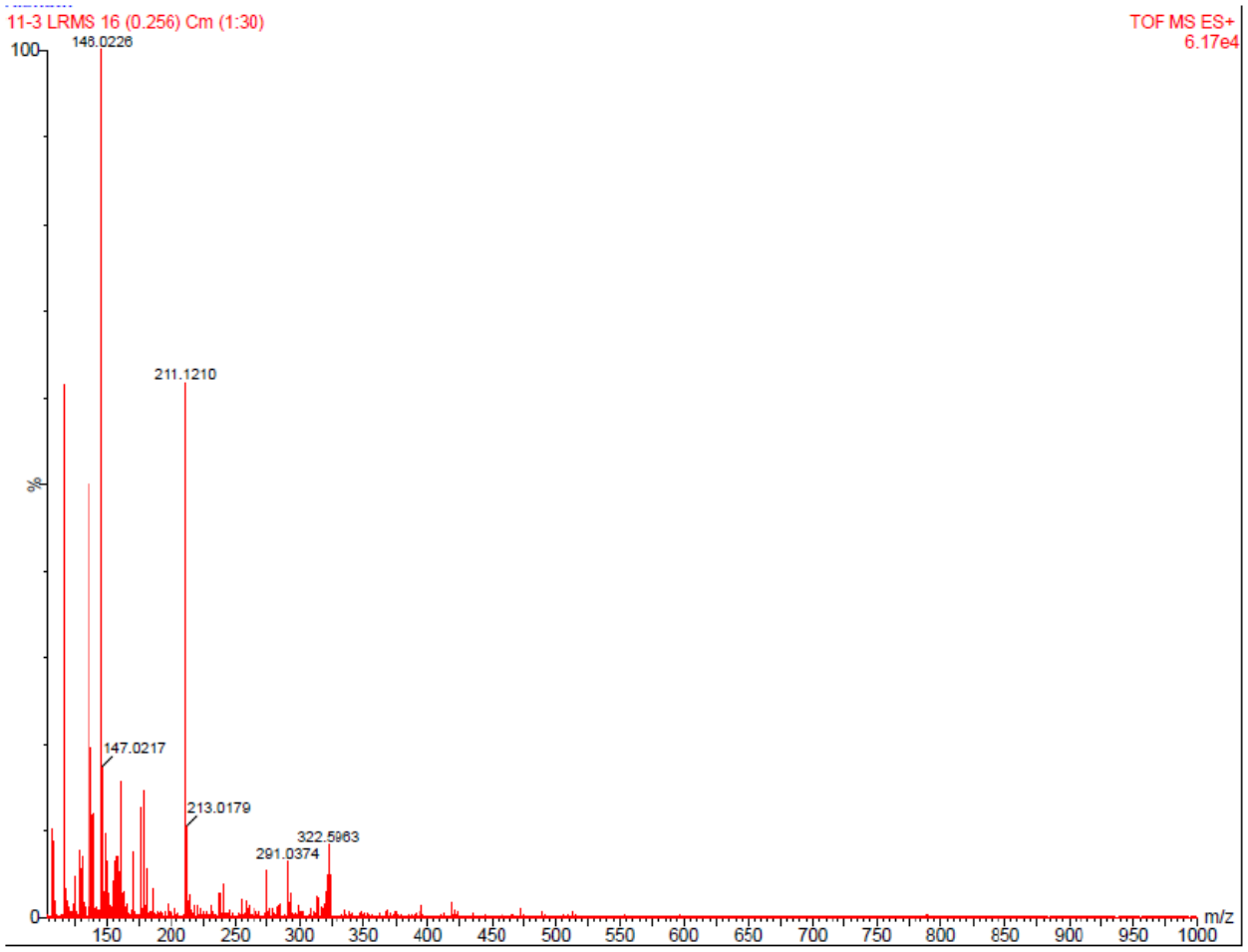


Figure SI 5.12 Low resolution ESI mass spectrum of **Pt2-Cl**.

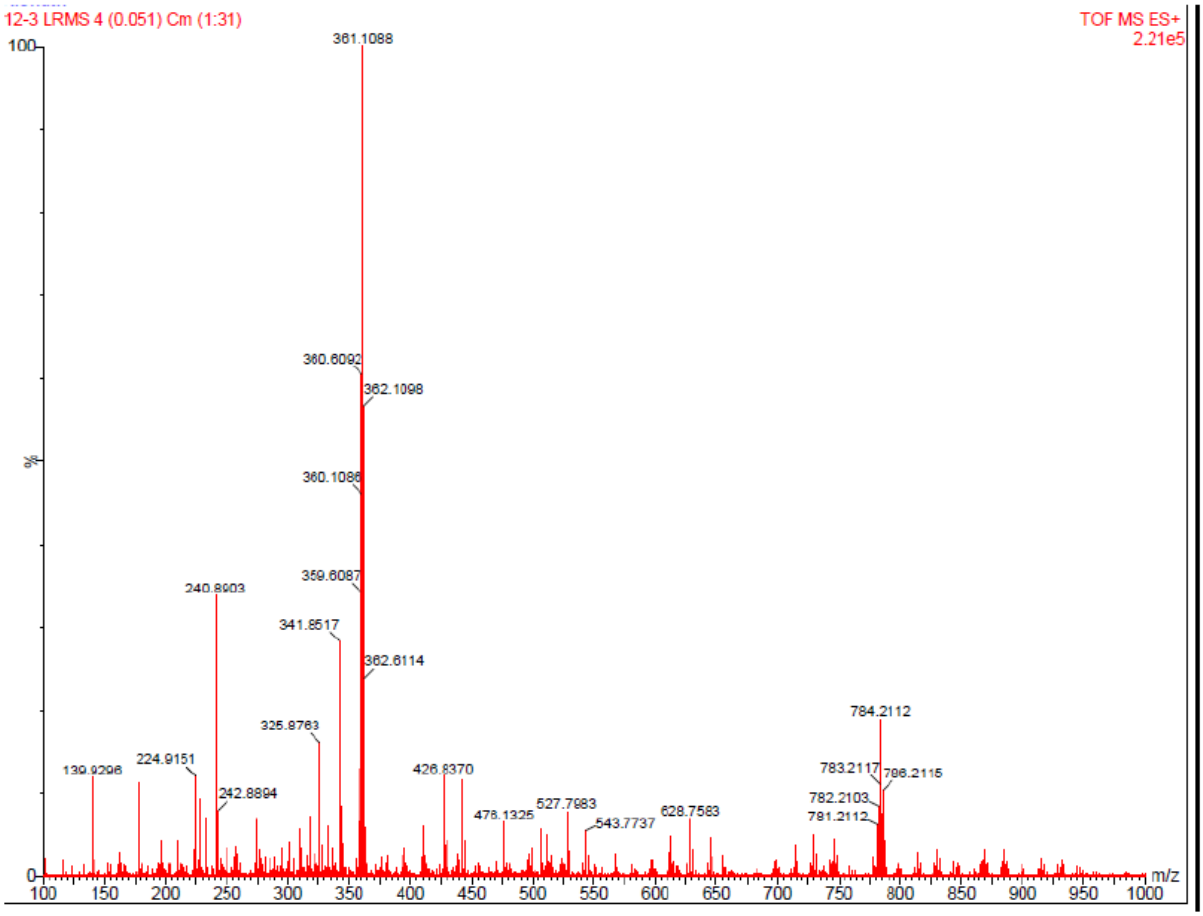


Figure SI 5.13 Low resolution ESI mass spectrum of $[Ru(qpy)_2Cl_2]$.

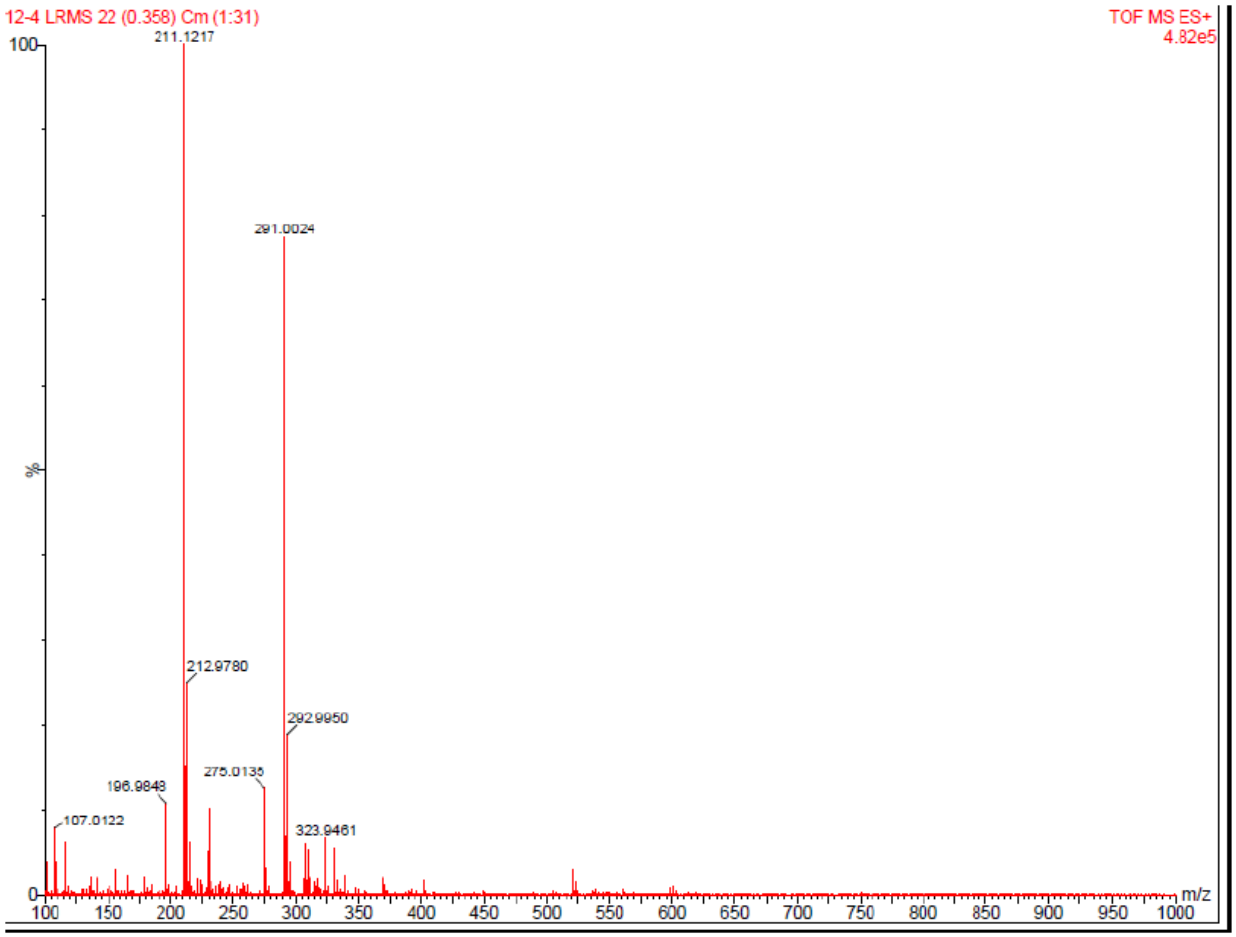


Figure SI 5.14 Low resolution ESI mass spectrum of **Pt3-Cl**.

Experimental SI

Preparation of about 0.1 M Ruthenium(III) Solution

$RuCl_3 \cdot 3H_2O$ (~1.5 g, 5.7 mmol) was refluxed in a mixture (70 mL) of a 1 M HCl and EtOH (v:v = 1:1) for 3 hours. The mixture was cooled and filtered then the filtrate reduced *in vacuo* to 10 mL. An aqueous solution of 1 M HCl was used to dilute the solution to the required acidified ~ 0.1 M Ru(III) solution.

[Ru(tpy)Cl_3]

Equal amounts of $RuCl_3 \cdot 3H_20$ (~150 mg, 0.574 mmol) and terpyridine were refluxed in absolute EtOH (125 mL) for 3 hours. The resulting reaction mixture was cooled to room temperature and the precipitate was filtered, washed with cold absolute EtOH (5 mL)

followed by copious amount of ethylether and dried *in vacuo*. Yield: 191 mg, 433 mmol, (76 %), brown precipitate.

[Ru(qpy)Cl_3]

The ruthenium moiety was synthesized following the literature procedure. The ligand qpy (100 mg; 0.323 mmol) was refluxed in MeOH (25 mL) until it dissolved. To this solution, a 0.1 M Ru(III) solution (3.25 mL; 0.33 mmol) was added drop-wisely. The reaction mixture was refluxed for 1.5 hours. The precipitated crude product was filtered hot. The filtrated was cooled to 253 K, which resulted in the precipitation of a relatively pure product. The product was filtered and dried. Yield: 84 mg, 0.162 mmol (49%).

Table SI 5.1 Summary of the selected wavelengths (nm) used in kinetic measurements

		Wavelength (nm)		
Nucleophile	Reaction step	**Pt1**	**Pt2**	**Pt3**
5'-GMP	1	302	318	320
GSH	1	280	254	255
L- met	1	253	307	310

Table SI 5.2 Average observed rate constants, k_{obs}/s^{-1}, for the substitution of aqua from **Pt1** by biological nucleophiles at 298K

GMP		L-met		GSH	
[Nu]/M	k_{obs}/s^{-1} x10^{-6}	[Nu]/M	k_{obs}/s^{-1}x10^{-5}	[Nu]/M	k_{obs}/s^{-1}x10^{-5}
0.00005	9.04122	0.002	5.73867	0.002	3.58854
0.00010	11.21200	0.004	13.05160	0.004	4.73328
0.00015	13.62436	0.006	20.44630	0.006	5.72506
0.00020	16.49708	0.008	26.28128	0.008	6.67013
0.00025	18.81848	0.010	33.38418	0.010	7.71892

Table SI 5.3 Average observed rate constants, k_{obs}/s^{-1}, for the substitution of aqua from **Pt2** by biological nucleophiles at 298K

GMP		L-met		GSH	
[Nu]/M	k_{obs}/s^{-1} x10^{-5}	[Nu]/M	k_{obs}/s^{-1}x10^{-5}	[Nu]/M	k_{obs}/s^{-1}x10^{-5}
0.0002	4.5206	0.00048	7.83379	0.00048	1.46018
0.0004	5.6806	0.00095	11.13365	0.00095	1.80422
0.0006	7.0848	0.00142	13.69427	0.00142	2.18808
0.0008	7.9192	0.00190	16.04602	0.00190	2.54188
0.0010	9.3060	0.00237	19.04784	0.00237	2.87680

Table SI 5.4 Average observed rate constants, k_{obs}/s^{-1}, for the substitution of aqua from **Pt3** by biological nucleophiles at 298K

GMP		L-met		GSH	
[Nu]/M	k_{obs}/s^{-1} x10^{-5}	[Nu]/M	k_{obs}/s^{-1}x10^{-4}	[Nu]/M	k_{obs}/s^{-1}x10^{-5}
0.00017	5.1725	0.00206	1.60706	0.00206	3.74528
0.00035	6.1709	0.00240	1.84105	0.00240	4.04918
0.00052	7.0176	0.00275	2.05766	0.00275	4.38437
0.00069	8.0329	0.00309	2.25939	0.00309	4.71918
0.00086	9.1443	0.00343	2.51745	0.00343	5.04833

Table SI 5.5 Temperature dependence of $k_2/M^{-1}s^{-1}$ for the substitution of aquafrom **Pt1**by biological nucleophiles at 298K

GMP		L-met		GSH	
T^{-1}/K^{-1}	$\ln(k_2/T)$	T^{-1}/K^{-1}	$\ln(k_2/T)$	T^{-1}/K^{-1}	$\ln(k_2/T)$
0.003413	-7.71105	0.003413	-9.57449	0.003413	-11.09727
0.003356	-7.33737	0.003356	-9.08327	0.003356	-10.55297
0.003300	-6.98185	0.003300	-8.62379	0.003300	-9.85440
0.003249	-6.59914	0.003249	-8.19471	0.003249	-9.50303
0.003195	-6.44595	0.003195	-7.65702	0.003195	-9.08925

Table SI 5.6 Temperature dependence of $k_2/M^{-1}s^{-1}$ for the substitution of aqua from **Pt2** by biological nucleophiles at 298K

GMP		L-met		GSH	
T^{-1}/K^{-1}	**$\ln(k_2/T)$**	**T^{-1}/K^{-1}**	**$\ln(k_2/T)$**	**T^{-1}/K^{-1}**	**$\ln(k_2/T)$**
0.003413	-8.34005	0.003413	-8.72795	0.003413	-9.68473
0.003356	-7.88286	0.003356	-8.03595	0.003356	-9.26151
0.003300	-7.29056	0.003300	-7.84709	0.003300	-8.92388
0.003249	-7.08330	0.003249	-7.45931	0.003249	-8.20170
0.003195	-6.51838	0.003195	-6.98736	0.003195	-7.75360

Table SI 5.7 Temperature dependence of $k_2/M^{-1}s^{-1}$ for the substitution of aqua from **Pt3** by biological nucleophiles at 298K

GMP		L-met		GSH	
T^{-1}/K^{-1}	**$\ln(k_2/T)$**	**T^{-1}/K^{-1}**	**$\ln(k_2/T)$**	**T^{-1}/K^{-1}**	**$\ln(k_2/T)$**
0.003413	-8.18892	0.003413	-8.59007	0.003413	-9.73104
0.003356	-7.69023	0.003356	-8.28971	0.003356	-9.30217
0.003300	-7.39088	0.003300	-7.96506	0.003300	-8.97050
0.003249	-6.86075	0.003249	-7.72011	0.003249	-8.50750
0.003195	-6.21909	0.003195	-7.46580	0.003195	-8.07989

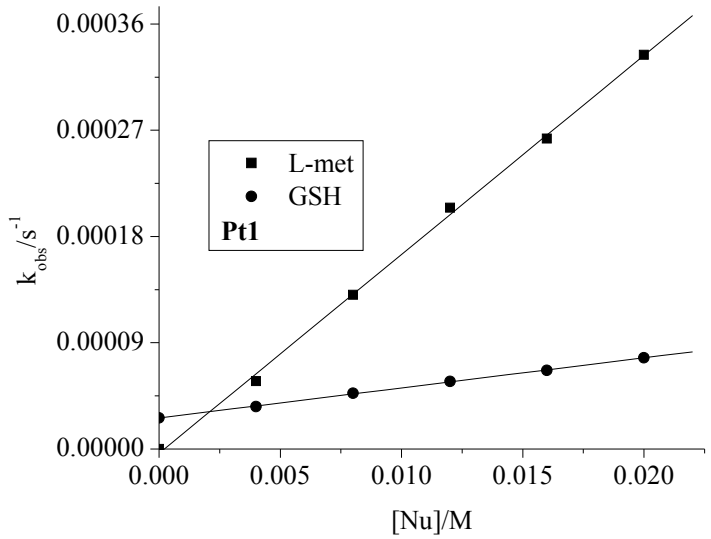


Figure SI 5.15 Concentration dependence plots of L-met and GSH nucleophiles for the aqua substitution on **Pt1** at 298K

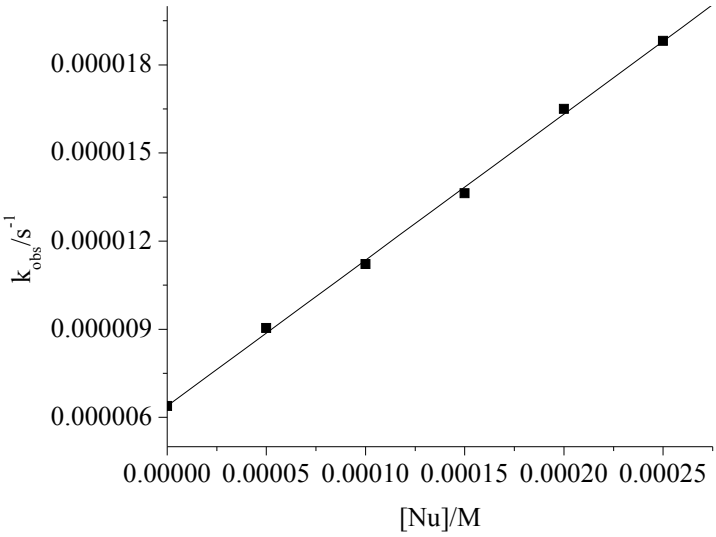


Figure SI 5.16 Concentration dependence plot of 5'GMP nucleophile for the aqua substitution on **Pt1** at 298K

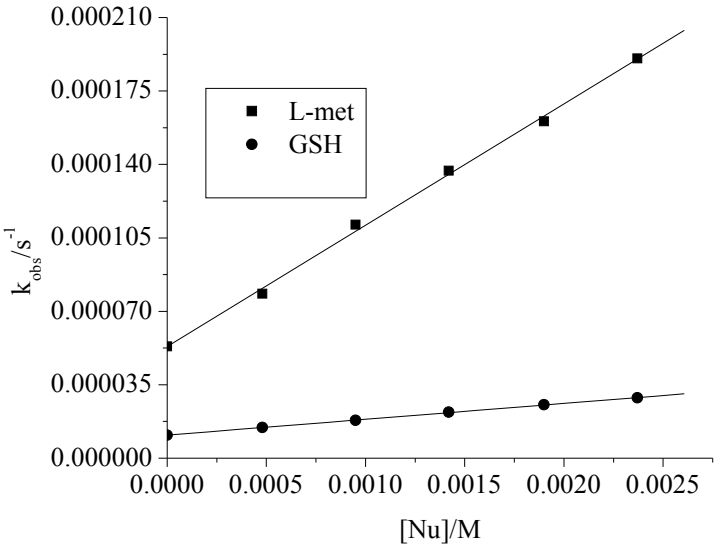


Figure SI 5.17 Concentration dependence plots of L-met and GSH nucleophiles for the aqua substitution on **Pt2** at 298K

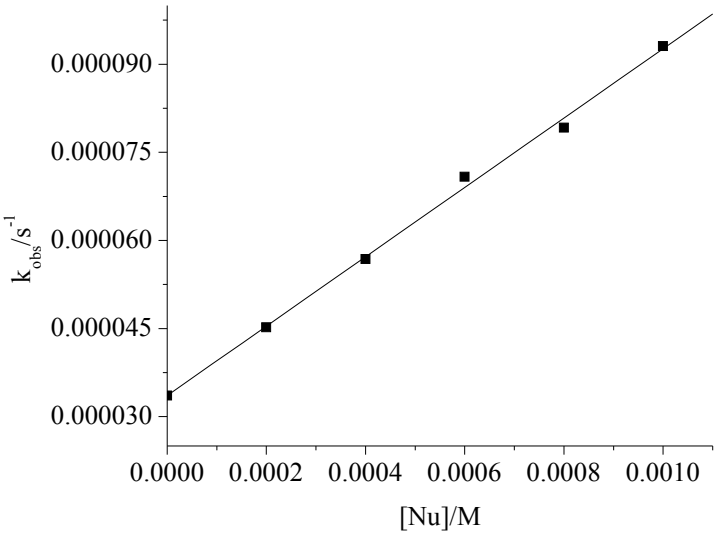


Figure SI 5.18 Concentration dependence plot of GMP nucleophile for the aqua substitution on **Pt2** at 298K

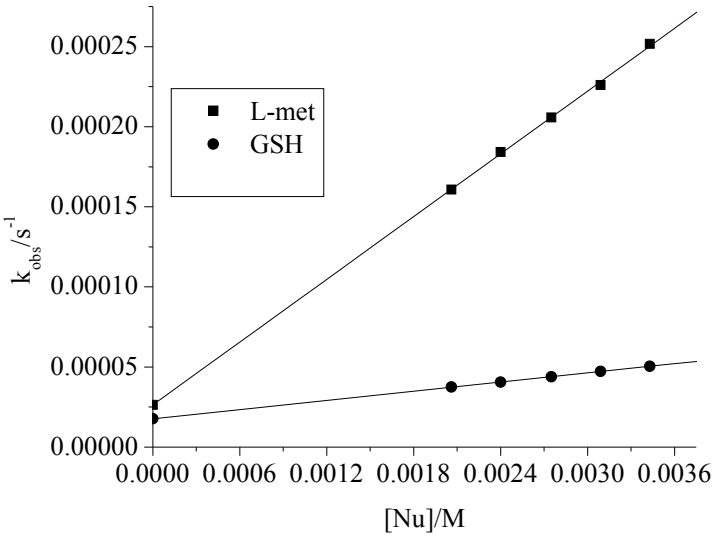


Figure SI 5.19 Concentration dependence plots of L-met and GSH nucleophiles for the aqua substitution on **Pt3** at 298K

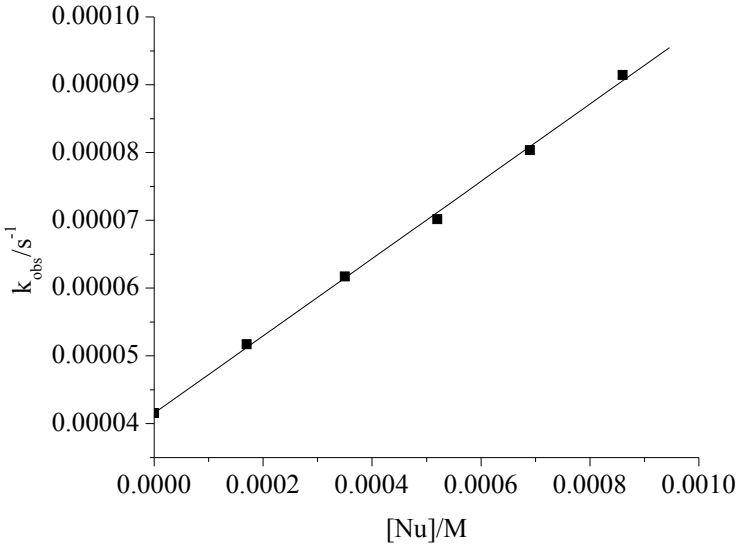


Figure SI 5.20 Concentration dependence plot of GMP nucleophile for the aqua substitution on **Pt3** at 298K

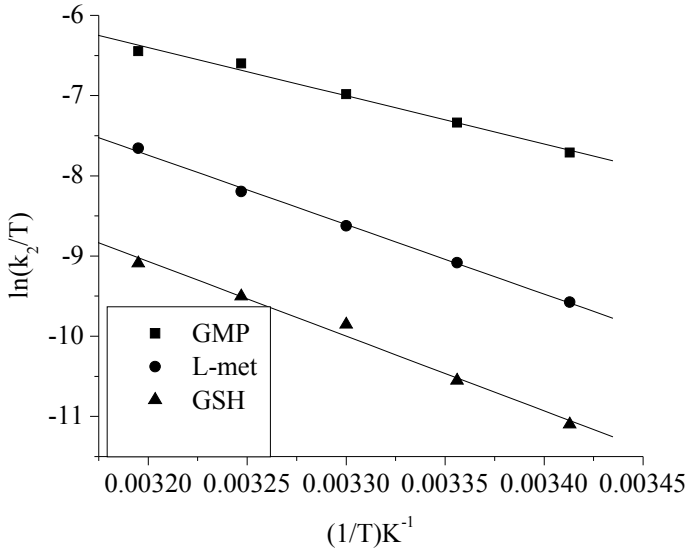


Figure SI 5.21 Eyring plots of **Pt1**with the biological nucleophiles at different temperatures in the range 20-40^0 C

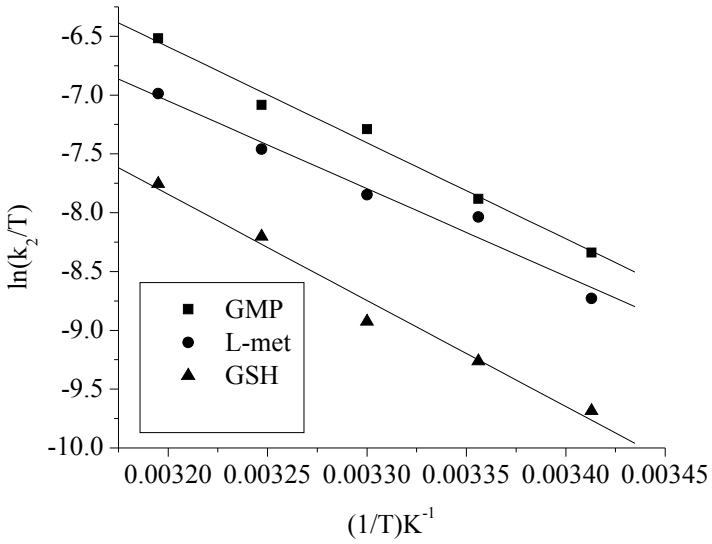


Figure SI 5.22 Eyring plots of **Pt2**with the biological nucleophiles at different temperatures in the range 20-40^0 C

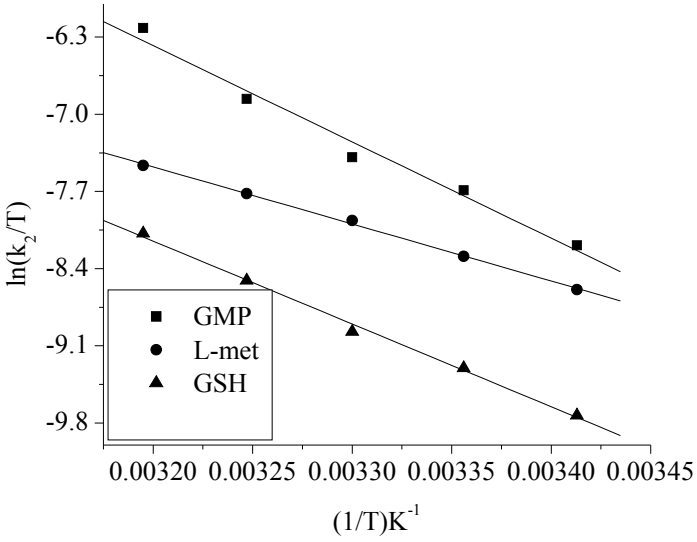


Figure SI 5.23 Eyring plots of **Pt3**with the biological nucleophiles at different temperatures in the range 20-40^0 C

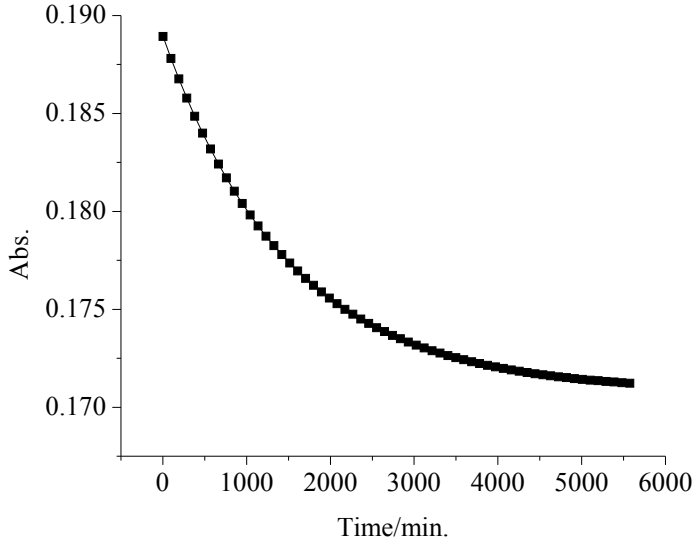


Figure SI 5.24 The kinetic trace for the reaction of **Pt1** with 20 fold GMP at 298K

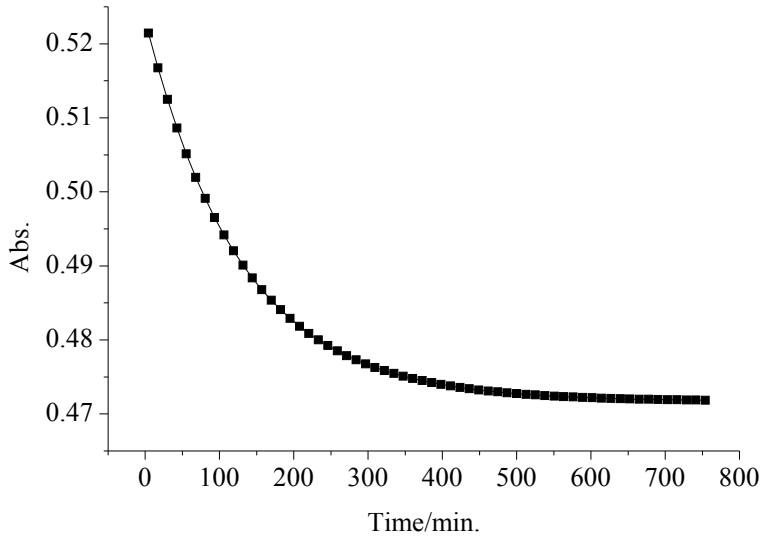


Figure SI 5.25 The kinetic trace for the reaction of **Pt1** with 40 fold L-met at 298K

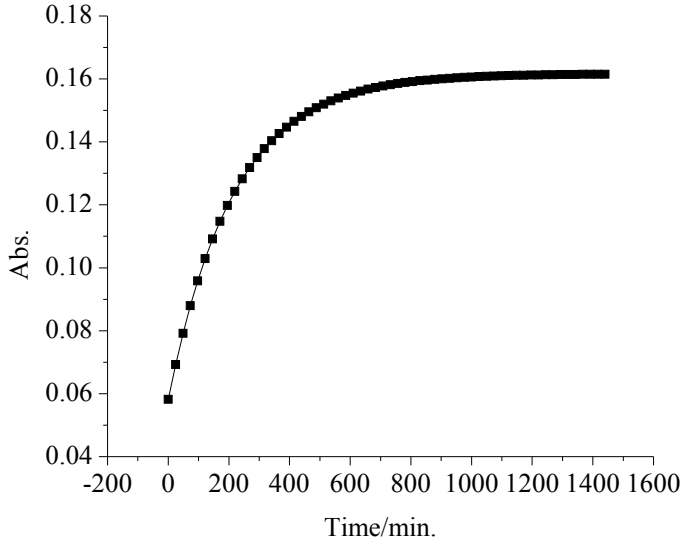


Figure SI 5.26 The kinetic trace for the reaction of **Pt1** with 100 folds GSH at 298K

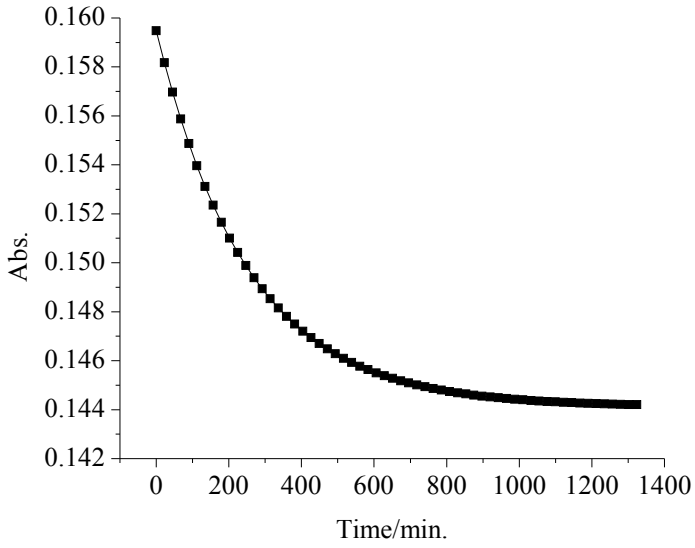


Figure SI 5.27 The kinetic trace for the reaction of **Pt1** with 30 folds GMP at 313K

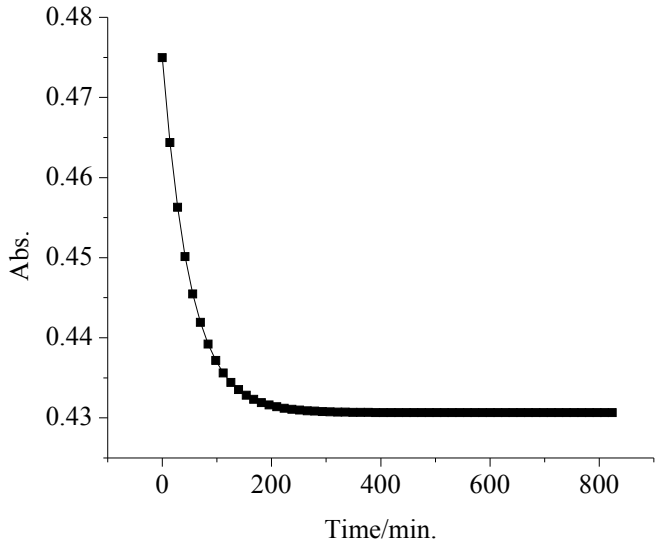


Figure SI 5.28 The kinetic trace for the reaction of **Pt1** with 60 folds L-met at 303K

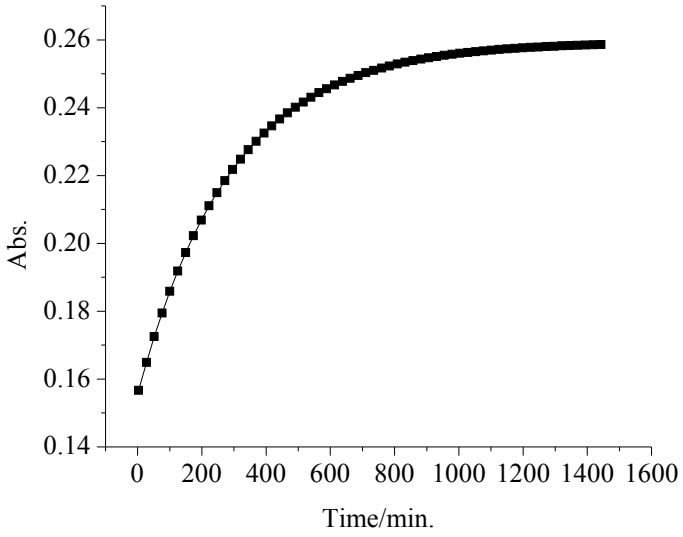


Figure SI 5.29 The kinetic trace for the reaction of **Pt1** with 60 folds GSH at 303K

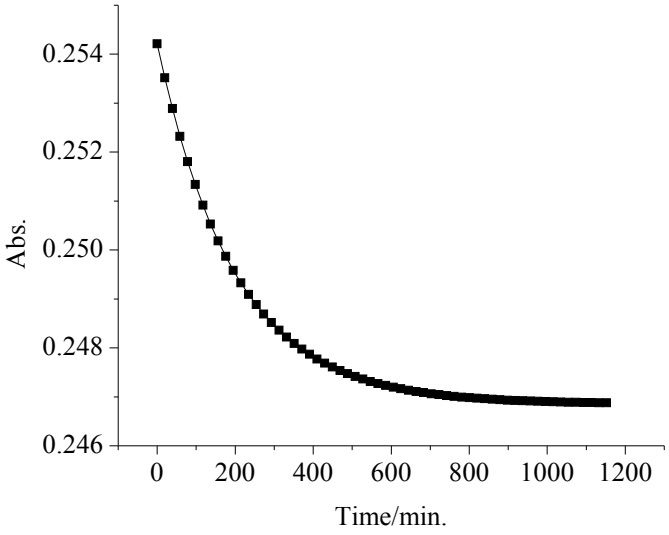


Figure SI 5.30 The kinetic trace for the reaction of **Pt2** with 50 folds GMP at 298K

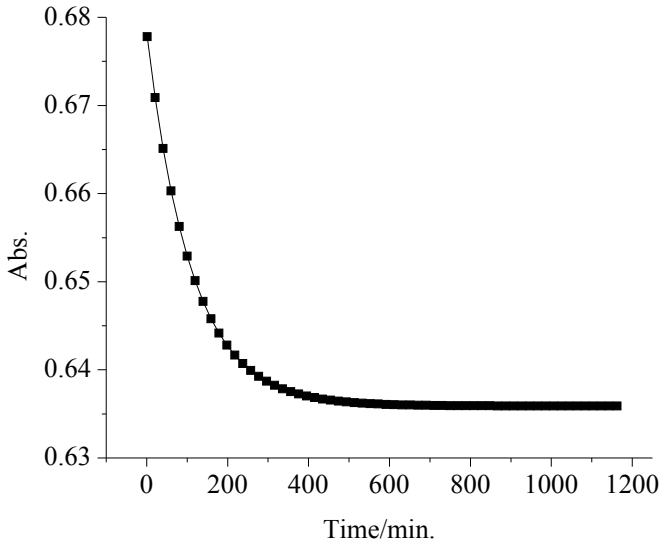


Figure SI 5.31 The kinetic trace for the reaction of **Pt2** with 80 folds L-met at 298K

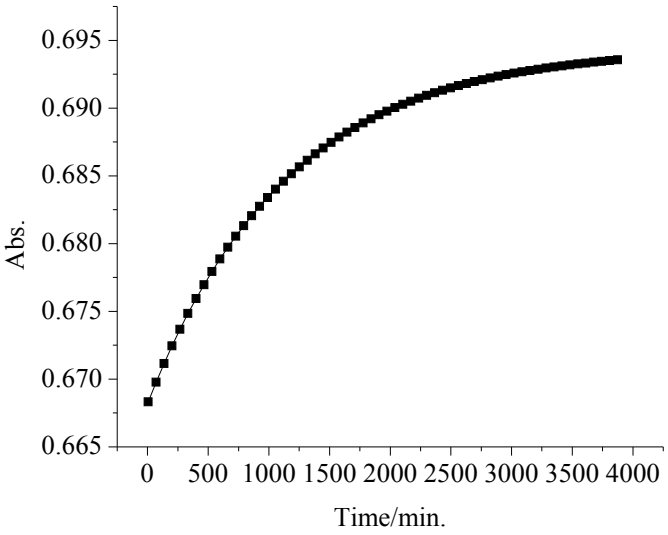


Figure SI 5.32 The kinetic trace for the reaction of **Pt2** with 20 folds GSH at 298K

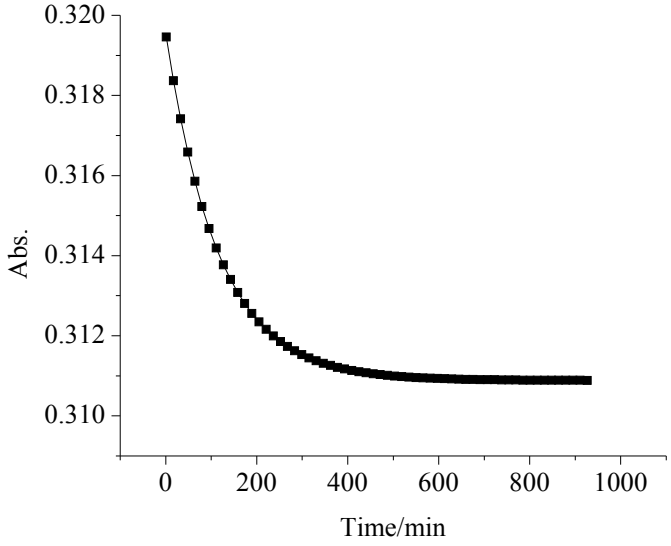


Figure SI 5.33 The kinetic trace for the reaction of **Pt2** with 30 folds GMP at 308K

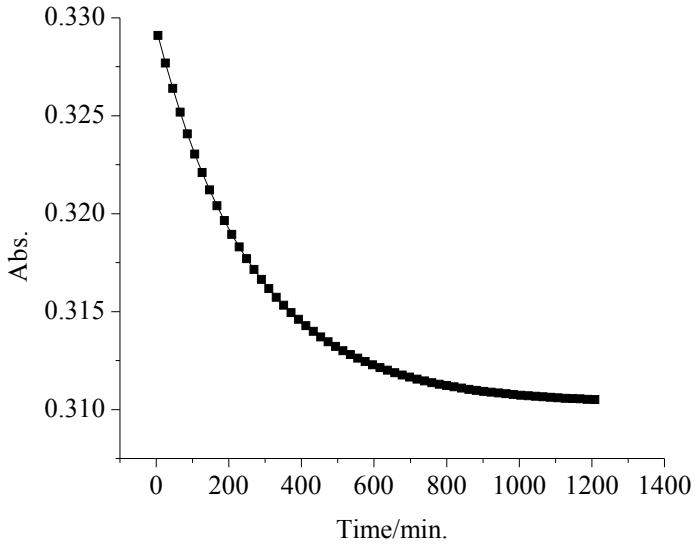


Figure SI 5.34 The kinetic trace for the reaction of **Pt2** with 60 folds GMP at 293K

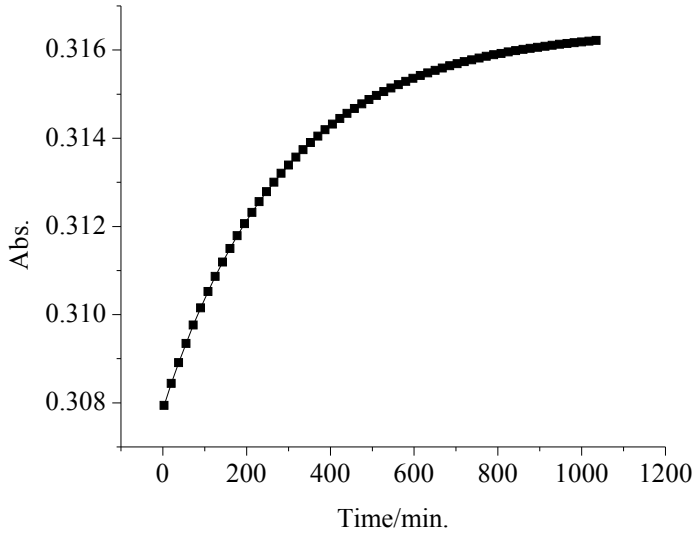


Figure SI 5.35 The kinetic trace for the reaction of **Pt2** with 60 folds GSH at 303K

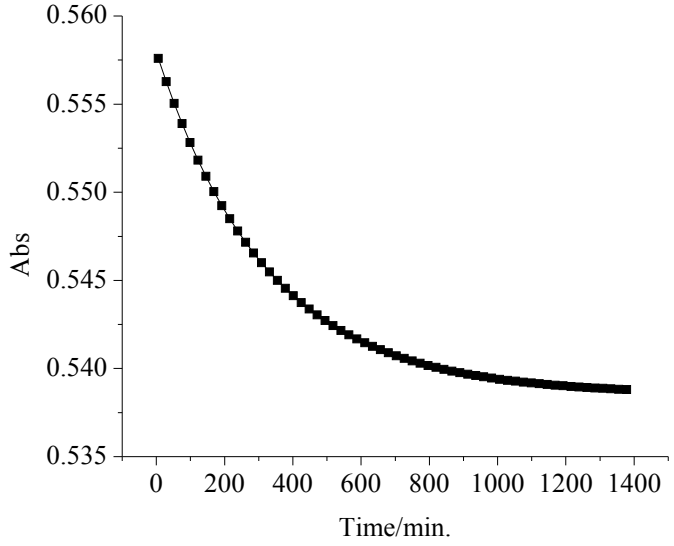


Figure SI 5.36 The kinetic trace for the reaction of **Pt3** with 10 folds GMP at 298K

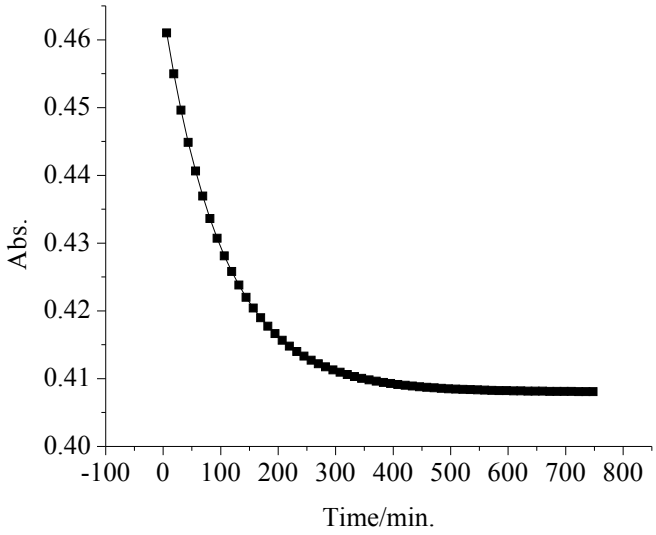


Figure SI 5.37 The kinetic trace for the reaction of **Pt3** with 120 folds L-met at 298K

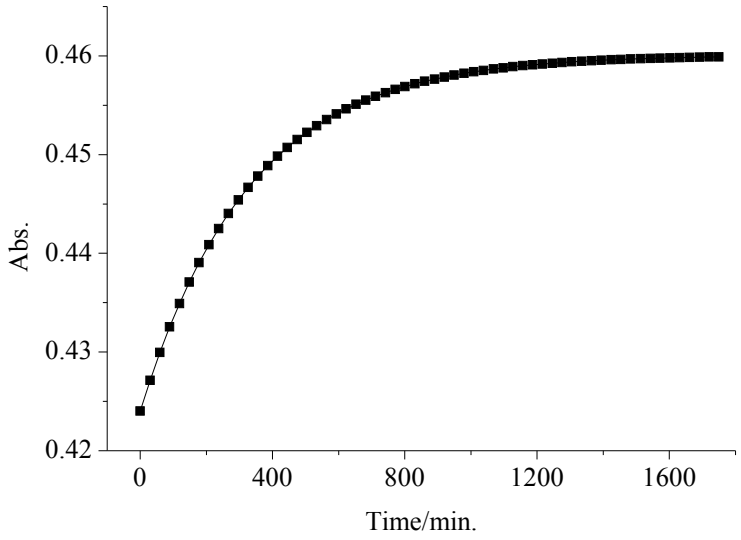


Figure SI 5.38 The kinetic trace for the reaction of **Pt3** with 200 folds GSH at 298K

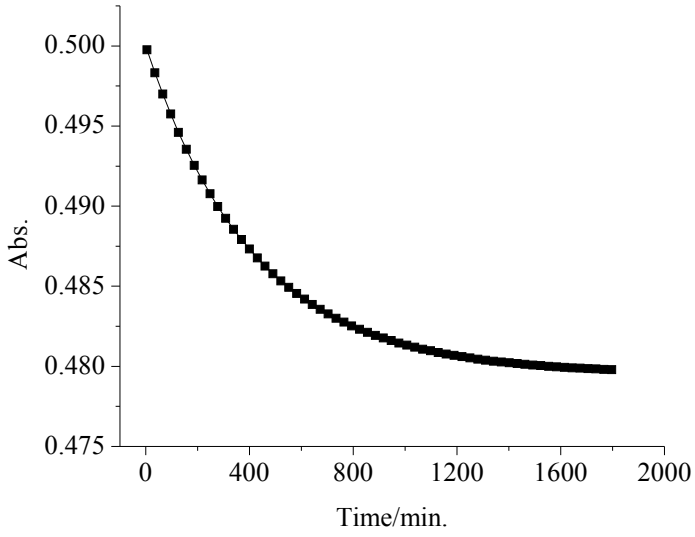


Figure SI 5.39 The kinetic trace for the reaction of **Pt3** with 30 folds GMP at 293K

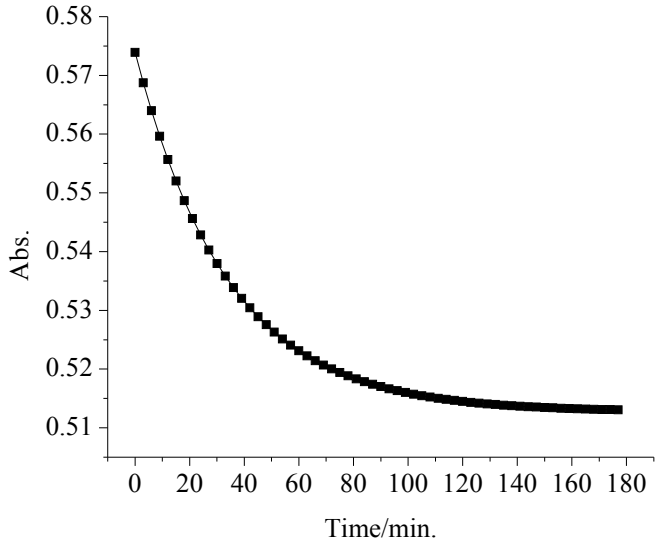


Figure SI 5.40 The kinetic trace for the reaction of **Pt3** with 160 folds L-met at 313K

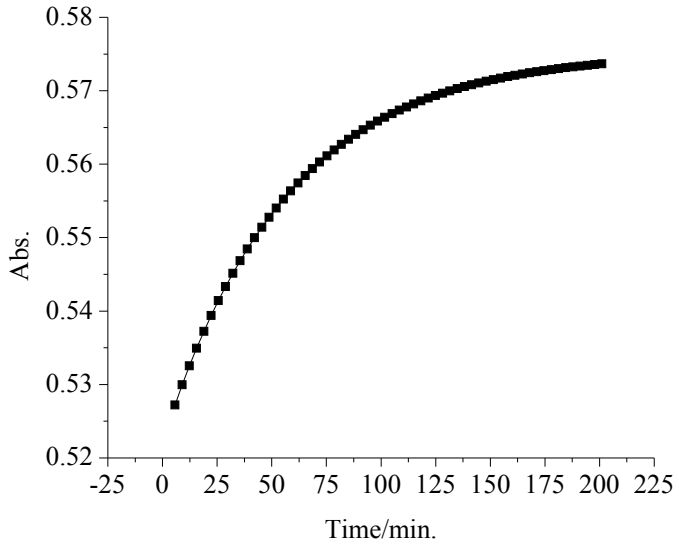


Figure SI 5.41 The kinetic trace for the reaction of **Pt3** with 160 folds GSH at 313K